RECONSTRUCTION OF PAST CLIMATES USING PINK PINE *(HALOCARPUS BIFORMIS)* TREE-RING CHRONOLOGIES

A thesis

submitted in partial fulfilment

of the requirements for the Degree of

Doctor of Philosophy

at

Lincoln University

by

Pavla Fenwick

Lincoln University

2003

Abstract of a thesis submitted in partial fulfilment of the
requirements for the Degree of Ph.D.

RECONSTRUCTION OF PAST CLIMATES USING PINK PINE (*HALOCARPUS BIFORMIS*) TREE-RING CHRONOLOGIES

by Pavla Fenwick

Knowledge of past climate variability is essential for understanding present and future climate trends. This study used *Halocarpus biformis* (pink pine) ring-width chronologies to investigate palaeotemperature history in Westland, New Zealand. The ensuing reconstruction is among the longest palaeoseries produced for New Zealand to date. It is in good agreement with other tree-ring-based records, and with instrumental (both local and hemispheric) data.

Thirteen pink pine chronologies were developed. Ring-width measurements were detrended using the Regional Curve Standardisation method to retain as much low-frequency variance as possible. Crossdating revealed the existence of a strong common signal among trees. Inter-site comparison indicated that a common control mechanism affected tree growth not only within sites, but also across sites.

To determine whether climate was the main factor that controlled the growth of pink pine in Westland, correlation and response function analyses were employed. Temperature, precipitation and the Southern Oscillation Index were tested for their relationship with tree growth. Mean monthly temperature was identified as the primary growth-limiting factor. Chronologies were positively correlated with temperature over an extended period (5-17 months), and climate response modelling showed that temperature explained 11-60% variance in the tree-ring data. The highest and most stable correlations occurred between tree growth and summer (January-March) temperatures.

Tree-ring data from the six sites that contained the strongest temperature signal were combined, and the Westland Regional Chronology (WRC) was developed. The WRC was then used to reconstruct January-March temperatures back to A.D. 1480. The calibration model explained 43% of the variance in temperature, and all calibration and verification tests were passed at high levels of significance. The reconstruction showed that temperatures in Westland have been following a positive trend over the last 520 years. The coolest 25-year

period was 1542-1566, while temperatures reached their maximum in 1966-1990. Spectral analysis of the Westland palaeotemperature record revealed cycles at periods of about 3, 5-6, 11, 14, 22, 45 and 125 years.

This study also confirmed that climate response is species-dependent. A separate exercise, which compared two species from the same site, demonstrated that while pink pine's growth was mainly influenced by summer temperatures, *Libocedrus bidwillii* was affected by conditions at the beginning of the growing season. However, the temperature signal in Westland's *Libocedrus bidwillii* was insufficient to produce a reliable reconstruction. It might be because the climate signal in this species was obscured by disturbances, as was shown in the final section of this project. Frequent growth releases and suppressions implied that *Libocedrus bidwillii* integrated both major (Alpine Fault earthquakes) and minor (windthrow) disturbances in its ring widths. Pink pine, on the other hand, was not sensitive to disturbance, and was therefore a better indicator of palaeotemperatures in Westland.

This research has strengthened the New Zealand network of chronology sites, and confirmed that pink pine has great dendroclimatic value. The last 520 years of temperature fluctuations were reconstructed with a high degree of fidelity – the model developed in this thesis is currently the most accurate estimate of a temperature-growth relationship in the country.

Keywords: climate response, dendrochronology, dendroclimatology, earthquakes, forest disturbance, *Halocarpus biformis*, *Libocedrus bidwillii*, New Zealand, palaeoclimate, temperature reconstruction, tree rings, Westland.

CONTENTS

Chapter 3: Climate response

Chapter 4: Temperature reconstruction

Chapter 5: Comparison with *Libocedrus bidwillii*

Chapter 6: Earthquakes

Chapter 7: Conclusions

LIST OF TABLES

LIST OF FIGURES

GLOSSARY

AC	Autocorrelation Coefficient
ACF	Autocorrelation Function
AHA	Ahaura (site / *Libocedrus bidwillii* chronology)
AIC	Akaike Information Criterion
AR	Autoregression
ARM	Armstrong Reserve (site / *Libocedrus bidwillii* chronology)
ARMA	Autoregressive Moving Average
ARS	Arstan chronology
a.s.l.	above sea level
BON	Mt. Bonar (site / pink pine chronology)
CE	Coefficient of Efficiency
CCP	Camp Creek (site / pink pine chronology)
CCP(LB)	Camp Creek (*Libocedrus bidwillii* chronology)
CRC	Cream Creek (site / *Libocedrus bidwillii* chronology)
CRG	Mt. Cargill (site / *Libocedrus bidwillii* chronology)
CRS	Croesus Track (site / pink pine chronology)
D_i	CCP(LB)-CCP (difference between *Libocedrus bidwillii* and pink pine tree-ring indices from Camp Creek, year *i*)
DBH	Diameter at Breast Height
ELD	Eldrig Peak (site / pink pine chronology)
ENSO	El Niño-Southern Oscillation
EPS	Expressed Population Signal
FLG	Batten Range – Flanagans Hut (site / *Libocedrus bidwillii* chronology)
GLS	Mt. Glasgow (site / pink pine chronology)
ITRDB	International Tree-Ring Data Bank
MAT	Matiri Range (site / pink pine chronology)
MEL	Mt. Elliot (site / pink pine chronology)
MGR	Mt. Greenland (site / pink pine chronology)
MLS	Mean Length of Series
MOA	Moa Park (site / *Libocedrus bidwillii* chronology)
MS	Mean Sensitivity
MSLP	Mean Sea Level Pressure
MTF	Mt. French (site / pink pine chronology)

MTF(LB)	Mt. French (*Libocedrus bidwillii* chronology)
MWP	Medieval Warm Period
OKA	Owaka (site / *Libocedrus bidwillii* chronology)
OMO	Omoeroa Saddle (site / pink pine chronology)
PAC	Partial Autocorrelation Coefficient
PACF	Partial Autocorrelation Function
PC	Principal Component
PCA	Principal Component Analysis
PM	Product Means test
PO	Pith Offset
R1	Serial correlation (autocorrelation at lag 1)
RAW	Raw chronology
RCS	Regional Curve Standardisation
RE	Reduction of Error
RES	Residual chronology
RP	Pearson's product moment correlation coefficient
RR	Robust correlation coeficient
RS	Spearman's coefficient of rank correlation
RSQ	Coefficient of determination
RUH	Rahu Saddle (site / *Libocedrus bidwillii* chronology)
SD	Standard Deviation
SOI	Southern Oscillation Index
SPD	Slopedown Hill (site / pink pine chronology)
ST	Sign Test
STD	Standard chronology
STPI	Summer Transpolar Index
TKG	Mt. Te Kinga (site / pink pine chronology)
TOS	Totara Saddle (site / pink pine chronology)
TRK	Tarkus Knob (site / *Libocedrus bidwillii* chronology)
WBF	Wilberforce (site / *Libocedrus bidwillii* chronology)
WLB	Westland *Libocedrus bidwillii* chronology
WRC	Westland Regional Chronology (pink pine)

Note: throughout the thesis, common name is used for Halocarpus biformis *(pink pine), while scientific names are used for all other species.*

Chapter 1

General introduction

1.1 Palaeoclimate

Over the last few decades, global increase in temperatures has become one of the principal environmental issues. The grave concern over climate warming is apprehensible – among potential impacts of climate change are, for example, increase in severity and frequency of climatic extreme events, changes in ecosystem composition, reduction in biological diversity, and damage to human health and economy (Intergovernmental Panel on Climate Change, 1996; Sturman and Tapper, 1996). Since the late 19th century, the world has warmed by about 0.6°C; the increase being continuous and more dramatic in the Southern Hemisphere (Jones *et al.*, 1986; Jones and Briffa, 1992; Jones *et al.*, 2001). In New Zealand, annual mean surface air temperatures have risen by 0.7°C between 1941-1950 and 1981-1990 (Salinger *et al.*, 1992a).

To increase the accuracy of future climate change scenarios, we first need to improve our understanding of the present climatic patterns. How much of the recent warming has been caused by anthropogenic influences? Is it unusual relative to the low-frequency variations in temperature that occur naturally? Long climatic records are essential for addressing these questions. Unfortunately, few instrumental records go back further than 100 years (Barry, 1978; Jones and Briffa, 1992). The longest continuous records in New Zealand are those from Auckland and Dunedin, where observations began in 1853 (Fouhy *et al.*, 1992). Information on earlier climate variability (palaeoclimate) can, however, be obtained from indirect sources, or "proxies."

Proxy climate data can be derived from historical records, or from a number of geological and biological phenomena. Ice cores, speleothems, glacier advances and recessions, corals, marine and terrestrial sediments, pollen, treeline changes, and tree rings are all examples of proxy climate indicators. Their applicability is restricted by both spatial and temporal limitations (Jones *et al.*, 1998). For example, the spatial extent of ice cores is limited to high latitudes and altitudes (Thompson *et al.*, 1998), whereas corals are available in the tropics only (Cook,

1995). Pollen spectra and sediment cores may encompass long time periods, but their resolution is low (McGlone *et al.*, 1993; Whitehouse, 1999). Tree rings span relatively short periods (centuries to millennia), but because of their high resolution (annual to seasonal) and replication, they are considered one of the most accurate providers of palaeoclimatic information in mid to high latitudes (Fritts, 1976).

1.2 Dendroclimatology

Dendroclimatology utilises dated tree-ring series (chronologies) to study climate. It is a subfield of dendrochronology, which can be broadly defined as "all tree-ring studies where the annual growth layers have been assigned to or are assumed to be associated with specific calendar years" (Fritts, 1976).

Dendrochronology is a "young" science, and it has been expanding rapidly since the pioneering work of an astronomer, Andrew Ellicott Douglass, in western North America in the early 20th century (Robinson, 1990). Originally, dendrochronological methods were developed for dating archaeological structures; but more recently, tree-ring analyses have been applied in other disciplines as well. These include ecology, geomorphology, hydrology, and – as mentioned earlier – climatology. One important development has been the establishment of the International Tree-Ring Data Bank (ITRDB) in 1974, which enables the global scientific community to contribute and freely access tree-ring data (Grissino-Mayer and Fritts, 1997). The background and concepts of dendrochronology and dendroclimatology have been described in great depth (e.g. Fritts, 1976; Cook and Kairiukstis, 1990), but new techniques are still being developed.

Cambial growth (production of xylem and phloem) occurs from meristematic activity in the vascular cambium, and it is reflected in tree-ring properties (e.g. width or density). In temperate zones, typically one ring is formed per year, with wood production beginning in spring/summer and ending with the onset of winter (Kramer and Kozlowski, 1979). Tree-ring properties are affected by a number of external and internal factors (Fritts, 1976; Kramer and Kozlowski, 1979). In some years, when the environmental conditions are highly limiting, no rings are produced, or they are absent from a part of the tree's circumference. Such rings are called missing (or partially missing) rings. At other times, two or more rings can be formed within a year, when a stress period occurs in the middle of the growing season. These are called false or double rings (Figure 1.1; Stokes and Smiley, 1968).

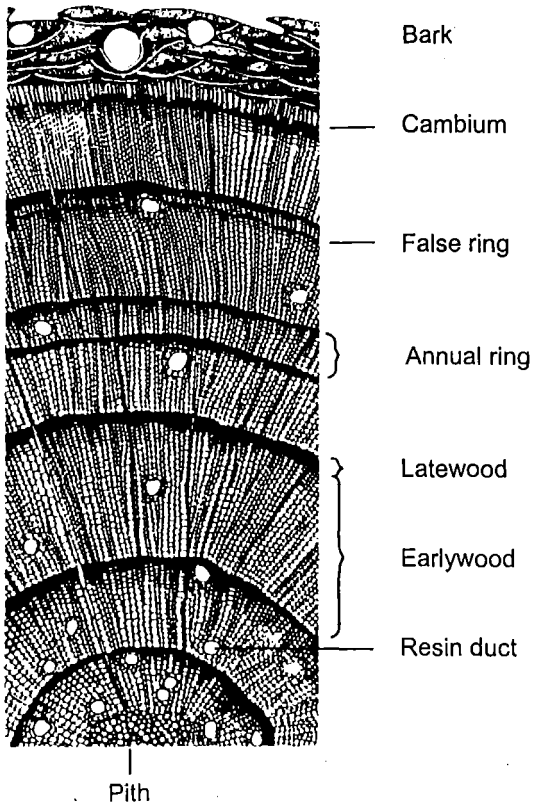

Figure 1.1 Tree rings and other characteristic features along a cross-section of a young conifer. Earlywood (produced at the beginning of growing season) is composed of large, thin-walled cells, whereas smaller cells with thicker walls form the latewood (at the end of the growing season). The abrupt change between the two types of cells is the ring boundary. False rings can be formed when growing conditions become temporarily severe during the growing season (small, thick-walled cells are produced). When the conditions improve, formation of larger cells with thinner walls is resumed. (Adapted from Fritts, 1976.)

The ability to form clear annual rings, longevity and wide geographical spread, are among the species-selection criteria for dendrochronological research (Stokes and Smiley, 1968). Other conditions that have to be met are: (1) only one environmental factor must dominate in limiting the growth of the tree; (2) this factor must vary in intensity from year to year and the resulting rings faithfully reflect such variation in their width; and (3) this growth-limiting factor must be uniformly effective over a large geographical area (Stokes and Smiley, 1968). The most common growth-limiting factors are precipitation and temperature. The more the tree is limited by environmental factors (usually near the margin of its natural range, i.e. treelines for temperature), the more the tree will exhibit variation in width from ring to ring. This variability in ring width is called sensitivity, while the lack of it is referred to as complacency (Stokes and Smiley, 1968; Fritts, 1976). Careful site (and tree) selection will result in the collection of sensitive tree-ring series.

The next stage after site selection and sampling is the process known as crossdating. Crossdating (comparing of ring-width patterns within and between trees) represents the most important tool of dendrochronology, as it determines the exact year of formation for each growth ring. Pilcher (1990) reviewed numerous visual and computer-aided crossdating techniques. The visual crossdating utilises sequences of unusually narrow and wide rings, and missing, false and frost rings to match the patterns (Stokes and Smiley, 1968; Fritts, 1976). The computer-aided procedures require that the ring widths be measured first, so that various correlation statistics can be calculated. Probably the most widely used crossdating software is COFECHA (Holmes, 1983).

Once a sufficient number of crossdated ring-width series has been obtained, the raw measurements can be standardised. Standardisation aims to remove individual growth trends from the ring-width series, while maximising the signal that is common to all trees at a site. This common signal is assumed to reflect climate (Graybill, 1982; Cook *et al.*, 1990a). Climate is only one of many variables that affect tree growth. A simplified linear model (Cook, 1985) views each ring width as an aggregate of the following inputs: (1) an age-size-related trend, (2) a climate-related trend, (3) an endogenous disturbance pulse, (4) an exogenous disturbance pulse, and (5) an unexplained variability. In dendroclimatology, the climate-related trend is considered signal, while all remaining variables are considered noise.

There are a number of deterministic and stochastic approaches to standardisation, which involve fitting of various curves to the individual ring-width series (Fritts, 1976, Cook and Kairiukstis, 1990). One of the newest methods is the regional curve standardisation (RCS), developed by Briffa *et al.* (1992). The RCS generates a single mean growth curve (common to all samples from a site) by aligning the ring-width measurements by their biological age. One major advantage of the RCS method is that it can preserve low-frequency variance in excess of the lengths of the individual series. However, the applicability of the RCS is somewhat limited in that it requires large data sets for the calculations (Esper *et al.*, 2003). In the past decade, the RCS has been successfully applied in several dendroclimatic studies in both hemispheres (Briffa *et al.*, 1992; Cook *et al.*, 2000a; Esper *et al.*, 2002). There are no simple rules for the selection of a suitable standardisation method. The choice is always dependent on the nature of the data and on the purpose of the study.

Through the standardisation process, the non-stationary ring-width measurements are transformed into stationary, dimensionless tree-ring indices. These indices are then used to

compute the final chronologies. Three methods are available to compute the mean-value function: (a) the arithmetic mean, (b) the biweight robust mean, and (c) a mean based on testing for a mixture of normal distributions in the sample (Cook *et al.*, 1990b). Methods (b) and (c) are used when outliers are present, and when the distribution of indices for each year appears to be bimodal or multimodal, respectively (Cook *et al.*, 1990b). Tree-ring series are often highly autocorrelated (Figure 1.2), a fact that violates the independence assumption necessary for most statistical analyses. Cook (1985) and Guiot (1986) developed techniques that remove autocorrelation from data (or "prewhiten" the data), based on the autoregressive moving average (ARMA) time series modelling (Box and Jenkins, 1970).

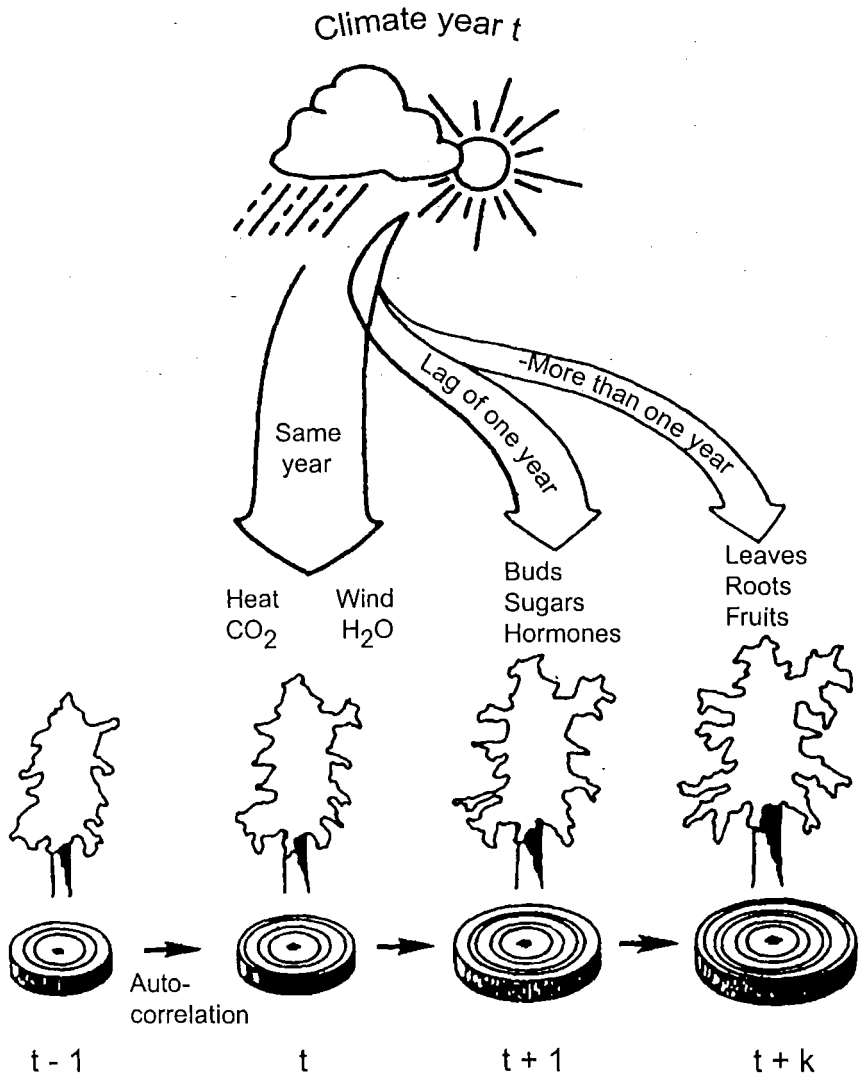

Figure 1.2 Autocorrelation in ring width. Climate of a given year mainly affects the ring width for the same year, but it can also affect ring widths in the following years through a number of biological and physiological processes. The ring widths from several consecutive years are thus statistically related. (Adapted from Fritts, 1976.)

Once the final chronologies are developed, the relationship between tree-ring data and instrumental climate data can be identified through correlation and/or response function analyses (Fritts, 1976; Blasing *et al.*, 1984). Response functions involve two steps – calibration and verification (Fritts, 1976; Cook and Kairiukstis, 1990). Calibration estimates the statistical relationship between tree rings and climate, using various regression techniques (Guiot, 1990). In these analyses, climate (typically monthly or seasonal data) is used as the independent variable (predictor), while the tree-ring data is the dependent variable (predictand). Verification is the independent testing of the calibration model – data estimated by the model are compared with observed data previously withheld from the calibration procedure. Fritts *et al.* (1990) described the commonly used verification statistics. Once the model has been verified, transfer function can be derived (where tree rings are the predictors and climate the predictand). By applying the transfer function to the entire chronology, climate from prior to the instrumental record is reconstructed.

1.3 Dendroclimatic research in the Southern Hemisphere

Compared with the Northern Hemisphere, few tree-ring based climate reconstructions exist for the mid-latitudes of the Southern Hemisphere (Norton and Palmer, 1992; Bradley and Jones, 1993; Jones *et al.*, 2001). This is partly due to the smaller landmass, and partly because less research has been undertaken. While southern Africa has a lack of suitable trees for dendrochronological studies (Norton, 1990), Argentina and Chile in South America, and Tasmania and New Zealand in the Australasian region, show great potential for providing reliable dendroclimatic records.

1.3.1 Dendroclimatic research in South America

In South America, tree rings have been used to study population dynamics (Villalba, 1995; Le Quesne *et al.*, 2000), glacier fluctuations (Villalba *et al.*, 1990) and climate (Villalba, 1990; Lara and Villalba, 1993; Villalba *et al.*, 1998). Villalba (1990) reconstructed summer temperatures since A.D. 870 in northern Patagonia. The longest temperature reconstruction (3622 years) has been produced from south-central Chile (Lara and Villalba, 1993). Both of these palaeotemperature records were derived from *Fitzroya cupressoides* (the second longest living tree species after *Pinus longaeva*) ring-width chronologies. Although chronologies from various other South American species show increased growth since the 1950s (Innes *et al.*, 2000; Szeicz *et al.*, 2000) or late 1970s (Villalba *et al.*, 1997a), the proxy temperature records obtained from *F. cupressoides* provide no evidence of a warming trend (Villalba, 1990; Lara and Villalba, 1993).

Other dendroclimatic studies have used tree rings to reconstruct precipitation (Villalba *et al.*, 1998; Schmelter, 2000) and changes in snow cover duration (Villalba *et al.*, 1997a). Several authors noted that the El Niño / Southern Oscillation phenomenon (ENSO) has a strong influence on tree growth in mid-latitudes of South America (Villalba, 1994; Villalba *et al.*, 1997a; Le Quesne *et al.*, 2000). Evidence has been found that ENSO forces the Southern Hemisphere climate system also in high latitudes (Villalba *et al.*, 1997b). Villalba *et al.* (1997b) used a network of chronologies from the southernmost forested land, Tierra del Fuego (*Nothofagus pumilio* and *N. betuloides*), and New Zealand (*Lagarostrobos colensoi* and *Halocarpus biformis*/pink pine) to reconstruct the last 250 years of monthly mean sea level pressure (MSLP) variability around Antarctica.

1.3.2 Dendroclimatic research in Australia

Few tree-ring studies have been conducted in mainland Australia. Although the subalpine *Eucalyptus pauciflora* exhibits some potential for crossdating (Ogden, 1982), species of the widely distributed *Eucalyptus* have, in general, shown little promise for dendrochronology (Ogden, 1978). The first chronologies in mainland Australia were developed by LaMarche *et al.* (1979a), who undertook limited sampling of both species and sites. These chronologies were only around 50 years long, as they were obtained from the short-lived conifer *Callitris* (LaMarche *et al.*, 1979a).

The vast majority of Australian dendroclimatic studies have been undertaken in Tasmania. The first Tasmanian chronologies were developed by LaMarche *et al.* (1979a), from both angiosperms (*Nothofagus gunnii*) and conifers (genera *Arthrotaxis* and *Phyllocladus*). The coniferous species have shown greater potential for tree-ring research, partly due to their longevity. LaMarche and Pittock (1982) used a subset of eleven chronologies (representing all three genera mentioned above) to reconstruct Tasmanian temperatures back to A.D. 1776. The same eleven chronologies were used by Campbell (1982) to produce a 199-year proxy record of stream flow in western Tasmania. More recently, Allen (1998) conducted an extensive dendroclimatic study of *Phyllocladus asplenifolius*.

Tasmania's most useful material for dendroclimatic reconstruction has proved to be *Lagarostrobos franklinii*, especially at high-altitude sites (Cook *et al.*, 1991; 1992; 1996a; 1996b; Buckley, 1997; Buckley *et al.*, 1997; Cook *et al.*, 2000a). The first temperature reconstruction derived from *L. franklinii* was 1090 years long, and it was based on living trees only (Cook *et al.*, 1992). The coldest 25-year period in this November-April proxy record

occurred from 1890 to 1914, and the warmest from 1965 to 1989 (Cook *et al.*, 1992). Subsequent collection of sub-fossil material enabled the reconstruction to be extended back to 800 B.C. (Cook *et al.*, 1996a; 1996b), and later to 1600 B.C. (Cook *et al.*, 2000a). Individual series in the early studies were standardised by fitting smoothing splines (Cook *et al.*, 1992) or linear/negative exponential growth trends (Cook *et al.*, 1996a) to the data. The final 3592-year reconstruction (Cook *et al.*, 2000a) was based on tree-ring series detrended by the regional curve standardisation (RCS) method (Briffa *et al.*, 1992). The RCS method retained great amounts of low-frequency variance in the data – oscillatory patterns of up to 588 years in length have been revealed in this improved November-April temperature reconstruction (Cook *et al.*, 2000a).

1.3.3 Dendroclimatic research in New Zealand

Early attempts to apply dendrochronological methods in New Zealand were largely inconclusive. Bell and Bell (1958), for example, had only limited success in crossdating several specimens of *Agathis australis* and *Podocarpus totara*. Most of the other examined species appeared unusable because of poorly defined rings, lack of circuit uniformity, complacency or short record (Bell and Bell, 1958). The first New Zealand chronologies were developed in the late 1970s (LaMarche *et al.*, 1979b; Dunwiddie 1979). This initial set comprised 20 chronologies from seven native coniferous species.

Several of these chronologies have been updated during the last two decades (D'Arrigo *et al.*, 1995; Xiong, 1995; D'Arrigo *et al.*, 1998; Xiong and Palmer, 2000a), and new records obtained from *Agathis australis* (Palmer, 1982; Ahmed, 1984; Ahmed and Ogden, 1985), *Libocedrus bidwillii* (Norton, 1983a; Xiong, 1995; Xiong and Palmer, 2000a), *Phyllocladus glaucus* and *P. trichomanoides* (Palmer, 1989), *Lagarostrobos colensoi* (Cook *et al.*, 2002a; 2002b) and pink pine (D'Arrigo *et al.*, 1995; D'Arrigo *et al.*, 1998; Xiong *et al.*, 1998). Chronologies were also developed from the angiosperms, *Nothofagus solandri* and *N. menziesii* (Norton, 1983a; 1983b; 1983c). Floating chronologies (i.e. chronologies not linked to a precise calendar date) exist from sub-fossil *Agathis australis* (3500-3000 B.P.; Bridge and Ogden, 1986) and *Phyllocladus trichomanoides* (2200-1800 B.P.; Palmer, 1989).

The first variables successfully reconstructed from New Zealand tree rings were river flow and precipitation in Canterbury (Norton, 1987). Four *Nothofagus solandri* ring-width chronologies were used to reconstruct Hurunui river summer flow and Lake Coleridge summer precipitation since A.D. 1879.

Norton *et al.* (1989) used a network of *Nothofagus solandri* and *N. menziesii* chronologies to reconstruct New Zealand summer temperatures back to A.D. 1730. Tree-ring data from ten subalpine stands (South Island) and temperature records from seven meteorological stations (entire country) were used in the analysis. Because of the methods used by Norton *et al.* (1989), little low-frequency variability was retained so that century-long trends were lost. However, the reconstruction provided estimates of annual to decadal temperature variation. The results indicate that cooler summers occurred in the early 1780s and late 1840s, whereas temperatures were above average in the 1750s. The warming trend of recent decades was not apparent in the reconstruction.

Salinger *et al.* (1994) estimated past temperatures and zonal and meridional flow over New Zealand from ring-width chronologies from five different species. The reconstructions extended back to A.D. 1731. Besides the multispecies approach, this study differed from Norton *et al.*'s (1989) in the standardisation techniques employed. Salinger *et al.* (1994) used cubic splines to retain more low-frequency climate-related variance in the chronologies. One of the prominent features of the November to March temperature reconstruction was the cool period from 1840 to the early 1860s, and around the 1900s. The recent increase in temperature was detected to some extent. The zonal pressure gradient record showed a distinctly weak circulation in the 1830s. The meridional pressure gradient reconstruction gave slightly contradictory results, depending on which period had been used for calibration.

Xiong and Palmer (2000b) reconstructed New Zealand temperatures back to A.D. 1720. February to March temperatures were estimated from eleven *Libocedrus bidwillii* chronologies, using a bootstrap transfer function. The warming trend after 1950 was apparent in the reconstruction. Spectral analysis of both the instrumental and the estimated temperature data revealed similar periodicities. The results also compared well with other proxy climate data.

The longest palaeotemperature record, and the only one produced specifically for Westland, is the Oroko Swamp series (Cook *et al.*, 2002b). Tree-ring data from *Lagarostrobos colensoi* were used to reconstruct the last 1100 years of summer (January to March) temperatures. Extensive collection of both living and sub-fossil material resulted in a chronology with sample depth of 260 ring-width series, which enabled the authors to use the RCS method. The RCS chronology was calibrated with Hokitika homogenised summer temperatures. The reconstruction shows unusual warming occurring after 1950. However, this rapid increase in

temperature is not statistically unprecedented when compared with the previous 1000 years. The above-average temperatures in the 12th and early 13th centuries provide evidence for the occurrence of the Medieval Warm Period (MWP) in New Zealand.

1.4 New Zealand environment

New Zealand (270,000 km^2) is located in the southwest Pacific Ocean between 34°S and 47°S latitude, and between 167°E and 179°E longitude. It is long (1900 km) and narrow (400 km at its widest point), with its main axis aligned in a northeast-southwest direction. The Southern Alps (with the highest peak, Mt. Cook, rising to 3764 m a.s.l.) are the most prominent physiographic feature of the South Island (41°S - 47°S, 167°E - 174°E). This mountain range subdivides the island into two distinct regions (east and west) that differ in geology, climate and vegetation.

1.4.1 Geology and soils

New Zealand is situated astride the Pacific and Australian plates. The Southern Alps began to rise about 5 million years ago, when the two colliding sections began to crumple (Institute of Geological and Nuclear Sciences, 1996). The uplift continues today, and the average plate-convergence is 3-4 cm per year (Aitken, 1999). The onshore boundary of the Australian and Pacific plates is called the Alpine Fault, and it is about 650 km long, extending from Milford to Blenheim. The major part of Alpine Fault is situated in Westland, which is therefore a region highly prone to earthquakes.

New Zealand's oldest rocks are granites. They were formed during the paleozoic, when 570-350 million years old sediments, once part of Australian and Antarctic Gondwana, were altered by heat and pressure. Granites can be found along the west coast of the South Island and on Stewart Island. The main ranges of the Southern Alps are formed by Torlesse greywackes, which are hardened sediments from between 280 and 200 million years ago (Institute of Geological and Nuclear Sciences, 1996). The West Coast's most recent rocks are the post-glacial marine, estuarine and coastal lagoonal deposits - sedimentary rocks from the upper cenozoic. Regionally metamorphosed rocks (basic paragneiss and amphibolite) are common in Fiordland. In the eastern part of the South Island, most rocks are sedimentary - e.g. greywackes, sandstone, siltstone, limestone and mudstone (New Zealand Geological Survey, 1972). In the immediate vicinity of the Alpine fault (Pacific plate), greywackes have been altered by intense heat and pressure to soft, easily eroded schists (Figure 1.3).

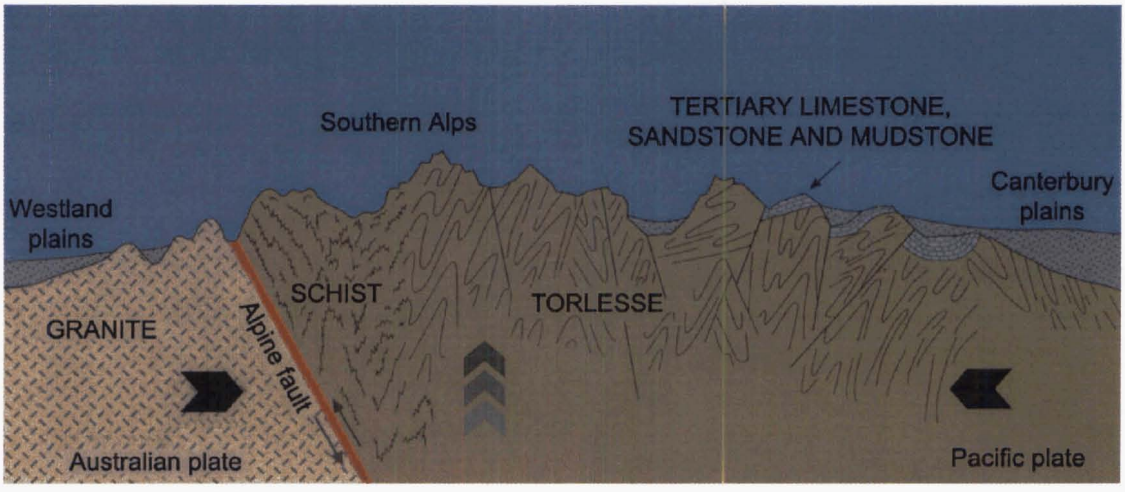

Figure 1.3 Cross-section of the South Island showing the major types of rocks. Torlesse greywackes on the eastern side of the Alpine Fault were transformed to schists due to movement of the plates, as indicated by arrows. (Adapted from Institute of Geological and Nuclear Sciences, 1996.)

Soils in the western part of the South Island are generally infertile, as abundant precipitation causes strong leaching. The common soil types in this area are yellow-brown earths, podzolised yellow-brown earths and podzols (New Zealand Soil Bureau, 1968). Steepland and skeletal soils are typical in montane areas, especially on granite parent rock. Skeletal soils are shallow, poor in nutrients, with a high content of rock fragments.

1.4.2 Climate

New Zealand's climate ranges from warm temperate in the north to cold temperate and alpine in the south (Tomlinson, 1976). Climatic conditions are moderated by oceanic influences, and vary with elevation and exposure to winds and sun. Because of its length, New Zealand extends across two circulation belts. While the north protrudes into the sub-tropical belt of anticyclones, the south of New Zealand lies in the westerly wind belt. As New Zealand is surrounded by ocean, the winds are laden with moisture before they reach the country (Salinger, 1988).

Two major atmospheric circulation systems that affect New Zealand's weather and climate are the Hadley Cell and the Walker circulation (Sturman and Tapper, 1996). The Hadley Cell transports air meridionally (northerly or southerly flow), while the Walker circulation moves air zonally (westerly or easterly flow). Zonal flow from the west leads to above-average

precipitation and lower temperatures in the west, while the eastern part of the South Island is drier and milder. The less frequent easterly circulation results in the opposite pattern. During southerly meridional flow, precipitation increases and temperature decreases in Southland, while the north is drier and milder. Northerly flow has the reverse effect (Salinger, 1980a; 1980b). Overall, the latitude-dependent climate change between north and south is more gradual than the west to east variation, where the magnitude of the anomalies is dependent on orography (The Royal Society of New Zealand, 1988).

One of the major atmosphere-ocean interactions that affects New Zealand's climate is Southern Oscillation (Sturman and Tapper, 1996). The Southern Oscillation is fluctuations in the intensity of the Walker circulation. The strength of the Walker circulation can be expressed by the Southern Oscillation Index (SOI), which is the normalised pressure difference between Tahiti and Darwin. The extreme phases of this oscillation are called El Niño (negative SOI) and La Niña (positive SOI). In New Zealand, El Niño events result in cold south-westerly flow, and therefore heavier than normal precipitation in the west and in the south of the South Island (Gordon, 1985). La Niña events, on the other hand, bring warm north-easterlies. The Southern Oscillation is quasi-periodical in the range of two to seven years, and the El Niño-Southern Oscillation (ENSO) events usually last between 18 and 24 months (Allan, 2000).

In the South Island, the regional weather and climate are strongly affected by the Southern Alps. During the prevailing west and southwest gradient flow, a perturbation of the pressure field occurs. While air is accumulated on the upwind side of the Southern Alps and a ridge of high pressure is formed, depleting air to the east creates a lee through (Sturman and Tapper, 1996). The distortion of the field is associated with a wind field that is three-dimensionally complex (Figure 1.4).

Clouds and fog are common, especially on the western coast of the South Island. This area also experiences 15-25 thunder days per year (Lydolph, 1985). Thunderstorms can act as a trigger mechanism for tornadoes, which in New Zealand achieve wind speeds up to 190 km/h. There are around 15 tornadoes recorded in New Zealand every year. They occur frequently along the west coasts of both islands, but particularly in north Westland (Sturman and Tapper, 1996).

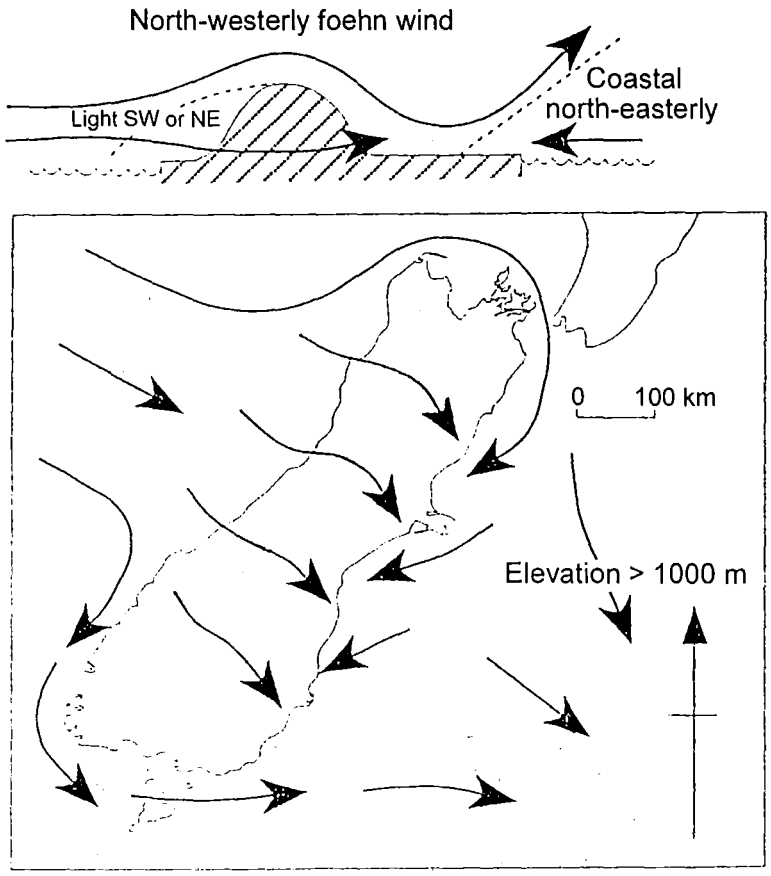

Figure 1.4 Effect of the Southern Alps on regional airflow. (Adapted from Sturman and Tapper, 1996.)

Annual average temperatures at sea level range from about 16°C in the north to about 10°C in the south (Salinger, 1988). Rainfall is highly dependent on topography. While much of the North Island receives 1000-2500 mm annually, the South Island shows more variation. In Alexandra, precipitation may be as low as 335 mm per year (Lydolph, 1985), whereas the annual rainfall in some parts of Westland may reach up to 11,000 mm (Griffiths and McSaveney, 1983).

Salinger (1981) used cluster and PCA techniques to identify New Zealand's temperature and rainfall response areas. Response areas are local areas that show homogenous temperature or rainfall anomalies in response to differing weather systems. In the South Island, there are four temperature response areas: West Coast, Southland, Inland Central Basins and Eastern South Island (Figure 1.5). As for the rainfall response areas, the South Island is divided into two main districts (western and eastern), which can be further subdivided as shown in Figure 1.6.

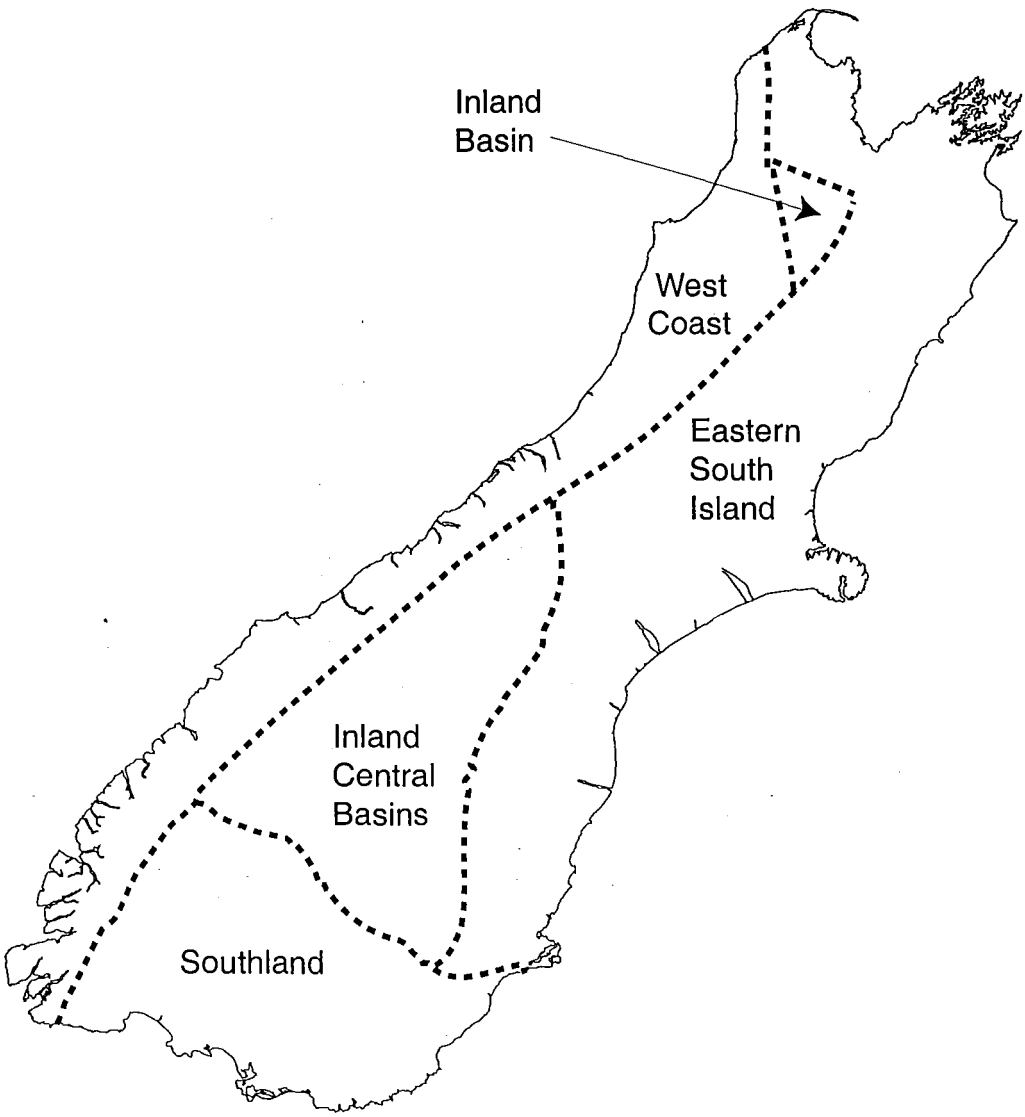

Figure 1.5 South Island temperature response areas. (Adapted from Salinger, 1981.)

Between 1941-1950 and 1981-1990, annual mean temperatures in New Zealand have increased by 0.5°C to 0.8°C (Salinger *et al.*, 1992a). North Island temperatures increased by 0.8°C. Increases of equal magnitude were recorded in the West Coast and Southland response areas of the South Island. Eastern South Island warmed by 0.7°C and inland basins by 0.5°C. No universal long-term trend in rainfall is apparent, however, there has been some variability on a regional scale. As winds from the east and northeast have become more frequent since 1950, the precipitation has increased in the north and east, while the west and south of both islands have become drier (Salinger, 1988).

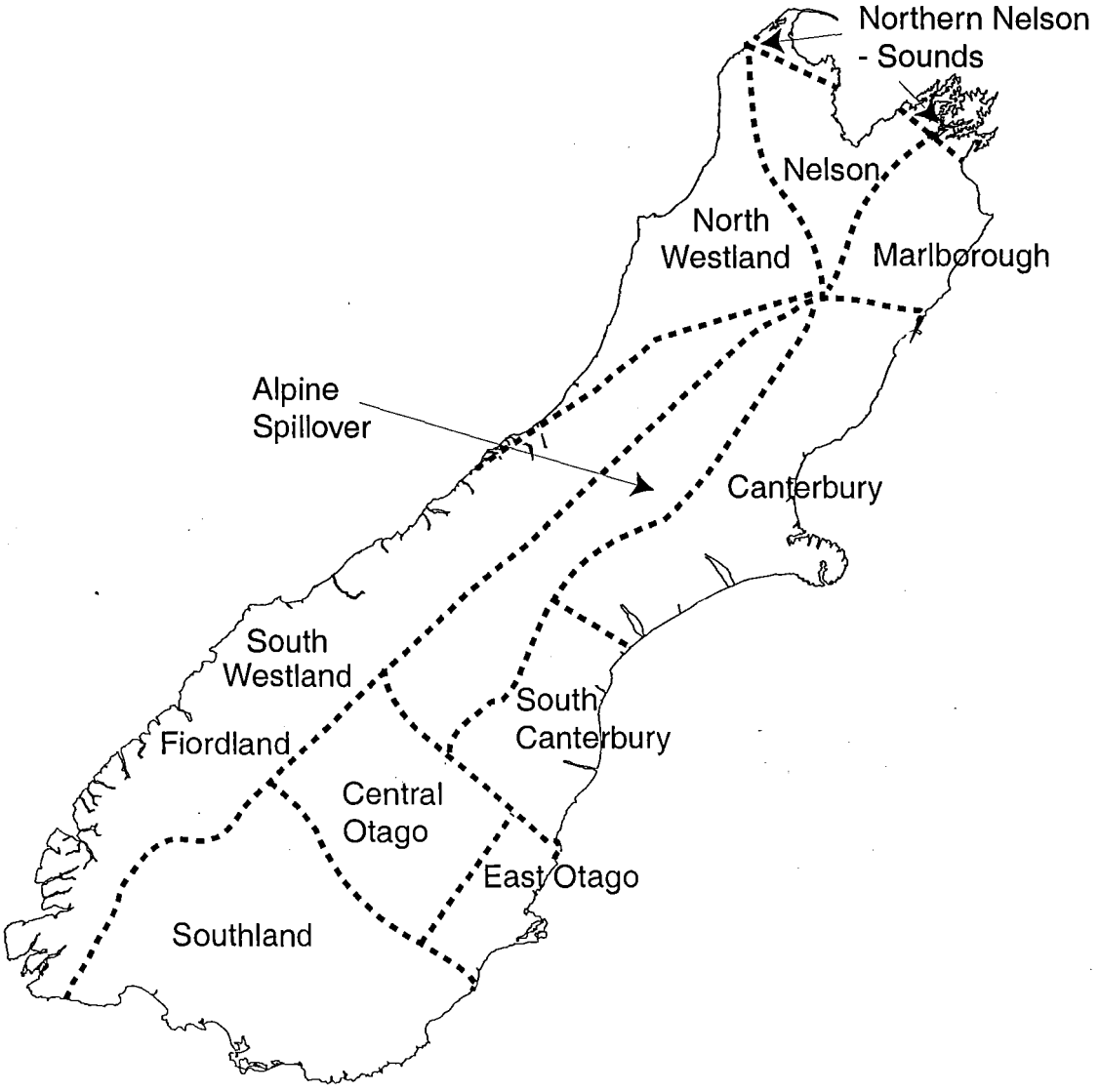

Figure 1.6 South Island rainfall response areas. (Adapted from Salinger, 1981.)

1.4.3 Vegetation

New Zealand indigenous forest communities can be divided into four major groups: (i) coastal forests, (ii) lowland conifer-broadleaved forests, (iii) upland conifer-broadleaved forests, and (iv) *Nothofagus* forests (Wardle, 1991). Prior to the arrival of the first settlers, New Zealand was mostly covered with evergreen rainforest (central Otago being the only larger area below treeline without complete forest cover), with the lowland conifer-broadleaved forests as the dominant type (McGlone *et al.*, 1993). However, Maori (after A.D. 1000) and European (after

A.D. 1800) settlers cleared nearly all the lowland conifer-broadleaved forest, and *Nothofagus*-dominated forests have become the most common indigenous forest type.

There are four species of *Nothofagus* in New Zealand. They are all tolerant of sub-optimal environments, and often form nearly pure stands (McGlone *et al.*, 1993). In montane and subalpine regions, especially in the northern part of the South Island and in Fiordland, *N. menziesii* and *N. solandri* are dominant at treeline.

In districts lacking *Nothofagus*, mixed forests (consisting of a variety of conifer and broadleaved species) occur. The upland conifer-broadleaved forests are floristically poorer than their lowland equivalents (Wardle, 1991). Broadleaved trees, or hardwoods, are here defined as all non-*Nothofagus* angiosperms. They range in size from canopy-dominant to stunted trees and shrubs at treeline. In lowland conifer-broadleaved forests, hardwoods usually form a lower tier, while conifers are typically tall and canopy-dominant trees. New Zealand conifers belong to three major families: Araucariaceae (represented by *Agathis australis* - New Zealand's largest tree, occurring in the northern part of the North Island), Cupressaceae (*Libocedrus bidwillii* and *L. plumosa*), and Podocarpaceae. New Zealand's podocarps include 17 species from the following genera: *Dacrycarpus*, *Dacrydium*, *Halocarpus*, *Lagarostrobos*, *Lepidothamnus*, *Phyllocladus*, *Podocarpus* and *Prumnopitys* (Salmon, 1996).

1.5 Pink pine

Halocarpus biformis (Hook.) Quinn, formerly known as *Dacrydium biforme* (Quinn, 1982), is a New Zealand indigenous species within the Podocarpaceae family. It is an evergreen conifer, with a distributional range extending from Mt. Tongariro and the Ruahine Mountains in the central North Island to Stewart Island (Stewart, 1984). In the South Island, it occurs predominantly in the west.

Pink pine occurs in association with other species within the conifer-broadleaved forest community. At low altitudes, it can be associated with *Lagarostrobos colensoi* and *Dacrydium cupressium*. Species that grow alongside pink pine at mid altitudes are, for example, *Metrosideros umbellata* and *Weinmannia racemosa*. In the subalpine zone, pink pine is often accompanied by trees and shrubs from the following genera: *Nothofagus*, *Dracophyllum* and *Olearia*. *Phyllocladus alpinus* occurs with pink pine at mid to high latitudes. From a dendroclimatic point of view, *Libocedrus bidwillii* is the most important

associated species, as it occurs at all altitudinal levels, and has been the subject of several dendrochronological studies (e.g. Dunwiddie, 1979; Norton, 1983a; Xiong, 1995; Xiong and Palmer, 2000a).

Pink pine is typically found on infertile soils in subalpine forest and scrub communities (Wardle, 1960). On Stewart Island, where the species reaches its highest latitudinal forest limit, pink pine descends to near sea level (Wilson, 1987a). At lower latitudes, it occasionally occurs at low altitudes, too - provided that the soils are poorly drained. Examples of such locations are the Totara Saddle and the Omoeroa Saddle in Westland. Trees are usually small, rarely exceeding 10 m in height and 60 cm in diameter (Figure 1.7), and they are often multi-stemmed (Figure 1.8). At high altitudes and on strongly exposed locations, pink pine occurs as a shrub (Figure 1.9). The outer bark is silver-grey, and it peels away in small thick flakes to reveal a reddish-brown inner layer (Figure 1.10). Pinkish colour of the wood gave the species its common name. All parts of the plant are very resinous.

Figure 1.7 Pink pine near treeline (Mt. French).

Figure 1.8 Pink pine tree with multiple stems (Matiri Range).

Figure 1.9 Shrub form of pink pine (Eldrig Peak).

Pink pine forms two types of leaves, juvenile and adult (Figure 1.11). Adult branchlets with their scale-like leaves are almost four-angled, 1.5 – 3.5 mm across (Wilson, 1987b). This gives the tree a heavy appearance, compared with other conifers with similar type of foliage (*Dacrycarpus*, *Dacrydium*, *Halocarpus*, *Lagarostrobos*, *Lepidothamnus* and *Libocedrus*). Leaves remain green and attached for as long 50 years (Wardle, 1963). Because of its harsh foliage with a low nutrient content, pink pine has an extremely low susceptibility to deer browsing (Wardle, 1974).

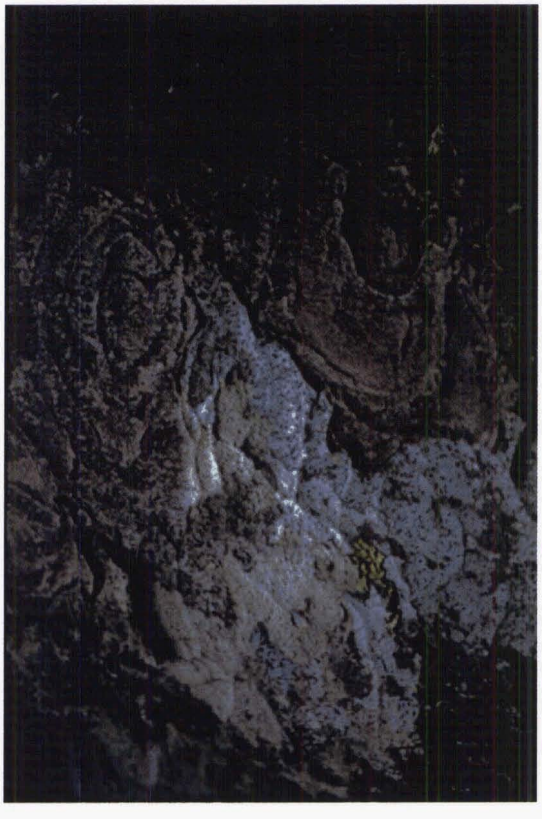

Figure 1.10 Characteristic colouring of pink pine's bark.

Figure 1.11 Pink pine's foliage. Juvenile leaves (left and right part of the picture) are longer and loosely arranged, whereas adult leaves (centre) are short and compact.

Apical buds lack any special protective structures, being sheathed only by developing foliage leaves (Wardle, 1963). However, this morphological disadvantage does not affect the hardiness of the species – pink pine is often found at the same altitudes as some species with specialised apical buds. In New Zealand shrubs and trees, physiological mechanisms seem to be more important for species distribution than morphological mechanisms.

Because of the oceanic climates, New Zealand plants have generally only a small degree of frost tolerance (Wardle, 1991). Pink pine is one of the most resistant species. Its freezing resistance, i.e. the lowest temperature at which the plant shows little or no damage, is -13°C (Sakai and Wardle, 1978). This value is about the same as that of *Lagarostrobos colensoi* and *Libocedrus bidwillii*. There are only five other species that can tolerate more severe frosts, the most resistant being *Halocarpus bidwillii*, which can survive temperatures as low as -25°C.

Pink pine is extremely slow growing. In subalpine trees, the annual shoot growth ranges from 10 to 18 mm (Wardle, 1963). As for cambial growth, pink pine can form rings only one or two cells in width (less than 0.1 mm) in certain years. When averaged for complete radii, the growth rates are around 0.2-0.4 mm / year. Initial estimates of pink pine's longevity were therefore very optimistic – the maximum age was expected to exceed 1,000 years (Wardle, 1960; Wardle, 1963). However, the oldest tree found so far was 663 years old. Tree rings are distinct (Wardle, 1963; Patel, 1967; Dunwiddie, 1979), and their boundaries have a characteristic wavy form (Figure 1.12).

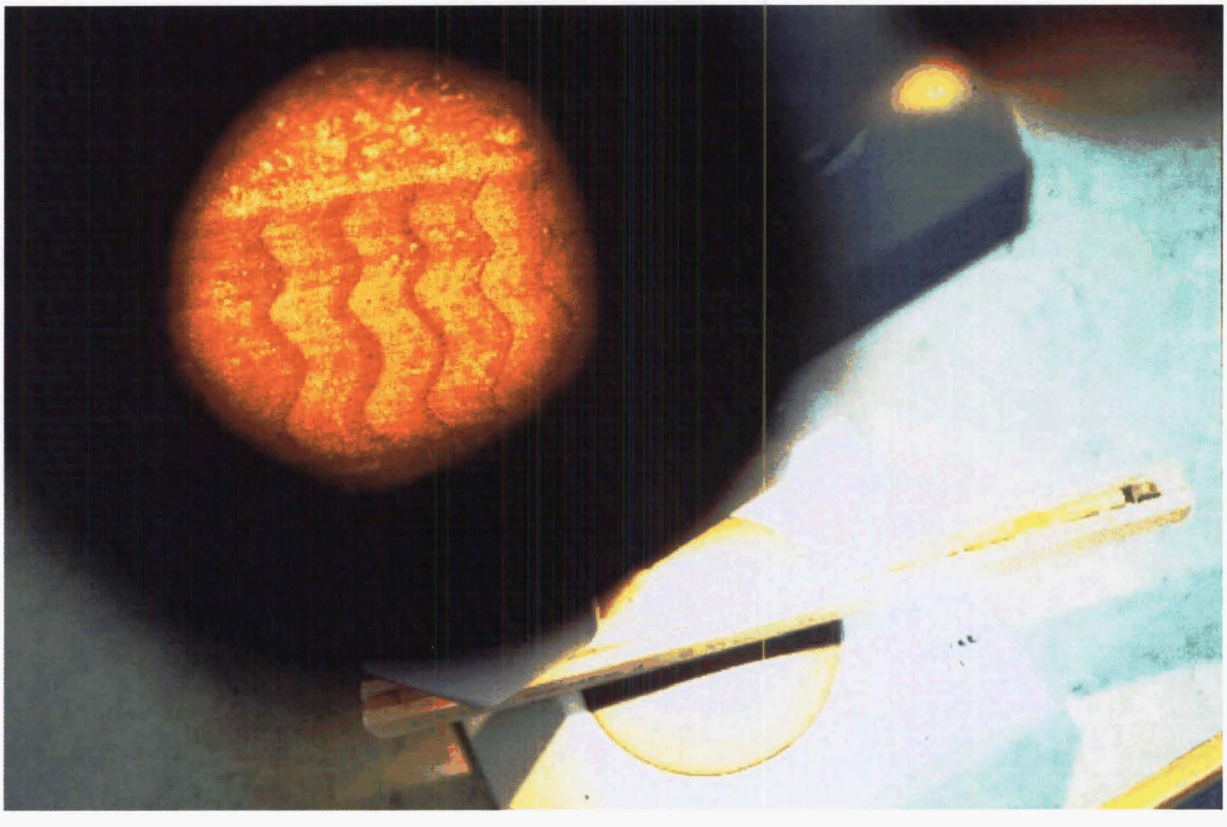

Figure 1.12 Typical wavy boundaries of pink pine's tree rings.

Little is known of pink pine's population dynamics. A study by Stewart and Rose (1989) in Camp Creek, Westland, concluded that it regenerates somewhat sporadically, probably following disturbance events (canopy breakdown). However, the regeneration pattern for pink pine appears to be more continuous than that for *Libocedrus bidwillii* (Stewart and Rose, 1989). Pilot dendroclimatological projects have shown that pink pine is sensitive to summer temperatures (D'Arrigo *et al.*, 1995; Xiong *et al.*, 1998), ENSO (Murphy, 1993), and in a smaller extent to precipitation (Xiong *et al.*, 1998).

1.6 Objectives

After the first exploratory collection, Dunwiddie (1979) developed one pink pine chronology from Fiordland, and classified pink pine as a species with promising dendroclimatic potential. Since then, only four pink pine chronologies have been developed – two from Stewart Island (D'Arrigo *et al.*, 1995), and two from the North Island (D'Arrigo *et al.*, 1998; Xiong *et al.*, 1998). To strengthen the New Zealand network of chronology sites, I propose to develop several new pink pine chronologies. Moreover, these chronologies will be produced from Westland, which is a region where few other chronologies exist.

Following the climate response analysis, I will use the pink pine chronologies to reconstruct past climates. This will be done specifically for Westland. As mentioned earlier, this region's climate differs from the rest of New Zealand due to orography. The uniqueness of the Westland region was also recognised by Xiong (1995), who found that three *Libocedrus bidwillii* chronologies from Westland correlated among themselves, but not with other chronologies from other parts of New Zealand. Nonetheless, climate reconstructions in New Zealand were typically produced by combining Westland chronologies with chronologies from other regions (Norton *et al.*, 1989; Salinger *et al.*, 1994). The only Westland summer temperature reconstruction is that from Oroko Swamp (Cook *et al.*, 2002b), which is of considerable length (1,100 years), however it utilises tree-ring proxies from a single site. The aim of this research is to reconstruct Westland's climate from a network of sites.

Pink pine often occurs in association with *Libocedrus bidwillii*, so another component of this work will be to compare climate sensitivity of the two species. Such *in situ* comparison could provide important new refinements to climate reconstructions. I will develop new *Libocedrus bidwillii* chronologies, and I will also use some existing data from the ITRDB.

As well as exhibiting a response to climate, trees can record the impacts of large-scale disturbances (e.g. Jacoby, 1997; see Section 6.1 for further details). This is particularly the case in Westland, where infrequent major earthquakes can have a substantial influence on tree establishment and growth (Stewart and Rose, 1989; Wells *et al.*, 1999). Another part of this project will therefore be to investigate the nature and extent of past earthquakes recorded in tree rings.

The specific objectives of this research are therefore:

1. To develop regional (Westland) long-term, high-resolution, precisely dated tree-ring chronologies from pink pine.
2. To analyse the relationship between tree-ring widths and instrumental climate records.
3. To reconstruct the last 500+ years of climate variation.
4. To compare pink pine's climate sensitivity with that of *Libocedrus bidwillii*.
5. To identify the temporal and spatial patterns of past major earthquakes in Westland in the last 500+ years.

1.7 Outline of thesis

This thesis consists of seven chapters and three appendices.

Chapter 1: The science of dendroclimatology, its importance in the study of palaeoclimate, and its main principles, are presented. An overview of dendroclimatic research in New Zealand and other parts of the Southern Hemisphere is given. New Zealand's physical environment and the native pink pine are described. Objectives of this study are stated.

Chapter 2: Thirteen pink pine chronologies are developed. Study sites, field and laboratory techniques, are described. Chronology statistics are presented. The effects of different standardisation methods on the data are investigated. The chronologies are compared by means of correlation and principal component analyses.

Chapter 3: The relationships between tree growth and climate (temperature, precipitation, SOI) are explored, using the correlation and response functions. The climatic variables that affected tree growth significantly are identified.

Chapter 4: The Westland temperature is reconstructed back to A.D. 1480. The results are compared with other proxy records.

Chapter 5: An inter-species comparison is carried out. The temperature response of pink pine is compared with that of *Libocedrus bidwillii*. Two original *Libocedrus bidwillii* chronologies were developed, and additional *Libocedrus bidwillii* tree-ring data were obtained from the ITRDB.

Chapter 6: Detection of earthquake signals in tree-ring data is attempted. Abrupt growth changes (suppressions and releases) are used to investigate the disturbance history.

Chapter 7: Final discussion, conclusions and suggestions for further research.

Appendices: Appendix 1 describes the methodology applied to estimate pith offset. Apendix 2 contains crossdated raw measurements and final chronologies from all sites. Appendix 3 contains the observed and reconstructed temperature data. The data in Appendices 2 and 3 are stored on a computer disk.

Chapter 2

Development of the ring-width chronologies

2.1 Introduction

This chapter describes the development of a new network of pink pine chronologies. A site description is followed by a brief account of standard field and laboratory techniques, which were implemented to collect and prepare the samples. A combination of visual and computer-aided techniques was used to crossdate ring sequences. Standardisation seeks to remove non-climatic signals from the tree-ring data, and the selection of a suitable standardisation method is arguably the most important step in dendroclimatic research. I investigate how two different standardisation techniques affect the final chronologies. Both the "traditional" (developed by applying negative exponential or linear curves to the ring-width series) and the regional-curve-standardised (RCS) chronologies, and their statistics, are presented. Finally, the chronologies are compared by the means of correlation analyses and PCA.

2.2 Site description

I established eleven study sites in central and northern Westland, and two sites in the southern South Island (Figure 2.1). The climate of the study area is humid, cool and cloudy. Rainfall ranges from about 1000-1500 mm/year in the Catlins (the SPD site; New Zealand Meteorological Service, 1984; Sandercock, 1987) to about 6000 mm/year at the high-altitude sites along the West Coast (Griffiths and McSaveney, 1983; New Zealand Meteorological Service, 1984). Snowfalls are common throughout winter. The soils are infertile, and drainage poor to moderate. For more details on Westland's environment, see Sections 1.4 and 3.2.
Site selection was based on several criteria: (1) good spatial representation of Westland, (2) altitudinal range, (3) tectonically stable areas, and (4) multiple species were required.

(1) *Spatial representation.* I explored potential locations along the West Coast; a number of sites could be found between 41°S and 43°S, but there is an obvious gap in the network of sites south of 43°30'S (Figure 2.1). This is because pink pine is a species characterised by a disjunct distribution, and most of this area is dominated by *Nothofagus* forests.

(2) *Altitudinal range.* Since trees growing close to their distributional limits are more likely to yield sensitive tree-ring series (Stokes and Smiley, 1968; Fritts, 1976), I established most sites at or near to treeline (Table 2.1). However, I have also included OMO and TOS in the selection – even though these sites were located at lower altitudes – because of the encouraging results by Cook *et al.* (2002a). The authors studied *Lagarastrobos colensoi* (another podocarp) from a nearby location, the Oroko Swamp (110 m a.s.l.), and found the tree growth to be significantly correlated with summer temperature.

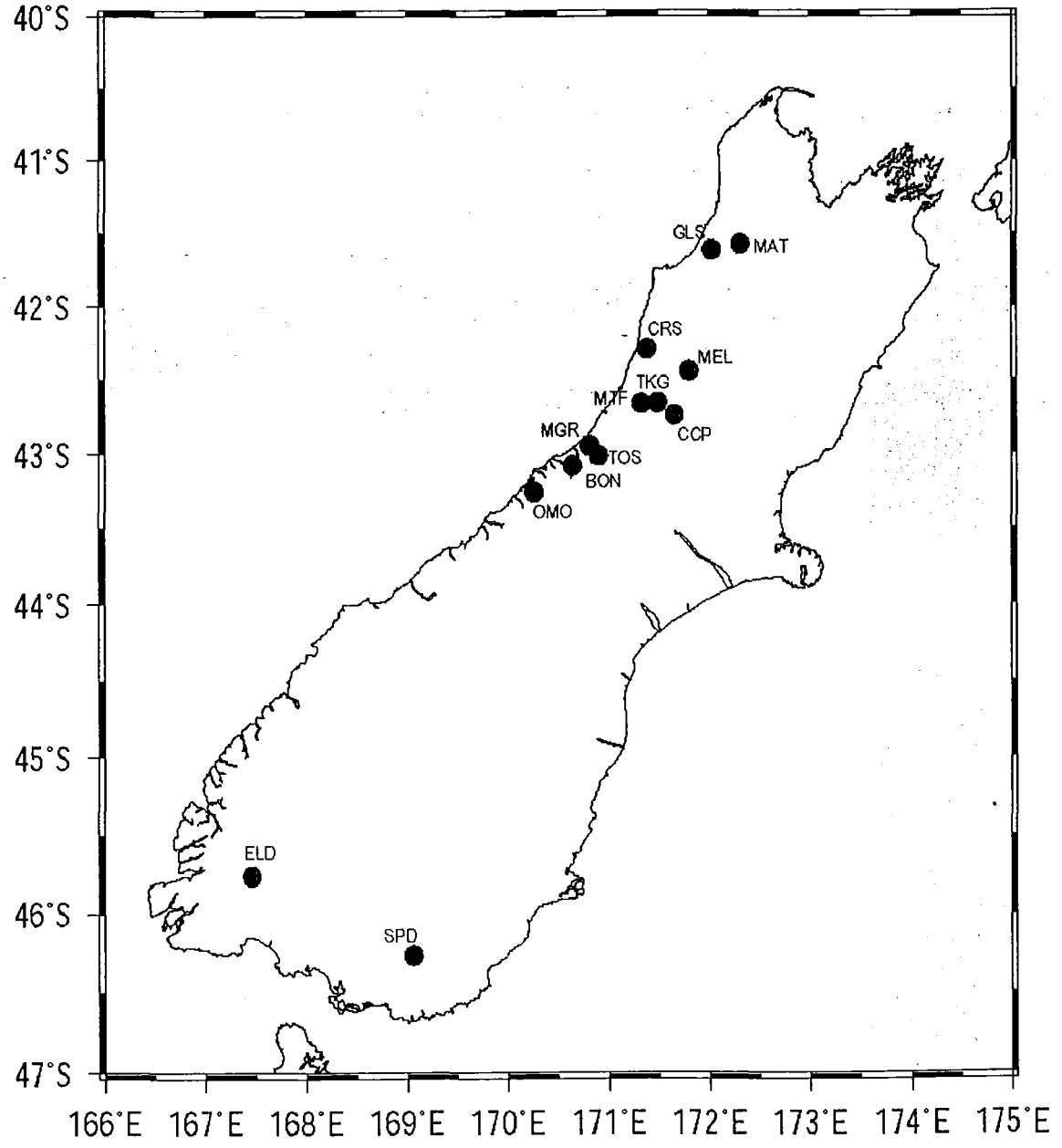

Figure 2.1 Location of the study sites.

(3) *Tectonically stable areas.* Most sites in central Westland were located very close to the Alpine Fault, i.e the climate signal in tree rings might be confounded by earthquake disturbance (Wells, 1998). Thus sites distant from the fault (ELD and SPD) were added to the network, to help with identification of potential disturbance pulses in the Westland trees.

(4) *Multiple species.* Because inter-species comparison is an important part of this research (Chapter 5), I wanted to sample pink pine at sites where it was associated with other species, especially *Libocedrus bidwillii.* At most sites, pink pine occurred within conifer-broadleaved forest. *Libocedrus bidwillii* was present at nine sites (BON, CCP, CRS, MAT, MTF, OMO, SPD, TKG and TOS). Occasionally, pink pine was also associated with *Nothofagus* (ELD, GLS and MAT).

Table 2.1 Site characteristics.

#	Site	Site Code	Lat. (S)	Long. (E)	Altitude [m a.s.l.]	Aspect	Slope [°]
1.	Mt. Bonar	BON	43°05'	170°39'	850	W	5-25
2.	Camp Creek	CCP	42°43'	171°34'	970	NNE	5-20
3.	Croesus Track	CRS	42°17'30"	171°23'30"	900	E	0-20
4.	Eldrik Peak	ELD	45°45'30"	167°28'	750	NE	0-25
5.	Mt. Glasgow	GLS	41°37'	172°02'30"	950	NW	15-25
6.	Matiri Range	MAT	41°34'30"	172°19'	1060	(W)	0-15
7.	Mt. Elliot	MEL	42°30'	171°50'	1050	W	15-40
8.	Mt. Greenland	MGR	42°57'	170°49'	865	NNE	0-5
9.	Mt. French	MTF	42°40'	171°20'30"	750	N	15-25
10.	Omoeroa Saddle	OMO	43°24'30"	170°06'30"	320	-	0
11.	Slopedown Hill	SPD	46°22'30"	169°03'	560	(SW)	0-5
12.	Mt. Te Kinga	TKG	42°39'30"	171°30'	950	NE	15-35
13.	Totara Saddle	TOS	42°59'	170°51'	210	-	0

Mixed forests typically formed a very dense canopy (Figure 2.2). The few exceptions were the CRS, MAT and MEL sites. At MAT, small groups of trees and shrubs were scattered on a montane plateau (Figure 2.2). At CRS and MEL, I mainly sampled individual trees above the forest limit, in a relatively open environment. At least two sites were disturbed by human activities within the last 50 years. The TOS site was subject to logging in the 1950s-1970s (B. Brown, pers. comm.). At BON, several trees and shrubs were cleared along the ridge in the early 1970s, when cables were laid from a transmitter station located on top of Mt. Bonar (M. Vronsky, pers. comm.). Also, many trees in the Mt. Bonar forest were killed or injured in the early 1950s, when a severe storm affected this area (M. Vronsky, pers. comm.).

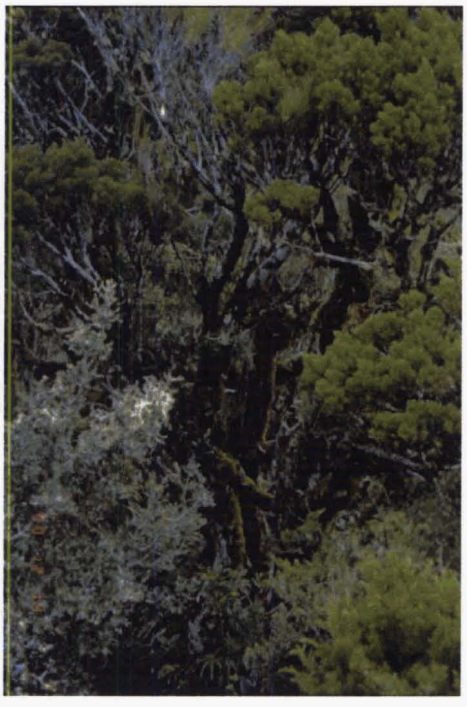

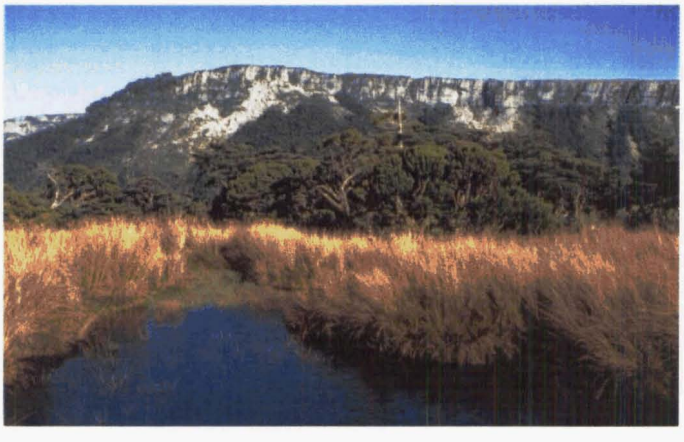

Figure 2.2 Pink pine at several of the study sites. Top left: dense forest on a gentle slope near the top of Mt. Greenland (MGR). Middle left: mid-altitude pink pine forest (MTF). Bottom left: high-altitude, poorly drained plateau (MAT); the landslide in the background was triggered by the 1929 Murchison earthquake. Top right: dense canopy near treeline (CCP). Bottom right: pink pine forest at ELD, where some of the oldest trees were found.

2.3 Materials and methods

2.3.1 Sampling and sample preparation

All samples were obtained by using increment borers (Figure 2.3), because the vast majority of sampled trees were living. Occasional dead trees were encountered that were still standing and their trunks were relatively solid, so it was still possible to use increment borers. On average, I sampled 28 trees from each site, ranging from 16 (MEL and SPD) to a maximum of 53 trees (CCP). Only trees with a diameter-at-breast-height (DBH) of 20 cm or more were sampled. This is because I assumed that greater DBH indicated greater ages – and old trees are required for dendroclimatic studies to obtain a chronology of maximum duration (Fritts, 1976; Schweingruber *et al.*, 1990). The DBH of most sampled trees ranged from 30 to 50 cm. Typically, two cores per tree were removed. Where possible, I took the cores from the opposite sides of the tree, parallel to the slope. I avoided all injuries and branches, following the methods of Stokes and Smiley (1968).

Figure 2.3 Extracting a core from a pink pine tree at Mt. French (MTF).

For the duration of the fieldwork, plastic straws were used to store the cores. These were subsequently mounted (Figure 2.4) and sanded (Figure 2.5) in the laboratory, following standard dendrochronological procedures (Stokes and Smiley, 1968).

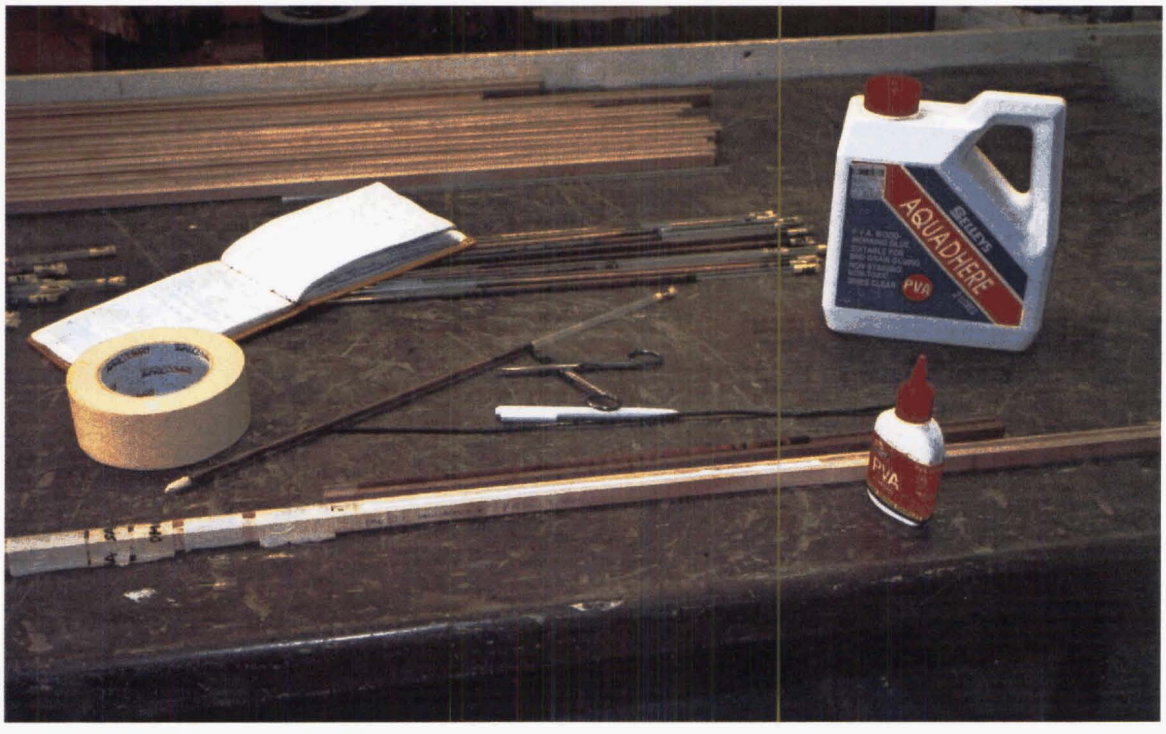

Figure 2.4 Mounting of cores. Using a water-soluble adhesive, cores were glued onto wooden mounts, and allowed to air-dry slowly.

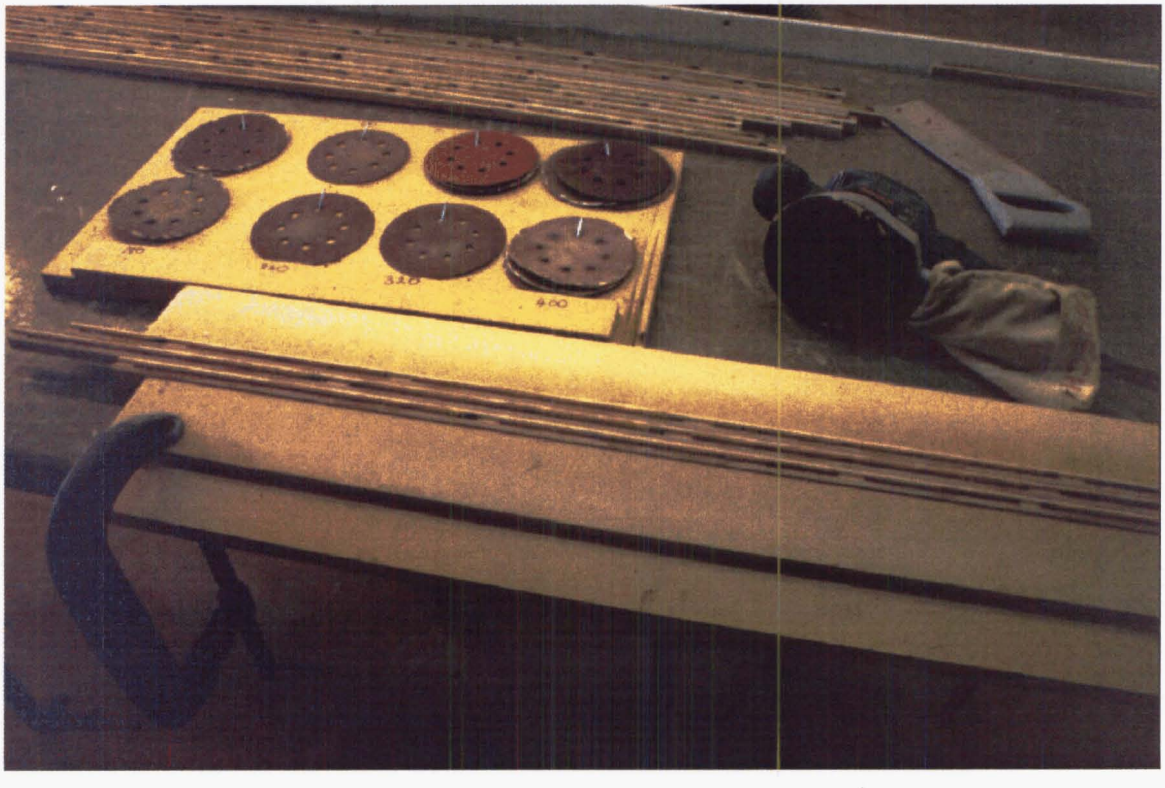

Figure 2.5 Sanding. Orbital sanders were used to gradually polish the surface of the cores (starting with an 80-grit and finishing with a 400-grit sanding paper).

2.3.2 Measuring and crossdating

As the New Zealand growing season covers two calendar years, rings were assigned to the year in which growth began – for example, the ring from the 1999/2000 summer was dated as 1999 (Schulman, 1956). I crossdated the samples first by visual means, and then by employing computer-aided crossdating procedures. The visual examination (under a binocular microscope) involved matching of ring-width patterns, first within trees, and then among trees (Stokes and Smiley, 1968; Fritts, 1976). I used marker rings (unusually narrow and wide rings in most cases) to match the patterns. I found that in the pink pine samples, the ten narrowest rings in the last 400 years occurred in these years: 1634, 1660, 1676, 1791, 1799, 1807, 1833, 1878, 1912 and 1983.

The visual crossdating was followed by measuring. I measured the ring widths using a Velmex measuring stage (Figure 2.6). The precision of the measurements was 0.001 mm. To verify the dates, and to date the samples where visual means were insufficient (e.g. because of a major distortion in a part of the core, such as ring wedging), I used the COFECHA software (Holmes, 1983). COFECHA is a quality control programme that uses correlation statistics to test the crossdating of measured ring-width series.

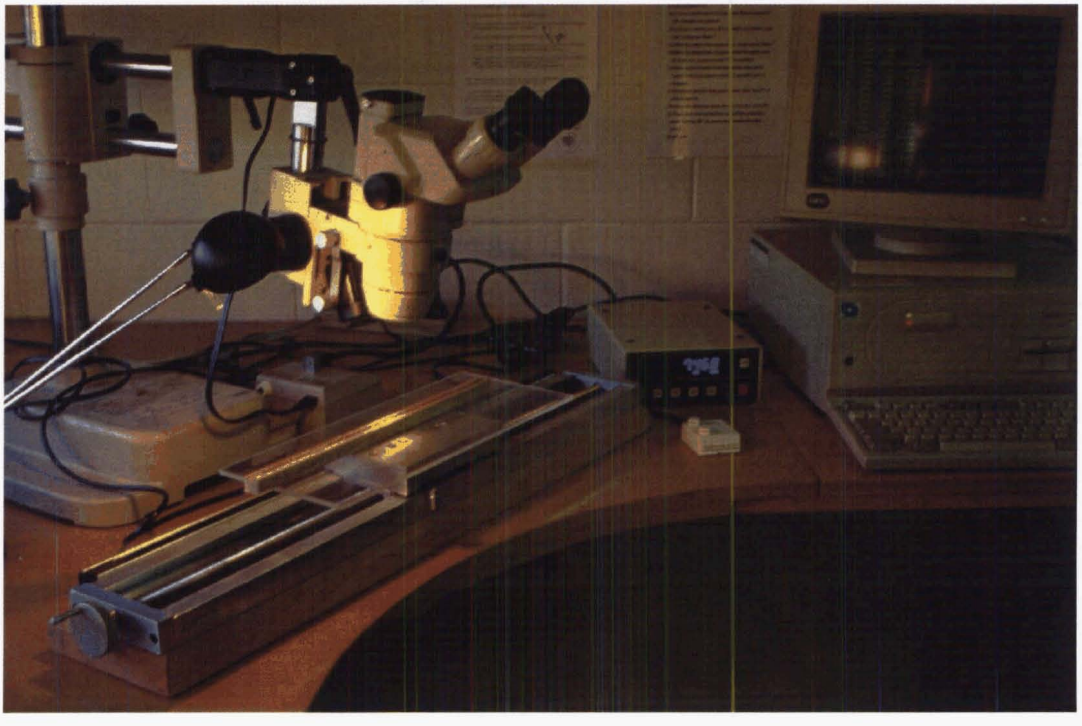

Figure 2.6 The measuring stage. Attached are a digital display unit and a computer, where the data are recorded.

From every site, up to three cores were separated into dated fragments by gaps spanning over several years to several decades. These undatable gaps occurred either when wood was missing (rotten or lost), or when the growth in that section was too suppressed. This introduced the problem called the "many fragments curse" (Sheppard *et al.*, 1997), a special case of the "segment length curse" (Cook *et al.*, 1995). To preserve the low-frequency variance contained in the entire series, I connected the fragments by replacing the undatable rings with estimated values. These values were calculated by the ARSTAN programme (Cook, 1985; updated version: E. Cook, pers. comm.). For every site, ARSTAN uses the measurements of all crossdated series to fill-in the gaps. Less than 0.3% of the data were thus estimated. Another measure I took to exorcise the segment length curse, was the discarding of short series. With the exception of four series that were 85-100 years long, I only included series of more than 100 years in the chronologies. The four short series spanned periods in the early part of the record, and their retention was thus important with respect to sample depth.

2.3.3 Standardisation

Figure 2.7 shows the various growth trends as exhibited by seven series (five trees) from the Camp Creek site. No universal growth trend is apparent. While the growth of series CCP25-2 resembles a negative exponential curve, linear trends can be detected in some of the others series: negative (CCP44-1), positive (CCP51-1) or horizontal (CCP26-2). I often noted a suppressed growth in the first few decades or centuries, followed by a period of fast growth, and then by a gradual decrease in ring width – such example is CCP23-1. The initial slow growth might indicate that the tree had developed under a closed canopy, competing for light and nutrients. The decrease in the recent centuries is probably the effect of tree ageing / increasing tree size. Competition and tree ageing are both examples of factors that result in growth trends unique to individual trees, and which standardisation seeks to remove.

I tested a variety of deterministic and stochastic methods of standardisation. The options investigated included fitting a linear or negative exponential curves to the individual series (Fritts, 1976), single detrending with cubic-smoothing splines of different 50% cut-off lengths (Cook and Peters, 1981), and various combinations of the above (double detrending). I examined the resulting plots and statistics, and I decided to use single detrending, namely the fitting of negative exponential or linear (any slope) curves to the series (henceforth referred to as the "single detrending method"). As this method of standardisation is very rigid, it preserves the low-frequency variance due to climate better than the more flexible cubic-smoothing splines and double-detrending methods (Cook and Briffa, 1990).

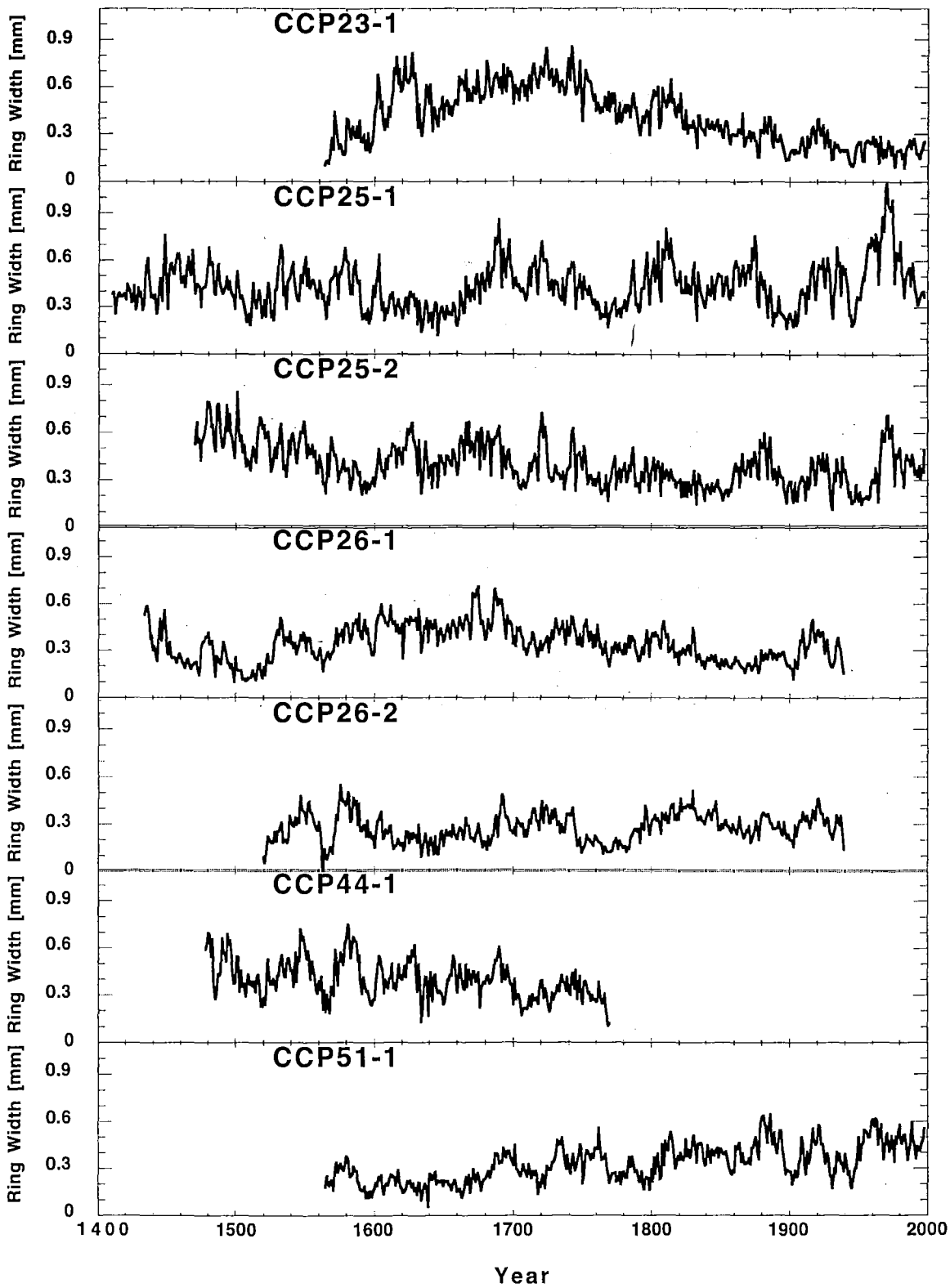

Figure 2.7 Examples of the various growth trends from the Camp Creek site.

The initial visual examination of the cores suggested that the ring-width patterns and trends were similar across the sites. This was confirmed later, when I compared chronologies based on the single-detrended data by the means of correlation and principal component analyses (Section 2.4.3). This indicated the potential for applying the Regional Curve Standardisation (RCS) method (Briffa *et al.*, 1992) to the series.

The RCS method requires aligning the individual series by cambial age to estimate a mean age-related growth curve, which is typical for the species in a given site or region. This curve is assumed to reflect biological noise only, and all deviations of the individual series from the mean curve are interpreted as climatic signals (Briffa *et al.*, 1992). With the core samples, the cambial age of the rings (i.e. the number of years from the pith) is usually unknown, as the pith is often missing from the samples. Such was the case here, hence I needed to estimate the pith offset of each series first (see Appendix 1 for details).

To decide whether sub-samples of trees from different sites belong to the same population (i.e. whether their biological growth can be described by the same basic curve) (Esper *et al.*, 2003), I developed mean growth curves for each individual site. The age-aligned mean growth curves for all 13 sites are presented in Figure 2.8. The series are noisier (more variable) both at the beginning and at the end due to smaller sample sizes. Two distinct growth trends are apparent: the horizontal or negative exponential trends that occur in the relatively open stands (CRS, MAT and MEL); and a growth trend that is typical for the closed-canopy trees – a slow initial growth, followed by increased ring widths at about 200-400 years of age, and a decline in growth as the trees age (the remaining ten sites).

I separated the series into two populations, OPEN and CLOSED, accordingly. The OPEN population contains 133 series (all samples from CRS, MAT and MEL), while the CLOSED population comprises the remaining 465 series. I generated one mean growth curve for each population (Figure 2.9). I truncated the CLOSED growth curve at 1000 years, because the increase in the last 100 years (biological age > 1000 years) was not age-related. It resulted from the low sample size - only three series were classified as older than 1000 years (and that may have been an overestimate of the true pith offset). The OPEN growth curve did not require truncation, but it exhibits higher variability overall, because it is based on fewer series. As the growth curves were still noisy, I superimposed simple theoretical growth curves (cubic-smoothing splines) over them. These smooth curves are the regional curves that were used to standardise individual ring-width series within each population (Figure 2.9).

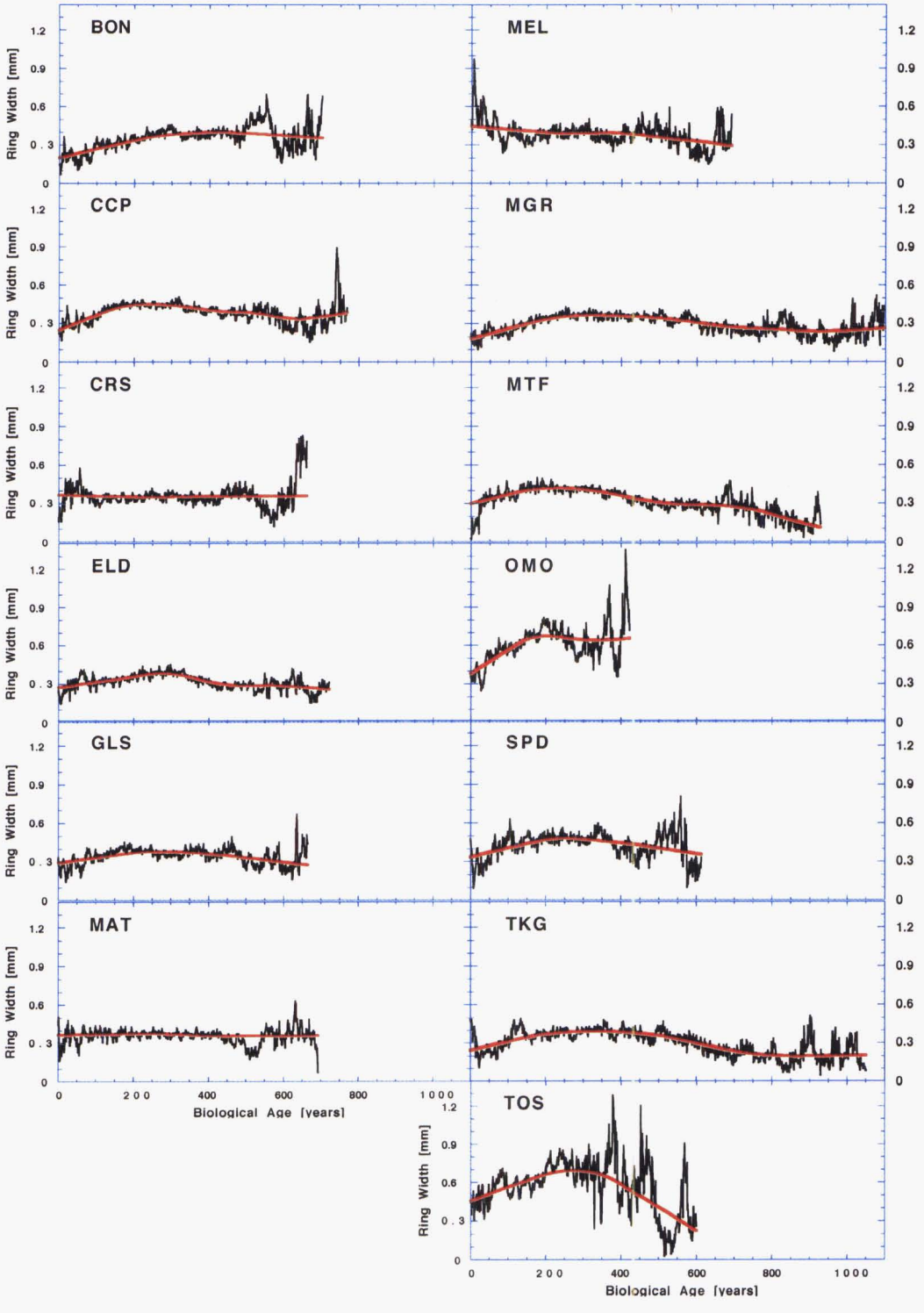

Figure 2.8 The age-aligned mean curves for the individual sites (sub-samples). Smooth curves (in red) are the corresponding splines. 1/3 splines were used for the CCP, ELD, MGR, MTF and TKG sites; 2/3 splines for the remaining eight sites.

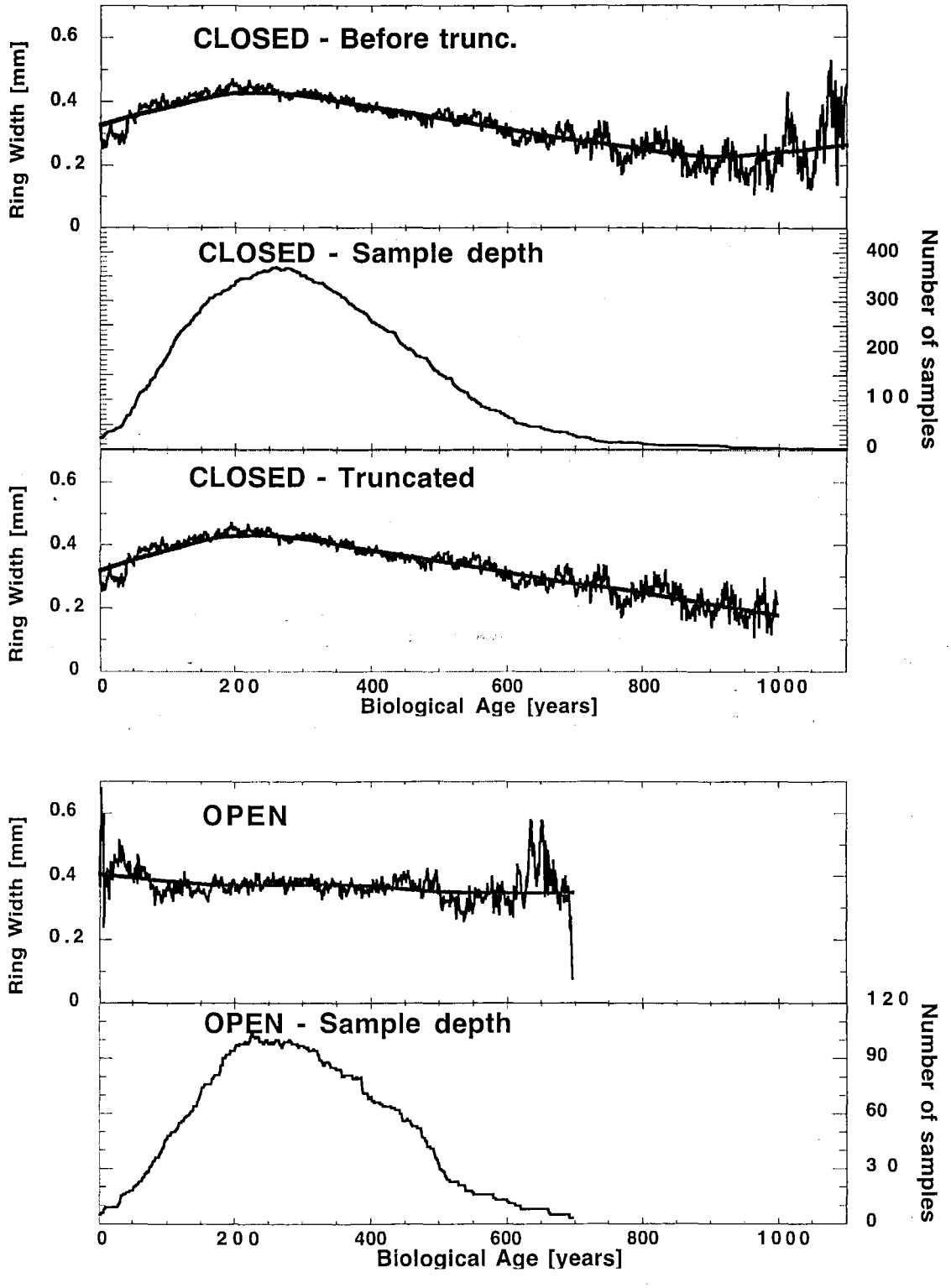

Figure 2.9 The age-aligned mean curves for the two populations (CLOSED and OPEN). The length of the CLOSED curve is truncated at 1000 years. The corresponding regional curve splines (heavy line): 1/3 spline was used for CLOSED; 1/2 spline for OPEN.

In both methods of standardisation (single detrending and RCS), I converted the non-stationary ring-width measurements into the stationary indices by the traditional RATIO procedure (Fritts, 1976). The tree-ring index I_t is calculated by dividing each measured ring-width value R_t by its expected value G_t (Equation 2.1).

$$I_t = R_t / G_t \qquad (2.1)$$

The expected value G_t represents the non-climatic, mostly age-related growth trend; it is the theoretical curve value determined by the detrending method. The new series of relative tree-ring indices have a defined mean of 1.0 and a relatively constant variance (Cook *et al.*, 1990a). I used the ARSTAN programme (Cook, 1985; updated version: E. Cook, pers. comm.) for all standardisation procedures.

2.3.4 Computation of the final chronologies

Once the ring-width measurements have been converted into the dimensionless tree-ring indices, the estimation of the common signal can proceed. To compute the mean-value function, I used the biweight robust mean (Cook *et al.*, 1990b). This method is suitable when outliers (i.e. extreme values caused by endogenous disturbances) are present in the detrended series. I selected this method of computation since outliers frequently occur in closed-canopy forest tree-ring data (Cook *et al.*, 1990b), and most of the trees I had sampled grew in such dense forests.

Another important step is the removal (total or partial) of autocorrelation from the series. I used autoregressive (AR) modelling (Cook, 1985), based on the autoregressive moving average (ARMA) time series modelling (Box and Jenkins, 1970). The order of the AR process was determined by the Akaike Information Criterion (AIC) (Akaike, 1974). Autocorrelation refers to the serial dependence of the observations in a time series (Figure 1.2), and it is measured by the autocorrelation function (ACF) and by the partial autocorrelation function (PACF). The autocorelation pattern is often described by a set of the autocorrelation coefficients (ACs; also called the serial correlation coefficients) that measure the correlation between observations at different times apart (lags). The ACF, or correlogram, is then a graph showing the ACs plotted against the corresponding lags. The partial autocorrelation refers to the autocorrelation at different lags while allowing for the effects of autocorrelation at

intermediate lags. Both the ACF and the PACF are used to select AR models that best describe the time series (Brown and Rothery, 1993).

For the single-detrended data, three types of chronologies were produced: standard (STD), residual (RES) and arstan (ARS). The STD chronology is computed from the detrended series, without autoregressive modelling. The RES chronology is produced by averaging residuals from AR modelling of the detrended series (white noise). The RES chronology is whitened by modelling the portion that contains four or more series, and applying the model to the entire chronology. The ARS version is created by reincorporating the pooled AR model into the RES chronology. The pooled autoregression contains the persistence that is common to a large proportion of the series (assumed to be related to climate and species physiology), and it excludes the persistence found in one or very few series (assumed to be caused by endogenous or exogenous disturbance events). The ARS series is thus intended to contain the strongest climatic signal possible (Cook, 1985).

For the RCS data, I aligned the ring-width measurements by cambial age, and detrended them by fitting a mean growth curve to the data. After obtaining the RCS indices, I converted the biological age back into calendar years, and calculated the mean RCS chronology. I used the ARSTAN programme (Cook, 1985; updated version: E. Cook, pers. comm.) to compute all chronologies. In this chapter, I present chronologies computed both from the single-detrended and RCS data, to demonstrate the effects of different standardisation methods.

The statistics I used to describe the chronologies include: standard deviation (SD), mean sensitivity (MS), mean Rbar, mean expressed population signal (EPS), serial correlation (R1), AR model (selected AR order), and variance due to pooled autoregression. The relevance of SD, MS and R1 to dendrochronology was described by Fritts (1976). Standard deviation is a measure of scatter of the tree-ring indices from their mean (which is equal to 1.0). When data are normally distributed, about two thirds of the data lie within one SD, and 95% within two SDs on each side of the mean. Mean sensitivity is a measure of the relative change in tree-ring indices from one year to the next, and it reflects the high-frequency variance in the chronologies. The MS values range from zero to two. Serial correlation is the autocorrelation at lag of one year, and it is a measure of the low-frequency variance contained in the data.

RBar is the average correlation between all possible series (Briffa and Jones, 1990), and it was calculated for 50-year windows lagged by 25 years. RBar is an indication of common

variance, and it is independent of sample size. The EPS, which partly depends on sample size, measures how well the finite chronology compares with a theoretical infinite population (Wigley *et al.*, 1984). The EPS values range from zero to one, and there is no test for a threshold level of the statistics. Wigley *et al.* (1984) suggested the value of 0.85 for a threshold, however the choice depends on the user's subjective evaluation of accuracy needs.

2.3.5 Chronology comparison

I used correlation and principal component analysis (PCA) to compare chronologies from the different sites (13 in total). I compared the high-frequency and low-frequency signals in both the RCS chronologies and in the ARS chronologies (computed from the single-detrended data; henceforth referred to as the "ARS chronologies"). To extract the high-frequency component from the data, I used a high-pass filter, which transmitted frequencies higher than 25 years and blocked most of the variance with wavelengths longer than 25 years. The low-pass filter blocked wavelengths of less than 25 years and passed low frequencies (wavelengths greater than 25 years). I compared all 13 chronologies over their entire common period (1590-1998). I used the SVDPCA5 programme (E. Cook, pers. comm.) for all procedures.

In the correlation analysis, I calculated Pearson's product moment correlation coefficients. I used cross-correlation matrices to simply compare chronologies with one another. A PCA (Cooley and Lohnes, 1971) is a more complex technique, which explains the variance-covariance structure of the data through a few linear combinations of the original variables. The general objectives of a PCA are (a) to reduce and (b) to interpret the data. A PCA transforms a number of correlated variables into a smaller number of uncorrelated (orthogonal) variables called principal components (PCs). Each successive PC explains the maximum remaining variance in the data (Peters *et al.*, 1981). Varimax rotation simplifies the structure of the PCs – a rotated PCA (Richman, 1986) makes it easier to distinguish group patterns in the data. I therefore used the rotated PCA to compare the chronologies. Several criteria may be applied to reduce the number of PCs (Guiot, 1990). I rotated only the PCs that were identified as significant ($P<0.05$) by the Monte Carlo analysis (Preisendorfer *et al.*, 1981). The Monte-Carlo red-noise criterion (Preisendorfer *et al.*, 1981) is very strict, as it retains only the largest and most important PCs. This method is well suited for cases where only interpretation is important (Guiot, 1990).

2.4 Results

2.4.1 Raw data

On average, I crossdated 90% of all collected samples (Table 2.2). Crossdating was least successful with the samples from Croesus Track (CRS), where only 70% of cores could be included in the chronology. However, the relatively high rejection rate (30%) was not caused by the lack of a common tree-ring pattern, but rather by the poor physical quality of the samples – several cores were too short to be included in the chronology, or the tree rings were too narrow to be measured. From several sites (CCP, MEL and TKG), I could crossdate all cores (Table 2.2).

The crossdating success resulted in high replication – on average, every chronology contained 46 radii from 27 trees, with the minimum of 25 radii and 12 trees from Slopedown Hill (SPD; Table 2.2). The chronologies spanned over 543 years on average, with values ranging from 409 years (TOS) to 662 years (ELD). The mean segment length was 291 years (Table 2.2). The average ring width was 0.44 mm; with the fastest growing trees unsurprisingly from the low-altitude sites, OMO and TOS, where the mean growth rates were over 0.6 mm/year (Table 2.2). Another factor that contributed to the crossdating success was the low occurrence of missing rings – only 0.065% of all crossdated rings were absent in the radii (Table 2.2).

Table 2.2 Raw data statistics. No. Trees = the total number of crossdated trees (i.e. the total number of trees included in each chronology); Series (% Sampl.) = the total number of crossdated series (followed in parentheses by the percentage of all samples collected that could be included in each chronology); MLS = the mean length of series [yrs.]; Mean Ms. – the mean ring-width measurement [mm]; Max Ms. = the maximum measurement [mm]; Miss. Rings = the percentage of absent rings; Series Interc. = the series intercorrelation.

Site	No. Trees	Series (% Sampl.)	Time Span	MLS	Mean Ms.	Max. Ms.	Miss. Rings	Series Interc.
BON	25	51 (98%)	1463-1999	351.2	0.41	2.09	0.056%	0.668
CCP	53	72 (100%)	1410-1998	327.4	0.44	1.74	0.055%	0.634
CRS	35	52 (70%)	1483-1999	272.0	0.38	2.03	0.049%	0.603
ELD	26	52 (78%)	1338-1999	311.5	0.36	1.61	0.025%	0.569
GLS	26	48 (98%)	1461-1999	275.8	0.40	1.75	0.076%	0.636
MAT	28	51 (85%)	1508-1999	261.0	0.39	1.71	0.015%	0.565
MEL	16	30 (100%)	1440-1999	269.3	0.41	1.67	0.037%	0.692
MGR	26	48 (94%)	1400-1999	355.8	0.35	1.52	0.059%	0.606
MTF	31	56 (98%)	1367-1999	347.1	0.39	1.45	0.093%	0.660
OMO	20	34 (85%)	1578-1999	227.9	0.65	2.53	0.065%	0.517
SPD	12	25 (83%)	1447-1999	283.2	0.49	2.57	0.099%	0.644
TKG	27	47 (100%)	1450-1999	304.6	0.38	1.50	0.091%	0.656
TOS	20	32 (76%)	1590-1998	197.1	0.66	2.13	0.127%	0.507

The series intercorrelation (i.e. the mean correlation with master chronology, as produced by the COFECHA programme; a measure of crossdating quality) was 0.612 on average, with the lowest values occurring in the two low-altitude sites (Table 2.2). Steepness of sites also affects the series intercorrelation. Trees on steep slopes tend to produce ring-width patterns common to more individuals within a site, as indicated by the higher series-intercorrelation values (Spearman's coefficient of rank correlation: RS = 0.8, P<0.01; Figure 2.10).

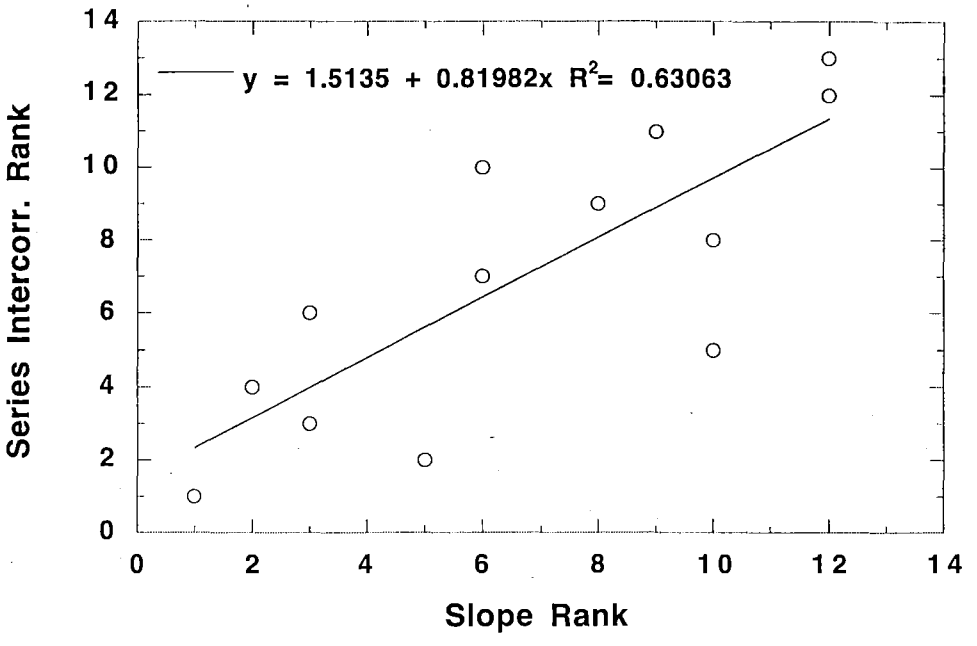

Figure 2.10 Dependence of series-intercorrelation values on site slope. Sites were ranked according to their slope (mean values from Table 2.1) and series-intercorrelation values (Table 2.2). Highest ranks (1, 2, ...) indicate the steepest sites and the highest series-intercorelation values.

2.4.2 Chronologies

Pink pine chronologies from all thirteen sites are presented in Figures 2.11 - 2.23. Each figure is composed of six plots: the raw chronology (i.e. the biweight robust mean of crossdated ring-width measurements); the sample depth (which shows how the number of series changes over time); the standard, residual and arstan chronologies (based on the single-detrended data); and the RCS-method chronology. One of the most striking features of the chronology plots is the close resemblance between the raw and the RCS chronologies (e.g. Figure 2.13). Also, the overall trend at the majority of sites is positive, and is especially evident in the raw and RCS chronologies. The positive trend is most pronounced at the OMO site (Figure 2.20). Many sites show increased growth in the second half of the 20th century, which is typically

present in the raw and RCS chronologies only (it has been removed or de-emphasised by the single detrending method). The sites that show such marked increase are, for example, CRS (Figure 2.13) and GLS (Figure 2.15). Nevertheles, several sites show only average growth during the 20th century, e.g. ELD (Figure 2.14) and MTF (Figure 2.19).

Different standardisation methods can have a profound effect on the final data, as is evident both from the chronology plots (Figures 2.11-2.23) and statistics (Table 2.3). Compared with the ARS chronologies (SD=0.175; mean for all 13 chronologies), the standard deviation was much higher for the RCS chronologies (SD=0.290). This is not surprising, since the RCS method is noisier than the traditional approaches (single detrending in this case). The mean-sensitivity values differed little between the two standardisation methods (MS=0.127 for ARS; MS=0.133 for RCS). RBar was much higher for the single-detrended data (RBar=0.381) – the mean RBar for the RCS data was only 0.226. The EPS values remained nearly equal (EPS=0.915 for ARS; EPS=0.881 for RCS). There was a remarkable increase in the serial correlation values (R1=0.584 for ARS; R1=0.829 for RCS), indicating that the RCS method retained much more low-frequency variance in the data. The simpler first order of autoregression was selected more often for the ARS chronologies, whereas higher orders – most often AR(4) – were used to model the RCS chronologies. The variance due to pooled autoregression increased accordingly – from 36.1% (the average for ARS), it has nearly doubled to 71.8% (RCS).

I investigated the autocorrelation properties of the ARS and RCS chronologies by calculating the autocorrelation coefficients (ACs) and partial autocorrelation coefficients (PACs) for the first ten lags (one lag being equal to one year). The autocorrelation structure is very similar across all of the sites. In the ARS chronologies (Figure 2.24), there is a rather sharp drop in autocorrelation from lag 1 to lag 2, which is most pronounced in the CCP, MEL, MTF, SPD and TKG chronologies. The PACFs for the ARS chronologies (Figure 2.25) show the predominance of AR(1) processes in the series, which is in agreement with the models selected by the ARSTAN programme (Table 2.3). In the RCS chronologies (Figure 2.26), not only are the lag-1 ACs substantially higher than those from the ARS chronologies (Table 2.3), but the coefficients remain high for all ten lags. It implies that more low-frequency signals were retained in the RCS chronologies. The PACFs for the RCS chronologies (Figure 2.27) indicate that AR(1) processes account for most of the autocorrelation in the series; however, the selection of higher-order AR models by ARSTAN (Table 2.3) is also acceptable.

Table 2.3 Chronology statistics. Top values describe the ARS chronologies; the values in bottom rows describe the RCS chronologies. St. Dev. = the standard deviation; Mean Sens. = the mean sensitivity; Mean EPS = the mean value of the expressed population signal; Serial Corr. = the serial correlation; AR Model = the selected autoregression order; RSQ = the variance due to pooled autoregression.

Site	St. Dev.	Mean Sens.	Mean RBar	Mean EPS	Serial Corr.	AR Model	RSQ
BON	0.229	0.129	0.442	0.965	0.747	1	56.2%
	0.396	0.138	0.366	0.957	0.894	3	83.7%
CCP	0.156	0.119	0.393	0.940	0.564	3	34.6%
	0.241	0.123	0.249	0.917	0.802	1	65.0%
CRS	0.174	0.130	0.365	0.935	0.566	1	32.4%
	0.265	0.137	0.201	0.894	0.795	5	67.7%
ELD	0.168	0.121	0.323	0.926	0.590	2	35.6%
	0.221	0.125	0.139	0.882	0.861	7	76.6%
GLS	0.176	0.117	0.418	0.861	0.669	1	45.4%
	0.324	0.128	0.264	0.852	0.918	4	87.5%
MAT	0.172	0.111	0.301	0.895	0.665	1	44.9%
	0.250	0.118	0.232	0.889	0.856	3	75.2%
MEL	0.213	0.169	0.463	0.918	0.480	3	26.5%
	0.314	0.170	0.253	0.857	0.751	4	59.9%
MGR	0.166	0.112	0.375	0.921	0.656	1	43.1%
	0.256	0.122	0.291	0.894	0.869	4	78.1%
MTF	0.176	0.138	0.423	0.942	0.527	3	30.2%
	0.227	0.141	0.233	0.926	0.784	8	64.5%
OMO	0.144	0.109	0.310	0.881	0.545	1	29.8%
	0.396	0.117	0.150	0.873	0.872	4	78.3%
SPD	0.165	0.128	0.431	0.915	0.533	4	30.4%
	0.272	0.136	0.225	0.855	0.761	4	59.9%
TKG	0.171	0.145	0.449	0.916	0.460	3	24.3%
	0.248	0.148	0.241	0.856	0.781	4	65.0%
TOS	0.165	0.120	0.254	0.876	0.596	1	35.5%
	0.362	0.122	0.090	0.807	0.833	4	71.5%

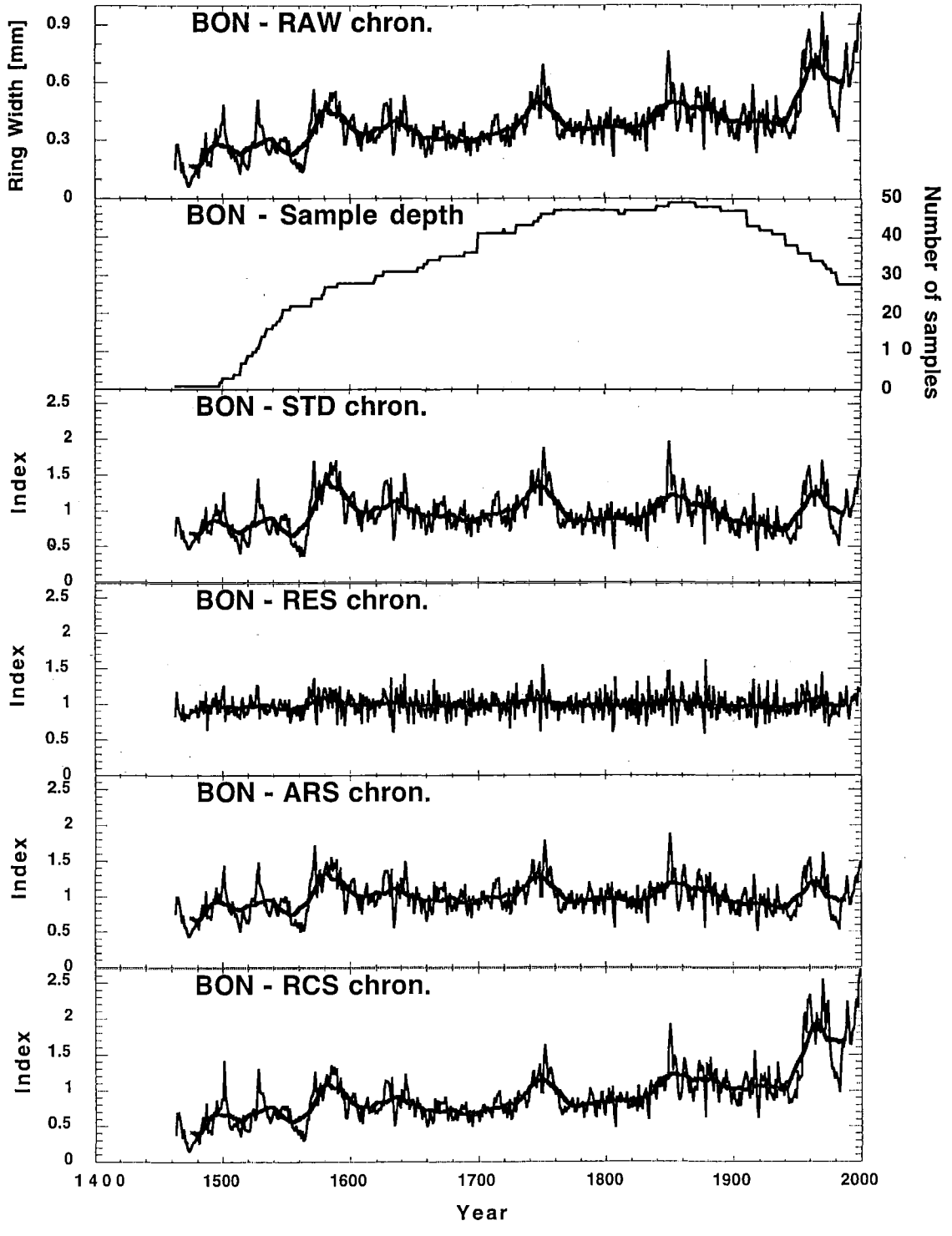

Figure 2.11 The Mt. Bonar chronology plots (1463-1999). Smoothed with a 25-year running mean (heavy line). The well-replicated BON chronologies show periods of increased growth in the 1580s, and around 1750 and 1850. The sharpest increase in growth occurs after 1954, and it is followed by a period of very slow growth in 1975-1983. Both abrupt growth changes (in the 1950s and 1970s) are most likely disturbance-related (Section 2.2).

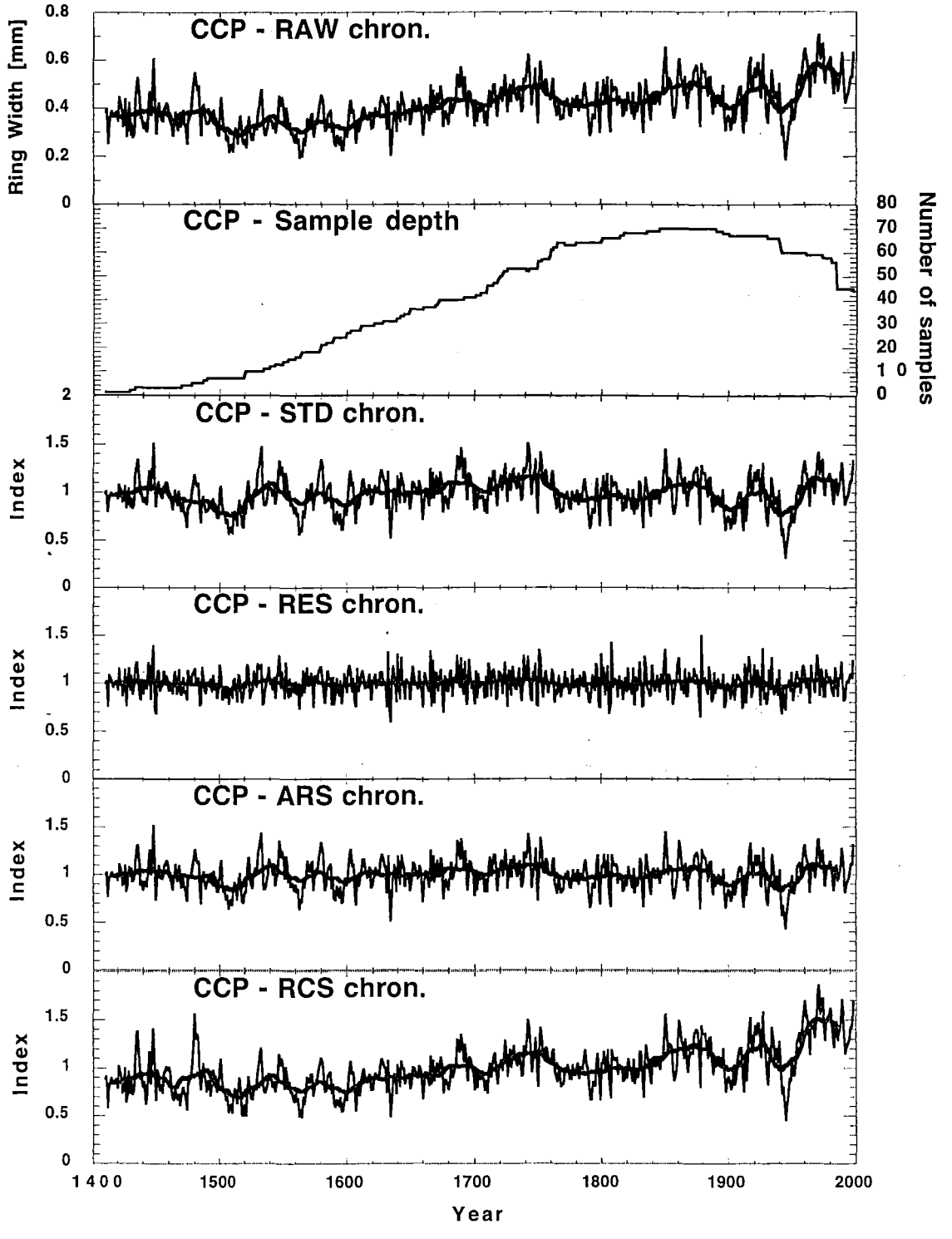

Figure 2.12 The Camp Creek chronology plots (1410-1998). Smoothed with a 25-year running mean (heavy line). The CCP chronologies have the highest replication of all thirteen sites. The high growth at around 1480 (most pronounced in the RCS chronology) may not reflect stand-wide trends since only five series are included at this point. A steady increase in growth over the entire 17th century peaks around 1750, and another period of high growth occurs in the mid-19th century. Growth is very slow in the 1940s.

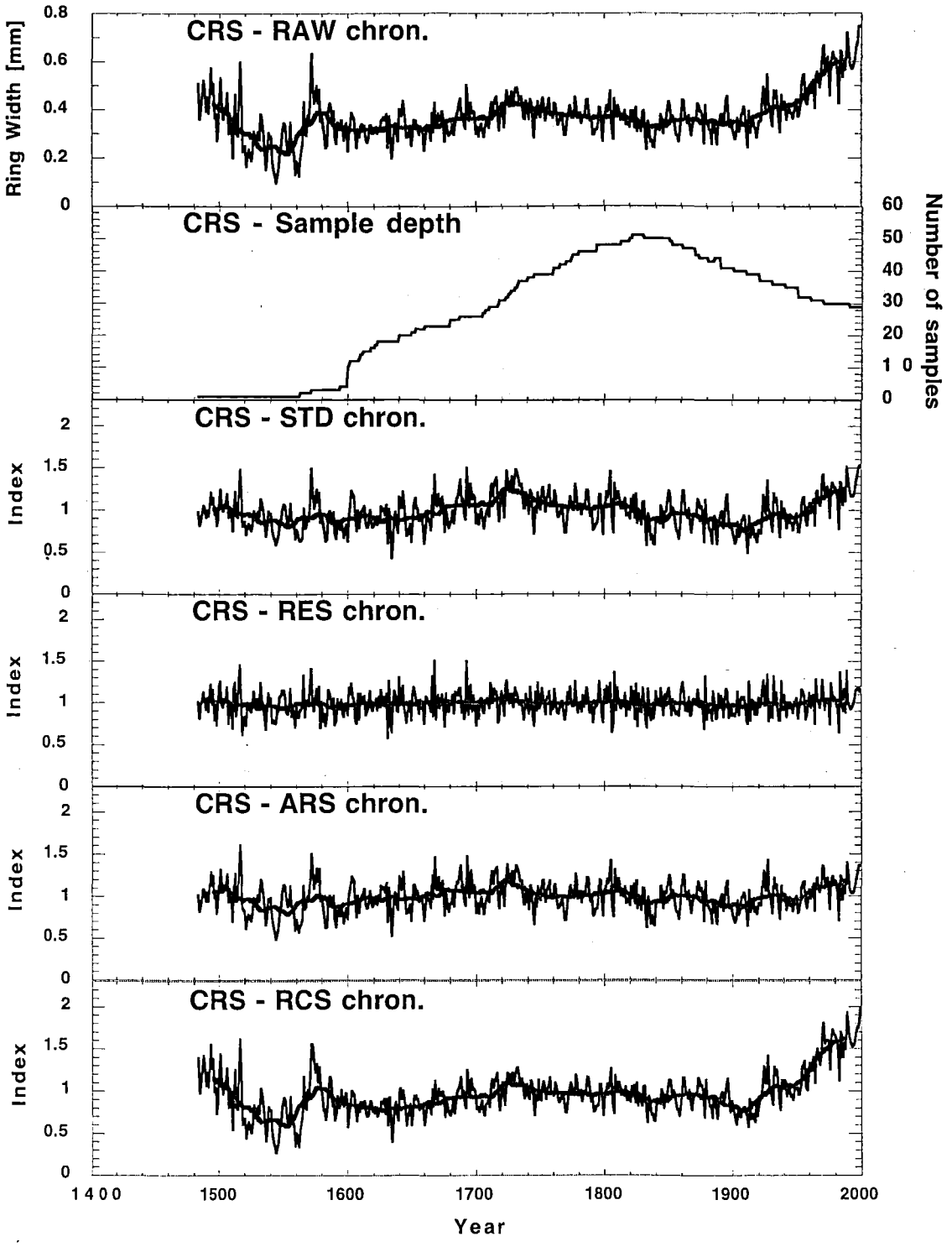

Figure 2.13 The Croesus Track chronology plots (1483-1999). Smoothed with a 25-year running mean (heavy line). The initial large variability in the CRS chronologies is entirely due to a low sample size. Except for a peak around 1730, the variability is low from 1600 to 1900. A sharp increase in ring widths / RCS indices occurs over the 20th century.

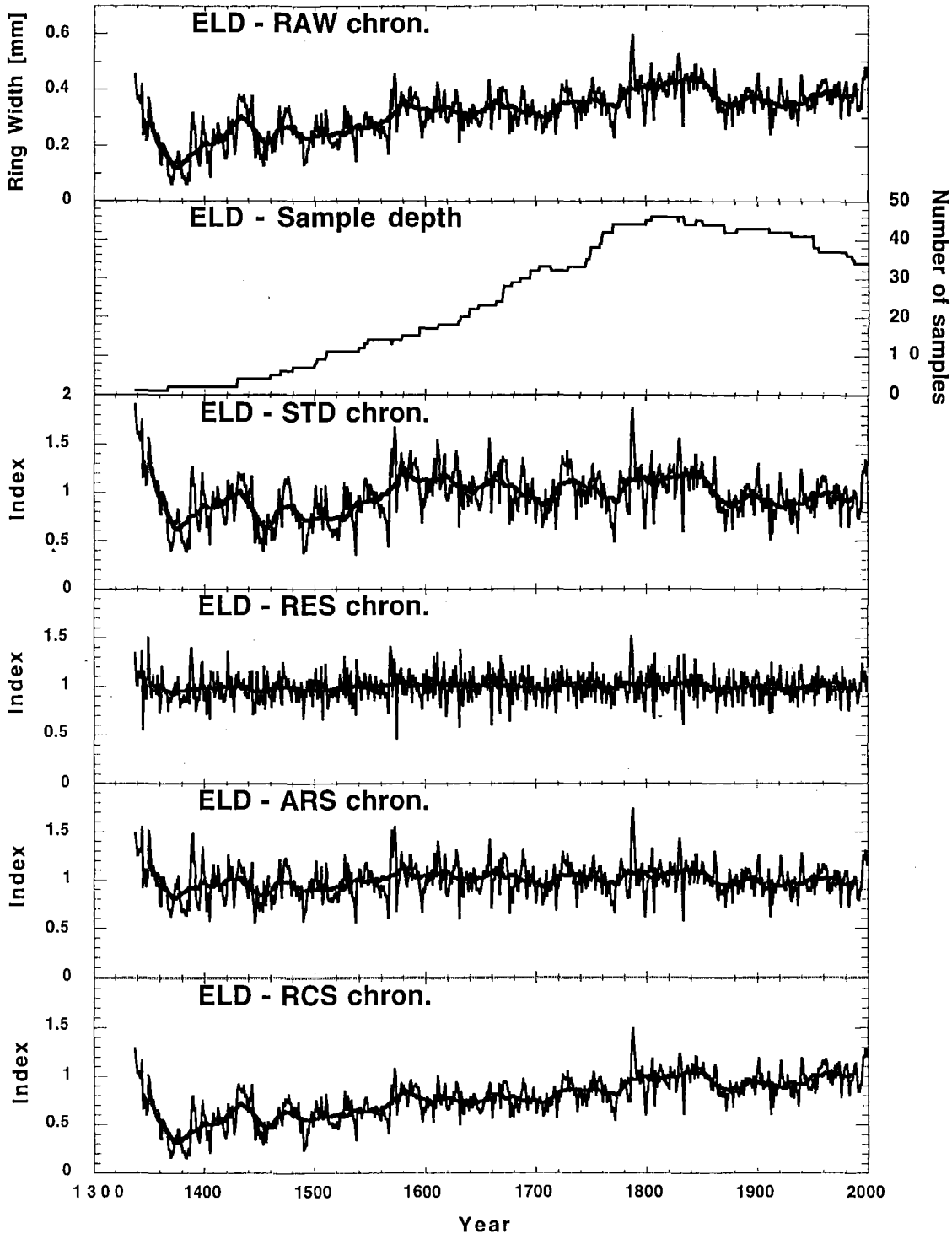

Figure 2.14 The Eldrig Peak chronology plots (1338-1999). Smoothed with a 25-year running mean (heavy line). In the ELD chronologies, the widest rings occurred in the late 1780s. Growth was also quite high in the first half of the 19th century, but average during the 20th century. However, the overall trend is positive.

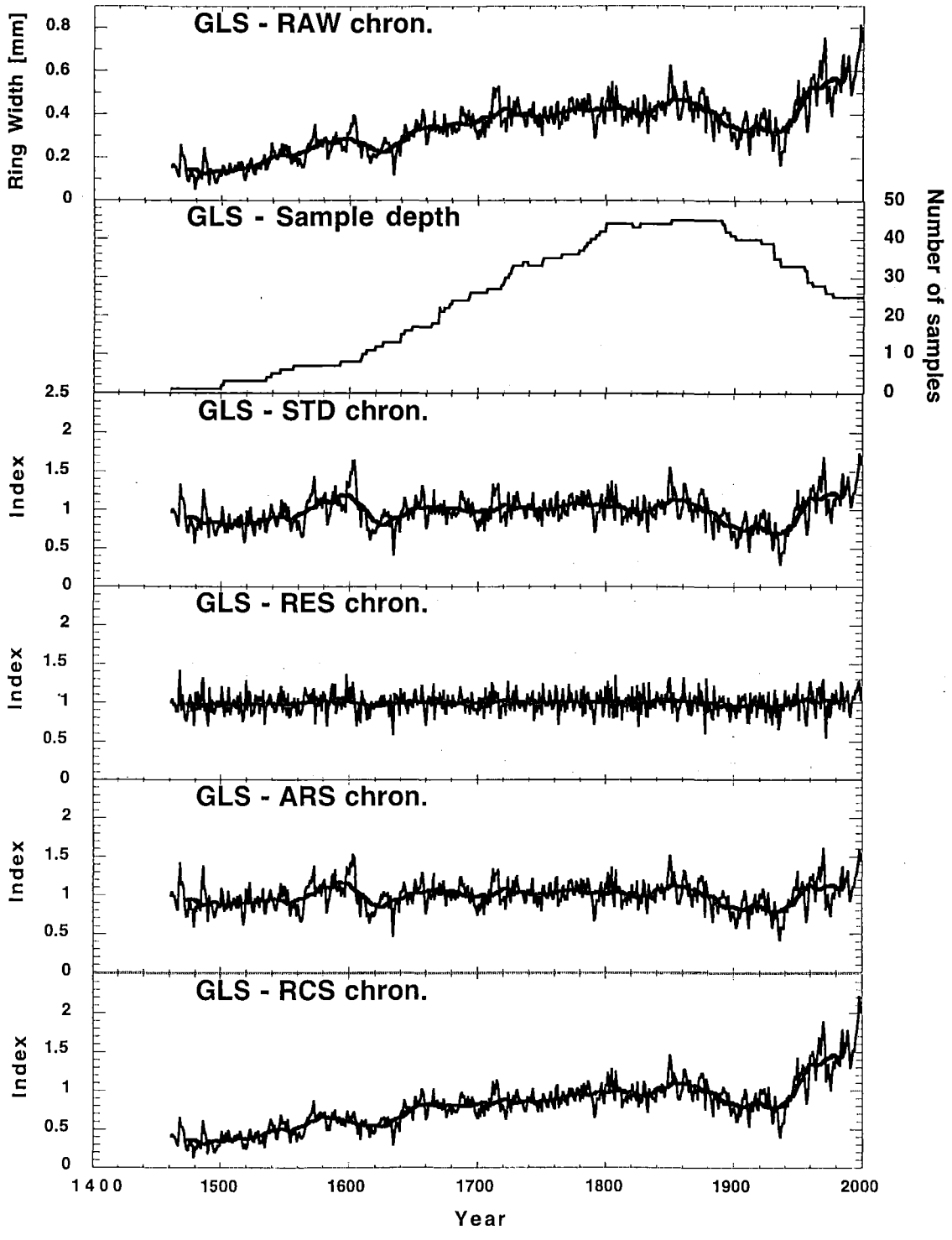

Figure 2.15 The Mt. Glasgow chronology plots (1461-1999). Smoothed with a 25-year running mean (heavy line). In the GLS chronologies, the positive growth trend peaks in the mid-19th century. The narrow rings of the 1930s are succeeded by faster growth for the rest of the 20th century. High growth in the 1570s and in the early 1600s is emphasised in the STD and ARS chronologies.

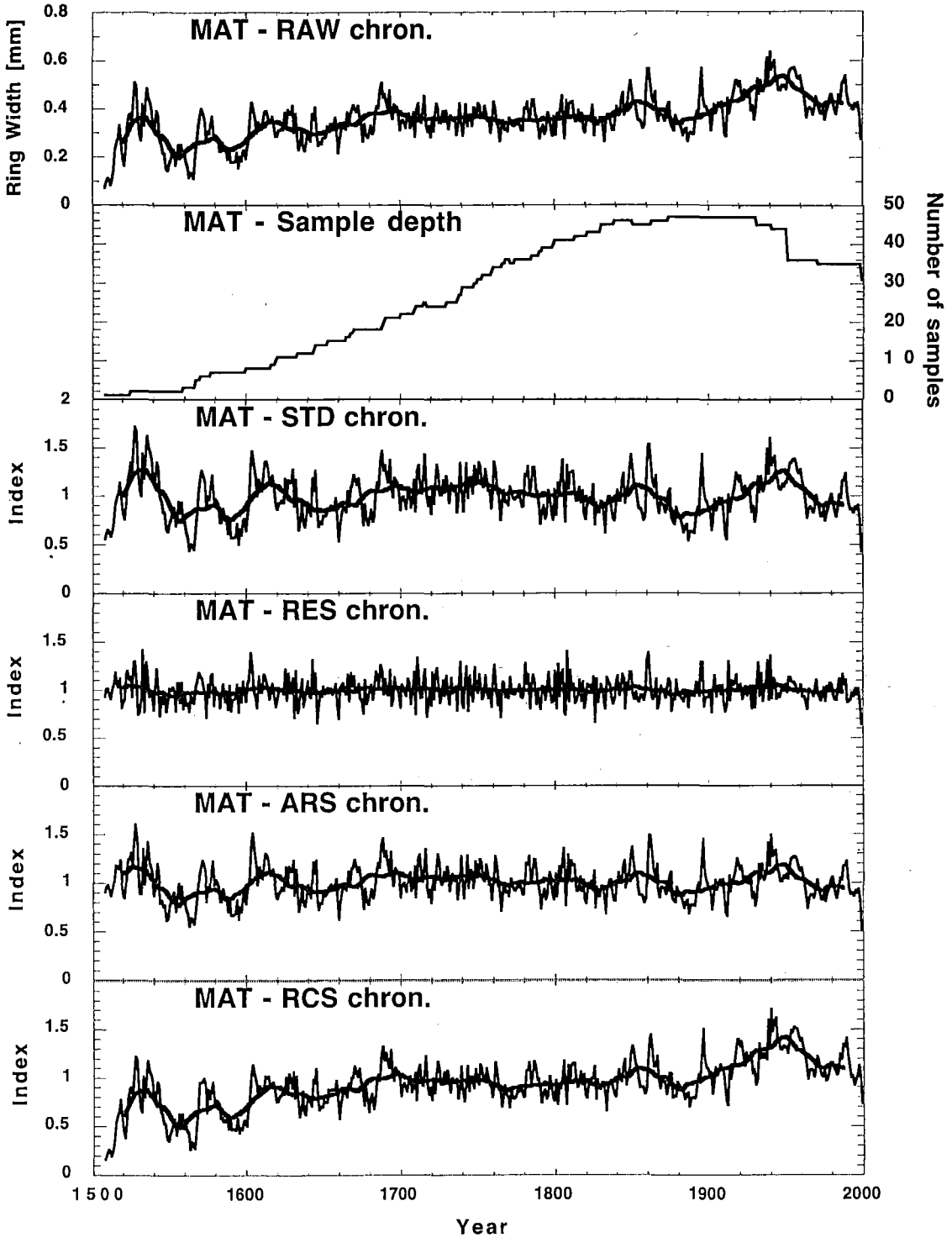

Figure 2.16 The Matiri Range chronology plots (1508-1999). Smoothed with a 25-year running mean (heavy line). The MAT chronologies show little variability in the 18th century, and periods of low growth in the 1590s and 1890s. The widest rings were formed around 1940.

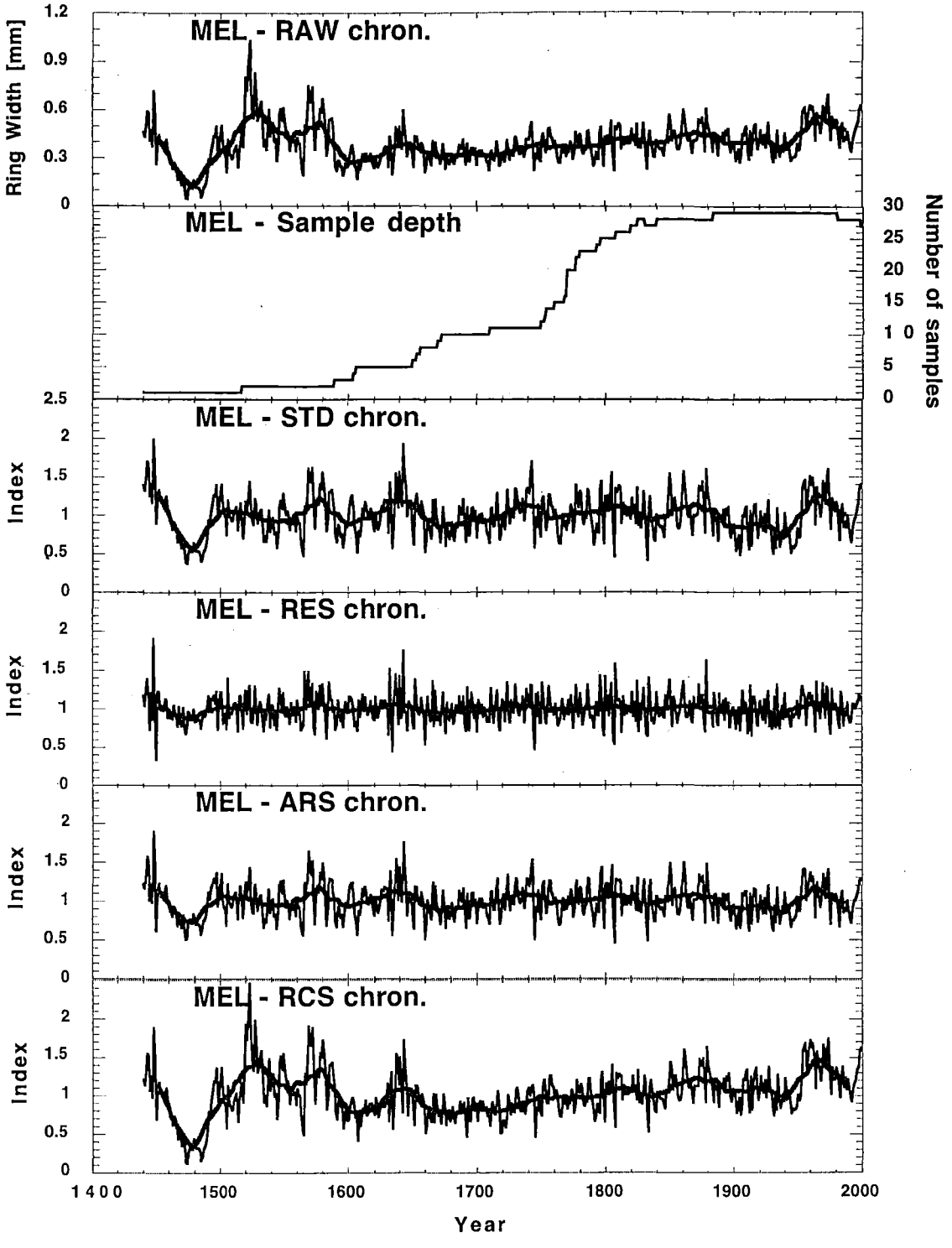

Figure 2.17 The Mt. Elliot chronology plots (1440-1999). Smoothed with a 25-year running mean (heavy line). The initial high variability in the MEL chronologies was again caused by the low replication. Periods of high growth occurred in the mid-19th century, and in the 1950s to mid-1970s.

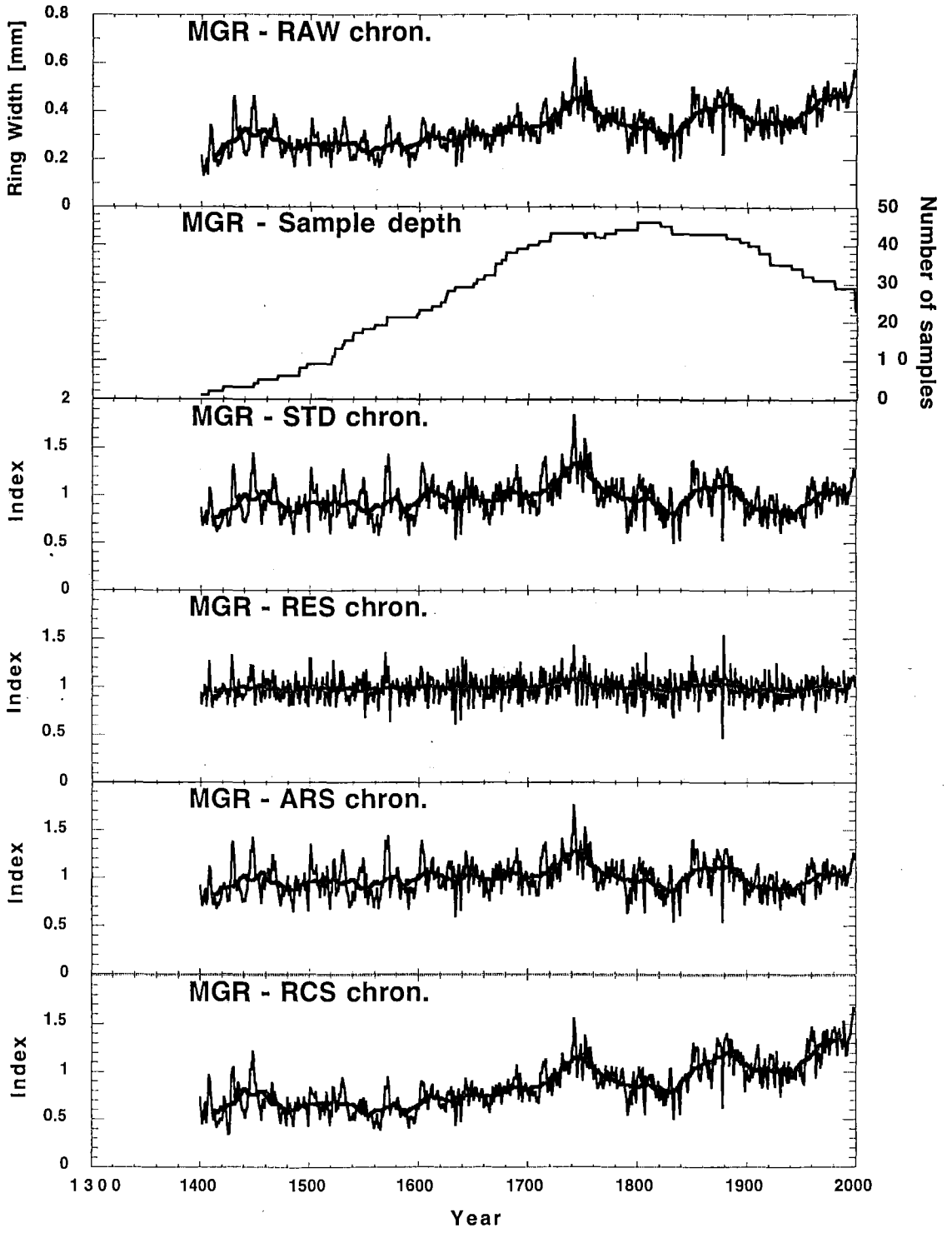

Figure 2.18 The Mt. Greenland chronology plots (1400-1999). Smoothed with a 25-year running mean (heavy line). In the MGR chronologies, the fast growth of the late 20th century was emphasised by the RCS method. The peak around 1740 was followed by slow growth in the 1830s, and then increased growth until the early 1890s.

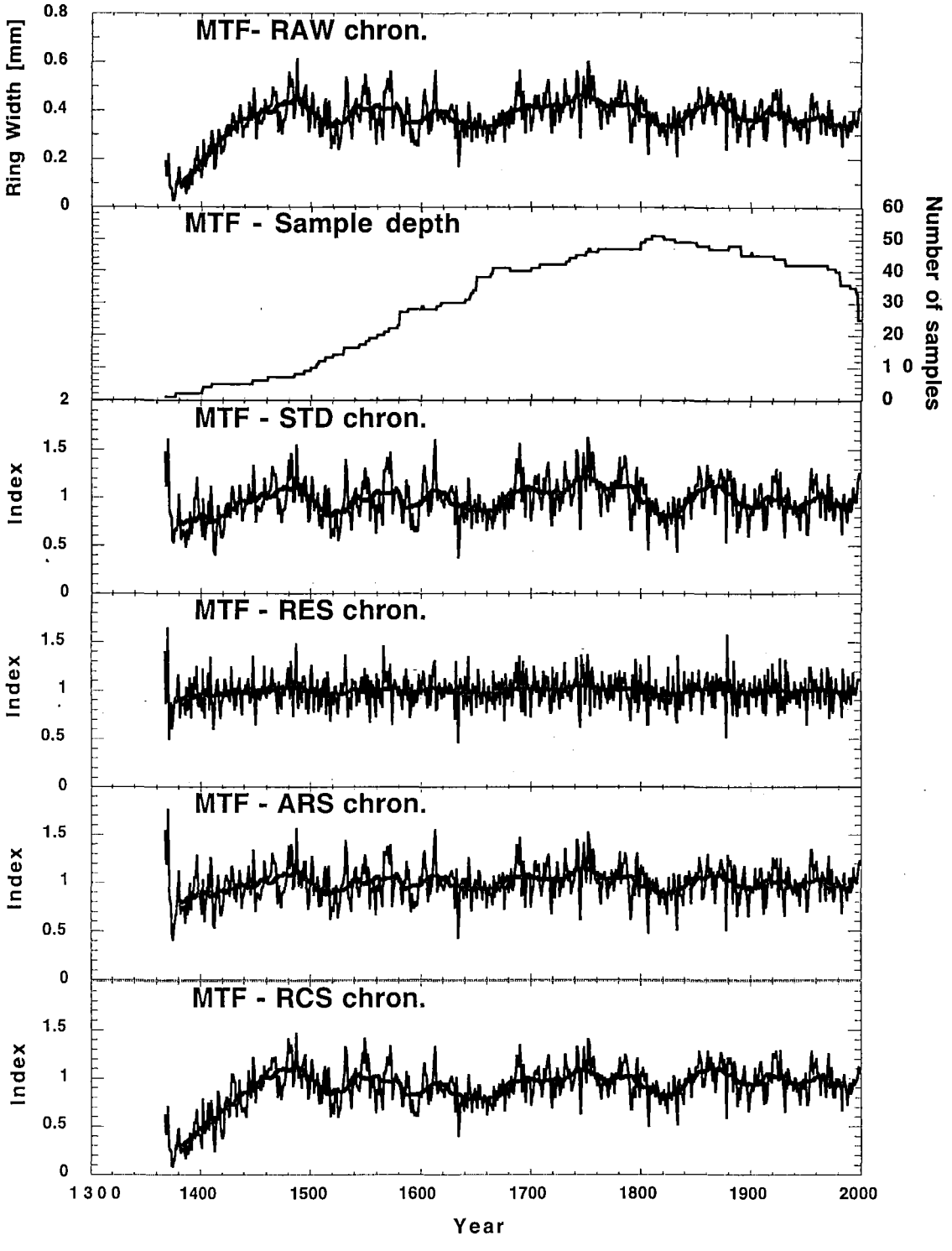

Figure 2.19 The Mt. French chronology plots (1367-1999). Smoothed with a 25-year running mean (heavy line). The MTF chronologies show periods of slow growth around 1520, in the mid-17th century and in the early 19th century. Wide rings were formed over the entire 18th century, and between the 1850s and 1870s.

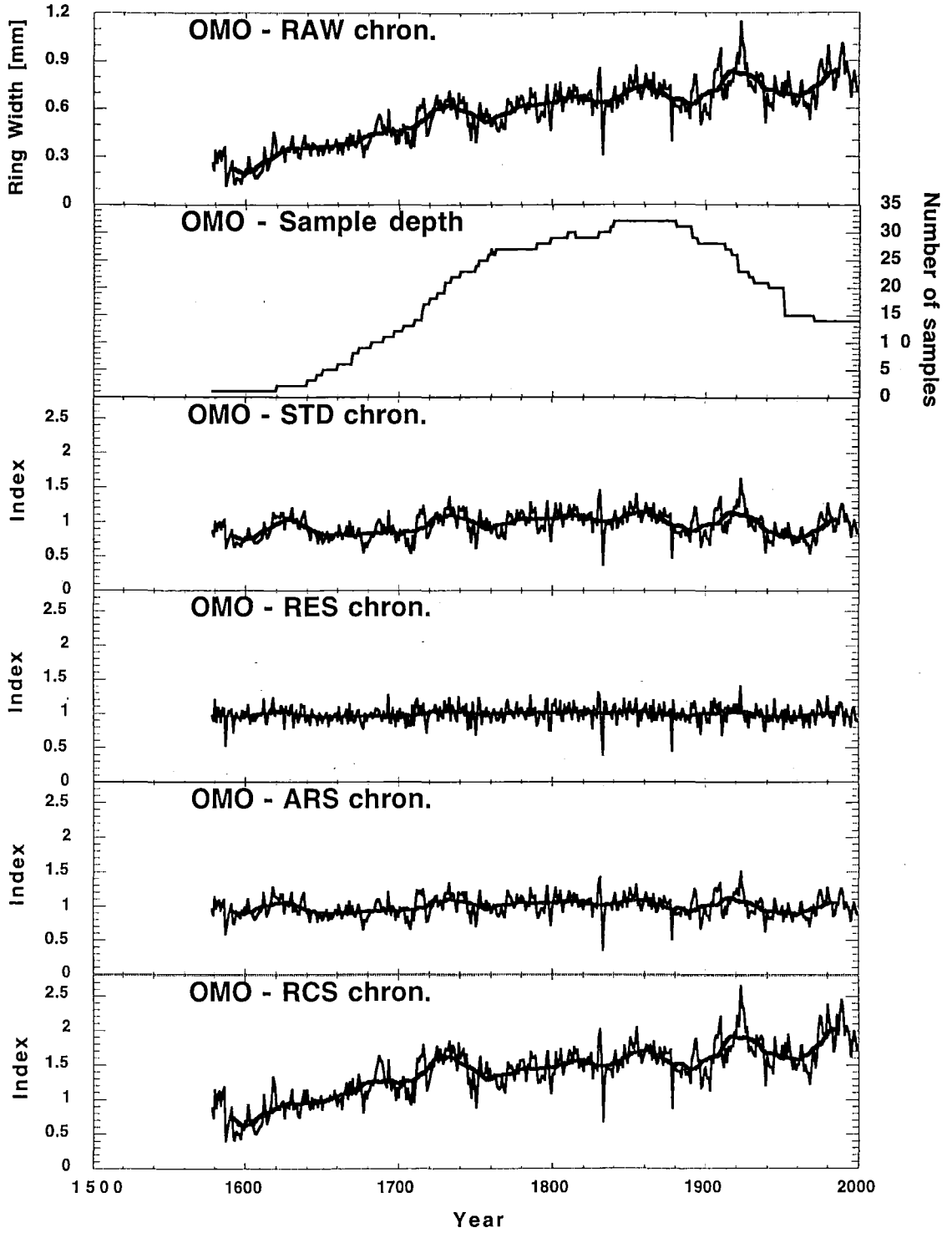

Figure 2.20 The Omoeroa Saddle chronology plots (1578-1999). Smoothed with a 25-year running mean (heavy line). At the OMO site, crossdating difficulties resulted in low sample depth of the chronologies in the 20th century. The overall trend at OMO is strongly positive, with the highest peak occurring around 1920.

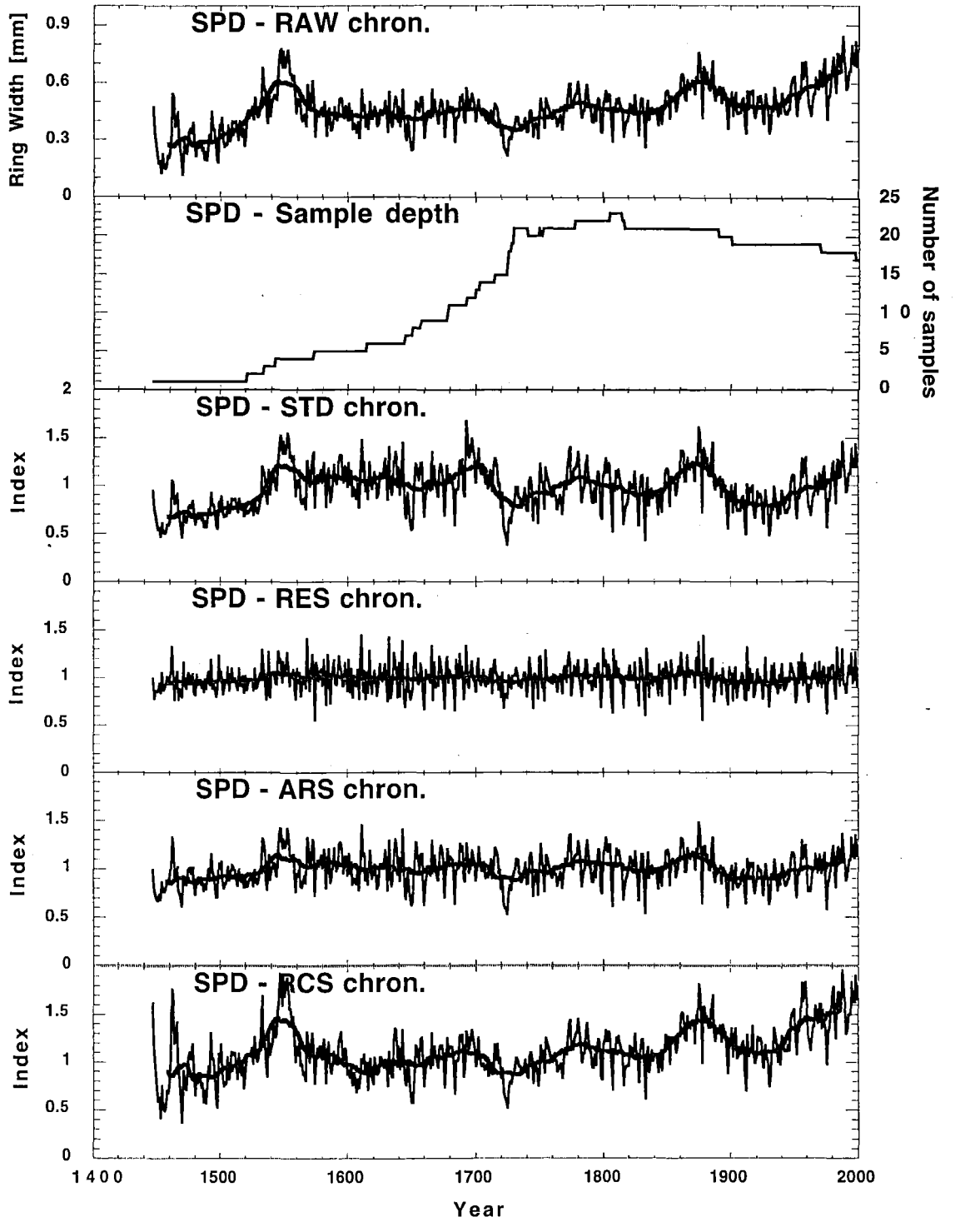

Figure 2.21 The Slopedown Hill chronology plots (1447-1999). Smoothed with a 25-year running mean (heavy line). The poorly-replicated SPD chronologies show a remarkable growth suppression in the 1720s. Peaks in growth occurred around 1550 (four series), and in the late 19th century.

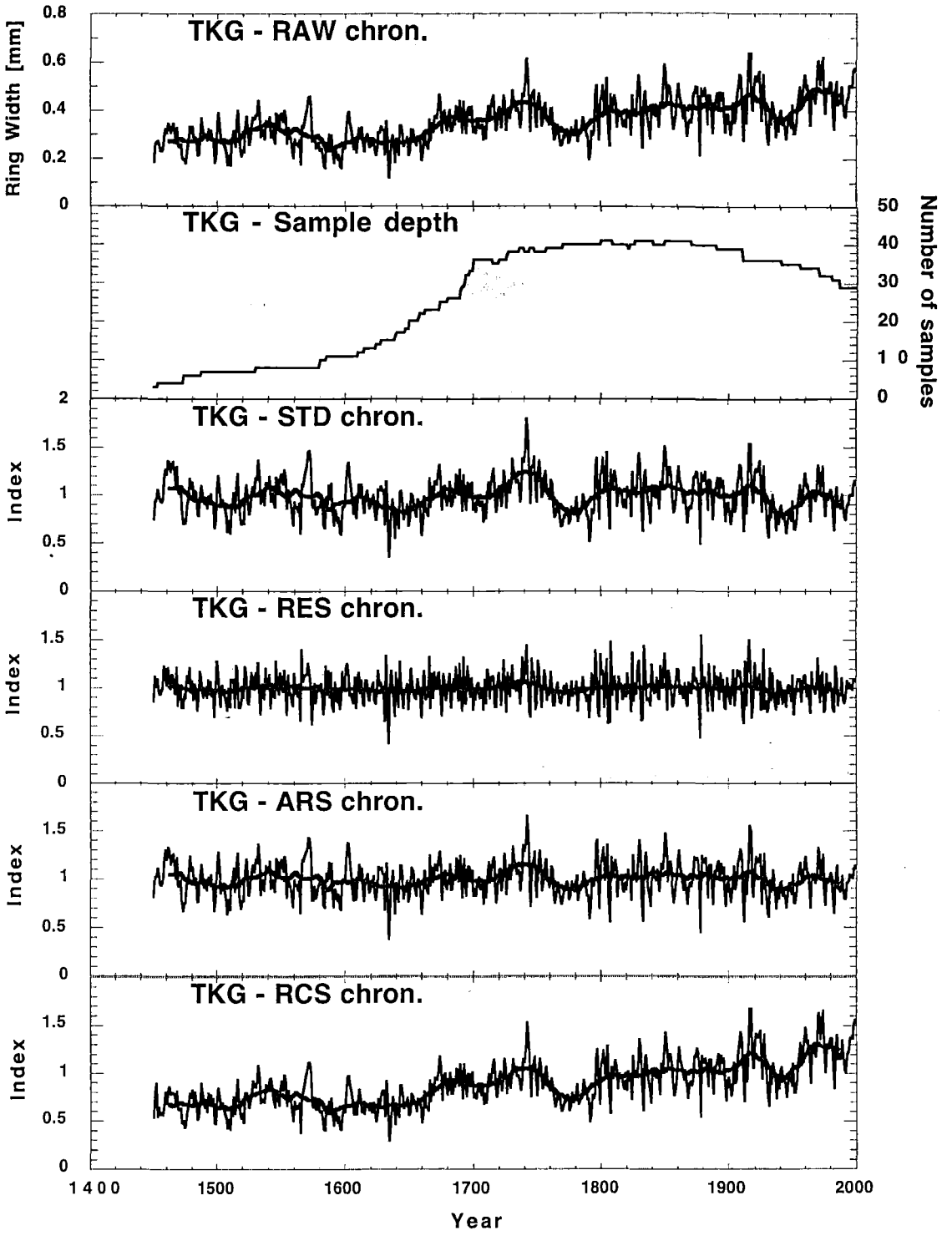

Figure 2.22 The Mt. Te Kinga chronology plots (1450-1999). Smoothed with a 25-year running mean (heavy line). In the TKG chronologies, the slow growth in the first half of the 17th century is followed by peaks around 1680 and 1740. Narrow rings were formed around 1770. The 19th century shows little long-term variability.

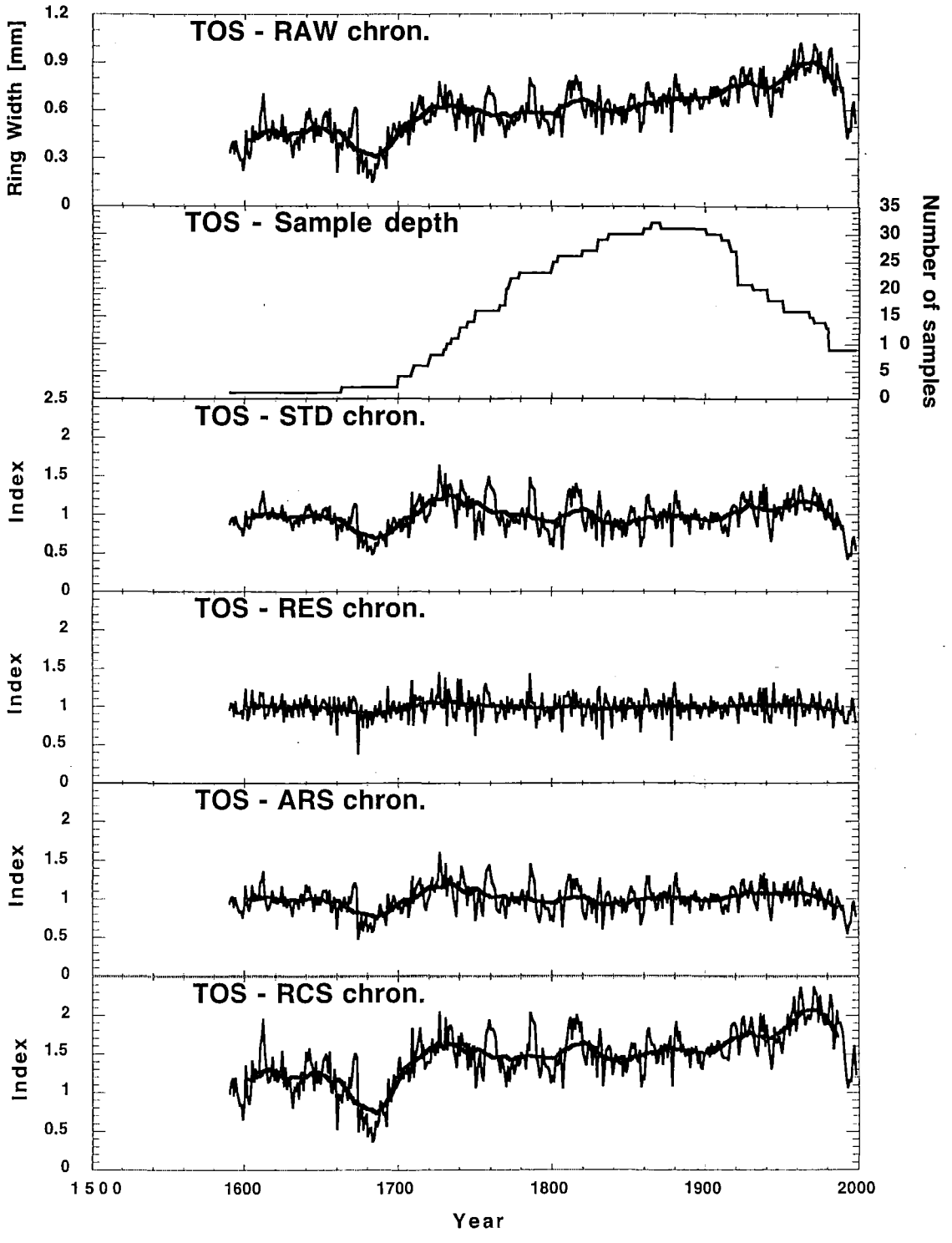

Figure 2.23 The Totara Saddle chronology plots (1590-1998). Smoothed with a 25-year running mean (heavy line). In the TOS chronologies, anthropogenic disturbances (Section 2.2) have probably caused inconsistent ring-width patterns over the 20th century. The poor crossdating led to a drop in sample size below 10 series after 1980. The growth suppression evident around 1680 is based on two series only, so care must be taken in interpreting this suppression. Periods of high growth occurred around 1730 and 1760, in the late 1780s and in the 1810s.

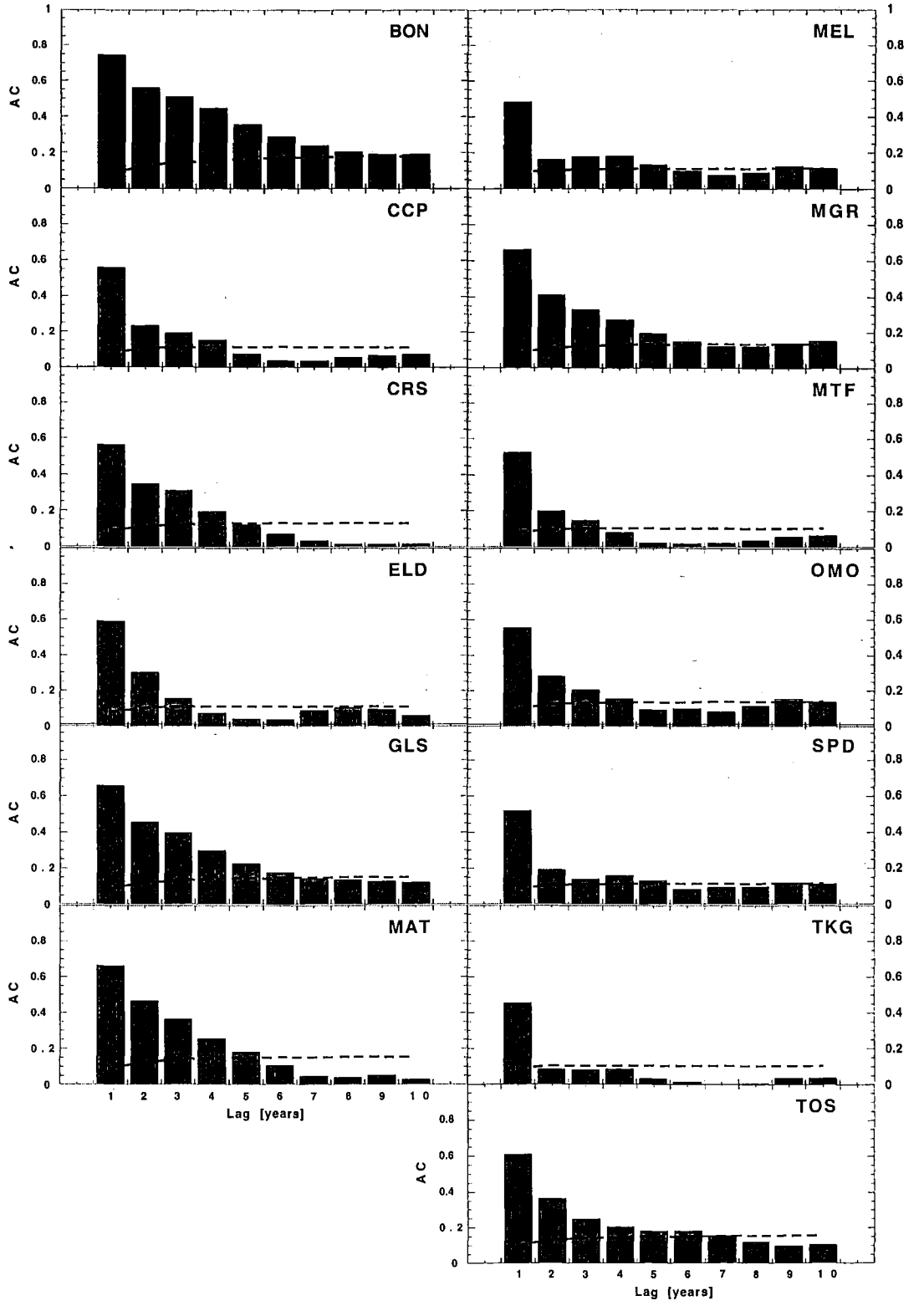

Figure 2.24 Correlograms for the ARS chronologies. The autocorrelation coefficient (AC) values were calculated out to 10 lags. Dashed lines indicate 95% confidence limits.

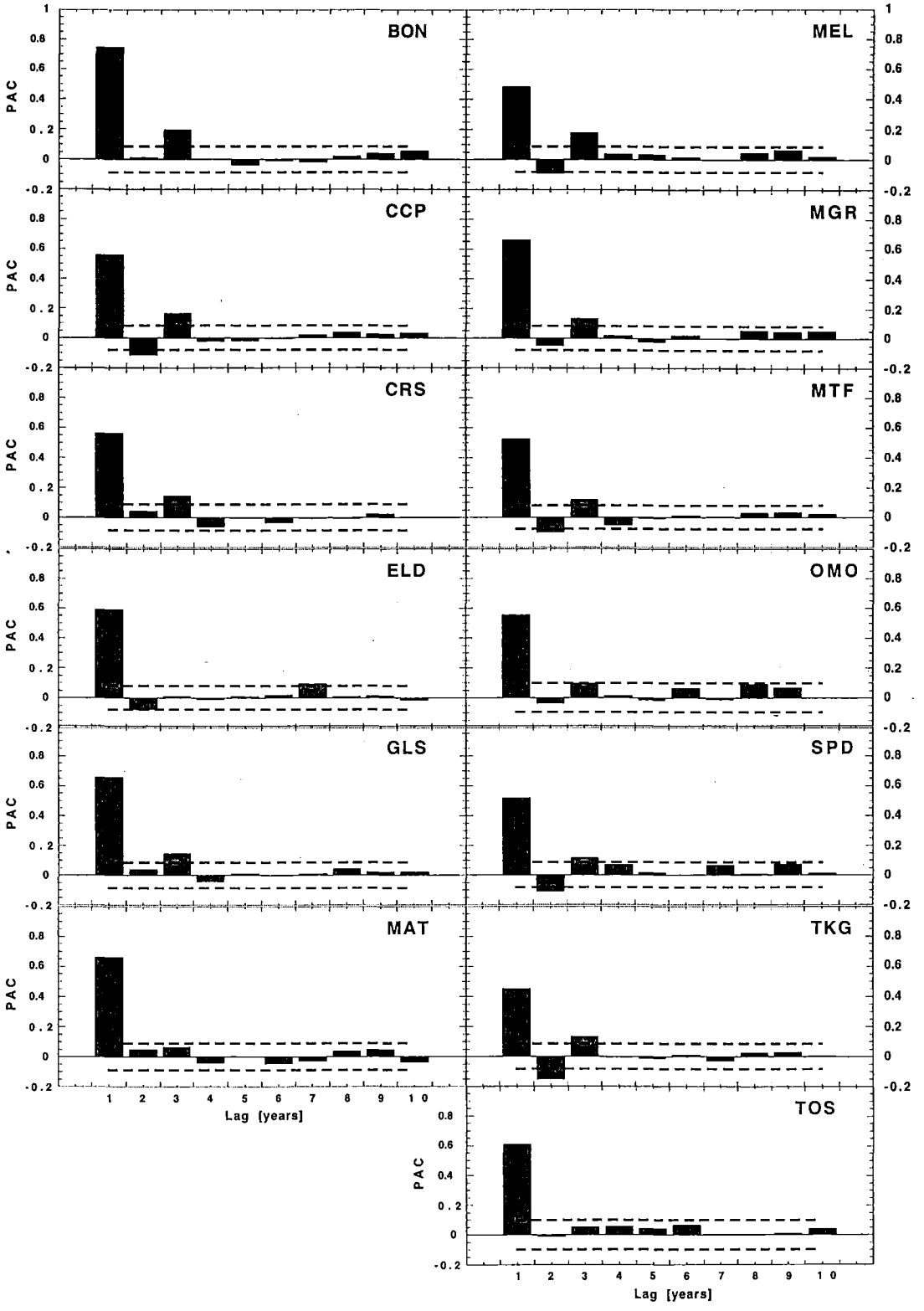

Figure 2.25 Partial autocorrelation function (ARS chronologies). The partial-autocorrelation coefficient (PAC) values were calculated out to 10 lags. Dashed lines indicate 95% confidence limits.

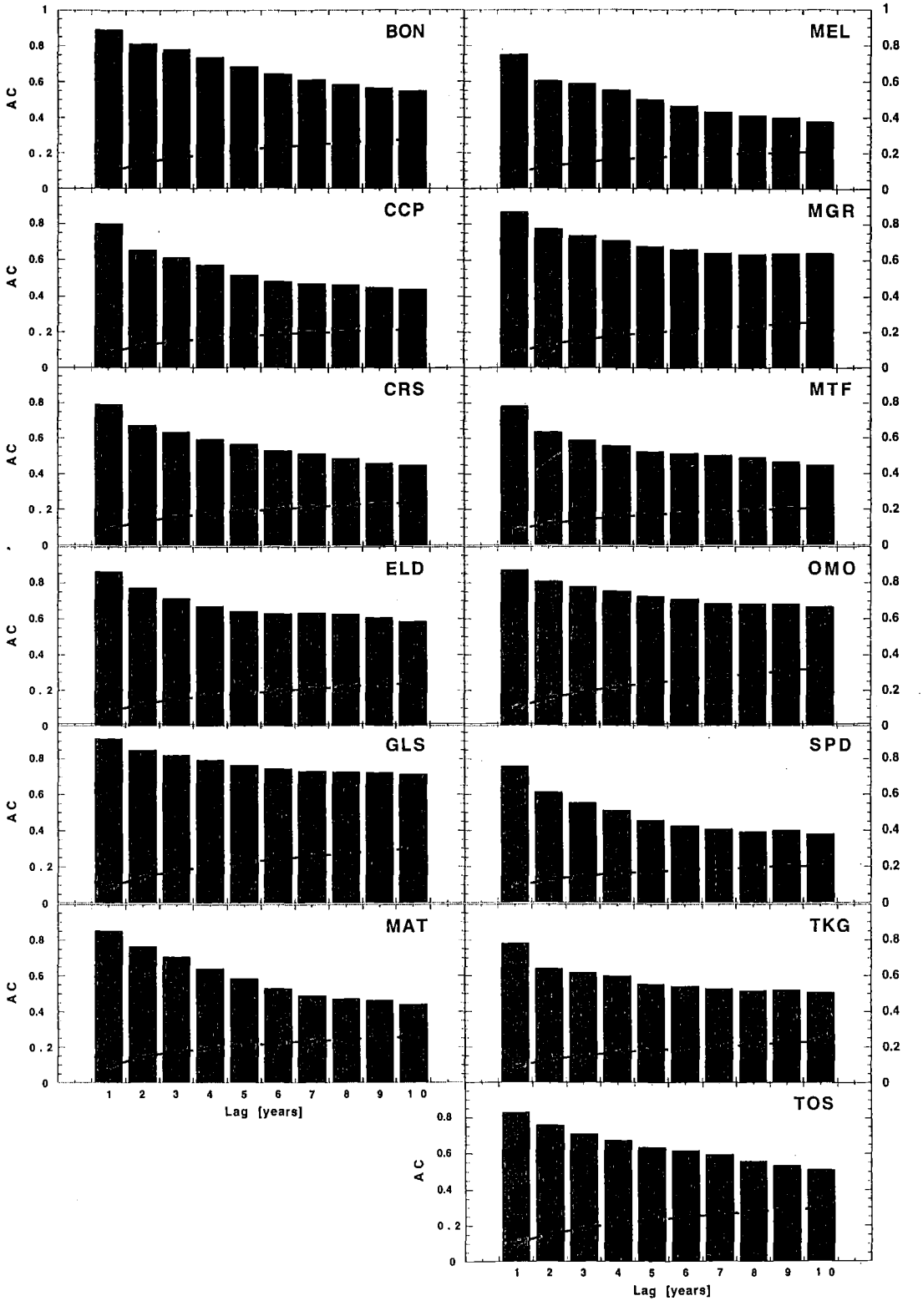

Figure 2.26 Correlograms for the RCS chronologies. The autocorrelation coefficient (AC) values were calculated out to 10 lags. Dashed lines indicate 95% confidence limits.

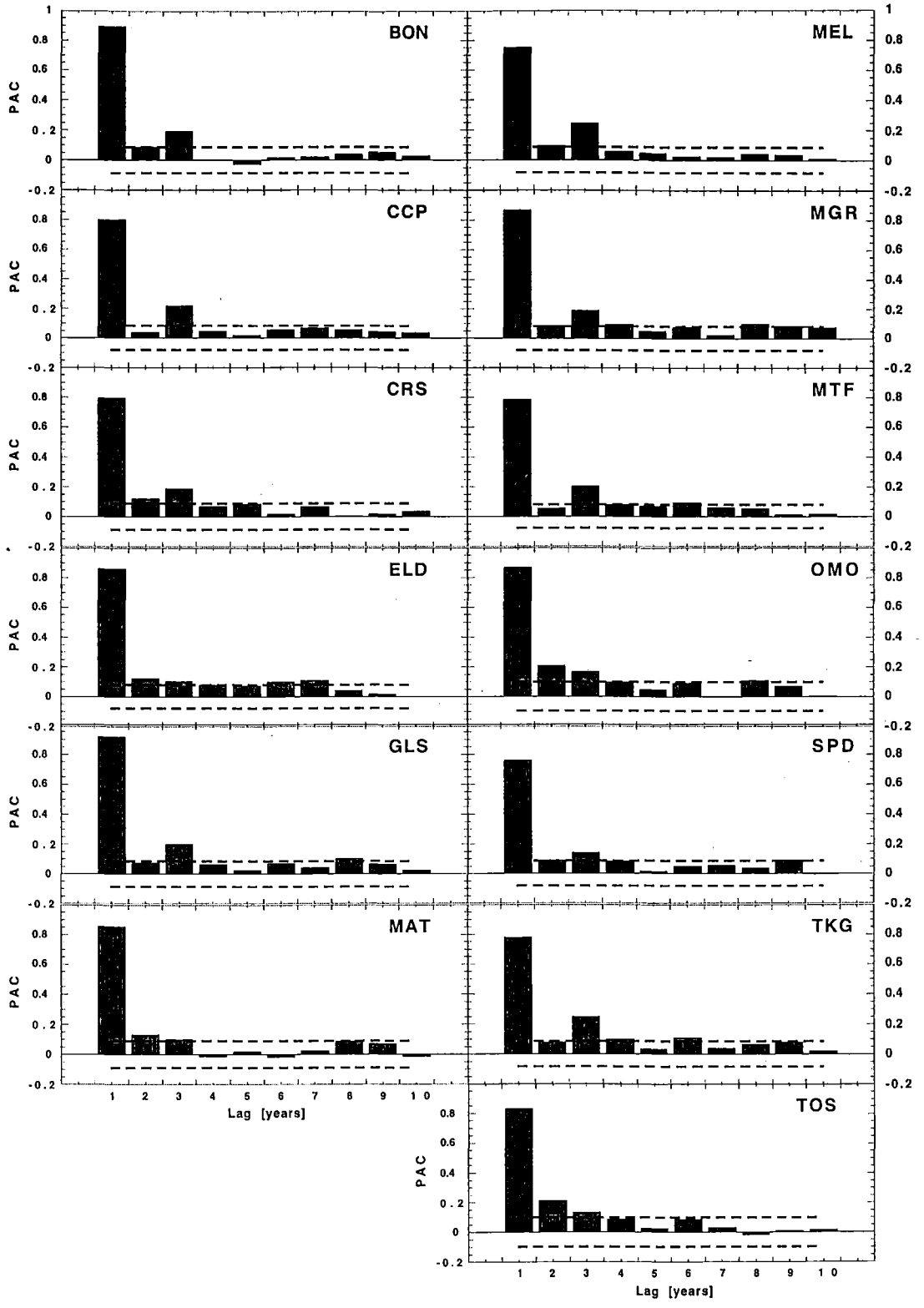

Figure 2.27 Partial autocorrelation function (RCS chronologies). The partial-autocorrelation coefficient (PAC) values were calculated out to 10 lags. Dashed lines indicate 95% confidence limits.

2.4.3 Chronology comparison

The correlation coefficients for the high-pass (<25 years) filtered ARS chronologies (Table 2.4) are all positive and highly significant (P<0.001), indicating a strong agreement between the high-frequency component of the chronologies. The three sites located near Lake Brunner (CCP, MTF and TKG) and MGR exhibit some of the highest correlations (RP>0.80). The low-altitude TOS site shows the least agreement with the other sites, and unsurprisingly, it is most similar to OMO, another low-altitude site. The low-frequency component (>25 years) of the ARS chronologies varies greatly from site to site, as both negative and positive significant values are present (Table 2.4). SPD differs from the remaining sites the most, as it shows five negative correlations, four of them significant at the 5% level.

Table 2.4 Double correlation matrix for the ARS chronologies. Period of analysis is 1590-1998. Values in the lower-left half of the table are for the low-pass filtered data, whereas the upper-right half contains correlation coefficients for the high-pass filtered chronologies. Number of stars below each value indicates its level of significance: ***P<0.001; **P<0.01; *P<0.05.

	BON	CCP	CRS	ELD	GLS	MAT	MEL	MGR	MTF	OMO	SPD	TKG	TOS
BON	**1**	.84 ***	.69 ***	.50 ***	.66 ***	.53 ***	.77 ***	.81 ***	.76 ***	.42 ***	.60 ***	.82 ***	.27 ***
CCP	.51 ***	**1**	.76 ***	.57 ***	.73 ***	.65 ***	.84 ***	.83 ***	.82 ***	.50 ***	.59 ***	.90 ***	.34 ***
CRS	.07	.61 ***	**1**	.55 ***	.71 ***	.65 ***	.76 ***	.71 ***	.70 ***	.42 ***	.52 ***	.76 ***	.30 ***
ELD	.22 ***	.11 *	.11 *	**1**	.47 ***	.51 ***	.57 ***	.52 ***	.47 ***	.38 ***	.57 ***	.55 ***	.38 ***
GLS	.44 ***	.37 ***	.39 ***	.16 **	**1**	.58 ***	.69 ***	.66 ***	.64 ***	.43 ***	.49 ***	.72 ***	.25 ***
MAT	-.05	.14 **	.32 ***	.12 *	-.12 *	**1**	.58 ***	.48 ***	.48 ***	.29 ***	.36 ***	.55 ***	.28 ***
MEL	.60 ***	.57 ***	.36 ***	.12 *	.32 ***	.00	**1**	.76 ***	.77 ***	.44 ***	.63 ***	.86 ***	.24 ***
MGR	.60 ***	.67 ***	.40 ***	.06	.40 ***	.19 ***	.50 ***	**1**	.85 ***	.56 ***	.54 ***	.85 ***	.38 ***
MTF	.45 ***	.62 ***	.35 ***	.02	.19 ***	.52 ***	.32 ***	.71 ***	**1**	.49 ***	.57 ***	.85 ***	.27 ***
OMO	-.03	.27 ***	.28 ***	.05	-.07	.20 ***	.22 ***	.14 **	.17 ***	**1**	.29 ***	.49 ***	.46 ***
SPD	.26 ***	.14 **	.04	-.12 *	.52 ***	-.16 **	.21 ***	.18 ***	.16 **	-.08	**1**	.62 ***	.18 ***
TKG	.44 ***	.66 ***	.28 ***	.20 ***	.19 ***	.17 ***	.35 ***	.55 ***	.43 ***	.34 ***	-.14 **	**1**	.26 ***
TOS	.16 **	.10 *	.13 **	.02	-.19 ***	.20 ***	.38 ***	.22 ***	.18 ***	.25 ***	-.47 ***	.13 **	**1**

For the high-pass filtered (<25 years) RCS chronologies, all correlations are positive and highly signigicant (P<0.001; Table 2.5). As with the ARS chronologies, the highest correlations occur among the CCP, MGR, MTF and TKG sites. The site that shows the poorest agreement with the remaining twelve sites is again TOS, followed by OMO and MAT. The RCS chronologies differ from the ARS chronologies in their low-frequency (>25 years) component. As can be seen from Table 2.5, all chronologies are positively correlated at high levels of significance (P<0.001). This may be an effect of the overall positive trend exhibited by most RCS chronologies, which was lost from the ARS chronologies due to detrending. The fact that MTF (the site with no positive trend; Figure 2.19) shows the lowest correlations (Table 2.5), would support this observation.

Table 2.5 Double correlation matrix for the RCS chronologies. Period of analysis is 1590-1998. Values in the lower-left half of the table are for the low-pass filtered data, whereas the upper-right half contains correlation coefficients for the high-pass filtered chronologies. All values are significant at 0.1% level (P<0.001).

	BON	CCP	CRS	ELD	GLS	MAT	MEL	MGR	MTF	OMO	SPD	TKG	TOS
BON	**1**	.79	.61	.47	.56	.48	.71	.75	.70	.40	.52	.78	.23
CCP	.80	**1**	.72	.56	.66	.62	.79	.82	.80	.51	.55	.87	.31
CRS	.74	.77	**1**	.51	.66	.58	.71	.68	.67	.42	.48	.71	.25
ELD	.64	.54	.51	**1**	.43	.50	.56	.51	.47	.38	.54	.54	.38
GLS	.80	.77	.83	.68	**1**	.50	.61	.61	.58	.40	.46	.67	.18
MAT	.46	.52	.44	.51	.44	**1**	.52	.44	.46	.29	.33	.53	.27
MEL	.81	.72	.52	.59	.69	.39	**1**	.74	.72	.44	.57	.81	.21
MGR	.79	.87	.72	.53	.77	.56	.69	**1**	.86	.56	.52	.87	.33
MTF	.32	.55	.21	.22	.28	.45	.27	.60	**1**	.50	.52	.82	.26
OMO	.53	.75	.60	.68	.69	.69	.55	.76	.48	**1**	.28	.48	.41
SPD	.75	.65	.63	.52	.79	.42	.75	.72	.25	.55	**1**	.57	.18
TKG	.73	.87	.64	.66	.73	.61	.64	.83	.49	.84	.58	**1**	.25
TOS	.61	.64	.54	.62	.52	.55	.69	.65	.34	.66	.41	.63	**1**

The rotated PCA emphasised the similarities and differences among the data. In most cases, only the first eigenvector was selected by the Monte-Carlo red-noise criterion as significant (Table 2.6), explaining around 60% of the variance and indicating that all chronologies could potentially be grouped into a single set. Only the low-pass filtered ARS chronologies showed some spatial variability, with two eigenvectors identified as significant. Together the first two eigenvalues account for 50% of the total variance of all thirteen series (Table 2.6).

Table 2.6 Results from the rotated PCA. Two eigenvectors were rotated from the low-pass filtered ARS chronologies. In the remaining analyses, only the first eigenvector was significant at 95% level.

Chronology type	No. of eigenvectors	Eigenvalue	Retained variance
High-pass ARS	1	8.1181	62.4%
Low-pass ARS	2	4.4401 / 2.0869	50.2% (34.1% + 16.1%)
High-pass RCS	1	7.7170	59.4%
Low-pass RCS	1	8.4186	64.8%

Figures 2.28-2.31 present the varimax loadings. Among the high-pass filtered ARS chronologies (Figure 2.28), TOS and OMO (the two low-altitude sites) show the lowest values. The low-frequency signals in the ARS chronologies (Figure 2.29) seem to depend both on altitude and latitude. The first rotated PC shows high loadings for the high-altitude sites in central Westland (BON, CCP, CRS, MEL, MGR, MTF and TKG). The sites with low varimax loadings are those from low altitudes (TOS and OMO), those from the southern South Island (ELD and SPD), and the northernmost site (MAT). It is not clear what kind of separation pattern is indicated by the second rotated PC.

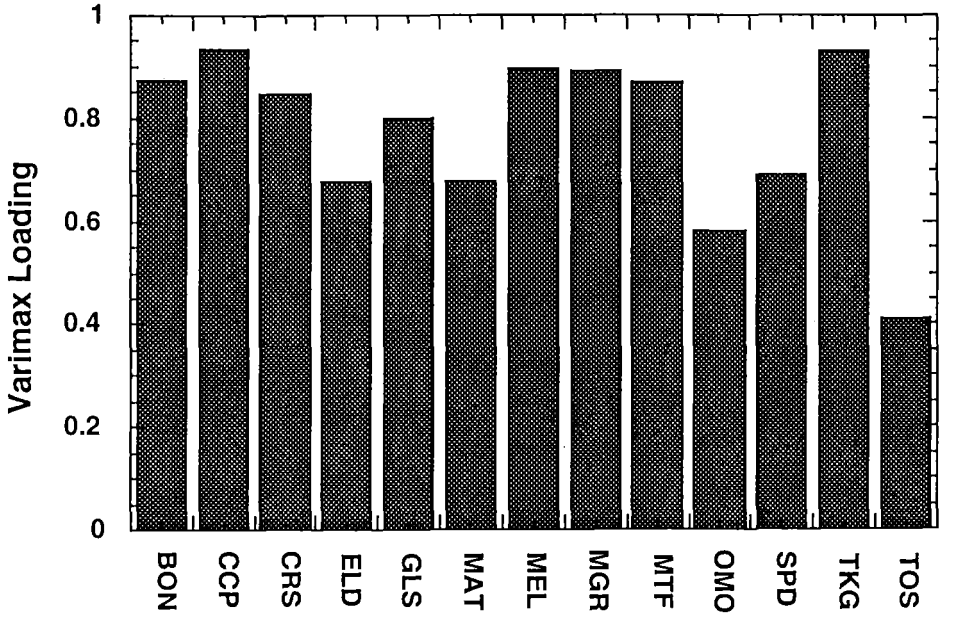

Figure 2.28 Varimax loadings for the high-pass filtered ARS chronologies.

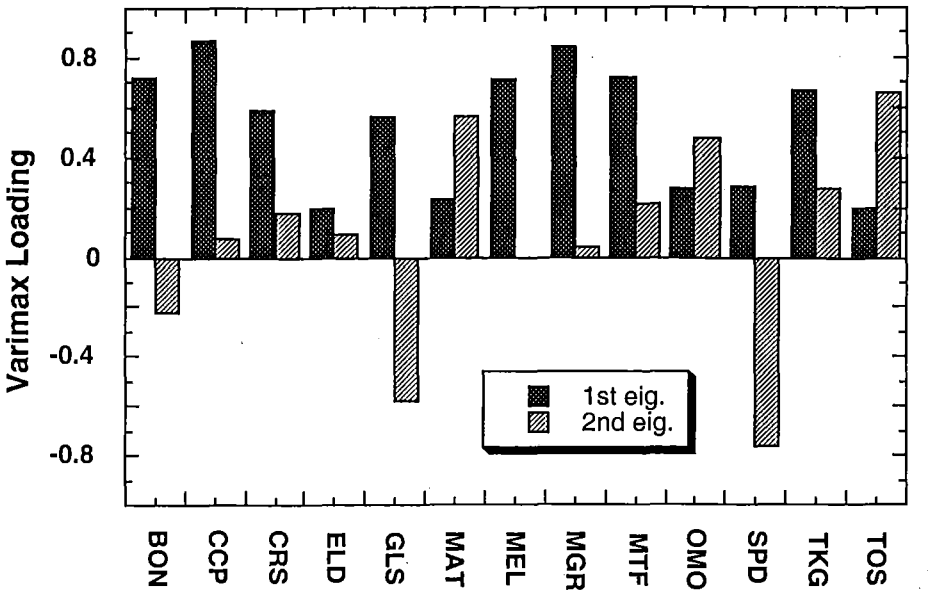

Figure 2.29 Varimax loadings for the low-pass filtered ARS chronologies.

The high-frequency component of the RCS chronologies (Figure 2.30) is nearly identical to that of the ARS chronologies. The difference is again in the longer-term trends. The varimax loadings for the low-pass filtered RCS chronologies are all very high, with the exception of the MTF site (Figure 2.31).

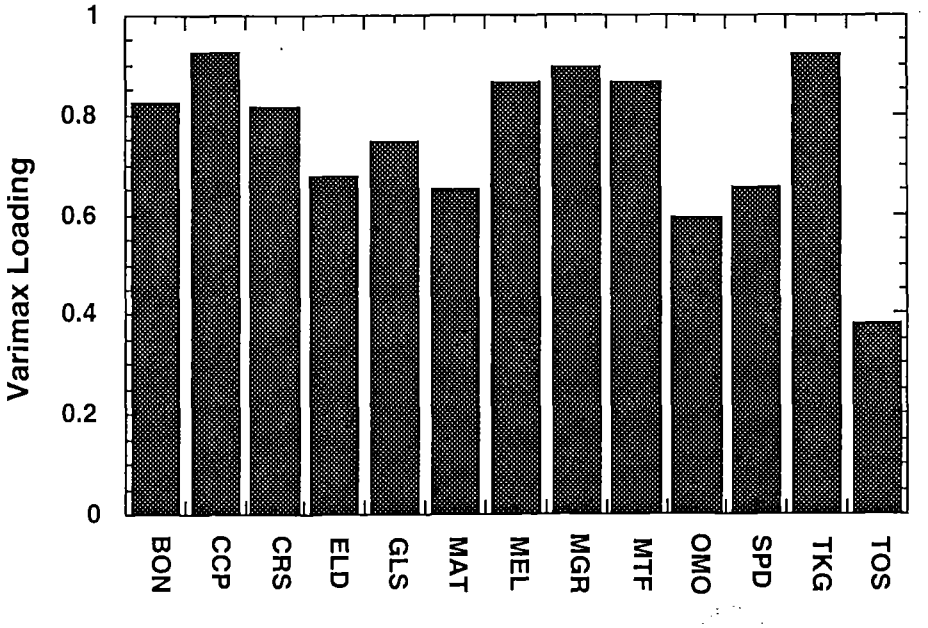

Figure 2.30 Varimax loadings for the high-pass filtered RCS chronologies.

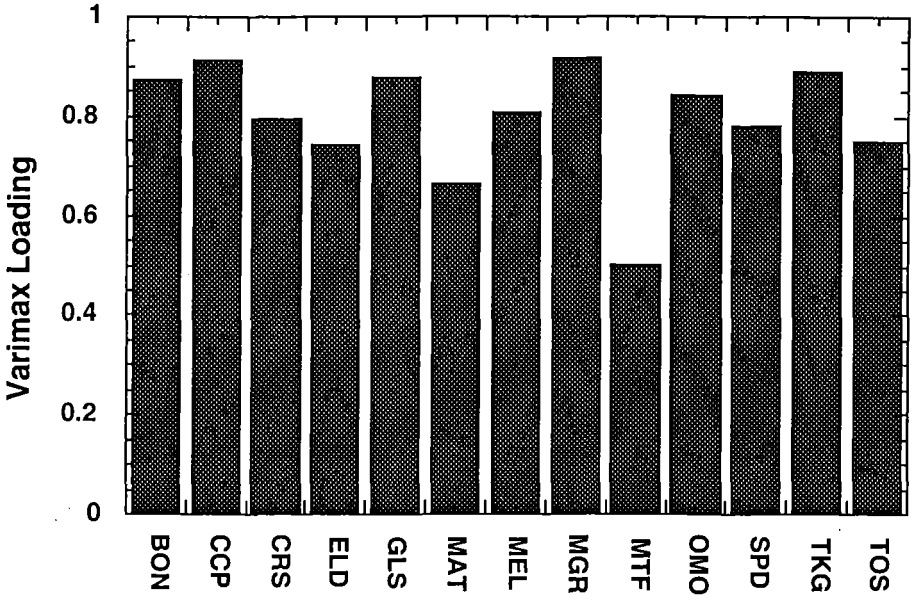

Figure 2.31 Varimax loadings for the low-pass filtered RCS chronologies.

2.5 Discussion

Pink pine trees exhibit common growth trends within individual sites, as has been shown by the high proportion of samples that could be crossdated (Table 2.2). Such synchronous variations in ring widths can be caused by climate or by large-scale disturbances. Since the inter-site comparison showed that tree-ring patterns were similar across the entire study area (RCS chronologies), it is most likely that climate was the primary limiting environmental factor. It appears that the ring widths reflected variations in temperature, because narrow rings were often formed in years in which below-average temperatures were recorded at the Hokitika meteorological station. For example, 1912 has been the coldest year on record (Salinger *et al.*, 1992a), and the ring that formed in the same year was the narrowest in the 20th century.

The increased growth in the second half of the 20th century, which was noted at most sites, coincided with increase in the mean annual temperatures in this area (Salinger *et al.*, 1992a). Similar periods of faster growth were identified in pink pine from Stewart Island and from the North Island (D'Arrigo *et al.*, 1995; D'Arrigo *et al.*, 1998), in *Lagarostrobos colensoi* (D'Arrigo *et al.*, 1998), and in the Tasmanian *Lagarostrobos franklinii* (Cook *et al.*, 1991; Cook *et al.*, 1992). In another Tasmanian conifer, *Phyllocladus asplenifolius*, the increased

growth of the recent decades was present in the raw data, but it has been removed by standardisation (Allen, 1998). In this study, similar removal or reduction of this phenomenon occurred when applying the single-detrending method to the data, while the RCS method resulted in no remarkable changes. The difference between the ARS and RCS chronologies shows how profoundly standardisation affects the tree-ring data and any potential climatic reconstruction.

In the single-detrending method, linear curves of any slope (negative, horizontal or positive) were fitted to the raw ring-width data. It is questionable whether the fitting of lines with positive slope was appropriate, because tree growth typically shows a decline with increasing age and size of the tree, not an enhancement (Fritts, 1976). It is possible that the positive trend was related to stand dynamics – most sampled trees were living, and belonged to a single cohort. As trees were getting older, more light may have been available, which in turn may have resulted in the increased growth. In this case, removal of the trend would be correct. However, I do not think that the positive trend was related to cohort development – if it were so, the mean growth curves that were developed for the RCS method (Section 2.3.3) would have revealed this trend. It is more likely that the positive trend was climate-related, and valuable information has been lost by its removal.

The close resemblance between the raw data and the RCS chronologies could be explained in two ways: (a) the age-related trends were very weak, and climate was the main factor that influenced tree growth, or (b) the RCS method failed to recognise and remove the age-related trends in the ring-width data. One potential source of error in the RCS method are the pith-offset estimates, which may potentially be incorrect. However, the RCS method is not very sensitive to even relatively large inaccuracies in the PO estimates (Esper *et al.*, 2003). In several cases, the RCS has been successfully applied when no PO information was available, and the first crossdated ring was simply considered to represent the first year of cambial age (Briffa *et al.*, 1992; Cook *et al.*, 2000a).

Another point of uncertainty in the RCS method was the separation of sites into two populations. Possibly, a third population should have been identified, one that would include the low-altitude, faster-growing trees (OMO and TOS). The argument against creating the third population was that the tree-ring data would be thus broken into too many small fragments, whereas a large sample size is one of the essential requirements for the RCS method (Briffa *et al.*, 1992; Esper *et al.*, 2003). The similar shapes of the mean growth curves

justify the inclusion of OMO and TOS within the CLOSED population. Since both of the above issues (the accuracy of the PO estimates and the identification of populations) appear to be negligible, the RCS chronologies are likely to be a faithful depiction of the tree growth as influenced by climate.

The chronology statistics are consistent with the results of other studies in the New Zealand – Tasmanian region. Low mean sensitivity is typical not only for pink pine (Dunwiddie, 1979; Murphy, 1993; Xiong *et al.*, 1998), but also for other conifers (with the exception of *Phyllocladus* spp., where alternating narrow and wide rings result in higher MS values) (Dunwiddie, 1979; Palmer, 1989; Xiong, 1995; Buckley, 1997; Allen, 1998). The mean sensitivity remained nearly equal in both types (ARS and RCS) of chronologies, but the RCS improved some of the other statistics remarkably, namely the serial correlation). The high serial correlation values (0.829 on average for the RCS chronologies) reflect the great amount of low-frequency variance that has been retained in the tree-ring data. On the other hand, the RBar values are rather low in the RCS chronologies (compared with the ARS chronologies). They typically range from 0.2 to 0.3, and for further research, it will be important to see how stable the values are over time.

Both the correlation analysis and the principal component analysis revealed a high degree of similarity among most chronologies. This is not surprising, because all chronologies were developed from the same species, they all cover approximately the same time period, and the sites were located in a region that is subject to similar climatic and weather patterns (Section 1.4.2). The similarities were especially high among the RCS chronologies, and among the high-pass filtered ARS chronologies. The low-pass filtered ARS chronologies showed certain variation in correlation strength, but again, some longer-term trends there had been lost due to the standardisation method used.

2.6 Summary and conclusions

Thirteen original pink pine chronologies were developed from the South Island, New Zealand. Eleven sites were located near treeline and two sites were located at lower altitudes. The chronologies spanned periods from 409 to 662 years. The two low-altitude chronologies were also the two shortest ones, and fewer trees exhibited a common growth pattern. These facts emphasise the importance of careful site selection for dendroclimatic research. I experimented with two methods of standardisation: single detrending (fitting of negative exponential or linear curves to the individual series) and the RCS. For the purpose of the RCS, two distinct

populations were identified, the classification being based on the openness of the canopy. The chronologies developed by the RCS method showed less common variance compared with the single-detrended data (as demonstrated by the RBar values). The high-frequency component was similar in both types of chronologies. The standardisation method mainly affected the chronologies in their low-frequency component. Greater amount of the low-frequency variance was retained when applying the RCS method to the data (as demonstrated by the serial correlation values). The inter-site comparison indicated that a common signal exists not only between individuals on a single site, but also on a larger, regional scale. One factor that typically influences tree growth on such broad scales is climate. The types and strength of the climatic signal that is contained in the tree-ring data will be investigated in the following chapter. Since the low-frequency variance is crucial in dendroclimatic studies, only the RCS chronologies will be used for further research.

Chapter 3

Climate response

3.1 Introduction

It has been shown that climate influences tree growth of both New Zealand conifers and angiosperms (e.g. Norton, 1983a; Palmer, 1989; Xiong, 1995). It is difficult to determine how the dendroclimatic potential of New Zealand species compares with other countries/regions, because results of climate-response studies have been highly variable throughout the world (Fowler, 1988). But in general, it might be said that the climate signal that is reflected in ring widths of New Zealand trees is more complex than the signal found in tree-ring data from the Northern Hemisphere (Graybill and Shiyatov, 1989; Briffa *et al.*, 1995; Kalela-Brundin, 1999), and especially the southwestern USA (Fritts, 1976). The New Zealand situation is comparable with South America (Lara and Villalba, 1993; Villalba *et al.*, 1998) and Tasmania (Buckley, 1997; Allen, 1998; Cook *et al.*, 2000a).

The strength of temperature and/or precipitation signal in tree-ring chronologies has been investigated in several New Zealand species: pink pine (D'Arrigo *et al.*, 1995; D'Arrigo *et al.*, 1998; Xiong *et al.*, 1998), *Lagarostrobos colensoi* (D'Arrigo *et al.*, 1998; Cook *et al.*, 2002a), *Libocedrus bidwillii* (Xiong, 1995; Xiong and Palmer, 2000b; Palmer and Xiong, 2003), *Phyllocladus trichomanoides* and *P. glaucus* (Palmer, 1989; Salinger *et al.*, 1994), *Agathis australis* (Ogden and Ahmed, 1989; Salinger *et al.*, 1994; Buckley *et al.*, 2000), and *Nothofagus menziesii* and *N. solandri* (Norton, 1984; Norton, 1987; Salinger *et al.*, 1994). Three studies have focused on broad-scale climate variables. In the first, Villalba *et al.* (1997b) examined the relationship between pink pine and *Lagarostrobos colensoi* tree-ring data and the mean sea level pressure (MSLP). Linking these results with similar data from Tierra del Fuego led then to the reconstruction of the summer transpolar index (STPI). The other two studies investigated the response of pink pine (Murphy, 1993) and *Agathis australis* (Fowler *et al.*, 2000) chronologies to the El Niño / Southern Oscillation (ENSO).

ENSO is the most important coupled ocean-atmosphere phenomenon to cause global climate variability on interannual time scales. Instrumental measures of ENSO are based either on

atmospheric [the Southern Oscillation Index (SOI)] or oceanic [the sea surface temperature (SST)] measurements. A strong SOI signal has been found in tree rings in northern Mexico and southwestern / southcentral USA (Cleaveland *et al.*, 1992; D'Arrigo and Jacoby, 1992; Lough, 1992; Meko, 1992; Stahle and Cleaveland, 1993; Stahle *et al.*, 1998; Cook *et al.*, 2000b), and more recently in Java (Stahle *et al.*, 1998; Cook *et al.*, 2000b). However, besides the tropics and subtropics, ENSO also affects many mid-latitude regions, including New Zealand (Gordon, 1985; Mullan, 1995). The STPI reconstruction (Villalba *et al.*, 1997b) provided evidence for long-term forcing of the Southern Hemisphere climate system by ENSO also in the high latitudes.

The aim of this chapter is to identify the climate variables that have a significant effect on the growth of pink pine. This is achieved through correlation analyses and response function modelling. First, I correlated the tree-ring data against four variables: mean monthly temperature, monthly precipitation, monthly SOI and seasonal SOI. Since the results indicated that temperature was the main growth-limiting factor, I used only the mean monthly temperature data in the response function. A model for each site was calibrated using the principal component regression technique, and verified on an independent data set.

3.2 Climate data

3.2.1 Temperature

To investigate the temperature signal that is contained in the tree-ring chronologies, I used data from the Hokitika meteorological station. Hokitika is located in central Westland (42°43'S, 170°59'E), in close proximity to most of the tree-ring sites. Its instrumental record is one of the longest in New Zealand (Fouhy *et al.*, 1992). I considered Hokitika's climate to be representative of the local climates for all of the sites. Twelve out of thirteen tree-ring sites are located in one temperature response area, the "West Coast" (Salinger, 1981; see Section 1.4.2 for details). The SPD site is located in the Southland response area; however, experimentation with meteorological data from Hokitika, Invercargill and Dunedin showed that also for SPD, the Hokitika record was the most suitable.

Temperatures have been recorded in Hokitika since 1866, with a 13-year gap between 1881 and 1893 (Figure 3.1). The mean annual temperature in Hokitika is 11.3°C, with temperatures being higher in the second half of the 20th century. 1912 was the coldest year on record and 1971 the warmest (Figure 3.1). Throughout its history, the station has been located at four

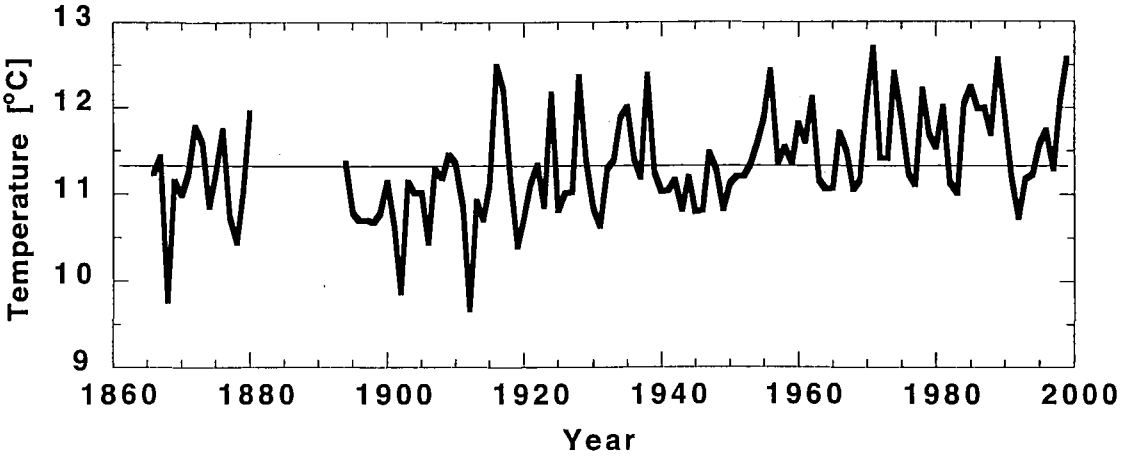

Figure 3.1 Hokitika mean annual temperatures. The Hokitika station recorded data from 1866 to 1880, and then continuously since 1894. (Data source: E. Cook, pers. comm.)

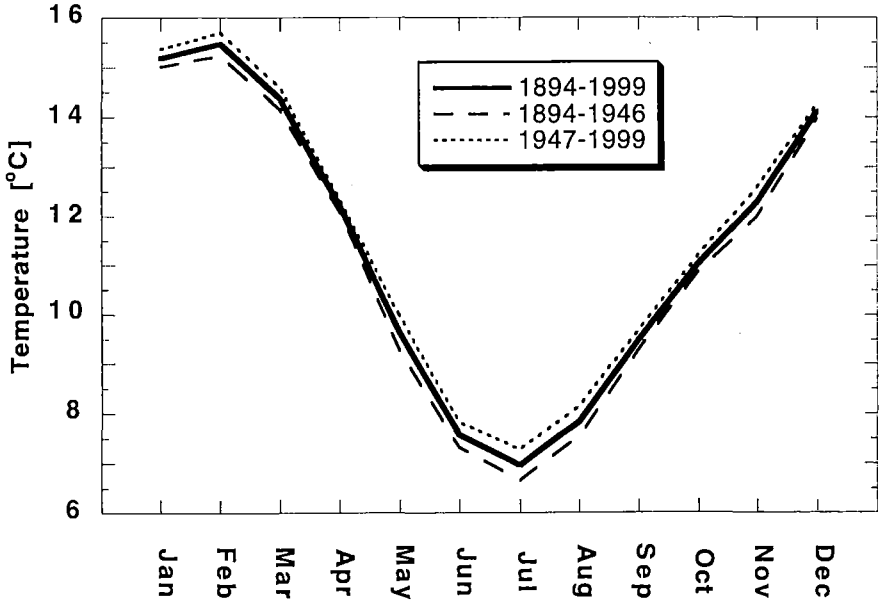

Figure 3.2 Hokitika mean monthly temperatures. The averages were calculated over three different periods: 1894-1999 (solid line), 1894-1946 (dashed line) and 1947-1999 (dotted line).

different sites (Fouhy *et al.*, 1992). To adjust for the different locations and to remove errors from the record, the data have been homogenised (Salinger *et al.*, 1992a). In all further analyses, I use the continuous part of the record since 1894. This still provides observations from more than 100 years for calibration and verification purposes. There is no major loss in not using the 1866-1880 data, since the early record is poorly documented and has greater variance that failed to be reduced by homogenisation (S. Larsen, pers. comm.). Also, this way it is unnecessary to estimate the missing values, which could introduce uncertainty into the calculations and into the interpretation of results.

Figure 3.2 shows the mean monthly temperatures. The warmest month in Hokitika is February, closely followed by January (both over 15°C). With a mean temperature of less than 7°C, July is the coldest month. Division of the data set into two equal parts reveals consistently higher temperatures in the late period of the record. The mean monthly temperatures in 1947-1999 were nearly 0.5°C higher than those in 1894-1946. The biggest increase, over 0.6°C, occurred in the late autumn and winter (May to August).

3.2.2 Precipitation

As for temperature, the precipitation data used in this study were recorded at the Hokitika meteorological station. The observations began in 1866, stopped temporarily in 1880, and were renewed in 1894 (Figure 3.3). The mean total precipitation is approximately 2830 mm per annum. 1878 was by far the wettest year on record - the total annual precipitation reached nearly 4000 mm. The driest year was 1930, in which the rainfall amounted to just over 2000 mm (Figure 3.3). The data were homogenised by Salinger *et al.* (1992b). In further analyses, I only use the continuous part of the record since 1894.

The precipitation is distributed evenly throughout the year, with a minimum (194 mm) in February and a maximum (273 mm) in October (Figure 3.4). No consistent change in the amount of precipitation is apparent when comparing the early and the late periods of the record.

I did not expect the tree-ring data to prove to be sensitive to precipitation. Firstly, because of the large amounts of rainfall the West Coast is experiencing, precipitation is not likely to be a growth-limiting factor there. Secondly, unlike temperature, rainfall is highly variable in space. Griffiths and McSaveney (1983) showed how dramatically precipitation changes along a West Coast transect, depending both on altitude and on the distance from the sea coast (Figure 3.5).

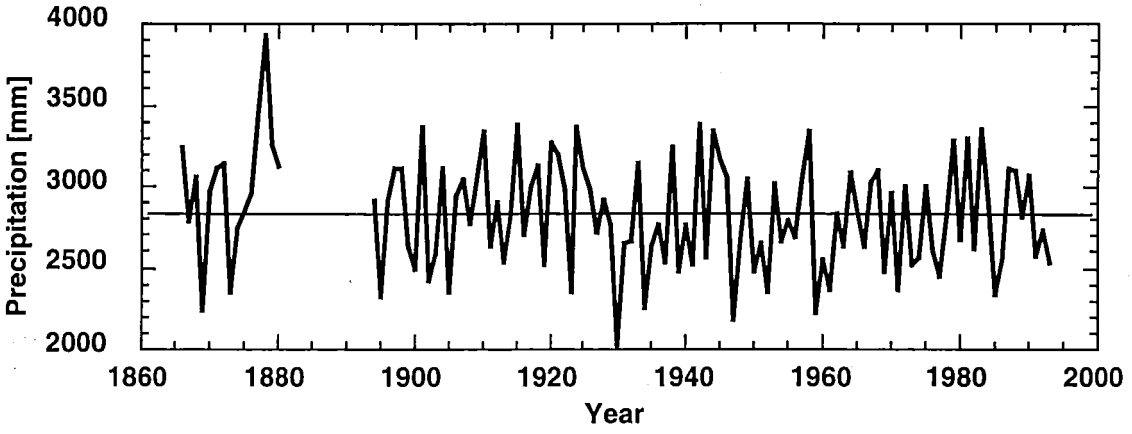

Figure 3.3 Hokitika total annual precipitation. As for temperature, no data were recorded between 1881 and 1893. (Data source: L. Xiong, pers. comm.)

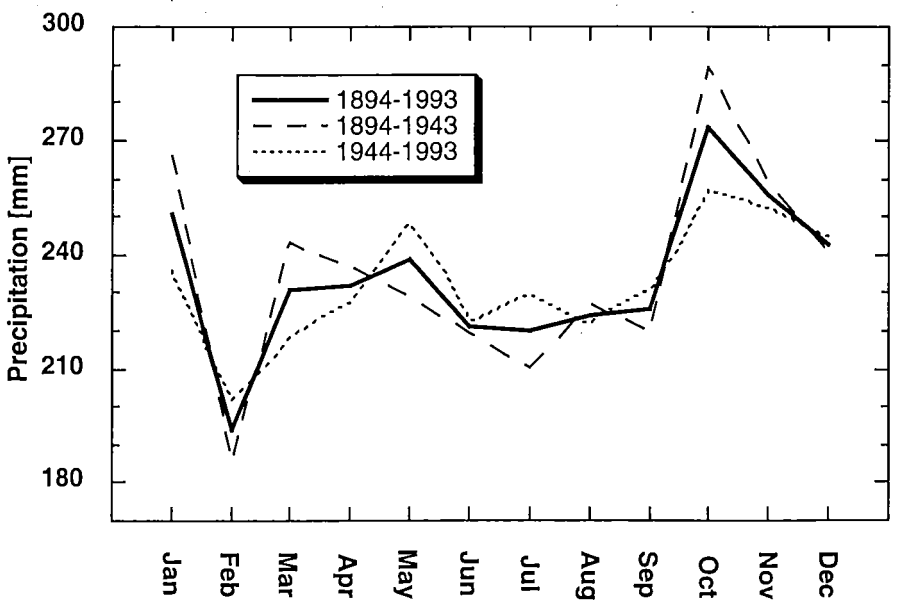

Figure 3.4 Hokitika mean monthly precipitation. The averages were calculated over three different periods: 1894-1993 (solid line), 1894-1943 (dashed line) and 1944-1993 (dotted line).

It is doubtful that Hokitika's precipitation is an adequate representation of the rainfall at the tree-ring sites - not only because of the horizontal distance that separates Hokitika from the individual sites, but also because of the differences in altitude. The Hokitika meteorological station is located at 38 m a.s.l. (Fouhy *et al.*, 1992), while most of the sites are near the treeline. However, even though I did not expect rainfall to affect tree growth significantly, it was still important to explore the relationship.

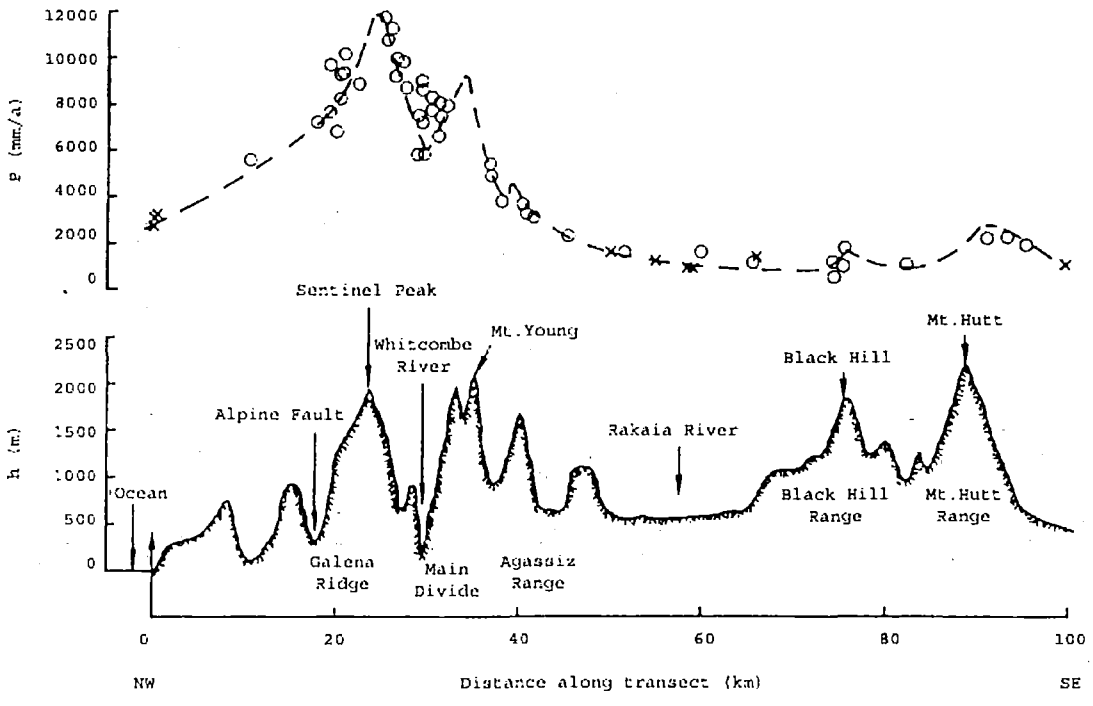

Figure 3.5 Rakaia transect showing the topographic profile *h* and the spatial distribution of rainfall *P*. The rainfall data points are marked as open circles and crosses. The transect is oriented in NW-SE direction, between 43°01'S and 43°33'S, and between 170°44'E and 171°40'E. (Adapted from Griffiths and McSaveney, 1983.)

3.2.3 Southern Oscillation Index

The Southern Oscillation Index (SOI) is calculated from the monthly or seasonal anomalies in the mean sea level pressure (MSLP) difference between Tahiti and Darwin. There are several methods of computation of the SOI (Ropelewski and Jones, 1987; Allan *et al.*, 1996). I used the monthly data provided by the Australian Bureau of Meteorology (2002), who adopted the Troup SOI technique (McBride and Nicholls, 1983). The index is calculated as follows:

$$SOI = 10 * (Pdiff - Pdiffav) / SD \qquad (3.1)$$

In Equation 3.1, the *Pdiff* represents the difference between the mean monthly Tahiti MSLP and the mean monthly Darwin MSLP, *Pdiffav* is the long-term (1933-1992) average of *Pdiff* for the month in question, and *SD* is the long-term (1933-1992) standard deviation of *Pdiff* for the month in question. The monthly SOI values range from about –35 to about +35. The mean annual values are shown in Figure 3.6.

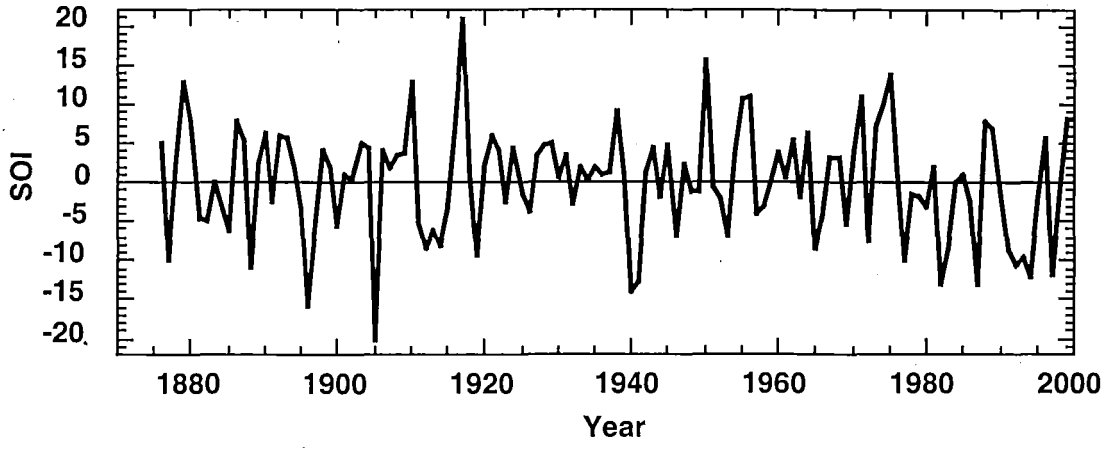

Figure 3.6 Mean annual SOI. Continuous record since 1876. (Data source: Australian Bureau of Meteorology, 2002.)

Negative values of SOI are associated with El Niño events, while positive values with La Niña. The average event lasts for 18-24 months and shows characteristics of being locked to the seasonal cycle (Allan *et al.*, 1996). Seasonal persistence is weakest in austral autumn, when new events are likely to develop and existing conditions collapse. Typically, ENSO is strong in spring to summer. ENSO reoccurs in the range of 2-7 years, but there are also various ENSO-like patterns in the climate system on decadal to multidecadal timescales (Allan *et al.*, 1996). Since the mid-1970s, the El Niño phases have been predominant over the La Niña phases (Allan, 2000). Some of the strongest El Niño events occurred during this period: in 1982-1983 and in 1997-1998. The latter has been dubbed "the climate event of the century" (Changnon, 2000). A protracted El Niño or sequence of El Niños occurred in the first half of the 1990s and in 1939-42 (Figure 3.6).

Extensive literature exists on ENSO, e.g.: Diaz and Markgraf (1992; 2000), Allan *et al.* (1996), Glantz (1996), and Caviedes (2001). Information on ENSO can be also obtained from numerous websites. An excellent example is the "El Niño / La Niña Home" (Climate Prediction Center, 2002), which is administered by the National Oceanic and Atmospheric Administration (NOAA), USA.

3.3 Materials and methods

The relationship between tree-ring data (the RCS chronologies developed in Chapter 2) and climate was identified through a process known as the response function (Fritts, 1976). A response function is a form of regression equation, in which the climate is used as the independent variable (predictor), and the tree-ring data as the dependent variable (predictand). Since the climate variables are intercorrelated, they need to be orthogonalised prior to regression (i.e. transformed into principal component eigenvectors).

Blasing *et al.* (1984) noted that the response function can be affected in unpredictable ways by, often subjective, decisions about the number of climate variables to include, confidence limits, number of eigenvectors to allow as candidate predictors in regression, etc. Since correlation functions are more objective and easy to interpret, the authors have recommended publishing the correlation function in addition to the response function. As the initial step, I therefore calculated the correlation functions for the tree-ring data and the individual climate variables (mean monthly temperature, monthly precipitation, monthly SOI and seasonal SOI). For the monthly data, the dendroclimatic window consisted of 22 months, from September at the beginning of the previous growing season to June at the end of the current growing season. For the seasonal SOI data, the dendroclimatic window was more extensive: it contained 15 seasons, starting with spring (September to November) three years prior to the growing season, and ending with autumn (March to May) at the end of the current growing season.

I included the climate data from the previous year(s) in the analyses, because Fritts (1976) and many other authors (in New Zealand, for example: Xiong, 1995; Buckley *et al.*, 2000; Fowler *et al.*, 2000; Palmer and Xiong, 2003) have shown that climate often affects tree growth not only in the current year, but also in several following years. This phenomenon is called physiological preconditioning, and it is statistically expressed as autocorrelation in ring widths. To remove the autocorrelation, I prewhitened both the tree-ring and the climate data through autoregressive modelling (Box and Jenkins, 1970). The selection of the AR order was based on the minimum AIC (Akaike, 1974). The prewhitening was done over the common period between the tree-ring and the climate data, which differed according to each climate variable.

After the AR modelling, I calculated the correlation functions for all sites. The Pearson's product moment correlation coefficient was calculated for the tree-ring data and the individual

monthly or seasonal climate data, over the entire common period. In addition, I examined the temporal integrity of the relationship between tree growth and mean monthly temperature. This was achieved by dividing the data sets into two periods of equal length, and by calculating two separate correlation functions – one for the early, the other for the late period.

I then used the mean monthly temperatures for the climate-response modelling (separate models were developed for each site). To estimate the statistical relationship between tree growth and climate, i.e. to calibrate the models, I used the principal component (PC) regression analysis (Cooley and Lohnes, 1971). Using an independent data set, the estimated data were then compared with observed data previously withheld from the calibration procedure, i.e. the models were verified (Fritts, 1976). I employed the split calibration / verification method, dividing the data into two halves. I used one for calibration and the other for verification, and then I reversed the order. The PC regression technique was applied to the prewhitened data (see above), and the predictors were first screened by their correlation with predictands. Only the predictors that were correlated with tree-ring data at 0.05 or higher probability level entered into the PCA. I eliminated the high-order eigenvectors (that account for very little variance) by retaining only eigenvectors with eigenvalues larger than one in the model. I used the PCREG software (E. Cook, pers.comm.) for all procedures.

The degree of similarity between estimated and observed data can be measured by a number of verification statistics (Fritts, 1976; Fritts *et al.*, 1990; Cook, 1992). In this study, I used the following to assess the reliability of the calibration models: the Pearson's product moment correlation coefficient (RP), the robust correlation coefficient (RR), the Spearman's coefficient of rank correlation (RS), the product means test (PM), the sign test (ST), the reduction of error statistic (RE), and the coefficient of efficiency (CE).

The RP statistic measures the covariance that is common to two data sets. It is insensitive to differences in mean and variance between the two data sets, and it reflects the entire spectrum of variation, including both high and low frequencies. The robust correlation coefficient (RR) is based on a biweight influence curve. The RS is a nonparametric test that measures association between two data sets by ranking the data and then calculating the correlation of the assigned ranks.

The sign test (ST) is a nonparametric test that simply counts the number of times that the signs of the departures from the mean agree or disagree. The ST is considered a success when

the sign of the estimate is more often correct than would be expected from random numbers. The PM accounts for both the sign and the magnitude of the departure from the calibration average. It is computed from the product of the estimated and observed departures from the mean, with the positive and negative products summed separately. The mean is calculated for each group, and the difference between the two absolute values is then tested for significance.

The RE is a highly-sensitive measure of reliability, and it is calculated by dividing the sum of the squared differences between observed and estimated values by the sum of the squared differences between observed values and the calibration mean, and subtracting that value from one. The CE is very similar to the RE, but it uses the verification mean for the calculation. CE is almost always less than RE, and that makes it the most difficult statistic to pass. Both the RE and the CE values can range from negative infinity to one, which indicates perfect estimation. The RE and the CE cannot be tested for significance, but in general, any positive values indicate some skill in the regression model.

3.4 Results

3.4.1 Correlation functions – temperature

The original common period between the tree-ring and the mean monthly temperature data (1894-1998 or 1894-1999, according to each site) was reduced by three or four years, to 1897-1998. This loss of data occurred for the following reasons: (a) the climate data were shifted backwards by one year to account for the Southern Hemisphere growth season, (b) the 22-month climatic window was used for the analyses, and (c) both the tree-ring and the climate data were prewhitened to remove autocorrelation.

Correlations between the prewhitened RCS chronologies and mean monthly temperatures, calculated over 102 years (1897-1998), are shown in Figure 3.7. Most sites exhibit a strong positive response over the entire growing season, broadly from September to May (and in several cases, even up to June). The current January-March temperatures appear to have the strongest influence on tree growth, with the highest correlations occurring in February. Twelve sites (with the exception of TOS) show significant ($P<0.05$) response to the February mean temperature. The ring widths are also affected by spring temperatures, especially in September, when again all sites except TOS show significant correlations with climate. At many sites, the winter temperatures (just prior to the growing season) seem to be of some importance.

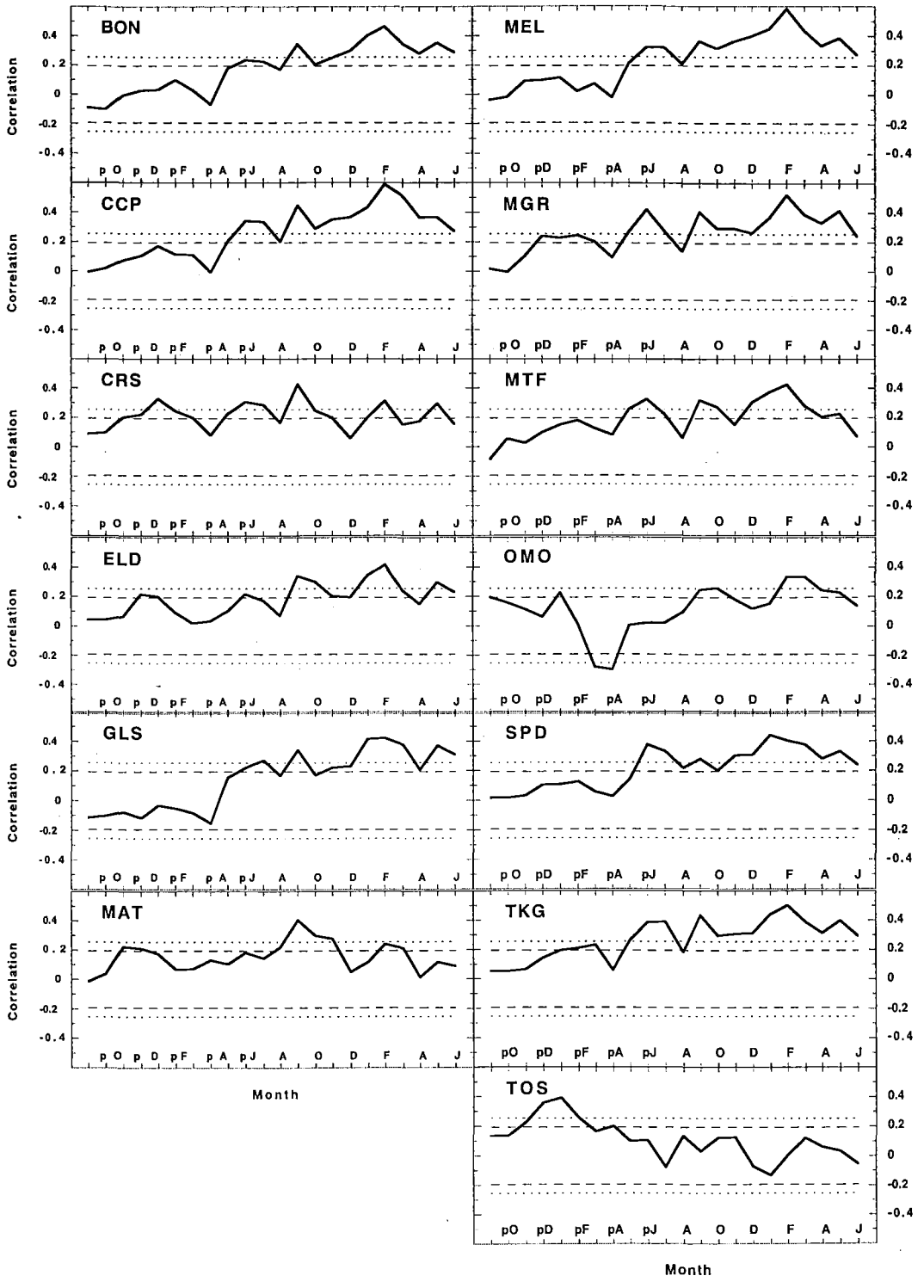

Figure 3.7 Correlation of site chronologies with the mean monthly temperature (Hokitika climate station). The period of analysis is 1897-1998. Climatic window is September of the previous growing season to June at the end of the current growing season. Dashed and dotted lines indicate 95% and 99% confidence limits, respectively.

TOS is the only site that does not respond to the temperatures in the current growing season – the only significant correlations occur during the previous growing season. Several other sites are also positively correlated with temperatures during the previous growing season, although the relationships are not as strong. The only significant negative correlations between ring widths and temperature occur at OMO, for the early autumn (March and April) of the previous year. The results of the correlation functions are summarised in Table 3.1. On average, tree-ring data were significantly correlated with temperatures over twelve months, ranging from five for TOS to seventeen for MGR.

Table 3.1 Correlation between the mean monthly temperature and the tree-ring data (1897-1998). The plus symbols indicate significant positive correlations ($P<0.05$), and the minus symbols indicate significant negative correlations ($P<0.05$). Total = the total number of significant variables (both positive and negative) for each site/month.

Month	BON	CCP	CRS	ELD	GLS	MAT	MEL	MGR	MTF	OMO	SPD	TKG	TOS	Total
prev. Sep										+				**1**
prev. Oct														**0**
prev. Nov			+			+							+	**3**
prev. Dec			+	+		+		+					+	**5**
prev. Jan			+	+				+		+		+	+	**6**
prev. Feb			+					+				+	+	**4**
prev. Mar			+					+		-		+		**4**
prev. Apr										-			+	**2**
prev. May		+	+				+	+	+			+		**6**
prev. Jun	+	+	+	+	+		+	+	+		+	+		**10**
Jul	+	+	+		+		+	+	+		+	+		**9**
Aug		+				+	+				+			**4**
Sep	+	+	+	+	+	+	+	+	+	+	+	+		**12**
Oct	+	+	+	+		+	+	+	+	+	+	+		**11**
Nov	+	+	+	+	+	+	+	+			+	+		**10**
Dec	+	+		+	+		+	+	+		+	+		**9**
Jan	+	+	+	+	+		+	+	+		+	+		**10**
Feb	+	+	+	+	+	+	+	+	+	+	+	+		**12**
Mar	+	+		+	+	+	+	+	+	+	+	+		**11**
Apr	+	+			+		+	+	+	+	+	+		**9**
May	+	+	+	+	+		+	+	+	+	+	+		**11**
Jun	+	+		+	+		+	+			+	+		**8**
Total	**12**	**14**	**14**	**12**	**11**	**8**	**14**	**17**	**11**	**10**	**13**	**16**	**5**	**157**

The temporal inconsistency of the relationship between tree growth and temperature is apparent, when the correlations are calculated over two separate 51-year periods (Figure 3.8). In the early period (1897-1947), spring temperatures have the biggest influence. This is

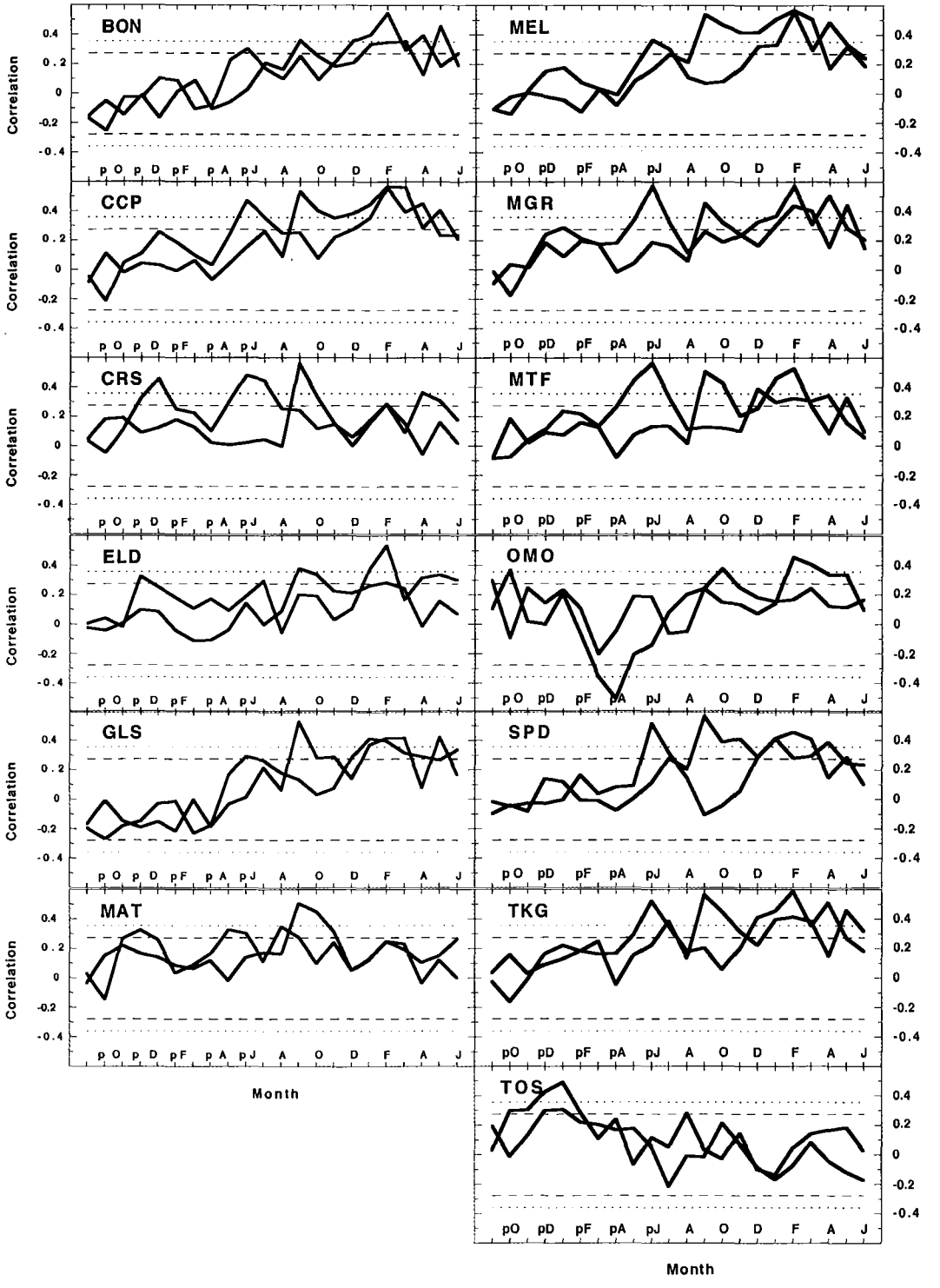

Figure 3.8 Temporal variability of the tree growth – mean monthly temperature relationship. Correlations were calculated for early (1897-1947; blue) and late (1948-1998; red) periods. Climatic window is from previous September to current June. Dashed and dotted lines indicate 95% and 99% confidence limits, respectively.

especially true for September. The positive (TOS) and negative (OMO) correlations in the previous growing season are also much stronger in the early period. The late period (1948-1998) shows, on the other hand, that temperatures significantly affect tree growth in winter prior to the growing season. Also, correlations between the chronologies and current-April temperature are remarkably higher (except for OMO and TOS) in the late period. The only months, in which the relationship is consistently significant for most of the sites, are January, February and March.

3.4.2 Correlation functions – precipitation

The relationship between tree-ring data and precipitation is very weak (Figure 3.9). It is only the negative correlations with January precipitation that stand out – the correlation coefficient is significant ($P<0.05$) for eight sites. There are occasional other significant relationships between the chronologies and the monthly data, both positive (CRS, SPD, TOS) and negative (BON, CRS, GLS, MTF, TOS), but they lack any consistent pattern. Two sites (ELD and OMO) show no significant correlation for any of the 22 months examined. The initial 1894-1993 common period was reduced by four years to 1897-1992 for the analytical purposes, due to the reasons stated earlier (Section 3.4.1).

3.4.3 Correlation functions – SOI

Even though the SOI record starts in 1876, the relationships between SOI and tree growth could only be investigated over the shortened periods of 1879-1998 (for the 22-month dendroclimatic window) and 1881-1998 (for the 15-season dendroclimatic window). Explanation for the loss of several years of data is given earlier (Section 3.4.1). Most chronologies and the monthly SOI are positively correlated over the growing season, and in winter prior to the growing season (Figure 3.10). The correlation coefficient values often exceed the 5% significance limit. OMO (with the exception of September and October) and TOS (August) do not show any significant relationships over this period. The correlations between tree growth and SOI in the previous year are seldom significant - only a few negative (GLS, SPD) and positive (MTF, OMO, TOS) responses can be detected. Three chronologies (CRS, ELD and MAT) exhibit no significant relationship with any of the 22 monthly SOI values.

The extended dendroclimatic window compares the chronologies with the seasonal SOI values over the current growing season, and back to three years prior to the growing season (Figure 3.11). Current year's SOI is positively correlated with tree growth, which is consistent

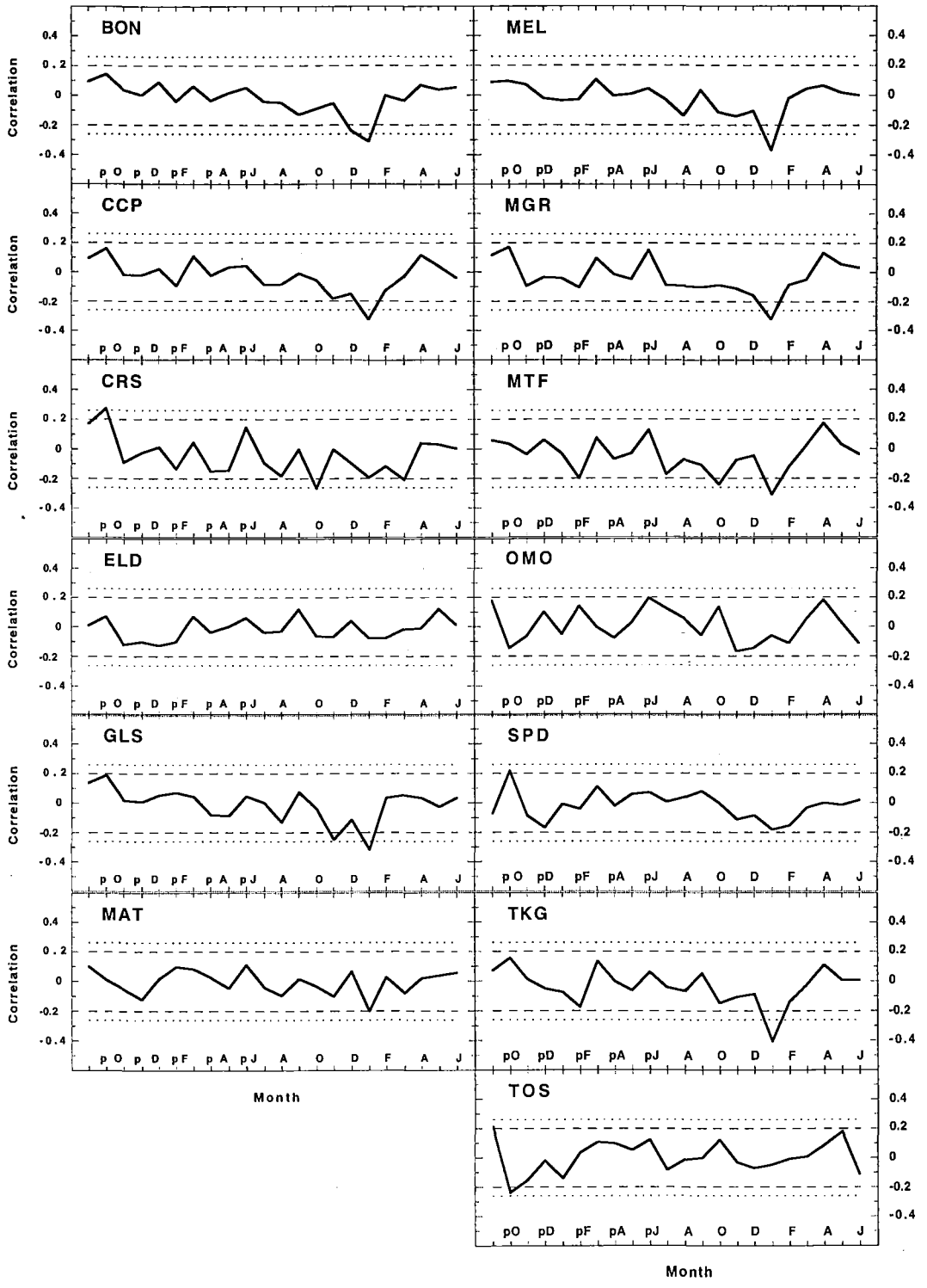

Figure 3.9 Correlation of site chronologies with the monthly precipitation (Hokitika climate station). The period of analysis is 1897-1992. Climatic window is September of the previous growing season to June at the end of the current growing season. Dashed and dotted lines indicate 95% and 99% confidence limits, respectively.

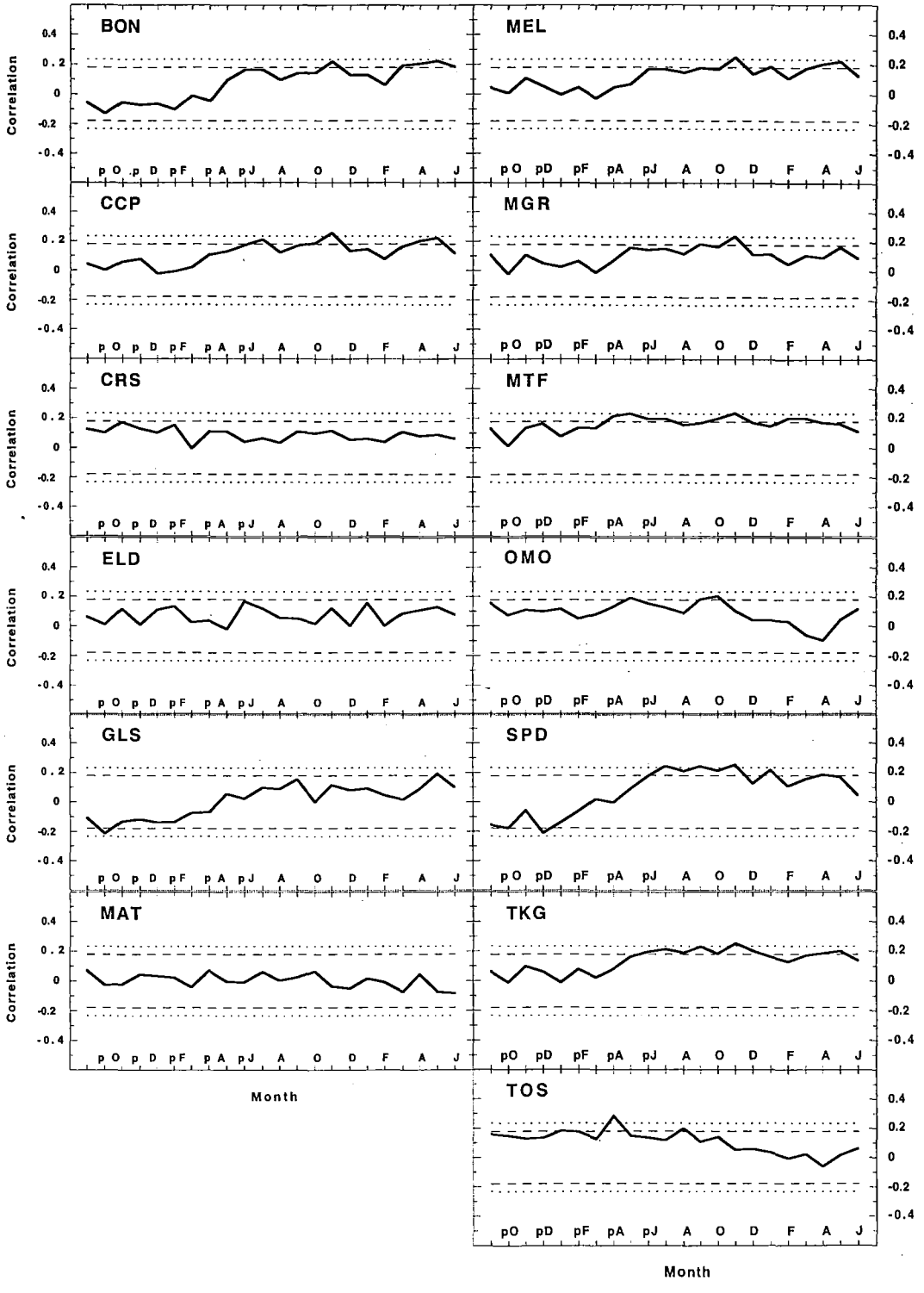

Figure 3.10 Correlation of site chronologies with the monthly SOI. The period of analysis is 1879-1998. Climatic window is September of the previous growing season to June at the end of the current growing season. Dashed and dotted lines indicate 95% and 99% confidence limits, respectively.

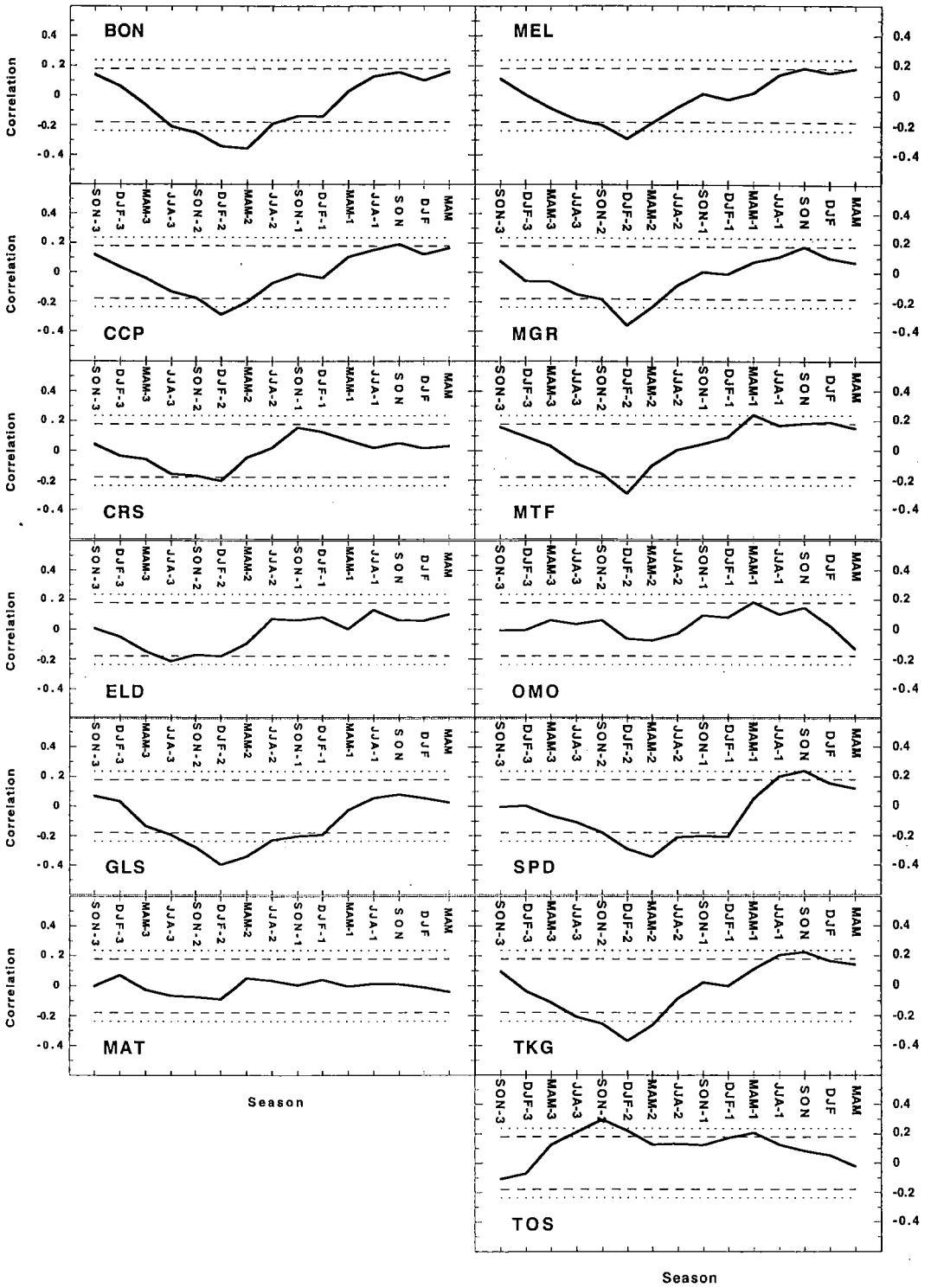

Figure 3.11 Correlation of site chronologies with the seasonal SOI. The period of analysis is 1881-1998. Climatic window is spring (September to November) three years prior to the growing season, to autumn (March to May) at the end of the current growing season. Dashed and dotted lines indicate 95% and 99% confidence limits, respectively.

with the results obtained from monthly data. This is especially true for spring (September to November), since November was the month in which SOI best correlated with the tree-ring data (significant for seven sites; Figure 3.10). However, the most striking feature of the correlation plots in Figure 3.11 is the strong negative response to SOI two years prior to the growing season. The inverse relationship between the tree-ring data and the summer SOI two years prior to the growing season is significant ($P<0.05$) for ten sites. The three exceptions are: MAT (no significant relationship whatsoever), OMO (one barely significant positive relationship in autumn of the previous growing season) and TOS (a pattern opposite to the other sites – strong positive relationships with SOI two years prior to the growing season).

3.4.4 Temperature response models

It is clear from the correlation functions that temperature is the main growth-limiting factor. The tree-ring data also show occasional significant relationships with precipitation and SOI over the 22-month dendroclimatic window, but this is likely the result of intercorrelation among the climate variables. For example, in January (1894-1993), temperature is correlated negatively with precipitation (Pearson's product moment correlation coefficient: $RP = -0.216$, $P<0.05$) and positively with SOI (Pearson's product moment correlation coefficient: $RP = 0.276$, $P<0.01$). It appears that cloudiness (sunshine hours, inversely) is an important common factor that is partly responsible for the intercorrelation among the variables (Table 3.2).

Table 3.2 Correlation matrix for the four different climate variables. The January values are compared over the common period of 1912-1993. The sunshine hours were recorded by the Hokitika meteorological station (data source: L. Xiong, pers. comm.). Number of stars indicates the level of significance: ***P<0.001; **P<0.01; *P<0.05.

	Temperature	Precipitation	SOI	Sunshine
Temperature	1			
Precipitation	-0.182	1		
SOI	0.244*	-0.210	1	
Sunshine	0.258*	-0.477***	0.283**	1

I created the calibration and verification periods by dividing the data into two equal parts: 1897-1947 ("early") and 1948-1998 ("late"). The 22 predictors (mean monthly temperature) were screened and only those that correlated significantly ($P<0.05$) with the predictand (tree-ring data) entered into the PCA. Their number was thus reduced to about six in the early, and to about seven in the late calibration period (Figure 3.8; Table 3.3a; Table 3.4a). The amount of variance explained by temperature increased accordingly, from 36% in the early calibration

period (Table 3.3a) to 39% in the late calibration period (Table 3.4a). The biggest changes in the amount of variance explained occurred in MGR (increase from 34% to 60%) and OMO (decrease from 47% to 18%).

Tables 3.3a and 3.3b Calibration (a) and verification (b) statistics for the temperature response model for the early calibration period (1897-1947). RP = the Pearson's product moment correlation coefficient; RR = the robust correlation coefficient; RS = the Spearman's coefficient of rank correlation; PM = the product means test; ST = the sign test; RSQ = the variance explained; Pred. = the number of predictors that entered into the PCA (i.e. the number of monthly variables that correlated with the tree-ring data at 5% significance level); RE = the reduction of error; CE = the coefficient of efficiency. In italics: non-significant statistics (P>0.05), and negative values of RE and CE.

Table 3.3a Calibration (1897-1947).

Site	RP	RR	RS	PM	ST	RSQ	Pred.
BON	0.54	0.64	0.60	0.010	38+ 13-	0.30	5
CCP	0.72	0.73	0.76	0.018	41+ 10-	0.52	9
CRS	0.51	0.53	0.53	0.005	38+ 13-	0.26	3
ELD	0.43	0.43	0.42	0.003	*31+ 20-*	0.18	3
GLS	0.57	0.56	0.59	0.007	36+ 15-	0.33	7
MAT	0.53	0.48	0.53	0.008	33+ 18-	0.28	3
MEL	0.68	0.69	0.69	0.017	39+ 12-	0.47	8
MGR	0.59	0.63	0.63	0.007	37+ 14-	0.34	6
MTF	0.65	0.67	0.74	0.006	43+ 8-	0.43	5
OMO	0.69	0.69	0.71	0.028	38+ 13-	0.47	7
SPD	0.64	0.70	0.67	0.011	38+ 13-	0.40	9
TKG	0.65	0.70	0.68	0.017	38+ 13-	0.42	9
TOS	0.48	0.49	0.49	0.007	34+ 17-	0.23	6

Table 3.3b Verification (1948-1998).

Site	RP	RR	RS	PM	ST	RE	CE
BON	0.56	0.59	0.53	0.010	37+ 14-	0.38	0.24
CCP	0.52	0.50	0.46	0.007	36+ 15-	0.44	0.25
CRS	0.30	0.26	0.26	*0.003*	*30+ 21-*	0.19	0.06
ELD	0.42	0.47	0.43	0.002	*29+ 22-*	0.30	0.10
GLS	0.42	0.44	0.41	0.007	*28+ 23-*	0.27	0.14
MAT	0.27	0.24	0.23	*0.001*	*31+ 20-*	*-0.38*	*-0.38*
MEL	0.49	0.53	0.53	0.009	33+ 18-	0.41	0.21
MGR	0.59	0.59	0.60	0.006	33+ 18-	0.48	0.27
MTF	0.35	0.38	0.38	*0.001*	34+ 17-	*-0.10*	*-0.10*
OMO	*0.20*	*0.18*	*0.18*	*0.003*	*30+ 21-*	*-0.08*	*-0.10*
SPD	0.33	0.31	0.24	0.009	*27+ 24-*	0.31	0.06
TKG	0.57	0.59	0.57	0.010	35+ 16-	0.42	0.32
TOS	0.29	0.31	0.30	0.003	*30+ 21-*	0.11	0.08

Tables 3.4a and 3.4b Calibration (a) and verification (b) statistics for the temperature response model for the late calibration period (1948-1998). RP = the Pearson's product moment correlation coefficient; RR = the robust correlation coefficient; RS = the Spearman's coefficient of rank correlation; PM = the product means test; ST = the sign test; RSQ = the variance explained; Pred. = the number of predictors that entered into the PCA (i.e. the number of monthly variables that correlated with the tree-ring data at 5% significance level); RE = the reduction of error; CE = the coefficient of efficiency. In italics: non-significant statistics (P>0.05), and negative values of RE and CE.

Table 3.4a Calibration (1948-1998).

Site	RP	RR	RS	PM	ST	RSQ	Pred.
BON	0.60	0.59	0.58	0.025	35+ 16-	0.36	7
CCP	0.70	0.70	0.66	0.012	38+ 13-	0.49	6
CRS	0.69	0.67	0.68	0.019	34+ 17-	0.48	8
ELD	0.65	0.66	0.63	0.005	36+ 15-	0.43	7
GLS	0.54	0.54	0.51	0.013	32+ 19-	0.29	7
MAT	0.53	0.53	0.51	0.002	35+ 16-	0.28	5
MEL	0.68	0.69	0.68	0.016	38+ 13-	0.46	8
MGR	0.77	0.78	0.78	0.010	43+ 8-	0.60	10
MTF	0.67	0.72	0.65	0.006	39+ 12-	0.45	8
OMO	0.42	0.41	0.42	0.007	36+ 15-	0.18	2
SPD	0.60	0.61	0.58	0.013	37+ 14-	0.37	7
TKG	0.77	0.78	0.79	0.014	45+ 6-	0.59	8
TOS	0.33	0.35	0.33	0.005	*31+ 20-*	0.11	2

Table 3.4b Verification (1897-1947).

Site	RP	RR	RS	PM	ST	RE	CE
BON	0.37	0.36	0.33	0.016	*30+ 21-*	0.16	*-0.13*
CCP	0.66	0.67	0.61	0.013	39+ 12-	0.52	0.42
CRS	*0.19*	0.25	*0.21*	*0.001*	*31+ 20-*	*-0.13*	*-0.38*
ELD	0.25	0.33	0.29	*0.001*	33+ 18-	0.10	*-0.10*
GLS	0.37	0.38	0.39	0.006	33+ 18-	0.16	*-0.13*
MAT	0.31	*0.19*	*0.22*	*-0.002*	38+ 13-	0.01	0.01
MEL	0.61	0.62	0.60	0.018	37+ 14-	0.49	0.32
MGR	0.50	0.56	0.50	0.008	34+ 17-	0.38	0.15
MTF	0.42	0.44	0.47	*0.004*	33+ 18-	*-0.13*	*-0.13*
OMO	*0.18*	*0.17*	*0.18*	*0.005*	*27+ 24-*	0.00	*-0.01*
SPD	0.50	0.53	0.48	0.013	32+ 19-	0.42	0.15
TKG	0.50	0.56	0.50	0.015	34+ 17-	0.28	0.19
TOS	0.50	0.52	0.49	0.007	33+ 18-	0.29	0.25

The results of the PC regression response functions are summarised in Tables 3.3a, 3.3b, 3.4a and 3.4b. In the early calibration period, the most successful models were developed for BON, ELD, MGR and TKG (Tables 3.3a and 3.3b). Several other sites (CCP, CRS, GLS, MEL, SPD and TOS) pass all or most of the verification statistics, however the poorer quality of the verification statistics (compared with the calibration statistics) indicates some artificial

predictability of these models. For MAT, MTF and OMO, the models were the least successful, as indicated by the negative values of both RE and CE.

In the late calibration period, the best models were developed for CCP, MEL and SPD (Tables 3.4a and 3.4b). For the TOS site, the model explains only 11% of variance in the calibration period, however the statistics markedly improve in the verification period. All the verification statistics for MGR and TKG are significant, but their values are substantially higher in the calibration period. BON, ELD and GLS pass most of the verification statistics, their weakest point being the negative values of CE. The MAT and OMO models perform badly, since the RE and CE statistics are near zero (values between –0.01 and +0.01), and most of the other verification statistics are not significant. The CRS and MTF models also fail to be successfully verified, with both RE and CE attaining negative values, and several other statistics below the 5% significance limit.

3.5 Discussion

Pink pine is sensitive to temperatures over most of the year, especially during the growing season (Figure 3.7). This response is consistent with results of other pink pine studies. Xiong *et al.* (1998) and D'Arrigo *et al.* (1998) have shown that two North Island chronologies were positively correlated with temperature at significant levels from September (November, respectively) to April. The Stewart Island chronologies (D'Arrigo *et al.*, 1995) exhibit a significant positive response for most of the months from September to May/June. Another New Zealand species that is positively correlated with temperature over the entire growing season is *Lagarostrobos colensoi* (D'Arrigo *et al.*, 1998; Cook *et al.*, 2002a). *Libocedrus bidwillii*, on the other hand, responds inversely to the late summer (February to March) temperatures of the previous growing season (Xiong and Palmer, 2000b; Palmer and Xiong, 2003). It must be noted, however, that none of the *L. bidwillii* sites were located in Westland, and that the temperature data used in the above two studies were the national average series (Salinger *et al.*, 1992a).

The significant response of pink pine's growth to the temperatures in the late autumn is surprising. It seems unlikely that growing season (especially at higher altitudes) would last until May or June. However, there is no specific information on the growth of pink pine. As Norton (1990) pointed out, the paucity of knowledge on the ecology and life history of many of the tree species investigated represents the most serious limitation in Southern Hemisphere dendrochronology. Although Xiong *et al.* (1998) suggest that the growing season lasts

approximately from September to April, results of this study indicate that final cell development persists at least into May. Similar findings by D'Arrigo *et al.* (1998) also support this. Wardle (1963) noted that in fact, only two seasons can be recognised in the New Zealand mountains: the warm season, when growth takes place; and the cold season, when plants are inactive. It is possible that in some cases, this cold season could last only for two to three months.

The dependence of the temperature response on altitude is uncertain. Buckley *et al.* (1997) found that the relationship between the Tasmanian *Lagarostrobos franklinii* and the current season's temperature is strong and positive, provided sites are located at high altitudes. Low-altitude *L. franklinii* chronologies showed weaker, direct response to the current season's temperature, and a strong, negative correlation over the previous season. Most of the high-altitude pink pine chronologies also show significant, positive relationships over the current year, and the low-altitude OMO site reacts in a manner similar to the low-altitude *L.franklinii*. However, the other low-altitude chronology (TOS) does not follow the pattern. TOS shows no response over the current year, and a significant positive relationship during the previous summer. Since TOS is a site that had been disturbed (logging), it is possible that the disturbance affected the shape of the correlation function. Although in that case, correlation between TOS and temperatures should have been different in early and late periods (the logging occurred only recently) – yet Figure 3.8 shows no such difference.

The temporal variability of the relationship between temperature and tree growth, exhibited by most chronologies (Figure 3.8), is of common occurrence in dendroclimatology (Briffa *et al.*, 1998a). In the Southern Hemisphere, Allen (1998) obtained similar results with the Tasmanian *Phyllocladus asplenifolius*. As Briffa *et al.* (1998a) noted, this change in tree-growth response has important implications for climate reconstructions – it may lead to inaccuracies in estimates of both past and future conditions. Thus although Figure 3.7 indicates that pink pine might be used to reconstruct temperatures over longer periods, only the months over which the relationships are time-stable (i.e. January-March; Figure 3.8) should be given priority.

The consistently strong response of pink pine to late-summer temperatures is in accordance with the results of Cook *et al.* (2002a). The authors compared the Oroko Swamp *Lagarostrobos colensoi* chronology with Hokitika's mean monthly temperatures, and found the January-March period to be the most stable and dependable temperature response model.

Precipitation does not seem to affect the growth of pink pine in any substantial way. These results were expected (see Section 3.2.2 for details). Most of the Westland chronologies exhibit only a significant negative response to January rainfall. This could be seen, in fact, as a temperature signal. Since increased cloudiness leads to cooler temperatures in summer, and to warmer temperatures in winter (S.Larsen, pers. comm.), more rainfall in January would be associated with more cloud cover and consequently, with lower temperatures for that month.

Relationships between the growth of pink pine and precipitation have also been investigated by Xiong *et al.* (1998). The authors have found that a North Island chronology was positively correlated with May precipitation (when using the New Zealand average climate data), and in addition to this, it also showed a significant negative response to August precipitation (when using the local climate series). These results (plus the strong temperature-growth relationships mentioned earlier) obtained by Xiong *et al.* (1998) emphasised that: (a) pink pine is better at reflecting temperature than precipitation conditions; (b) the choice of meteorological, and precipitation in particular, data (regional v. local) has a great effect on the final outcome; and (c) the growing season could indeed extend until May (as indicated by the significant response for this month, and as discussed earlier).

Pink pine responds positively to the current season's SOI, and negatively to the SOI two years prior to the growing season. In Northland, *Agathis australis* reacts in an exactly opposite manner (Fowler *et al.*, 2000). This is expected, given the nature of the relationships (teleconnections) between ENSO and New Zealand climate (Gordon, 1985; Mullan, 1995). Southwesterly airflow is prevalent during the negative phases of SOI (El Niño conditions), and this leads to cooler temperatures and to increased rainfall in the south and west of the South Island, while the north and east of the North Island are drier. La Niña brings northerly and northeasterly winds, and consequently warmer temperatures and less precipitation to the southwest, while the northeast usually experiences above-average precipitation. The rainfall pattern in Northland is therefore clearly opposite to that in Westland. The correlations between SOI and temperature are positive for the whole country, but here we must be aware of the fact that pink pine responds to temperature positively, while the relationship between the growth of *Agathis australis* and temperature is inverse (Buckley *et al.*, 2000). Thus the mirror-like shape of the correlation functions is absolutely sound.

Although the influence of ENSO on New Zealand climate is greatest in the spring (Mullan, 1995), the strongest relationships between the pink pine chronologies and SOI occurred in

December-February (two years prior to the growing season). Several other studies from Mexico and/or USA have also shown that the extratropical teleconnections of ENSO are strongest in December-February (Cleaveland *et al.*, 1992; D'Arrigo and Jacoby, 1992; Stahle and Cleaveland, 1993; Cole and Cook, 1998; Stahle *et al.*, 1998). The North American chronologies respond to SOI either concurrently, or follow it by one year (Stahle *et al.*, 1998). The lag of two years (between the instrumental SOI and the tree-ring data) was present in two other Southern Hemisphere studies, which investigated the climate response of *Agathis australis* (Fowler *et al.*, 2000) and *Tectona grandis* (Stahle *et al.*, 1998). Fowler *et al.* (2000) suggest that this may partly reflect the quasibiennial tendency of ENSO, but is more likely to be associated with tree phenology.

The significant relationships between SOI and most chronologies indicate that Westland pink pine might be useful in reconstructing past ENSO variability. Further research should explore this potential. However, in this thesis, I want to focus on the primary growth-limiting factor, which is temperature. As Jones *et al.* (2001) pointed out, "no climate proxy directly measures variability of the atmospheric circulation, but instead records its local environmental influence" (through the indirect effects on temperature or precipitation at the proxy sites). That is to say, the SOI signal that is contained in the pink pine chronologies is, for the most part, a temperature signal. This was also indicated by the intercorrelation among the climate variables (Table 3.2). I have therefore used only temperature as a predictor in the climate response models, to investigate the temperature-growth relationships in more detail (as temperature is the variable that will be reconstructed in Chapter 4).

Better calibration results were obtained when using the late period. However, those models were verified with less success than the models that were calibrated on the early period. One reason for both the calibration and the verification statistics being more satisfactory in the late period could be that climatic conditions in the second half of the 20th century were different from the conditions in the early part (Salinger, 1988). Also, meteorological data are of generally higher quality in the latter half of the record (Salinger, 1981). It is important to keep in mind that the climate-growth modelling involves a number of limiting assumptions (Fritts, 1990) that are seldom completely met, and that calibration is only a simplified version of the complex relationships between tree growth and climate. Therefore only some percentage (less than 50% for most sites) of the variance in tree rings could be explained by temperature.

3.6 Summary and conclusions

I investigated the nature and strength of the climate signal that was contained in thirteen pink pine chronologies. The dendroclimatic window over which the correlation functions were calculated extended over 22 months (mean monthly temperature, monthly precipitation and monthly SOI) or 15 seasons (seasonal SOI). I found that the growth of pink pine was directly affected by temperature. The tree-ring data were positively correlated with temperature over the entire growing season (approximately from September to May), and the strongest and most consistent relationships occurred in January-March. Chronologies were negatively correlated with January precipitation, but in general, the influence of rainfall on tree growth was negligible. The relationship with SOI was direct during the growing season (in agreement with the temperature response), and inverse when calculated for a lag of two years. The low-altitude chronologies (OMO and TOS) responded to climate in a different way than the remaining eleven chronologies, however, it was not clear whether this was an effect of altitude or disturbances.

Only the temperature data were used for the climate response modelling. Employing the principal component regression technique, I developed two models for each site. The models that were calibrated on the late period explained more variance, but were verified with less success than the early-period models. Although some of the chronologies will have to be rejected from further research, the results showed that overall, pink pine holds great potential for temperature reconstruction. A proxy record of the Westland temperature will be derived in the next chapter.

Chapter 4

Temperature reconstruction

4.1 Introduction

One of the first palaeotemperature records in New Zealand was derived from a stalagmite in a north-west Nelson cave (Wilson *et al.*, 1979). The series (annual temperatures smoothed with 50-year running mean) extended back to about 1150. Although the dating had been considered inaccurate (Burrows and Greenland, 1979; Burrows, 1982), recent research (Palmer and Xiong, 2003) indicates that the speleothem-derived data need to be offset by only 13 years. Concurrently with Wilson *et al.* (1979), Burrows and Greenland (1979) analysed the diverse evidence for temperature variation in New Zealand over the last 1000 years. Burrows and Greenland (1979) studied both instrumental records and proxies (i.e. indirect evidence from various natural phenomena, such as iceberg sightings or changes in glaciers, treeline and snowline). The authors noted that much of the evidence was weak, equivocal, difficult to interpret or difficult to place in time. When reviewing the usefulness of proxy records, Burrows (1982) emphasised that tree rings hold the greatest promise as the providers of precise and high-resolution palaeotemperature data.

New Zealand's first temperature reconstruction derived from tree rings was based on ten chronologies from subalpine *Nothofagus menziesii* and *N. solandri* (Norton *et al.*, 1989). The proxy record of summer (December-March) temperatures extended back to 1730. The three reconstructions that followed (Palmer, 1989; Salinger *et al.*, 1994; Xiong and Palmer, 2000b) were of similar length. Palmer (1989) used nine *Phyllocladus trichomanoides* and *P. glaucus* chronologies to reconstruct January-March temperatures back to 1750. Salinger *et al.* (1994) reconstructed November-March temperatures back to 1731, using eight chronologies from five different species (*Agathis australis*, *Phyllocladus trichomanoides*, *P. glaucus*, *Nothofagus menziesii* and *N. solandri*). Xiong and Palmer (2000b) derived their record (February-March temperatures; extending back to 1720) from eleven *Libocedrus bidwillii* chronologies. All four reconstructions were based on the New Zealand average temperature series (Salinger, 1980c).

Recently, three records longer than 500 years have been produced. January-March temperatures were derived from a *Lagarostrobos colensoi* tree-ring chronology from Oroko Swamp, using local (Hokitika) meteorological data. The first reconstruction (Cook *et al.*, 2002a) extended back to 1200. Additional sampling resulted in a reconstruction covering the past 1100 years (Cook *et al.*, 2002b). (Note: further details on the Oroko Swamp reconstruction are given in Section 4.2.3). The latest palaeotemperature record to be produced from New Zealand tree rings, is the series derived from five *Libocedrus bidwillii* chronologies located in the North Island (Palmer and Xiong, 2003). The updated New Zealand average temperature series (Salinger *et al.*, 1992a) were used to reconstruct February-March temperatures back to 1459.

In this chapter, I present a new palaeotemperature record, which focuses on regional (Westland) climate. All the previous multi-site reconstructions have been New-Zealand-wide, and only the single-site *Lagarastrobos colensoi* reconstruction (Oroko Swamp; Cook *et al.*, 2002b) has been from Westland. First, I created a composite chronology by merging tree-ring data from six Westland sites. I calibrated this RCS chronology with Hokitika summer temperatures, to obtain a reconstruction extending back to 1480. Finally, I compared the results with the Oroko Swamp proxy record (Cook *et al.*, 2002b).

4.2 Materials and methods

4.2.1 Development of a regional chronology

I created the Westland Regional Chronology (WRC) by merging ring-width series from six sites into one composite set. I selected sites that would contribute to the WRC using the results of Chapters 2 and 3. Six chronologies exhibited the highest degree of similarity (Section 2.4.3), and showed a strong, consistent response to January-March temperatures (Section 3.4.1). These were: BON, CCP, GLS, MEL, MGR and TKG. To exclude any potential effect the Mt. Bonar disturbance (Section 2.2) could have on the WRC, I truncated all BON samples at the year 1950. The remaining seven chronologies were not included in the WRC for the following reasons: (a) sites located outside of Westland (ELD, SPD), (b) a low-frequency component that was substantially different from the trends exhibited by other chronologies (MTF; Figure 2.31), and (c) weak response to summer temperatures (CRS, MAT, OMO and TOS, Figure 3.8).

I re-detrended this new subset of individual ring-width series using the RCS technique (Chapter 2). I developed a new mean growth curve, over which I superimposed a simple theoretical curve (1/3 spline). This fitted regional curve was then used for standardisation. I used the arithmetic mean method (Cook *et al.*, 1990b) for chronology computation. The regional chronology was low-pass filtered with a 25-year smoothing spline, and I estimated 95% confidence limits for the filtered series using the bootstrap method (Efron, 1987). I used the ARSTAN programme (Cook, 1985; updated version: E. Cook, pers. comm.) for all procedures. For further details on chronology development, see Chapter 2.

4.2.2 Temperature reconstruction

The WRC-based (henceforth referred to as "Westland") temperature reconstruction was produced following standard calibration and verification techniques (Fritts, 1976; Cook and Kairiukstis, 1990). The tree-ring indices (WRC) acted as a predictor in the transfer function. As the predictand, I used the January-March mean of Hokitika homogenised temperatures (Salinger *et al.*, 1992a; Section 3.2.1). I selected the late-summer season because Section 3.4.1 indicated that January-March temperatures had the most influence on tree growth, and that the relationship was stable in time.

I used simple linear regression analysis to transform the tree-ring data into the estimates of summer temperatures. Prior to regression, the tree-ring data were prewhitened as an AR(1) process. The AR order was determined by the minimum AIC procedure (Akaike, 1974). The climate data did not require prewhitening. To develop and validate the regression model, I used the split calibration / verification method. I divided the data into two equal periods (1894-1946 and 1947-1999), using one for calibration and the other for verification, then reversing the order. For further details on calibration and verification, see Section 3.3.

The frequency-domain fidelity of the reconstruction was evaluated using spectral and cross-spectral analyses (Koopmans, 1974; Kendall and Ord, 1990). I analysed both the observed and reconstructed data over the common period 1866-1999 (with missing values in 1881-1893 for the observed temperatures). The spectra were calculated from 33 lags (25% of the series length) of the autocovariance function. I also computed the spectrum of the entire reconstruction (1480-2000), and this was done from 130 lags, at wavelengths longer than 10 years. I used the ARAND software (Howell, 2001) for the analyses.

4.2.3 The Oroko Swamp proxy record

Using correlation analyses, the Westland reconstruction was then compared with a palaeotemperature series derived from *Lagarostrobos colensoi* growing in Oroko Swamp (Cook *et al.*, 2002b). The infertile and acidic Oroko Swamp is located in Westland (43°14'S, 170°17'E), at an elevation of 110 m a.s.l. The original *Lagarostrobos colensoi* ring-width chronology covered the period 816-1998 (the first tree-ring chronology from New Zealand to span the past millennium; Cook *et al.*, 2002a), and was positively correlated with September-May Hokitika temperatures. The strongest and most stable temperature-growth relationships occurred in January-March (Cook *et al.*, 2002a).

Subsequent addition of sub-fossil material resulted in a new, improved chronology, covering the period 700-1999 (Cook *et al.*, 2002b). The increased sample depth enabled the authors to use the RCS method (Briffa *et al.*, 1992), which preserved much of the low-frequency variance in the tree-ring data (Cook *et al.*, 2002b). Figure 4.1 shows the resulting Oroko Swamp *L. colensoi* (henceforth referred to as "Oroko") temperature reconstruction (Cook *et al.*, 2002b).

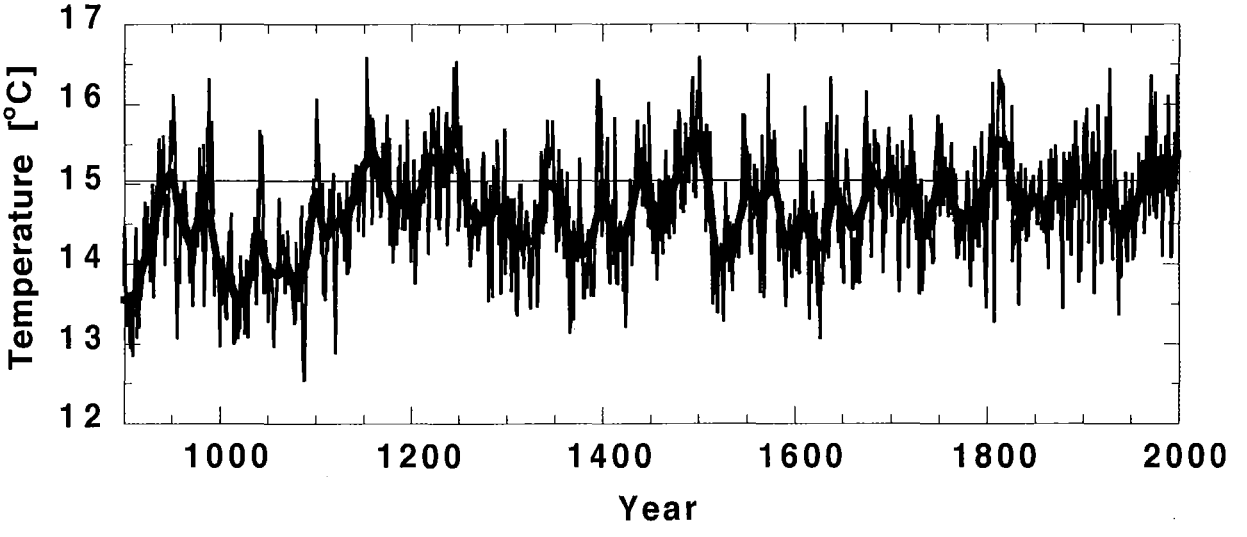

Figure 4.1 The Oroko Swamp summer (January-March) temperature reconstruction (900-1999). With overlaid 25-year smoothing (red), and the 20th century mean of Hokitika instrumental temperatures (black horizontal line). Note that after 1958, the temperature values are the observed Hokitika data. (Data source: E. Cook, pers. comm.).

The Oroko reconstruction was based on an 1894-1957 calibration period (RSQ = 0.38, RP = 0.62), while the 1866-1893 data were reserved for verification (RP = 0.65, RE = 0.35, CE = 0.35; temperature estimates were used for the 1881-1893 interval) (Cook *et al.*, 2002b). The post-1957 tree-ring data could not be used for either calibration or verification, because of a stand-wide disturbance that affected the trees (Cook *et al.*, 2002a). Among the most striking features of the 1100-year Oroko reconstruction (Figure 4.1) are: (1) the sustained low temperatures in the 993-1091 period, (2) the two above-average warm intervals in the 12th and 13th centuries, which are considered to be an expression of the Medieval Warm Period (Lamb, 1965) in New Zealand, (3) the sharp cooling at around 1500, and (4) the long-term warming trend since the 16th century, which includes the somewhat abrupt increase in temperatures after 1950 (Cook *et al.*, 2002b).

4.3 Results

4.3.1 The Westland Regional Chronology

The Westland Regional Chronology (WRC) spans 600 years (1400-1999), and contains 296 series from 173 trees (Figure 4.2). Mean segment length is 313 years, and average ring width is 0.41 mm. Increased growth is apparent in the mid-18th century, the second half of the 19th century and the second half of the 20th century. Tree growth was slow around 1560, 1900 and 1940, but the overall growth trend is positive. Also shown in Figure 4.2 is the age-aligned mean growth curve (truncated at 1000 years), and the fitted regional curve that was used to standardise the individual ring-width series.

The resulting RCS chronology (Figure 4.2) resembles the raw data closely, except for in the first few decades of the 15th century. The mean RBar of the RCS chronology / WRC is 0.202, standard deviation 0.221, mean sensitivity 0.115, and serial correlation 0.802. The first order of autoregression was selected and this AR(1) model explains 65.3% of the tree-ring variance. The running RBar and EPS plots (Figure 4.3) indicate that the WRC is reliable back to about 1480. Over the 1480-1999 period, the chronology is based on the mean of 20 or more series.

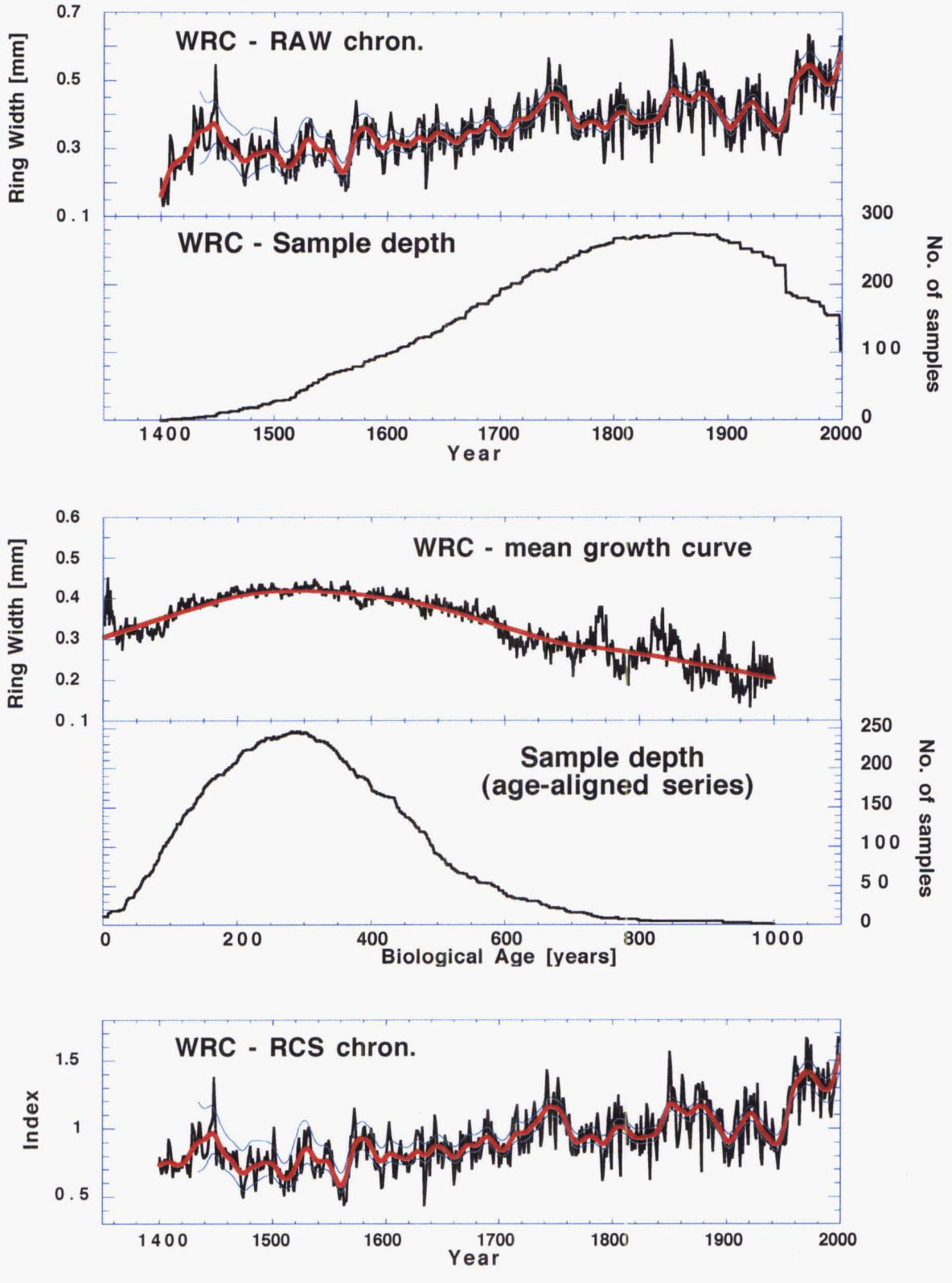

Figure 4.2 The Westland Regional Chronology plots (1400-1999). Top: The raw chronology and the sample size; middle: the age-aligned mean growth curve that was used to standardise the series (truncated at 1000 years), bottom: the RCS chronology. Red lines: overlaid smoothing (25-year splines were used for the chronologies, 1/3 spline for the growth curve). Bootstrap 95% confidence limits were computed for the chronologies (blue lines).

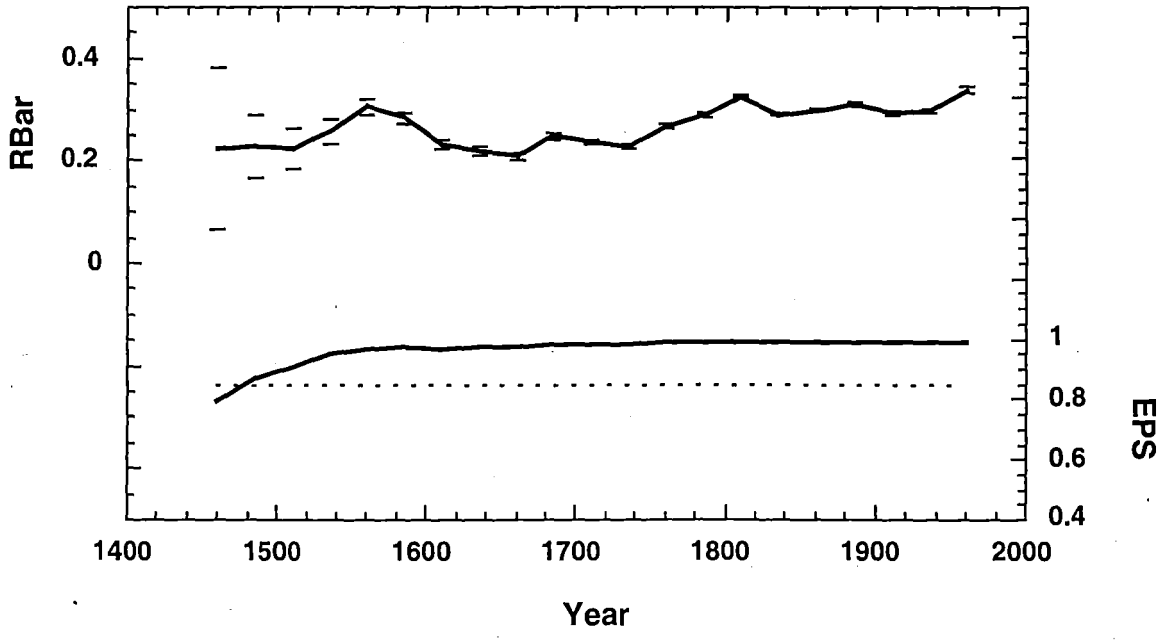

Figure 4.3 Running RBar and EPS plots for the Westland Regional Chronology. The RBar values ± 2 standard errors (horizontal markers) are in the upper part of the graph. The dotted line in the lower part of the graph indicates an EPS of 0.85.

4.3.2 Westland temperatures 1480-2000

Calibration and verification results for the Westland temperature reconstruction are shown in Tables 4.1a and 4.1b. The model calibrated on the early period (1894-1946) explains 42.9% of the variance in January to March temperatures (Table 4.1a), while the model based on the late period (1947-1999) explains 43.8% of the variance (Table 4.1b). Both models were validated successfully. RE>0.5, CE>0.4, and the high probability levels (P<0.001) for results of all remaining calibration and verification tests demonstrate the excellent performance of both models (Tables 4.1a and 4.1b). Using the entire period (1894-1999) for calibration, the tree-ring data explain 46.1% of the variance in temperature.

Because of the better verification statistics (Table 4.1a), I selected the early-calibration model to reconstruct Westland summer (January-March) temperatures back to 1480. The reconstructed data exhibit similar trends and amplitudes as the observed data over most of the common period (Figure 4.4), although occasional differences exist. The tree rings tend to overpredict the actual temperatures in the early part of the record – the estimated temperatures were higher (by more than 1°C) than the observed data in the following years: 1868, 1874,

1880, 1912, 1921, 1939 and 1950. Underpredicting (i.e. when reconstructed temperatures were lower than the recorded data by more than 1°C) occurred in 1894, 1904, 1918, 1929, 1938, 1958, 1965, 1975, 1984 and 1989. The year 1938 represents the most serious disagreement between the two records, since the actual January-March mean temperature was 2.5°C higher than its estimated value.

Tables 4.1a and 4.1b Calibration and verification statistics for the early (a) and late (b) calibration period. Stat. = statistic; P = probability level. RP = the Pearson's product moment correlation coefficient; RR = the robust correlation coefficient; RS = the Spearman's coefficient of rank correlation; PM = the product means test; ST = the sign test; RSQ = the variance explained; RE = the reduction of error; CE = the coefficient of efficiency.

Table 4.1a Early calibration.

Calibration (1894-1946)			Verification (1947-1999)		
Stat.	**Value**	**P**	**Stat.**	**Value**	**P**
RP	0.655	$< 10^{-5}$	RP	0.661	$< 10^{-5}$
RR	0.667	$< 10^{-5}$	RR	0.656	$< 10^{-5}$
RS	0.704	$< 10^{-5}$	RS	0.653	$< 10^{-5}$
PM	0.483	0.00034	PM	0.391	0.00024
ST	41+ 12-	0.00006	ST	40+ 13-	0.00018
RSQ	0.429	$< 10^{-5}$	RE	0.557	
			CE	0.422	

Table 4.1b Late calibration.

Calibration (1947-1999)			Verification (1894-1946)		
Stat.	**Value**	**P**	**Stat.**	**Value**	**P**
RP	0.661	$< 10^{-5}$	RP	0.655	$< 10^{-5}$
RR	0.656	$< 10^{-5}$	RR	0.667	$< 10^{-5}$
RS	0.653	$< 10^{-5}$	RS	0.704	$< 10^{-5}$
PM	0.346	0.00020	PM	0.404	0.00077
ST	40+ 13-	0.00018	ST	42+ 11-	0.00002
RSQ	0.438	$< 10^{-5}$	RE	0.508	
			CE	0.410	

Figure 4.5 shows the linear relationship between the continuous part of the instrumental record (1894-1999; 106 years) and the reconstructed data for the same period. The two datasets are highly correlated (Pearson's product moment correlation coefficient: RP = 0.69, P<0.001). Inclusion of the early record (1866-1880) increases the common period to 121 years, while reducing the correlation slightly (Pearson's product moment correlation coefficient: RP = 0.67, P<0.001).

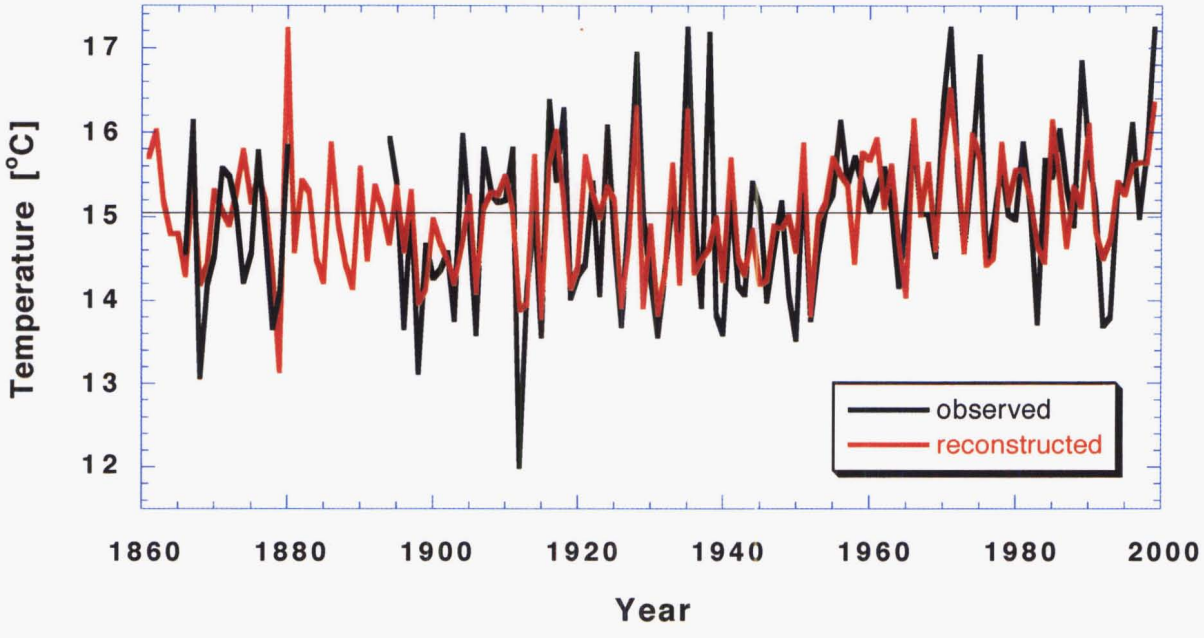

Figure 4.4 Observed (black) and reconstructed (red) Hokitika temperatures. Based on the 1894-1946 calibration period. The black horizontal line is the 20th century mean of Hokitika instrumental temperatures (January – March).

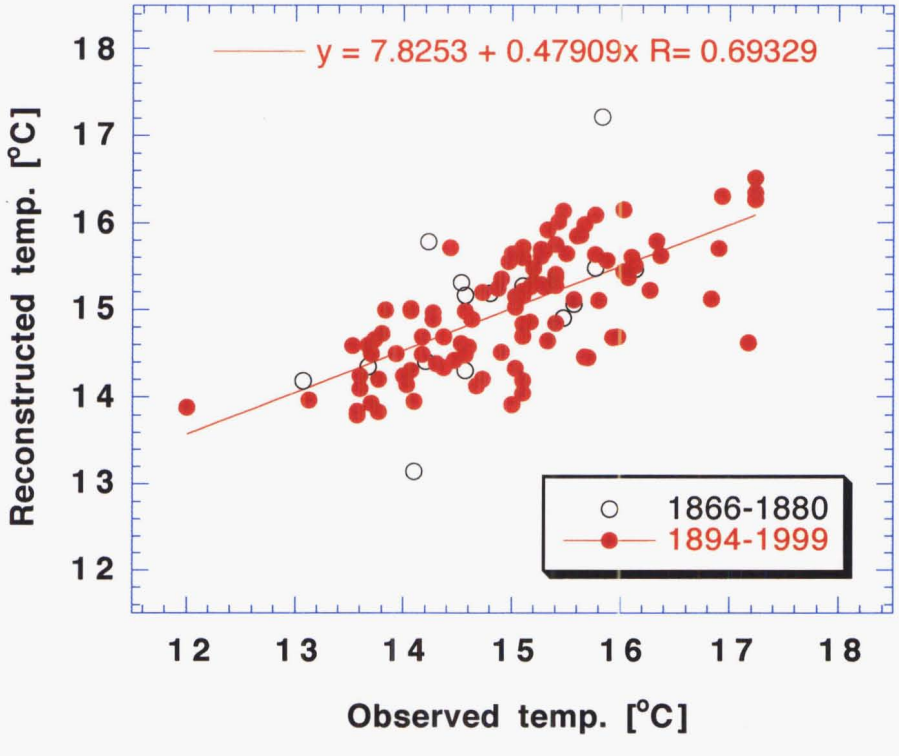

Figure 4.5 Scatter plot of the observed and reconstructed temperatures. Full red circles mark the data that were used for calibration and verification purposes (1894-1999). Early record (1866-1880) is indicated by open circles.

Based on the RBar and EPS statistics (Section 4.3.1), the Westland reconstruction is reliable back to 1480. Thus the proxy record is 400 years longer than the instrumental record (Table 4.2). The mean temperature over the entire period of reconstruction (1480-2000) is 0.22°C lower than the mean of January-March temperatures calculated from the Hokitika actual data (1866-1880 and 1894-1999). Both standard deviation and variance are much higher for the observed data. Distribution of the observed data is symmetrical (skewness near zero) and leptokurtic (positive kurtosis), whereas the reconstructed data are, over their entire length, right skewed and leptokurtic (Table 4.2). As the reconstructed data are not normally distributed (they are right skewed), some statistical assumptions may not be strictly valid.

Table 4.2 Statistics for the January-March observed (1866-1880 and 1894-1999) and reconstructed (A: 1866-1880 and 1894-1999; B: 1480-2000) temperature data.

	Obs. (1866-1880, 1894-1999)	**Rec. A (1866-1880, 1894-1999)**	**Rec. B (1480-2000)**
N [years]	121	121	521
Mean [°C]	15.00	15.02	14.78
Median [°C]	15.10	15.10	14.73
Minimum [°C]	12.00	13.14	13.14
Maximum [°C]	17.23	17.21	17.21
Standard deviation [°C]	0.957	0.699	0.584
Variance	0.915	0.488	0.341
Skewness	0.023	0.105	0.414
Kurtosis	0.261	-0.084	0.262

The reconstructed January-March Westland temperatures are shown in Figure 4.6. Summer temperatures have been steadily increasing over the entire length of the record, with highest values occurring after 1950. The abrupt change from the cold 1940s to the warm 1950s is comparable with another sharp increase in temperatures in the 1560s. Tables 4.3a and 4.3b list the coldest and warmest periods in the reconstruction, respectively. The mean temperature over the coldest 25-year period (1542-1566) was 14.39°C, i.e. 0.39°C below the 1480-2000 reconstruction mean (Table 4.3a). Because of the overall trend, fourteen out of fifteen coldest decades occurred before 1700. Over the last 300 years, the lowest temperatures occurred in 1898-1907 (Table 4.3a), which is consistent with the instrumental data (Salinger *et al.*, 1992).

The warmest 25-year period of the Westland reconstruction is 1966-1990, with an average temperature 0.56°C higher than the 1480-2000 mean (Table 4.3b). Besides the 20th century, temperatures were above the long-term average of 14.78°C also in the 1740s, 1750s, and in the 1830s to 1870s (Table 4.3b).

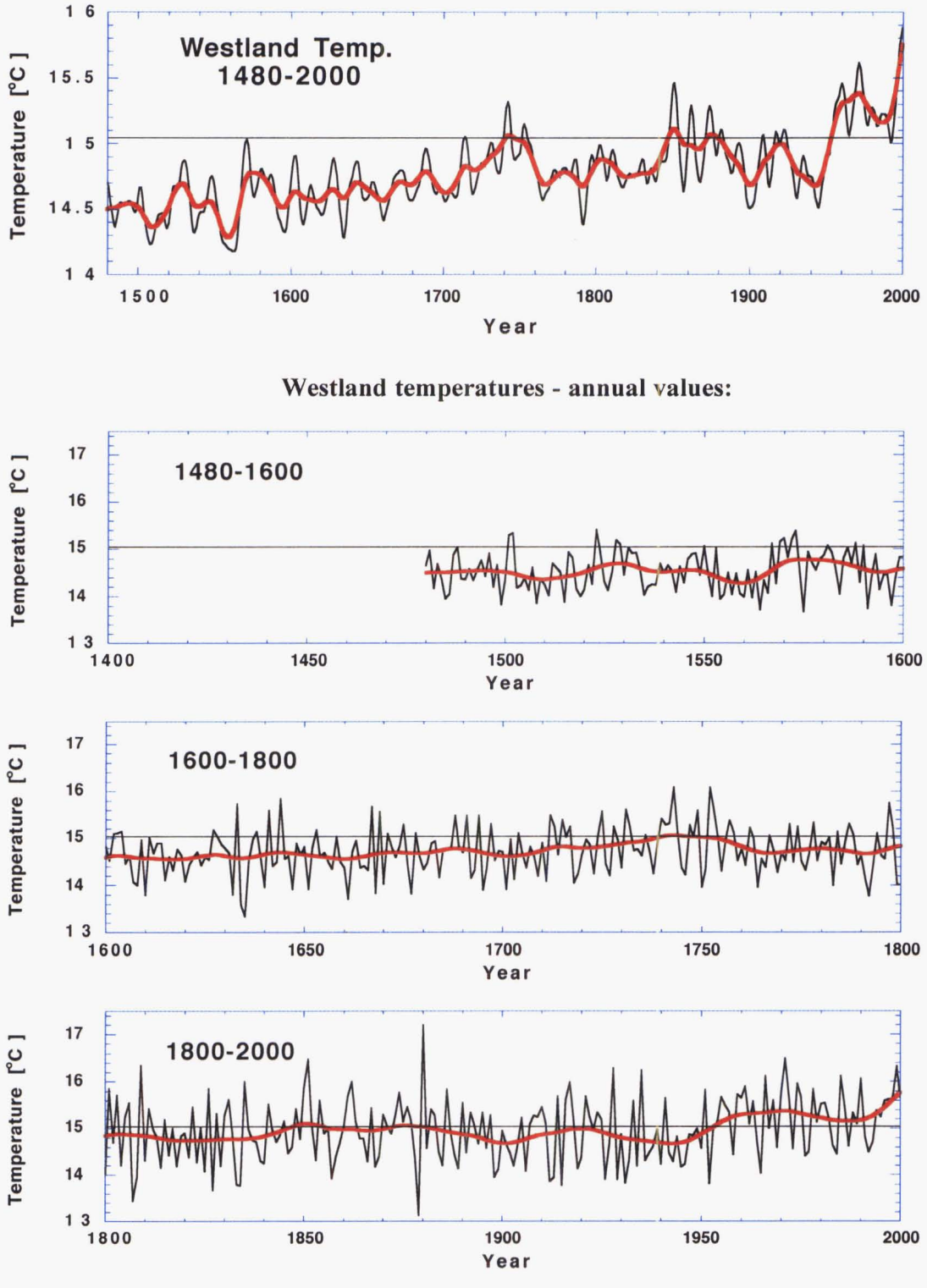

Figure 4.6 The Westland summer temperature reconstruction (1480-2000). With overlaid 25-year smoothing (red), and the 20th century mean of Hokitika instrumental temperatures (black horizontal line). Top plot shows the 10-year low-pass filtered series (to emphasise variance with wavelengths greater than 10 years) over the entire period of reconstruction. Remaining three plots show the yearly values in 200-year segments.

Tables 4.3a and 4.3b The five coldest (a) and five warmest (b) non-overlapping 25-year periods, and the fifteen coldest (a) and fifteen warmest (b) non-overlapping 10-year periods of the Westland temperature reconstruction. Units: °C. SD = standard deviation; Dep. = departures from the 1480-2000 reconstruction mean of 14.78°C.

Table 4.3a Cold periods.

Cold 25-year periods				Cold 10-year periods			
Interval	**Mean**	**SD**	**Dep.**	**Interval**	**Mean**	**SD**	**Dep.**
1542-1566	14.39	0.375	-0.39	1557-1566	14.19	0.282	-0.60
1503-1527	14.41	0.373	-0.37	1503-1512	14.28	0.254	-0.50
1591-1615	14.54	0.441	-0.24	1589-1598	14.38	0.415	-0.41
1616-1640	14.57	0.519	-0.21	1534-1543	14.39	0.243	-0.39
1646-1670	14.59	0.493	-0.19	1513-1522	14.41	0.358	-0.37
				1631-1640	14.44	0.756	-0.34
				1482-1491	14.45	0.353	-0.33
				1615-1624	14.48	0.239	-0.30
				1657-1666	14.49	0.373	-0.29
				1492-1501	14.54	0.408	-0.24
				1547-1556	14.54	0.429	-0.24
				1605-1614	14.55	0.444	-0.23
				1898-1907	14.55	0.451	-0.23
				1692-1701	14.56	0.535	-0.23
				1676-1685	14.57	0.392	-0.22

Table 4.3b Warm periods.

Warm 25-year periods				Warm 10-year periods			
Interval	**Mean**	**SD**	**Dep.**	**Interval**	**Mean**	**SD**	**Dep.**
1966-1990	15.35	0.615	+0.56	1966-1975	15.56	0.638	+0.77
1859-1883	15.07	0.753	+0.29	1954-1963	15.42	0.426	+0.64
1739-1763	15.03	0.554	+0.25	1990-1999	15.40	0.588	+0.62
1939-1963	15.01	0.603	+0.22	1978-1987	15.26	0.551	+0.48
1830-1854	14.98	0.662	+0.20	1847-1856	15.22	0.647	+0.43
				1916-1925	15.19	0.573	+0.41
				1740-1749	15.19	0.545	+0.40
				1874-1883	15.16	1.046	+0.38
				1752-1761	15.04	0.560	+0.26
				1858-1867	15.04	0.554	+0.26
				1797-1806	15.04	0.738	+0.26
				1886-1895	14.99	0.553	+0.21
				1724-1733	14.96	0.492	+0.18
				1835-1844	14.92	0.527	+0.14
				1712-1721	14.91	0.489	+0.13

Figure 4.7 shows the spectra of the instrumental record and of the reconstructed data. The spectral density of both series is the highest at periods of 3.4 years. Another peak in spectral density occurs at periods of around 5 years (4.8 years for the observed data; 5.0 years for the estimates). The coherency spectrum (Figure 4.8) indicates that the reconstruction is highly coherent ($P<0.05$) with the actual temperatures, especially in bandwidths smaller than 0.4 (i.e. periods longer than 2.5 years). The decadal cycle, which is apparent in the observed data, is only weak in the last 134 years of the reconstructed data (Figure 4.7). However, it becomes much more pronounced when analysing the entire length of the reconstruction (periods of 10.8 years; Figure 4.9). Figure 4.9 also reveals other long-term cycles that are present in the reconstruction: at periods of about 14, 22, 45 and 125 years.

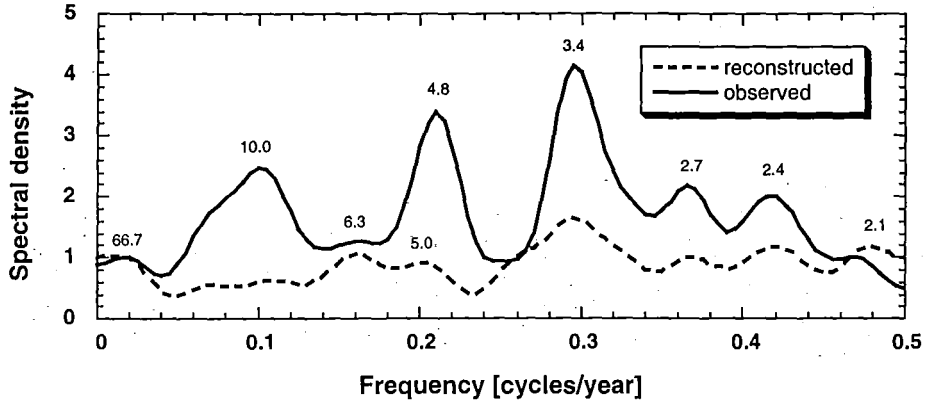

Figure 4.7 Spectral density of observed and reconstructed temperatures (1866-1999). Calculated from 33 lags. Length of cycles (in years) is indicated above each peak.

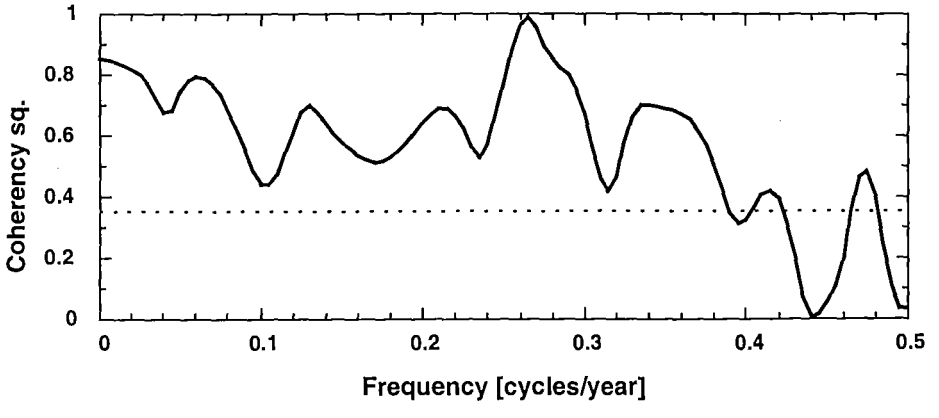

Figure 4.8 Coherency spectrum of observed and reconstructed temperatures (1866-1999). Dotted line indicates 95% confidence limit.

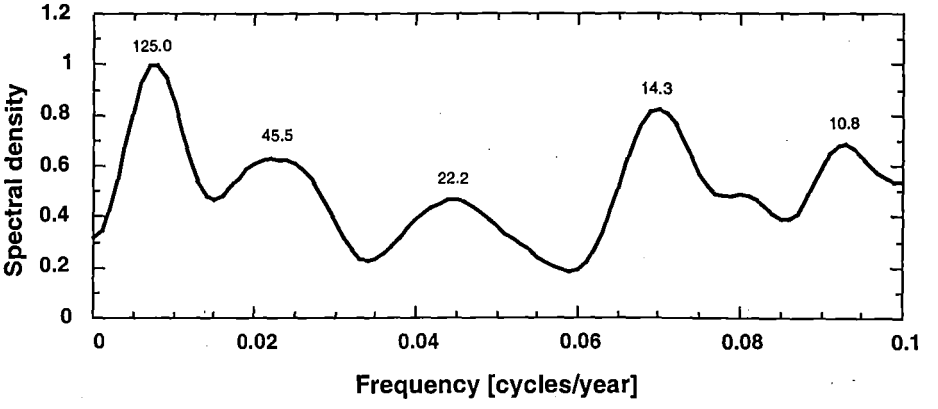

Figure 4.9 Spectral density of reconstructed temperatures (1480-2000) in the 0-0.1 bandwidth. Calculated from 130 lags. Length of cycles (in years) is indicated above each peak.

4.3.3 Comparison with the Oroko reconstruction

Figure 4.10 shows the Westland and Oroko temperature plots. While the two records exhibit a reasonable degree of similarity over most of the common period, there are also several shorter periods when the two proxies are markedly different. For example, Westland temperatures are lower than Oroko temperatures from the 1480s to early 1510s, the mid-1540s to early 1560s, and in the 1810s to mid-1820s. Higher Westland temperatures (compared with the Oroko reconstruction) occurred in the late 1510s to mid-1530s, the 1620s, the 1730s to mid-1740s, the early 1850s, and in the early 1860s. The mean temperature calculated over the 1480-1999 Oroko reconstruction period is 14.80°C, nearly equal to the 14.78°C mean based on the Westland series (Table 4.2).

An interesting period is 1480-1560, when the Westland and Oroko reconstructions are similar in year-to-year variability, but exhibit substantially different longer-term trends (Figure 4.10). This is mainly caused by a sharp drop (and subsequent recovery) in temperatures around 1500, apparent in the Oroko reconstruction, but absent from the Westland series.

Over the entire common period (1480-1999), the correlation between the two records is highly significant (Pearson's product moment correlation coefficient: RP = 0.43, P<0.001) (Figure 4.11). However, as mentioned earlier, the strength of the relationship is not constant over time. Figure 4.12 shows the changing correlations between 50-year sub-periods. For most sub-periods, the unfiltered Westland and Oroko temperature reconstructions are

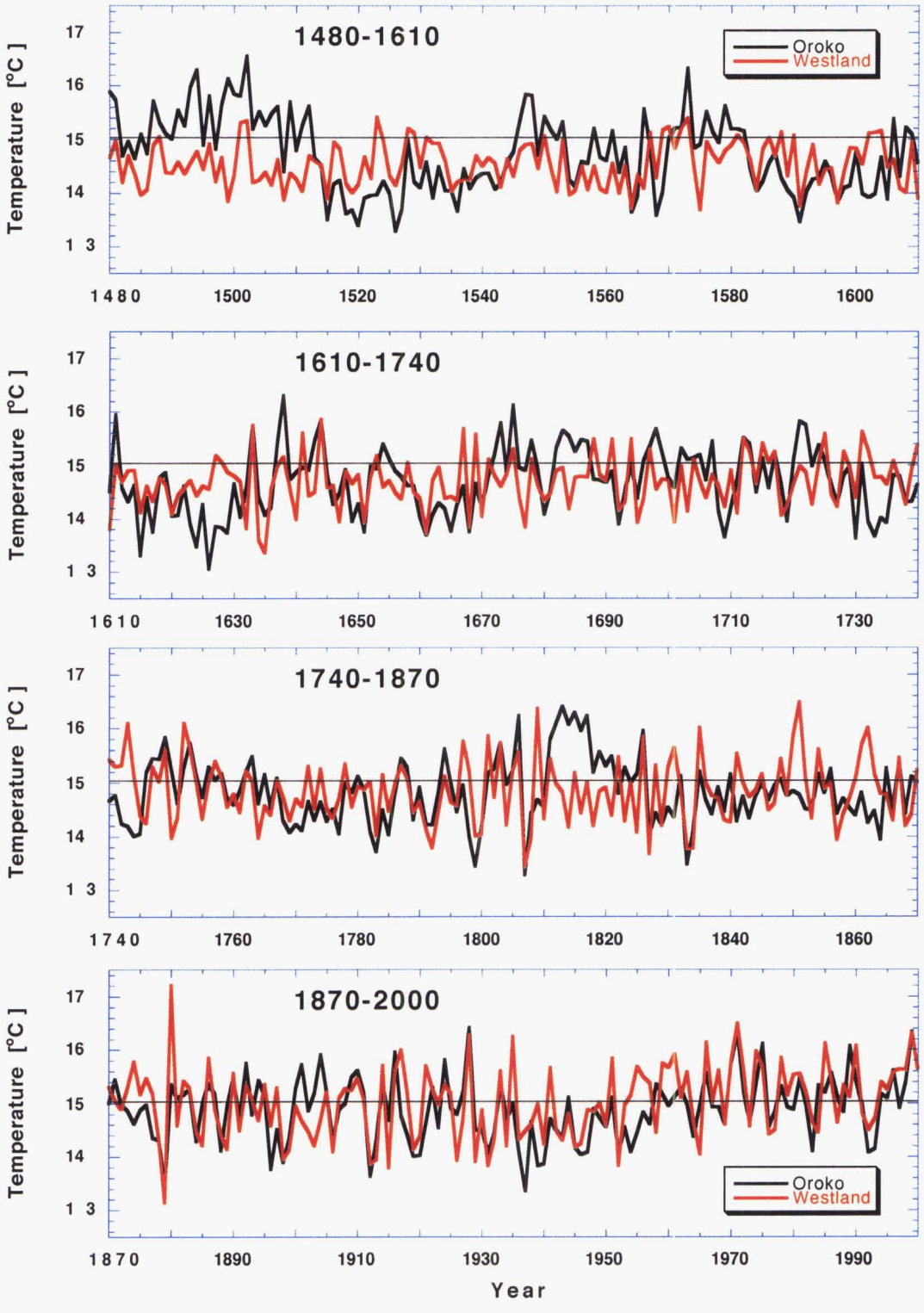

Figure 4.10 The Westland (red) and the Oroko (black) temperature reconstructions. The two proxy records are compared over the entire common period (1480-1999), in 130-year segments. The black horizontal line is the 20th century mean of Hokitika instrumental temperatures.

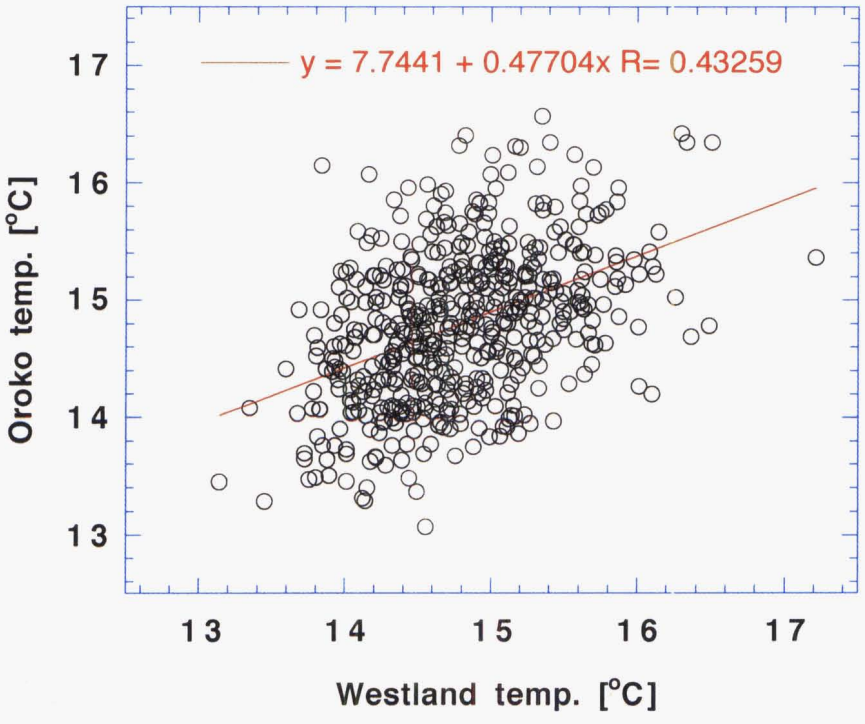

Figure 4.11 Scatter plot of the Westland and the Oroko temperature reconstructions. Based on 520 pairs of data (1480-1999).

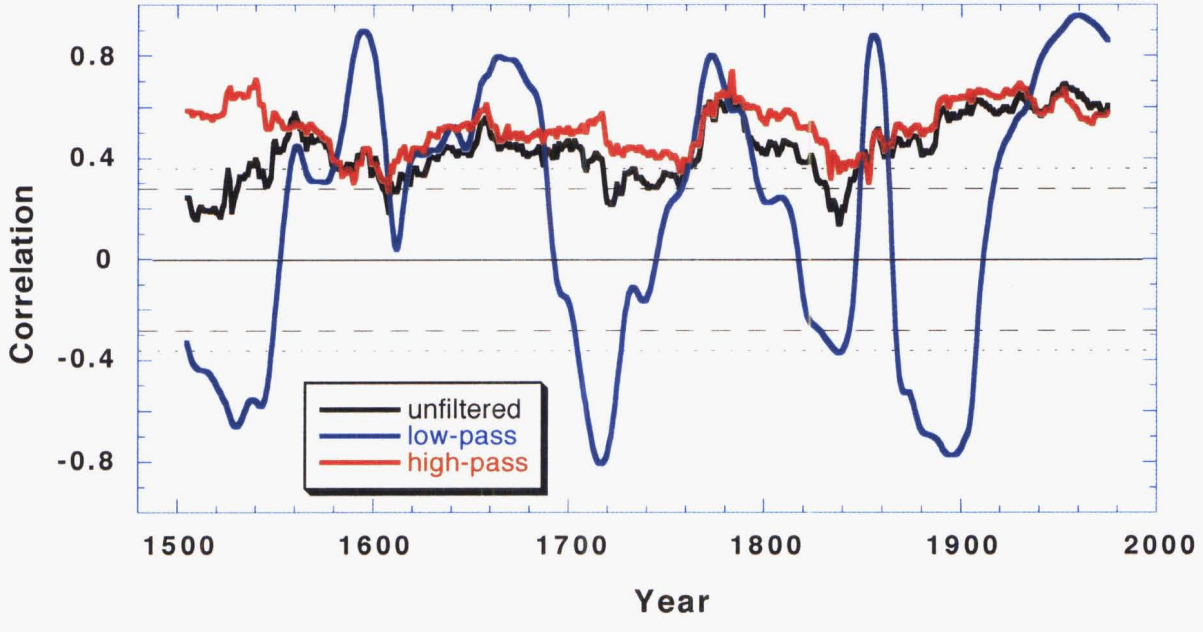

Figure 4.12 Running Pearson's correlation coefficients between the Westland and the Oroko temperature reconstructions. Calculated for the unfiltered data (black), and for their high-pass (<25 years; red) and low-pass (>25 years; blue) components. Plotted on the centroids of 50-year periods. Dashed and dotted lines indicate 95% and 99% confidence limits, respectively.

positively correlated at the 5% significance level. Besides the 20th century (when data were used to calibrate the models), the highest correlations occur in the second half of the 18th century, with a maximum in 1758-1807 (Pearson's product moment correlation coefficient: RP = 0.67, P<0.001). Weaker agreement between the two proxies is apparent around 1500, briefly in the early 17th and 18th centuries, and at around 1840. Here correlation values are either not significant, or if significant are much lower than for other periods. Minimum correlation occurred during the 1813-1862 sub-period (Pearson's product moment correlation coefficient: RP = 0.14, P>0.10).

The high-frequency components (wavelengths shorter than 25 years) of both records are very similar – the correlations are always significant at the 5% level, except for one marginal value over the 1583-1632 sub-period (Figure 4.12). It is clearly the low-frequency trends (wavelengths of more than 25 years) that are responsible for the occasional lack of agreement between the two proxies. The low-pass filtered series are negatively correlated in 1480-1550, in the first half of the 18th century, and over most of the 19th century (Figure 4.12).

4.4 Discussion

Pink pine tree rings performed very well as predictors of Westland temperatures. This is indicated by the large amount of variance explained, and also by the stability of the models – in both early and late periods, the calibration and verification statistics attained similar, highly reliable values (Tables 4.1a and 4.1b) – something not seen in many other attempts for reconstruction of New Zealand temperatures (Norton *et al.*, 1989; Palmer, 1989; Salinger *et al.*, 1994; Xiong and Palmer, 2000b). Over most of the common period, the reconstructed Westland temperatures show the same trends as the observed data (Figure 4.4). The spectral and cross-spectral analyses (Figures 4.7 and 4.8) show that the actual and estimated temperatures contain cycles of similar lengths.

The most pronounced peak in spectral density, which occurs at periods of 3.4 years (Figure 4.7), is most likely related to ENSO. Since ENSO reoccurs in the range of 2-7 years (Allan *et al.*, 1996), the same is probably true for peaks at around 5-6 years. A strong forcing of Westland temperatures by ENSO is also suggested by the cold summers in 1878, 1884, 1891, 1912, 1919, 1926, 1932, 1940, 1958, 1965, 1973, 1976, 1983, 1987 and 1992-1993 (showing both in the observed and reconstructed data), as those years were intensive El Niño years (Caviedes, 2001; Climate Prediction Center, 2002). The cold years that coincide with strong El Niño prior to the instrumental record (Ortlieb, 2000), are 1701, 1791, 1804 and 1814.

Another factor – large volcanic eruptions – may have contributed to the low temperatures in certain years (Briffa *et al.*, 1998b). The cooling in 1992-1993 was partly caused by the Mt. Pinatubo eruption in June 1991 (Folland and Salinger, 1995). Other major eruptions – the Indonesian volcanoes Tambora (1815), Krakatoa (1883) and Agung (1963) – were followed by a decrease in both hemispheric (Self *et al.*, 1981) and Westland temperatures (Figure 4.6). Hirschboeck (1979-1980) suggests that intensive volcanic activity in 1925-1945 led to a relative temperature decrease in the Southern Hemisphere during the 1930s. This is also supported by the results obtained in this chapter - both the instrumental (Salinger *et al.*, 1992a) and the reconstructed data (Figure 4.6) show that temperatures were cooler around that time.

Table 4.4 shows the spectral properties of the Westland palaeotemperature series. These are similar to the reconstructed New Zealand average data (Norton *et al.*, 1989; Xiong and Palmer, 2000b), especially at high frequencies. Fewer longer-term trends have been identified in the early studies (Table 4.4), probably because of the standardisation techniques employed. As mentioned above, the periods of 3.4, 5.0 and 6.3 years relate most likely to ENSO. The 10.8-year and 22.2-year cycles in the Westland reconstruction could be an expression of sunspot activity. The peak at 14.3 years coincides with a significant coherence at 14.5 years between the reconstructed STPI and the SOI (Villalba *et al.*, 1997b). The causes of the 45-year and 125-year cycles identified in the Westland reconstruction are not known. However, regular oscillations on the order of 40-60 years have been detected in other high-latitude reconstructions / chronologies from both the Northern and Southern Hemisphere (Cook *et al.*, 1992; Murphy, 1993; D'Arrigo *et al.*, 1996; Xiong and Palmer, 2000b). A long periodicity exceeding 125 years has been found in ring-width patterns of pink pine from Fiordland (Murphy, 1993), and a similar low-frequency (128-year) peak is evident in the spectra of Southern Hemisphere sea surface temperatures (Folland and Salinger, 1995).

Table 4.4 Cycles detected in the Westland and two earlier reconstructions.

Approximate length of a cycle	Value detected in the Westland reconstruction	Value detected in the rec. by Norton *et al.* (1989)	Value detected in the rec. by Xiong and Palmer (2000b)
3-4 years	3.4	3.1	3.8
5-6 years	5.0 and 6.3	5.0	4.8 and 5.9
10 years	10.8 and 14.3	9.3	9.5 and 12.5
20 years	22.2	20.0	-
45-50 years	45.5	-	50.0
125 years	125.0	-	-

Comparison of the Westland reconstruction with New Zealand's non-dendroclimatic proxies yielded mixed results. A lichenometric study at Mueller Glacier in the Mt. Cook region (Winkler, 2000) suggests that a local "Little Ice Age" [a period of low temperatures, variously dated within the 1550-1900 range (Bradley and Jones, 1993; Jones *et al.*, 2001)] occurred at around 1725-1730. This is not evident in the Westland series. The dates of glacial advances (Burrows and Greenland, 1979) are concurrent with below-average temperatures in Westland in the early 17th century, at around 1790, 1820-1830, 1890 and 1930. However, other periods in which glaciers advanced (1850 and 1740) were not reconstructed as being cool. According to the speleothem record (Wilson *et al.*, 1979), temperatures reached their minimum in the 17th century. The Westland reconstruction indicates temperatures were low at that time, but some even colder periods occurred in the 16th century (which is not apparent in the speleothem proxy). Although some of these results could be viewed as disappointing, it must be noted that many of the dates derived from indirect evidence other than tree rings are uncertain (Burrows and Greenland, 1979; Burrows, 1982; Section 4.1). More attention will therefore be given to comparing arguably more precise tree-ring palaeotemperature records.

I compared the Westland reconstruction with a proxy record derived from eleven *Libocedrus bidwillii* chronologies (Xiong and Palmer, 2000b). Over the common period (1720-1987), the series were positively correlated (Pearson's product moment correlation coefficient: RP = 0.24, P<0.001). This mainly reflects the year-to-year variability, since in the low-frequency domain, difficulties arise due to the relative shortness of the *L. bidwillii* record, and due to the different standardisation techniques employed. Also, Xiong and Palmer (2000b) used chronologies from the North Island and from northern South Island to reconstruct the New Zealand average temperatures. The season reconstructed from the *L. bidwillii* chronologies was February-March (cf. January-March for the Westland series). Considering all these differences and limitations, the correlation between the two records is reasonably high.

Since the focus of my study was on Westland climate, I have not examined correlations between the Westland reconstruction and any of the other series that used the New Zealand average temperatures (Norton *et al.*, 1989; Palmer, 1989; Salinger *et al.*, 1994; Palmer and Xiong, 2003). Instead, I carried out a detailed comparison of my results with the Oroko reconstruction (Cook *et al.*, 2002b). In the Oroko research, not only were Hokitika meteorological data used for the climate modelling, but also the tree-ring data were standardised using the same method (RCS), and the same season (January-March) was reconstructed.

Calibration and verification results are more satisfactory for the Westland reconstruction (e.g. RSQ = 43%, compared with RSQ = 38% for Oroko). This could be caused by a shortage of suitable data in the Oroko modelling – because of a stand-wide disturbance, Cook *et al.* (2002b) were unable to use the post-1958 tree-ring data for calibration/verification. The two records are highly correlated over the common period 1480-1999 (Figure 4.11), which indicates the two proxies are reconstructing same year-to-year variations in temperature in the same way. However, differences exist in the lower frequencies (Figure 4.12), which is not solely due to the use of different species or locations. It is possible that the negative correlations were caused by disturbances, but it would be difficult to determine which of the two series was affected. The fact that the Westland reconstruction is based on samples from six sites (cf. one site for Oroko) would give more credibility to the Westland series. On the other hand, the Oroko reconstruction combines samples from both living trees and sub-fossil material, whereas only living trees were used for Westland. Thus the WRC (and subsequently the Westland reconstruction) could be affected by stand dynamics in addition to climate.

It is unusual that the variability in the early part of the Westland record should be lower than the variability in the more recent decades (Figure 4.6). Chronologies (and hence reconstructions) often show greater variability in their early segments, as a results of smaller sample depth (e.g. Buckley, 1997; Cook *et al.*, 2000a). Again, the opposite pattern exhibited by the Westland reconstruction may have been caused by the fact that only living trees had been sampled. Four or five hundred years ago, these trees would typically be growing under a dense canopy, producing very narrow rings and not reflecting the fluctuations in temperature as dramatically as unrestrained trees. Such results emphasise the importance of obtaining tree-ring data from both living and dead trees. Where possible, the collection of sub-fossil material should become the main focus of any further research.

4.5 Summary and conclusions

Westland temperatures have been reconstructed back to 1480. The record is based on 296 pink pine tree-ring series from six high-elevation sites, located between 41°S and 43°S. Using simple linear regression, I calibrated the RCS chronology against January-March mean temperatures from Hokitika. The model, calibrated on the 1894-1946 period, explained 42.9% of the variance in temperature. All calibration and verification tests have been passed at high levels of significance ($P<0.001$). Over the 1894-1999 common period, the correlation between the observed and reconstructed data was 0.69 ($P<0.001$). The two series were highly coherent at all periods longer than 2.5 years. The Westland palaeotemperature record exhibited an

overall positive trend, with the lowest temperatures occurring in the mid-16th century, and with the maximum in the second half of the 20th century. The five coldest non-overlapping 25-year periods were 1542-1566, 1503-1527, 1591-1615, 1616-1640 and 1646-1670. The five warmest periods were 1966-1990, 1859-1883, 1739-1763, 1939-1963 and 1830-1854. Spectral analysis of the Westland reconstruction revealed cycles at periods of about 3, 5-6, 11, 14, 22, 45 and 125 years.

The Westland reconstruction showed only a moderate agreement with records derived from sources other than tree rings. I obtained much more encouraging results when comparing the Westland series with other tree-ring palaeotemperature records, especially the one from Oroko Swamp. The correlation between Westland and Oroko over the 1480-1999 common period was 0.43 ($P<0.001$). The high-frequency component contributed most to the strength of this value. I detected some serious disagreements in the lower frequencies, that may have been caused by disturbances at either Oroko or at some of the Westland sites. For example, earthquakes may have affected the Westland chronologies – and this possibility will be investigated in Chapter 6. To further improve the results, I also recommend collecting sub-fossil pink pine material to complement the existing data that had been derived from living trees only.

Chapter 5

Comparison with *Libocedrus bidwillii*

5.1 Introduction

In New Zealand, the greatest number (28) of chronologies have been developed from *Libocedrus bidwillii* (International Tree-Ring Data Bank, 2002). The chronology sites occur over a wide range of latitudes, longitudes and altitudes (Dunwiddie, 1979; Norton, 1983a; Xiong, 1995; Xiong and Palmer, 2000a). Several sites are located in Westland, where *Libocedrus bidwillii* is often associated with pink pine (Figure 5.1). This provides a unique opportunity for comparing the dendroclimatic potential of the two species effectively growing side by side. No similar study has been conducted in New Zealand before.

Figure 5.1 Upland conifer-broadleaved forest. In this example from Matiri Range (MAT), pink pine (right) grows alongside *Libocedrus bidwillii* (conical shape; centre-left) and *Nothofagus solandri* (left).

Paying particular attention to temperature response, I compared pink pine with *Libocedrus bidwillii* on two levels – regionally and locally. For the regional comparison, I created a composite *Libocedrus bidwillii* chronology (WLB), parallel to the Westland Regional Chronology (WRC; pink pine) developed in Chapter 4. The WRC has proved to be a good indicator of palaeotemperatures in this region (Chapter 4). One of the questions I asked was: Can Westland temperatures be reconstructed from *Libocedrus bidwillii* tree rings as well? Two previous studies, in which New Zealand temperatures have been derived from *Libocedrus bidwillii* tree-ring data, used chronologies from the North Island and Nelson area only (Xiong and Palmer, 2000b; Palmer and Xiong, 2003).

In a separate exercise, I compared two chronologies (pink pine and *Libocedrus bidwillii*) developed from the same site (Camp Creek – site code CCP). The objective was to investigate if the two chronologies exhibit different responses to climate. Is the climate response affected by site conditions only, or are there any other reasons that cause different species to react to temperature fluctuations in different ways? Chronologies developed from the same species over a range of sites often show different responses to climate (e.g. Chapter 3; Xiong, 1995) – this is probably the result of environmental conditions that vary from site to site. But what causes different species to respond differently? Until recently, the assumption has been that the same factor (varying site conditions) could be the reason. With two chronologies developed from different species, but from the same site (i.e. subject to identical climate), this case study aimed to either confirm or refute the assumption that only site factors explain variations in climate response.

5.2 Materials and methods

5.2.1 Libocedrus bidwillii chronologies

At some of my study sites, pink pine occurs in association with *Libocedrus bidwillii*. At Camp Creek (CCP) and Mt. French (MTF), I sampled both species, and in addition to the pink pine chronologies (Chapter 2), I also developed two *Libocedrus bidwillii* chronologies – CCP(LB) and MTF(LB). I crossdated 93% and 91% of all *Libocedrus bidwillii* samples from CCP and MTF, respectively. I encountered some difficulty in including the entire series in the chronologies – in many specimens (especially those older than 500 years), I was unable to measure the ring widths in the outer (most recent) 100-200 years, because of the suppressed tree growth in this period. This problem is consistent with Xiong (1995), who recommended collecting samples from both old and relatively young *Libocedrus bidwillii* trees.

For each crossdated series, I estimated the pith offset following the methodology described in Appendix 1. I used the RCS technique (Briffa *et al.*, 1992) to detrend the individual ring-width series. The age-aligned mean growth curves (not shown) for both CCP(LB) and MTF(LB) were similar to the curve in Figure 5.7, exhibiting the characteristics of a closed-canopy population (Section 2.3.3). For all further details on sampling, sample preparation and chronology development, refer to Chapter 2.

The resulting CCP(LB) and MTF(LB) chronologies are presented in Figure 5.2, and selected chronology statistics are listed in Table 5.1. With a time span of more than 900 years (Table 5.1), CCP(LB) is currently the longest *Libocedrus bidwillii* chronology yet available (International Tree-Ring Data Bank, 2002). However, it must be noted that because of the small sample size in the early part of the record, CCP(LB) is reliable back to only around 1530.

Table 5.1 CCP(LB) and MTF(LB) chronology statistics.

Statistic	CCP(LB)	MTF(LB)
No. of trees / series	24 / 42	24 / 40
Time span	1064-1998	1330-1999
Mean length of series [years]	359	278
Mean measurement [mm]	0.49	0.56
Standard deviation	0.316	0.304
Mean sensitivity	0.162	0.160
Mean RBar	0.217	0.231
Serial correlation	0.797	0.783

Large sample size is necessary for the RCS method to be truly effective (Esper *et al.*, 2003). Therefore, in addition to working with individual site chronologies, I decided to create a regional *Libocedrus bidwillii* chronology, similarly to the pink pine WRC (Chapter 4). Also, having a single series representing each species facilitates the comparison – it can be easily seen how well each integrates the regional climate signal. I obtained all *Libocedrus bidwillii* tree-ring data (crossdated ring-width measurements) that have been produced for the South Island, from the ITRDB (International Tree-Ring Data Bank, 2002). Figure 5.3 shows location of the sites. Table 5.2 provides further details on each site and collection, and identifies the contributors of the data. I used single detrending (fitting of negative exponential or linear curves) to develop chronologies from the ten sets of raw data obtained from the ITRDB. I did not apply the RCS method to them because of small sample size and/or unavailability of the pith-offset data.

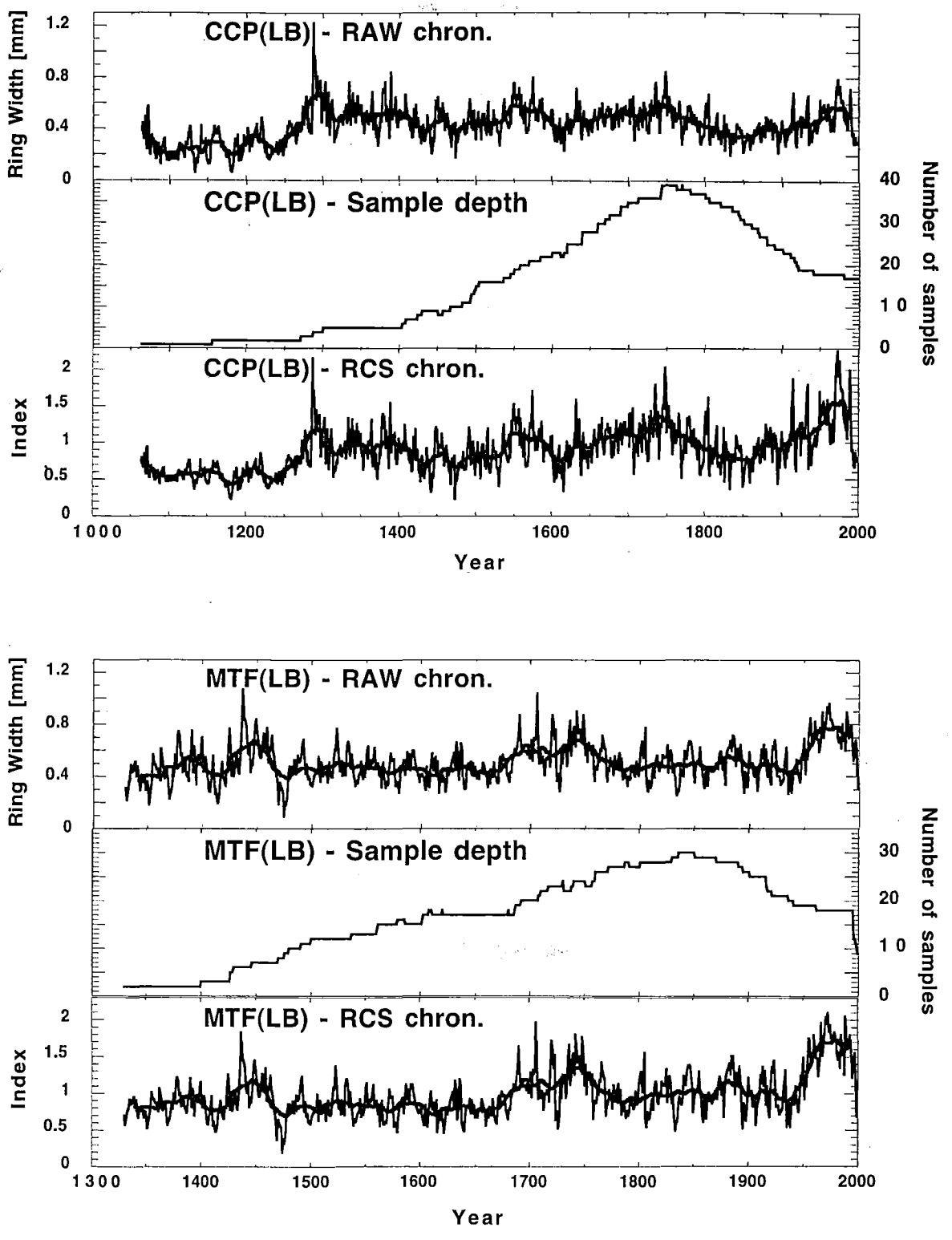

Figure 5.2 The Camp Creek (top three graphs; 1064-1998) and Mt. French (bottom three graphs; 1330-1999) *Libocedrus bidwillii* chronology plots. Smoothed with a 25-year running mean (heavy line).

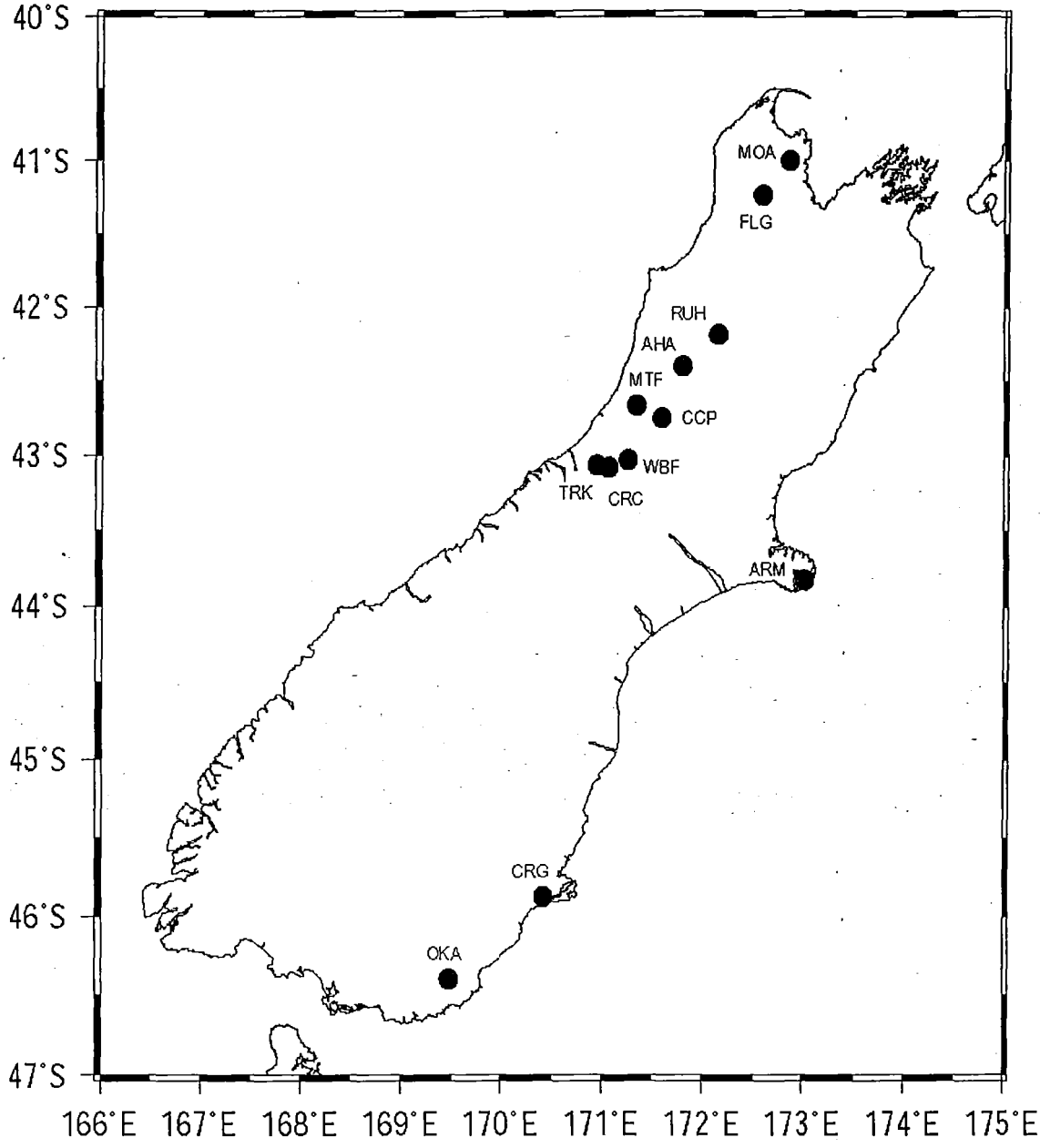

Figure 5.3 Location of the South Island *Libocedrus bidwillii* chronology sites. Note: site codes are consistent with Xiong (1995), ITRDB (2002) and this thesis.

To determine which *Libocedrus bidwillii* sites could be merged with CCP and MTF, i.e. to determine which sites form the same population, I performed rotated PCA on all twelve chronologies. The common period was 1732-1958. Since different standardisation methods had been used [RCS for CCP(LB) and MTF(LB); single detrending for the remaining ten chronologies], i.e. different amounts of low-frequency variance have been retained, I only compared the high-frequency signals. I used a high-pass filter that transmitted wavelengths

shorter than 25 years and blocked frequencies lower than 25 years. See Section 2.3.5 for further details on PCA.

Table 5.2 *Libocedrus bidwillii* site and chronology characteristics.

#	Site	Site code	Lat. (S)	Long. (E)	Altitude [m a.s.l.]	No. (trees / series)	Time span
1.	Ahaura	AHA[3]	42°23'	171°48'	244	32 / 59	1525-1992
2.	Armstrong Reserve	ARM[1]	43°50'	173°00'	731	22 / 46	1446-1958
3.	Camp Creek	CCP[4]	42°43'	171°34'	965	24 / 42	1064-1998
4.	Cream Creek	CRC[2]	43°05'	170°59'	800	15 / 25	1460-1978
5.	Mt. Cargill	CRG[1]	45°50'	170°32'	576	12 / 43	1492-1975
6.	Batten Range - Flanagans Hut	FLG[3]	41°16'	172°36'	950	20 / 33	1683-1991
7.	Moa Park	MOA[3]	40°56'	172°56'	1036	20 / 49	1490-1991
8.	Mt. French	MTF[4]	42°40'	171°20'	855	24 / 40	1330-1999
9.	Owaka	OKA[1]	46°23'	169°27'	305	14 / 47	1732-1976
10.	Rahu Saddle	RUH[3]	42°19'	172°07'	672	20 / 40	1560-1992
11.	Tarkus Knob	TRK[2]	43°05'	170°58'	925	21 / 27	1526-1978
12.	Wilberforce	WBF[3]	43°04'	171°17'	780	15 / 31	1674-1992

Source: [1] LaMarche *et al.* (1979); [2] Norton (1983a); [3] Xiong (1995), [4] this thesis.
Note: AHA - original data collected by LaMarche *et al.* (1979b); updated by Xiong (1995).

The PCA results (Section 5.3.1) revealed that CCP(LB) and MTF(LB) were very similar to two other Westland *Libocedrus bidwillii* chronologies, CRC and TRK. By merging ring-width series from these four sites into one composite set, I created the Westland *Libocedrus bidwillii* (WLB) chronology. Again, I used the RCS technique (Briffa *et al.*, 1992) to detrend the series. In the CRC and TRK chronologies, I was unable to estimate the pith offsets. Therefore, I considered the innermost ring of each tree to represent the first year of cambial age (Briffa *et al.*, 1992; Cook *et al.*, 2000a). For additional, but shorter series from the same tree, I calculated the pith offset accordingly. For example, for three series (from the same tree) starting in 1700, 1720 and 1750, the PO estimates would be 0, 20 and 50 years, respectively. Since the CRC and TRK series comprise less than 40% of the WLB chronology's sample depth, and since the RCS method is not very sensitive to inaccuracies in PO estimates (Esper *et al.*, 2003), this has not affected the resulting WLB chronology in any significant way. To compute the WLB chronology, I followed the same methodology as for WRC (Section 4.2.1).

5.2.2 Temperature response and modelling

As for pink pine, I used the Hokitika homogenised record (Salinger *et al.*, 1992a) to investigate the relationship between WLB tree-ring data and temperature. For all details on correlation and response functions, see Chapter 3.

5.2.3 Inter-species comparison

Pink pine has been compared with *Libocedrus bidwillii* on two scales: (a) within a region, and (b) within a site. On the regional scale, I used correlation analysis to examine the similarities and differences between WRC and WLB. To carry out the small-scale inter-species comparison, I investigated tree-ring data from the Camp Creek (CCP) site. I preferred CCP over MTF because (a) both for the pink pine and *Libocedrus bidwillii* chronologies, CCP had the highest replication; and (b) both the CCP and CCP(LB) chronologies were representative of the Westland regional tree-growth patterns (being part of WRC and WLB, respectively).

I compared the CCP and CCP(LB) tree-ring data over the years for which meteorological data were available (i.e. 1866-1880 and 1894-1998). I visually inspected the tree cores, attempting to identify marker rings, such as frost, light or double rings. I could not detect any frost rings (i.e. frost-damaged tracheid cells), probably because both pink pine and *Libocedrus bidwillii* are among the most frost-resistant tree species in New Zealand (Sakai and Wardle, 1978). Neither was I able to recognise any distinct and frequently-occurring variations in latewood density, perhaps because of the narrowness of the rings (typically less than 0.5 mm). The only noticeable differences between pink pine and *Libocedrus bidwillii* were related to ring widths, not to wood anatomy.

I found that in certain years, pink pine formed wider-than-average rings, while the ring widths in most *Libocedrus bidwillii* trees were relatively narrow (and vice versa). Figures 5.4 and 5.5 provide several examples of these differences. Both the pink pine (CCP05-1; Figure 5.4) and *Libocedrus bidwillii* (CCP106-1; Figure 5.5) trees were of similar size (DBH of 32.3 cm and 34.2 cm, respectively) and age (around 400 years), and they were located within thirty metres of each other. Being exposed to identical climatic conditions, it might be reasonable to expect that they would produce rings of similar relative widths. Yet this was not the case – comparison of the 1896 and 1915 ring reveals the opposite responses of the two species (Figures 5.4 and 5.5).

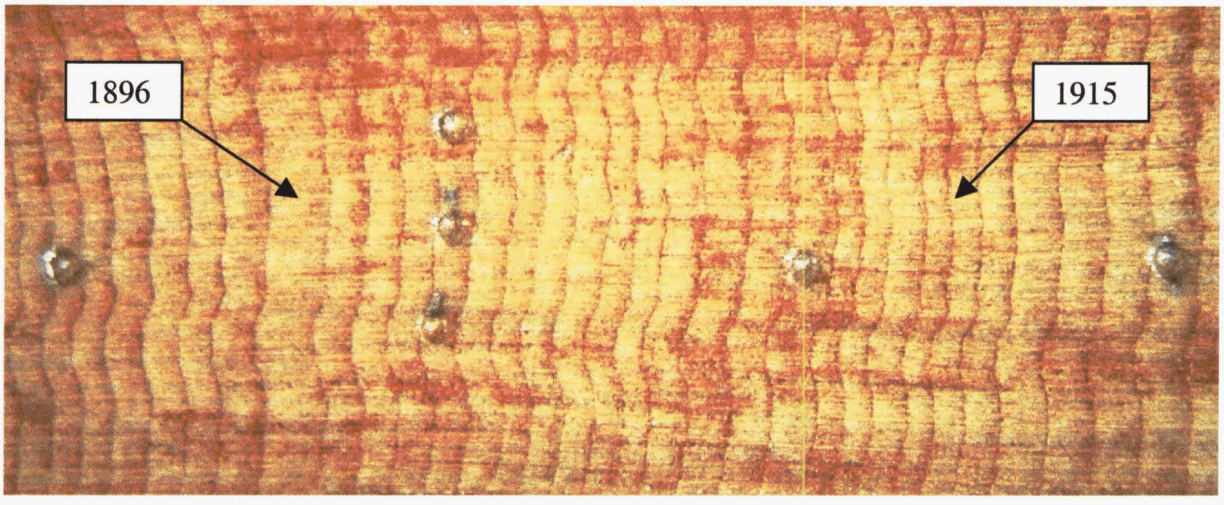

Figure 5.4 The 1890-1920 section of the CCP05-1 core (pink pine). Each decade is marked by one dot; three dots indicate the year 1900. Note the relatively wide rings in 1895, 1896, 1918 and 1919; and narrow rings in 1914 and 1915. The scale is 15:1 (approximately).

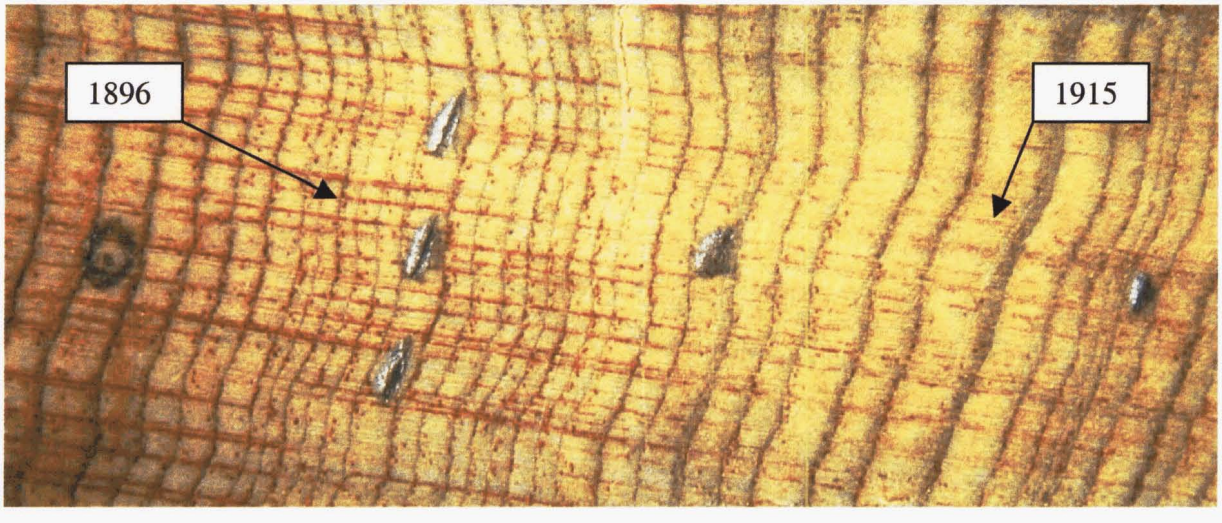

Figure 5.5 The 1890-1920 section of the CCP106-1 core (*Libocedrus bidwillii*). Each decade is marked by one dot; three dots indicate the year 1900. Note the relatively narrow rings in 1895, 1896, 1918 and 1919; and wide rings in 1914 and 1915. The scale is 15:1 (approx.).

To identify the years in which the relative ring widths between the two species varied most, I calculated the difference D for each year i by subtracting the pink pine tree-ring indices from the *Libocedrus bidwillii* tree-ring indices (Equation 5.1).

$$D_i = CCP(LB)_i - CCP_i \qquad (5.1)$$

I examined the instrumental climate record (Hokitika homogenised temperatures; Salinger *et al.*, 1992a), focusing on years in which *D* reached either very high (positive) or very low (negative) values. I noticed that *Libocedrus bidwillii* often formed narrower rings than pink pine ($D<0$) when cool conditions before/at the start of the growing season were followed by warm summers, and vice versa (Table 5.3).

Table 5.3 Selected tree-ring (CCP) and temperature (Hokitika) data. CCP(LB) and CCP = chronology indices; *D* = the difference between CCP(LB) and CCP; Cold/Warm months = departures of mean monthly temperatures from the 20th century mean. Note that the calendar years for January, February and March would be different from the dendrochronological years used in the table.

Year	1876	1935	1914	1952
CCP(LB)	0.81	0.65	1.44	1.49
CCP	1.23	1.06	0.71	0.69
D	-0.42	-0.41	+0.73	+0.80
Cold months	Jul –0.86°C Sep –0.81°C	Sep –1.31°C Nov –0.73°C	Dec –2.97°C Feb –2.33°C	Feb –0.63°C Mar –1.45°C
Warm months	Nov +1.87°C Dec +1.73°C	Dec +2.53°C Jan +1.11°C	Jul +0.54°C	Aug +1.11°C Nov +0.97°C

To further explore the relationships suggested above, I plotted normalised seasonal temperatures (two scatter diagrams – summer v. previous winter and summer v. spring) and determined the quadrants in which the years with extreme *D*-values tend to occur most frequently. The seasonal temperatures were 3-month averages, normalised (i.e. converted into *z*-scores) by dividing the difference between each value and the mean by the standard deviation (Mendenhall and Sincich, 1988). Normalised data have a mean of zero and a standard deviation that equals one. The advantage of using the normalised temperatures is that, based on the sign, cold (negative) and warm (positive) seasons can be readily identified.

5.3 Results

5.3.1 The Westland Libocedrus bidwillii chronology

In the rotated PCA, two eigenvectors were identified as significant by the Monte-Carlo red-noise criterion. The first two eigenvectors explain 55% of the total variance among the series (38% and 17%, respectively). The rotated varimax loadings (Figure 5.6) illustrate the separation of the *Libocedrus bidwillii* chronologies into three groups: western, eastern and

transitional. High loadings for the first eigenvector and low loadings for the second eigenvector show that CCP and MTF could be merged with other two sites on the West Coast, CRC and TRK. Opposite pattern (low loadings for the first eigenvector and high loadings for the second eigenvector) is typical for the chronologies from the eastern coast of the South Island (OKA, CRG and ARM), and also for the northernmost site (MOA). A transitional group (with about equal loadings for both eigenvectors) is formed by WBF, AHA, RUH and FLG. While AHA, RUH and FLG are located north-east of the western group, WBF is situated between CCP and CRC (Figure 5.3). The reason WBF does not load similarly with the western chronologies is probably that it lies east of the Southern Alps' main divide, whereas all four sites that comprise the Westland *Libocedrus bidwillii* chronology (CCP, CRC, MTF and TRK) are located west of the divide.

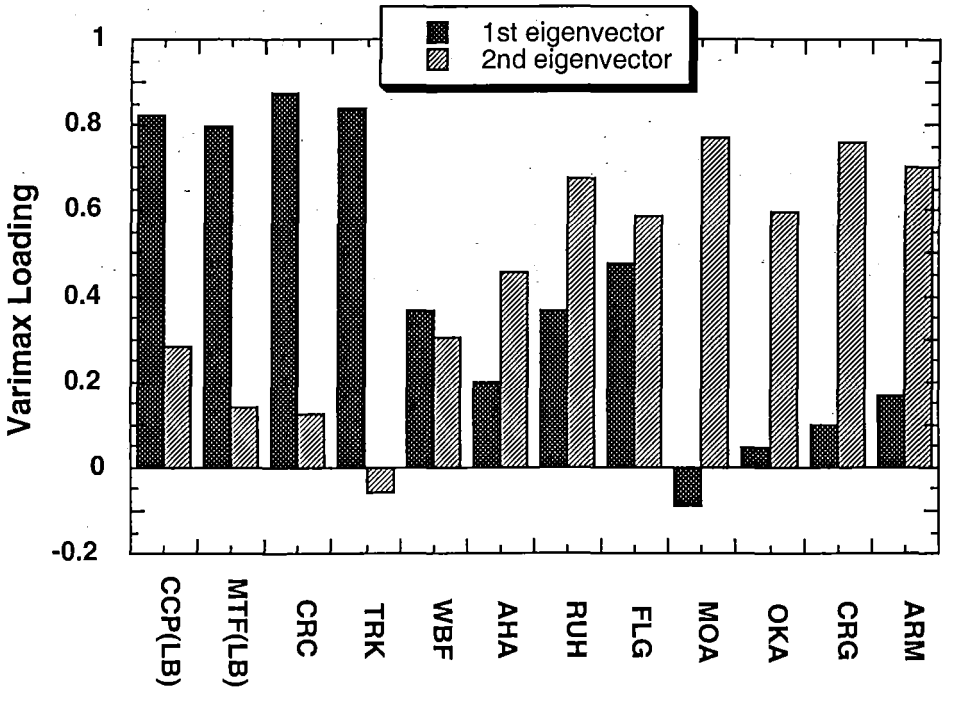

Figure 5.6 Varimax loadings for the high-pass (<25 years) filtered *Libocedrus bidwillii* chronologies. Period of analysis is 1732-1958.

The WLB chronology spans 936 years (1064-1999). Figure 5.7 presents only the 1450-1999 section, which is the period that had been identified as reliable (based on the results of RBar and EPS statistics; not shown). The WLB chronology contains 134 series from 84 trees. The sample size drops sharply after 1978 (Figure 5.7); 1978 being the last year in which the CRC and TRK series contribute to the chronology (Table 5.2). The mean segment length is 291

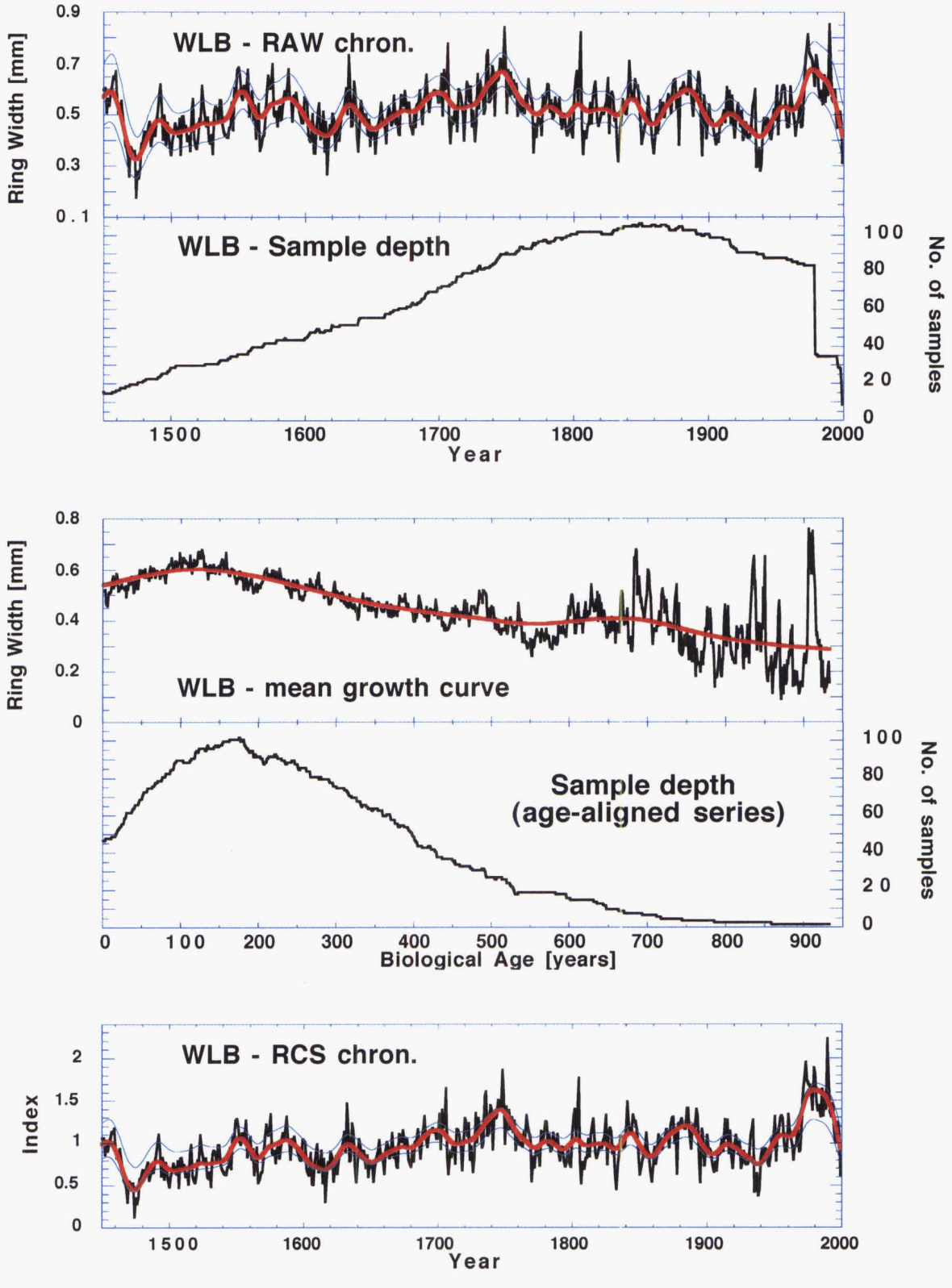

Figure 5.7 The Westland *Libocedrus bidwillii* chronology plots (1450-1999). Top: The raw chronology and the sample size; middle: the age-aligned mean growth curve that was used to standardise the series; bottom: the RCS chronology. Red lines: overlaid smoothing (25-year splines were used for the chronologies, 1/3 spline for the growth curve). Bootstrap 95% confidence limits were computed for the chronologies (blue lines).

years, and the average ring width 0.54 mm. Tree growth was suppressed in the 1460s and 1470s, in the early 17th century, and in the 1940s. The most prominent periods of increased growth occurred in the mid-18th century and in the second half of the 20th century. The age-aligned mean growth curve (Figure 5.7) becomes very noisy (highly variable) when the cambial age exceeds 600 years, as a consequence of the decreasing sample size. The resulting RCS chronology (Figure 5.7) is very similar to the raw data. The mean RBar (for the entire length of the WLB chronology, covering 1064-1999) is 0.148, standard deviation 0.291, mean sensitivity 0.155, and serial correlation 0.799.

The WLB chronology is very similar to the WRC (Figure 5.8). For the unfiltered data (Figure 5.8), the correlation between the two series is highly significant over the common period 1480-1999 (Pearson's product moment correlation coefficient: RP = 0.53, P<0.001). It is mainly the low-frequency trends (wavelengths longer than 25 years) that contribute to this value (Pearson's product moment correlation coefficient: RP = 0.73, P<0.001). The correlation between the high-frequency components (wavelengths shorter than 25 years) is somewhat weaker, however still significant (Pearson's product moment correlation coefficient: RP = 0.30, P<0.001).

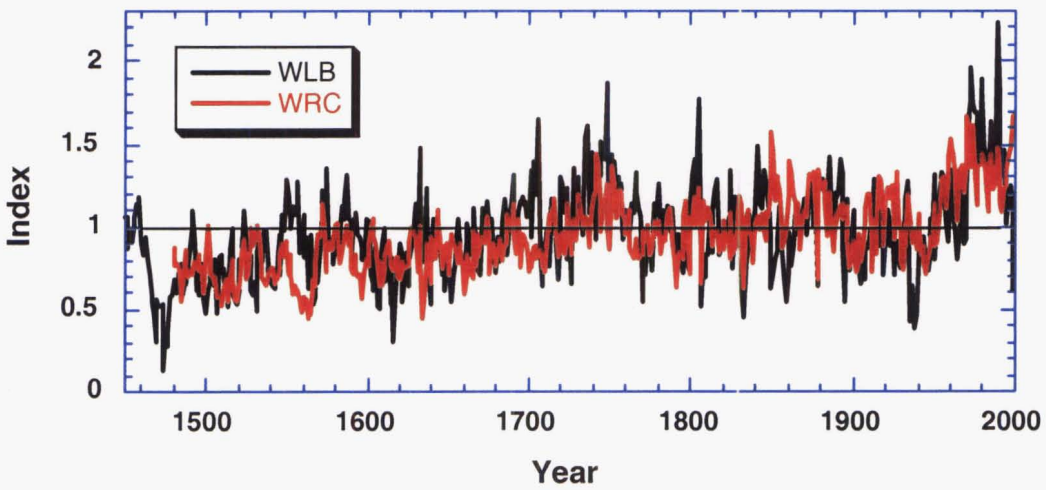

Figure 5.8 Comparison of the WLB chronology with the WRC (unfiltered data).

5.3.2 Regional WLB / temperature relationship

Figure 5.9 shows the correlations between prewhitened WLB tree-ring and climate data over the common period 1897-1998. Both series were modelled as AR(2) processes. Overall, the WLB chronology exhibits a positive response to mean monthly temperatures from about May (prior to the growing season) to April at the end of the current growing season. Summer

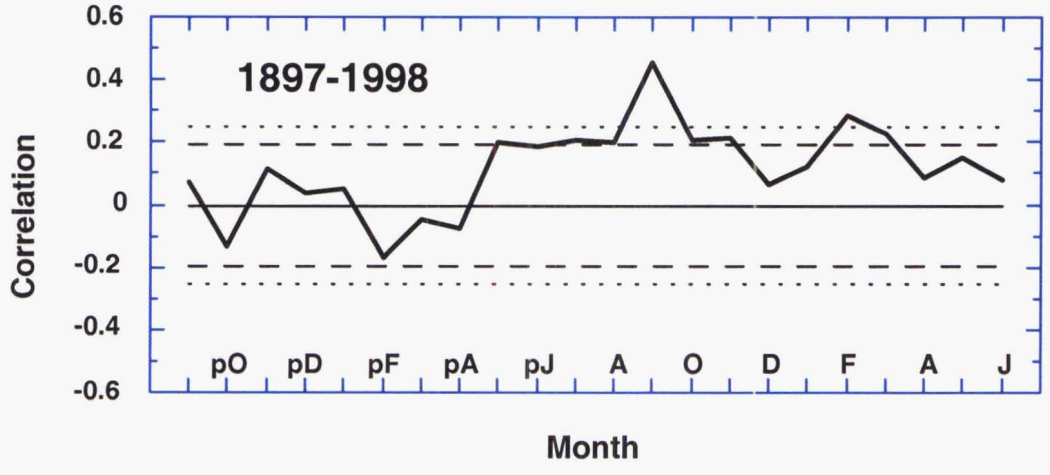

Figure 5.9 Correlation of the WLB chronology with the mean monthly temperature. The period of analysis is 1897-1998. Climatic window is September of the previous growing season to June at the end of the current growing season. Dashed and dotted lines indicate 95% and 99% confidence limits, respectively.

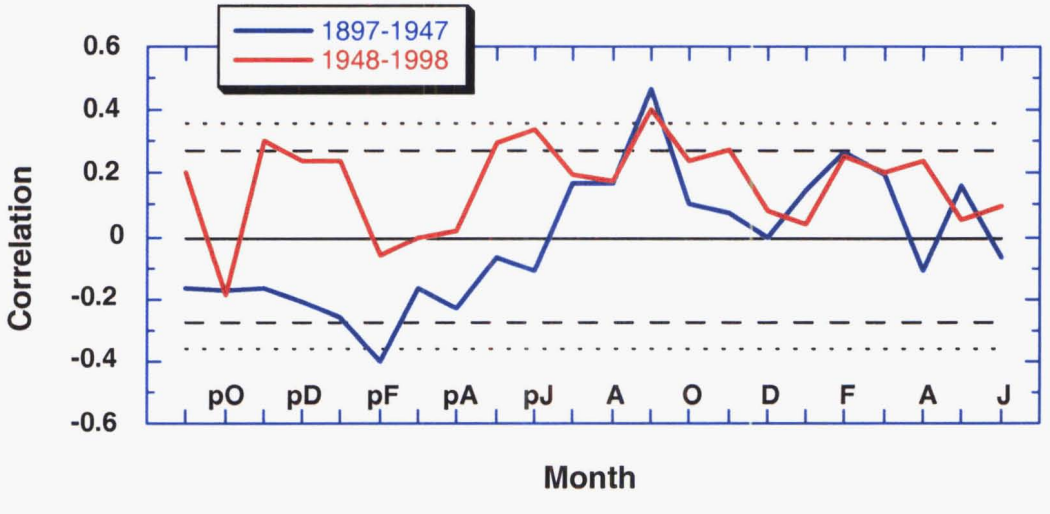

Figure 5.10 Temporal variability of the relationship between WLB tree-ring data and mean monthly temperature. Correlations were calculated for early (1897-1947; blue) and late (1948-1998; red) periods. Climatic window is September of the previous growing season to June at the end of the current growing season. Dashed and dotted lines indicate 95% and 99% confidence limits, respectively.

(December and January) temperatures appear to have less influence on the growth of *Libocedrus bidwillii*, and tree-ring widths are best correlated with current September (spring) and current February-March (late summer) temperatures. Instability of the relationship between WLB tree-ring data and temperature is revealed in Figure 5.10. In the early period (1897-1947), previous February (negative correlation) and current September (positive correlation) are the only two months, in which the relationship is significant ($P<0.05$). In the late period (1948-1998), tree growth is significantly affected by temperatures in November, May and June prior to the growing season; and in September and November at the beginning of the current growing season (all significant correlations are positive).

To assess the strength of the temperature signal that was contained in the WLB chronology, I performed four calibration/verification experiments on different monthly combinations. Table 5.4 presents the results for the models calibrated on the late period. The greatest amount of variance explained (24.9%) could be obtained when reconstructing mean May-October temperatures. However, only the calibration statistics are satisfactory – in the verification period, the model explains only 7.2% of the variance in temperature. More stable models could be produced for the shorter seasons (1-3 months in duration), but these explain less than 20% of the variance. Because of the poor results shown in Table 5.4 (and because calibrating on the early period produced, in general, even weaker results; not shown), no temperature reconstruction from *Libocedrus bidwillii* tree rings has been attempted.

Table 5.4 Calibration and verification results of four different temperature response models for the late calibration period (1947-1998). RSQ = the variance explained; RP = the Pearson's product moment correlation coefficient (observed v. reconstructed values). Number of stars indicates the level of significance: ***P<0.001; **P<0.01; *P<0.05.

Period	Number of months	RSQ (late calibr. model)	RP - calibration (1947-1998)	RP - verification (1895-1946)
May - October	6	24.9%	0.499***	0.269*
July - September	3	12.5%	0.354**	0.408**
September	1	16.4%	0.405**	0.449***
February - March	2	8.1%	0.284*	0.278*

5.3.3 Local comparison

At Camp Creek (CCP), over most of the 120 years of instrumental climate record (1866-1880 and 1894-1998), *Libocedrus bidwillii* tree rings were wider than pink pine rings (Figure 5.11). Figure 5.12 shows the twenty lowest (i.e. *Libocedrus bidwillii* < pink pine; $D<-0.15$) and the twenty highest (i.e. *Libocedrus bidwillii* > pink pine; $D>+0.56$) D-values.

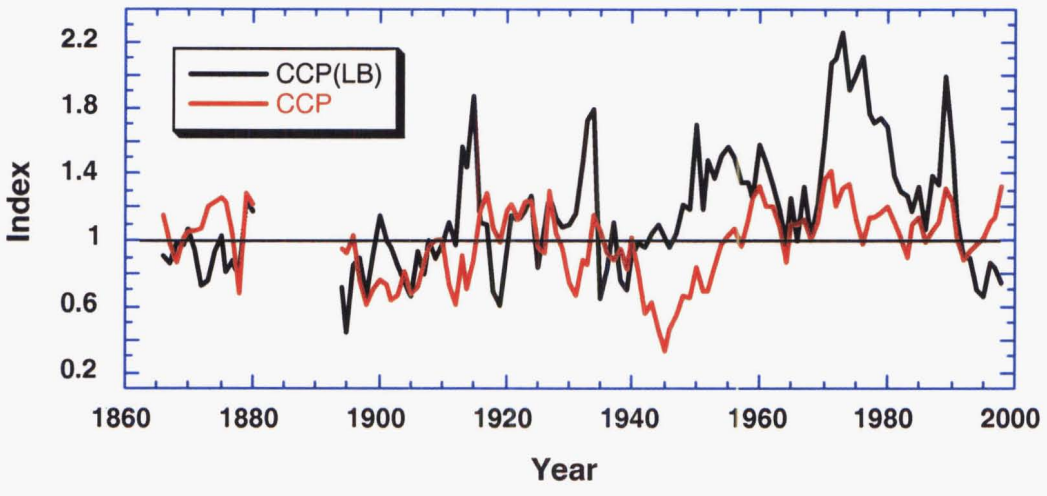

Figure 5.11 Pink pine (red) and *Libocedrus bidwillii* (black) tree-ring indices from the Camp Creek site. Shown are only the years for which meteorological data are available.

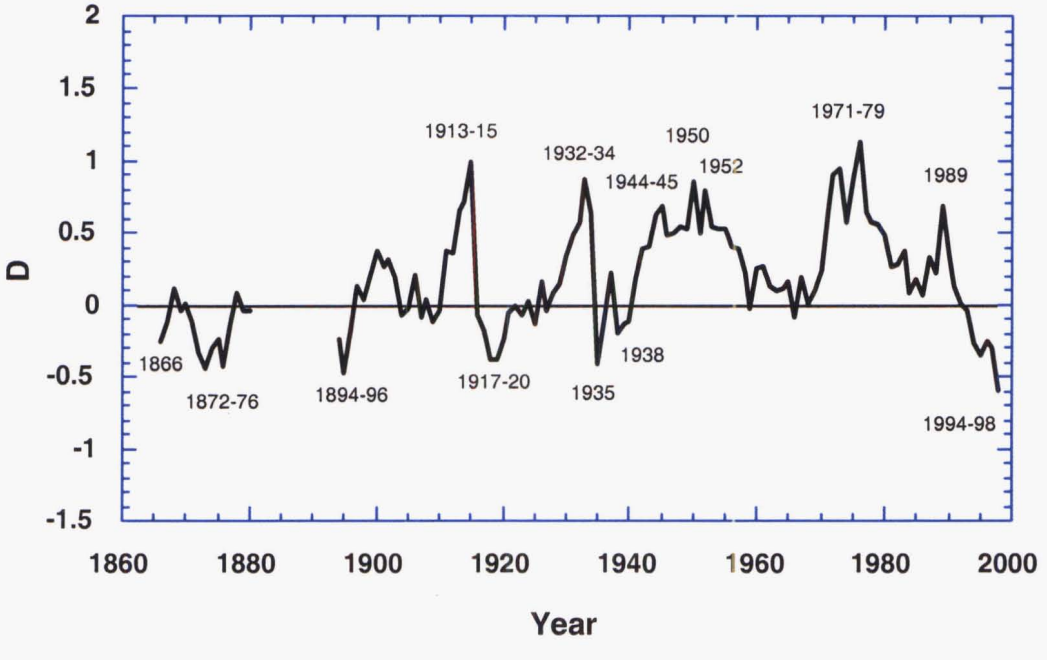

Figure 5.12 Difference (*D*) between *Libocedrus bidwillii* and pink pine tree-ring indices from the Camp Creek site. Indicated are the years in which *D* reached its twenty highest and twenty lowest values.

Figures 5.13 and 5.14 (with plotted seasonal temperatures from all 120 years) show that extreme *D*-values (*D*<-0.15 and *D*>+0.56) tend to occur within certain quadrants, i.e. that certain combinations of warm and cold seasons result in ring widths that are markedly different between the two species. For example, quadrant 2 (Figure 5.13) contains 10 out of the 20 lowest *D*-values (*D*<-0.15), indicating that *Libocedrus bidwillii* forms narrower rings than pink pine mostly when a cold previous winter is succeeded by a warm summer. Warm springs and warm summers (quadrant 5; Figure 5.14), on the other hand, typically lead to *Libocedrus bidwillii* rings that are wider than pink pine rings (11 out of the 20 highest *D*-values: *D*>+0.56). The results (the number of extreme events in each quadrant) are summarised in Tables 5.5a and 5.5b.

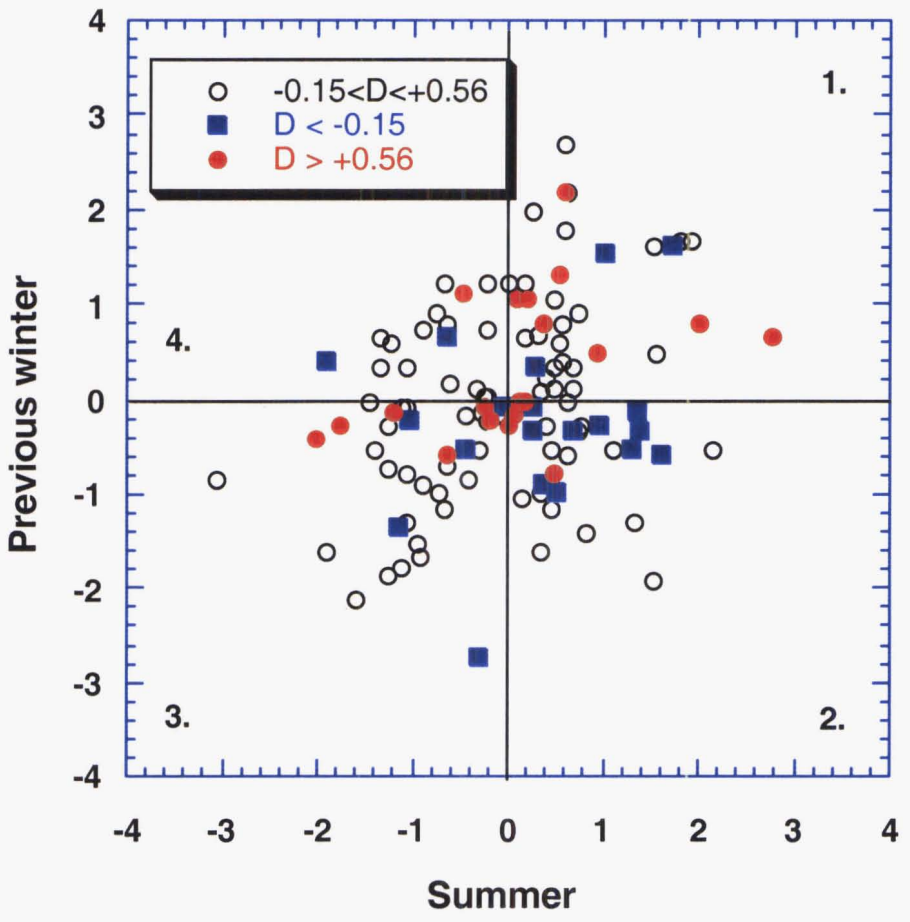

Figure 5.13 Scatter plot of the normalised temperatures: winter prior to the growing season (previous June-August) and summer (December-February). Based on 120 pairs of data (1866-1880 and 1894-1998). Red circles and blue squares indicate the years in which *D* reached its twenty highest (*D*>+0.56) and twenty lowest (*D*<-0.15) values, respectively. Individual quadrants are numbered 1 to 4.

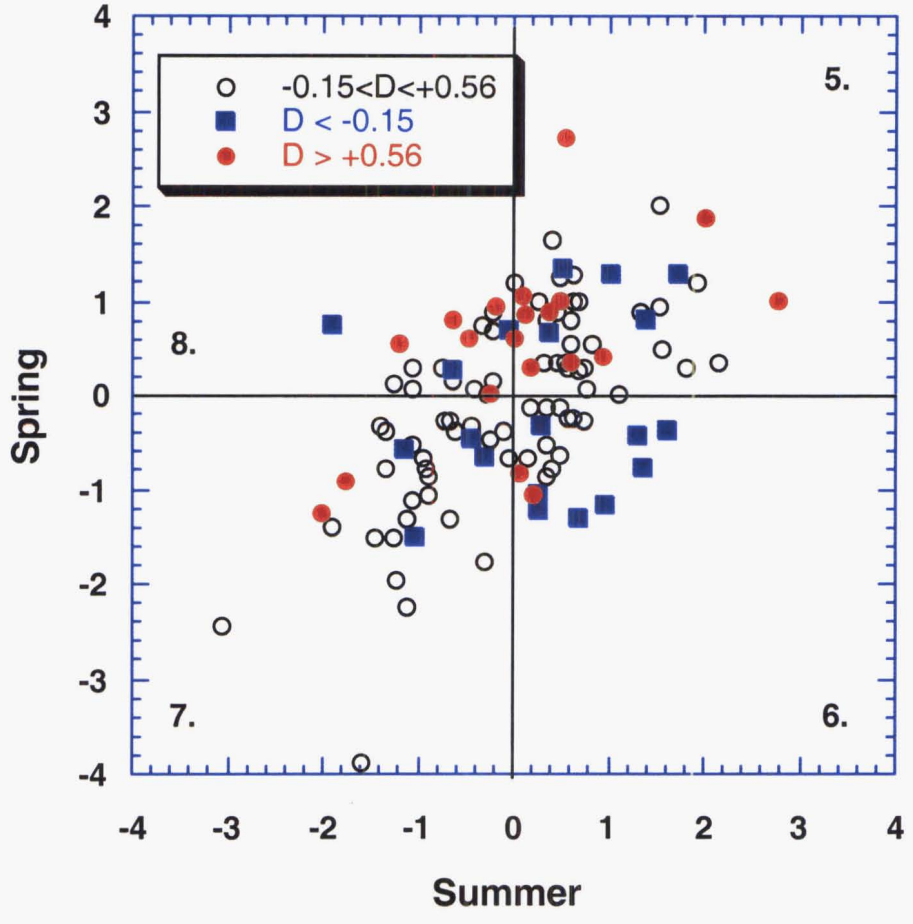

Figure 5.14 Scatter plot of the normalised temperatures: spring (September-November) and summer (December-February). Based on 120 pairs of data (1866-1880 and 1894-1998). Red circles and blue squares indicate the years in which *D* reached its twenty highest (*D*>+0.56) and twenty lowest (*D*<-0.15) values, respectively. Individual quadrants are numbered 5 to 8.

Table 5.5a shows that the occurrence of narrower *Libocedrus bidwillii* rings than pink pine rings (*D*<-0.15) is related to cold winters and springs. A significant majority (27 out of 40; Sign test: n=40, S=27, P<0.05) of these low *D*-values occurred when there had been a cold winter or spring (quadrants 2, 3, 6 and 7), compared with only 13 in warm winters and springs (quadrants 1, 4, 5 and 8). Low *D*-values (*D*<-0.15) are also associated with warm summers (quadrants 1, 2, 5 and 6) more frequently than cold summers (quadrants 3, 4, 7 and 8; Table 5.5a; Sign test: n=40, S=26, P<0.05). The opposite (wide *Libocedrus bidwillii* rings and narrow pink pine rings; *D*>+0.56) occurred when winter and spring temperatures were above average (quadrants 1, 4, 5 and 8), however this result is significant only when *D*-values within 0.25 SD of the mean are ignored (Table 5.5b; Sign test: n=36, S=25, P<0.05).

Tables 5.5a and 5.5b Number of low (a) and high (b) *D*-values within each temperature quadrant (Q1-Q8): summary of the results presented in Figures 5.13 and 5.14. Seasons were identified as "cold" or "warm" when the normalised 3-month averages were below or above zero, respectively. Numbers in brackets indicate the frequency when values within 0.25 SD of the mean (zero) are excluded from the analysis.

Table 5.5a $D < -0.15$ (*Libocedrus bidwillii* < pink pine).

Season	Cold summer	Warm summer	Total
Cold previous winter	Q3: 5 (4)	Q2: 10	**15 (14)**
Cold spring	Q7: 4	Q6: 8	**12**
Warm previous winter	Q4: 2	Q1: 3	**5**
Warm spring	Q8: 3	Q5: 5	**8**
Total	**14 (13)**	**26**	**40 (39)**

Table 5.5b $D > +0.56$ (*Libocedrus bidwillii* > pink pine).

Season	Cold summer	Warm summer	Total
Cold previous winter	Q3: 6 (5)	Q2: 5 (2)	**11 (7)**
Cold spring	Q7: 2	Q6: 2	**4**
Warm previous winter	Q4: 1	Q1: 8	**9**
Warm spring	Q8: 5	Q5: 11	**16**
Total	**14 (13)**	**26 (23)**	**40 (36)**

5.4 Discussion

The PCA output (Figure 5.6) confirmed that tree-growth patterns of Westland trees differ from patterns found in other regions of New Zealand. This is consistent with the results of Xiong and Palmer (2002a), who compared 23 *Libocedrus bidwillii* chronologies from both the North and the South Island, and found that most series were very similar. The only exceptions were AHA, CRC and TRK, which are all from Westland. From the high correlation value between CRC and TRK (Pearson's product moment correlation coefficient: RP = 0.77, P<0.001), Xiong and Palmer (2002a) inferred that these two sites had been subject to a strong regional influence.

This regional influence does not stem simply from a site being located in Westland. As both Xiong and Palmer (2002a) and this work (Figure 5.6) show, other Westland sites (AHA, RUH and WBF) are also different from CRC and TRK. It seems that to be part of a Westland regional population, sites need to meet additional requirements: (1) location west of the Southern Alps' main divide, (2) high elevation, and (3) location on a steep slope on the weather side of a mountain (western or northern exposure, typically). This observation is valid

for both *Libocedrus bidwillii* and pink pine, as can be seen from the composition of WLB and WRC, respectively. The regional chronologies comprise sites (CCP, MTF, CRC, TRK, BON, GLS, MEL, MGR and TKG; Chapters 4 and 5), that meet all three criteria.

Temperature is one of the factors that influence the growth of both *Libocedrus bidwillii* and pink pine in Westland. However, it is different months that have the biggest effect on each species. While pink pine is sensitive to summer temperatures (Chapter 3), *Libocedrus bidwillii* is responding to conditions in winter prior to the growing season and in spring (Figure 5.9). This difference in temperature response explains the correlations between WRC and WLB (highest value for the low-pass filtered data; Section 5.3.1). Because the WRC reflects mostly summer temperatures, but the WLB is more of an expression of temperatures earlier in the (biological) year, it is expected that the two chronologies are more similar in their low frequencies than they are in their high frequencies. This is because seasonal temperatures are more similar in the low-frequency domain, too. It has been shown for the Southern Hemisphere as a whole (Jones and Briffa, 1992), and for the Hokitika station in particular (Salinger *et al.*, 1992a). Year-to-year differences between seasons (and hence chronologies) are, on the other hand, greater due to short-term changes in circulation/weather patterns.

Three other studies in New Zealand have investigated the relationship between temperature and *Libocedrus bidwillii* tree-ring data (Xiong, 1995; Xiong and Palmer, 2000b; Palmer and Xiong, 2003). They found that in most chronologies, the strongest and most consistent climate signal was a negative response to February and March temperatures one year prior to the growing season. This is different from the results presented here. The sole indication of such relationship in this work is the negative correlation between WLB and temperatures in previous February, significant in the early period (1897-1947) only (Figure 5.10). Since shorter (both tree-ring and temperature) records were available for the previous studies (Xiong, 1995; Xiong and Palmer, 2000b; Palmer and Xiong, 2003), it is possible that the period of analysis affected the results. However, it is more likely that it was the type, not the length of the records, which led to identification of different climate signals. Xiong and Palmer (2000b) and Palmer and Xiong (2003) used the national average temperature series and *Libocedrus bidwillii* chronologies from the North Island / Nelson area, whereas the results presented in this chapter are based on meteorological data from Hokitika and chronologies from Westland.

Xiong (1995) calculated response functions for 23 *Libocedrus bidwillii* chronologies located on both islands of New Zealand, CRC and TRK among them. He found that CRC exhibited significant relationships with temperatures in July prior to the growing season (+), in current October (-) and February (+); while TRK responded to temperatures in previous February (-), in July (+) and in September (+) at the start of the growing season. Except for the negative response to October temperatures (CRC), the results are consistent with the correlations between temperature and WLB (Figure 5.9). Xiong (1995) also concluded that while the majority of *Libocedrus bidwillii* chronologies responded well to the national average temperature series, CRC and TRK performed best when modelled against local (Hokitika) data. This again emphasises the uniqueness of Westland's tree-growth patterns and climate.

The rather unusual temperature response exhibited by most non-Westland *Libocedrus bidwillii* chronologies (i.e. the negative relationship with previous February and March) is not completely understood. Buckley *et al.* (1997), who described similar response patterns in Tasmanian *Lagarostrobos franklinii*, suggested that a warm growing season results in optimum growth rates that in turn depletes reserves of carbohydrate and nutrients for the next year. Allen (1998), who detected a negative response to previous year's temperatures in *Phyllocladus asplenifolius*, offered another explanation. Allen (1998) hypothesised that the delayed response might relate to reproductive biology – low temperatures lead to limited floral primordial formation with little flowering the next year. This in turn results in fast tree growth, because there is reduced competition between the reproductive and non-reproductive tissues. Both theories could be applicable also to *Libocedrus bidwillii* (Xiong and Palmer, 2000b; Palmer and Xiong, 2003).

Allen (1998) also suggested that the negative relationship with temperature might be linked to water stress. It would explain why *Libocedrus bidwillii* in Westland does not show the inverse response to previous year's temperatures. Compared with other New Zealand's regions, the precipitation in Westland is very high and unlikely to be limiting to tree growth (Chapter 3). Indeed, a correlation analysis between Hokitika rainfall and the WLB data revealed no significant relationships over the 22-month dendroclimatic window, with the exception of one positive value for previous September.

As opposed to the non-Westland *Libocedrus bidwillii* series, the WLB chronology produced in this study shows a simpler, direct relationship with temperatures during the growing season, and in winter prior to the growing season (implying that cold winters can delay the

start of tree growth, and therefore reduce the ring widths). However, the factors that influence the growth of *Libocedrus bidwillii* in Westland appear to be more complex – winter and spring temperatures alone explain only a small amount of variance in the ring widths, making the WLB chronology unsuitable for a temperature reconstruction.

In previous studies, only chronologies from the North Island / Nelson area have been used to reconstruct temperatures from *Libocedrus bidwillii* tree rings (Xiong and Palmer, 2000b; Palmer and Xiong, 2003). The two models explained 42% of the temperature variance in calibration and 16% in verification (Xiong and Palmer, 2000b), and 27% of variance in calibration and 14% in verification (Palmer and Xiong, 2003). In this work, the best calibration model could explain 25% of the variance in Westland temperatures, but because of the unsatisfactory verification, the reconstruction did not proceed. Xiong (1995) experimented with the CRC and TRK tree-ring data, and his attempt to reconstruct Hokitika temperatures has also been unsuccessful.

The case study from Camp Creek (CCP; Section 5.3.3) confirmed that the response to climate is species-dependent. Pink pine tree-ring indices were similar to *Libocedrus bidwillii* indices, when temperatures were below average (e.g. 1868, 1878, 1902, 1911-12, 1930-31 and 1992-93) or above average (e.g. 1924, 1956 and 1962) throughout the year. The ring-widths differed from one species to the other only when temperatures fluctuated within a year, i.e. when both cool and warm seasons occurred within the same year. The results are in agreement with the temperature response exhibited by both species (Chapter 3; Figure 5.9). It may be that *Libocedrus bidwillii* commences its growth earlier than pink pine, and is thus affected mainly by winter/spring temperatures (cf. summer for pink pine). Xiong (1995) showed that the growth of *Libocedrus bidwillii* starts in spring (end of September). However, since no physiological study has been conducted for pink pine, it is impossible at this stage to determine what mechanisms are responsible for the different response.

5.5 Summary and conclusions

Two original *Libocedrus bidwillii* ring-width chronologies were developed from central Westland, New Zealand. With a time span of 935 years (1064-1998), the CCP(LB) chronology is the longest chronology developed from this species. The two chronologies were compared with other *Libocedrus bidwillii* chronologies from the South Island. The assumption that tree-growth patterns in Westland differ from those in other parts of New Zealand was corroborated by PCA, when four Westland sites were classified as a separate

group. These four sites were merged to form a regional chronology (WLB). On the regional scale, pink pine (WRC) was very similar to *Libocedrus bidwillii* (WLB). The highest correlation between WRC and WLB was achieved in the low-frequency domain. Some disagreements in the year-to-year variability were probably due to different climate response.

Westland's *Libocedrus bidwillii* was sensitive to temperatures in winter prior to the growing season, in spring and in late summer. The highest and most consistent correlations between WLB and temperature occurred in September, indicating that spring conditions had the greatest influence on tree growth. The relationship with temperature was direct, and although it was significant for most of the months from May to November, and in February and March, it was not as prominent as the summer response exhibited by pink pine. It also differed from the temperature-tree growth relationships of *Libocedrus bidwillii* from other parts of New Zealand. It appears that *Libocedrus bidwillii* is, in this region at least, a less reliable source of palaeotemperature data than pink pine. The WLB chronology was therefore not used to reconstruct Westland temperatures.

The small-scale comparison confirmed that winter/spring temperatures influenced the growth of *Libocedrus bidwillii*, while summer temperatures were more important for pink pine. In other words, it confirmed that climate response is species-dependent. The reasons are probably related to species physiology and phenology, but further investigation is required to clarify the mechanism.

Chapter 6

Earthquakes

6.1 Introduction

Major disturbances, such as strong earthquakes, can confound climate reconstructions (Kitzberger *et al.*, 1995). Recognition and mitigation of the effects of large disturbances on tree growth is therefore an important element of dendroclimatic research. Being situated astride two crustal plates (Australian and Pacific; Figure 6.1), New Zealand has a tectonically active landscape. The chronology sites, on which the Westland palaeotemperature record (Chapter 4) is based, are located in a vicinity of the plates' boundary – the Alpine Fault. The objective of this chapter is to investigate if/how past earthquakes affected the tree-ring data, and consequently the temperature reconstruction.

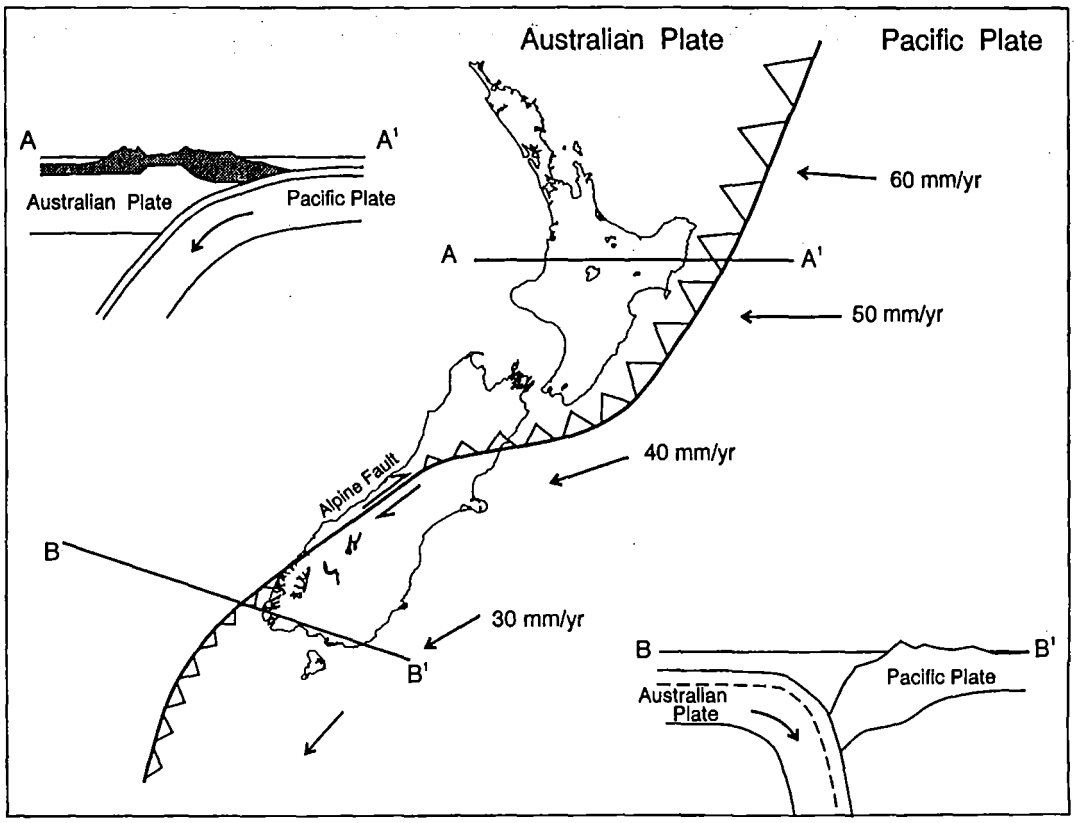

Figure 6.1 The Australian-Pacific plate boundary. Arrows show annual movement of the Pacific Plate relative to the Australian. (From Aitken, 1996).

Two scales – magnitude and intensity – are used to describe earthquakes. Magnitude is a measure of the amount of energy released during an earthquake. The first type of magnitude scale was devised by Charles Richter in 1935. Since then, several other techniques have been developed to determine the magnitude of an earthquake. Their applicability is dependent on the extent of the earthquake, the depth of its hypocentre (i.e. the place where the earthquake began), and the distance of the epicentre (i.e. the point on the Earth's surface directly above the hypocentre) from recording seismographs (Aitken and Lowry, 1995). While magnitude measures the original force at the hypocentre of the earthquake, intensity measures the degree of shaking that occurs at the surface. The intensity of an earthquake at a particular location indicates the local effects and damage of the earthquake upon people and their environment. The Modified Mercalli (MM) scale is used to determine the intensity values. It ranges from MM I (usually not felt by people) to MM XII (general panic and total destruction) (Eiby, 1966). Earthquakes may damage trees – directly through shaking, or indirectly through landslides – when their intensity reaches MM VI or higher (Table 6.1).

Table 6.1 The Modified Mercalli intensity scale. Earthquake effects on vegetation and landscape for MM ≥ VI. (Adapted from Eiby, 1966).

Intensity	Effects
MM VI	Trees and bushes shake, or are heard to rustle. Loose material may be dislodged from existing slips, talus slopes, or shingle slides.
MM VII	Trees and bushes strongly shaken. Small slips, and caving-in of sand and gravel banks.
MM VIII	Some tree branches may be broken off. Cracks appear on steep slopes and in wet ground. Landslips in roadside cuttings and unsupported excavations.
MM IX	Cracking of the ground conspicuous.
MM X	Large landslides on riverbanks and steep coasts.
MM XI	Great damage.
MM XII	Total damage. Large rock masses displaced. Visible wave-motion of the ground surface reported. Objects thrown upwards into the air.

Over the last 600 years, several earthquakes with epicentres in Westland were of 7+ magnitude, and their intensity reached MM X or higher. Two events (Murchison and Inangahua) are well documented, as they occurred only recently – in 1929 and 1968, respectively (Henderson, 1937; Benn, 1992; Anderson *et al.*, 1994; Downes; 1995). The sources of the Murchison and Inangahua earthquakes were two minor faults located west of the Alpine Fault – the White Creek and the Lyell faults, respectively (Anderson *et al.*, 1994). No seismicity associated directly with the Alpine Fault has been recorded over the last 160 years of European settlement. However, prehistoric dates of the three latest Alpine Fault

ruptures have been recently identified – these earthquakes, presumably stronger and more damaging than those at Murchison and Inangahua, occurred in 1717, at about 1630 and at about 1460 (Wells, 1998; Yetton *et al.*, 1998; Wells *et al.*, 1999).

Both direct and indirect indicators are used to investigate earthquake history. Evidence can be obtained, for example, from trenching, radiocarbon dating of organic material buried in landslides and river terraces, dating of earthquake-triggered tsunami deposits, or tree rings (Jacoby, 1997; Wells, 1998; Yetton, 1998; Yetton *et al.*, 1998; Wells *et al.*, 1999; Goff and McFadgen, 2001; Wells *et al.*, 2001).

Trees can respond to an earthquake on several scales, ranging from cells to stand-wide or regional levels. The changes in wood anatomy include formation of reaction wood, which occurs in conifers as dark, thick-walled cells (similar to latewood) on the downward side of a tilted trunk (Jacoby, 1997). Production of this compression wood also results in asymmetric growth (Berryman, 1980; Jacoby, 1997). Trees that survive damage to their tops and roots caused by shaking, or other injuries, may show growth suppressions (Kitzberger *et al.*, 1995; Jacoby, 1997; Wells *et al.*, 1999; Wells *et al.*, 2001). Other specimens may benefit from the death of neighbouring trees and show growth releases (Berryman, 1980; Veblen *et al.*, 1992; Kitzberger *et al.*, 1995; Jacoby, 1997; Vittoz *et al.*, 2001; Wells *et al.*, 2001). Another "earthquake signature" in tree-ring data may be a synchronous date of first (or last) ring, when trees colonise a disturbed surface (or suffer massive mortality), e.g. after a landslide (Veblen *et al.*, 1992; Jacoby, 1997). Earthquake impacts on forest age-class distributions have recently been identified for several South Island sites (Wells, 1998; Wells *et al.*, 1999; Vittoz *et al.*, 2001; Wells *et al.*, 2001).

No obvious changes in wood anatomy could be detected in the cores collected for this project (Section 5.2.3), and selective sampling (for the purpose of climate reconstruction) made it impossible to determine the age structure of stands. Therefore, only one indicator (changing growth rates, i.e. suppressions and releases) is used in this chapter to examine the disturbance history.

6.2 Materials and methods

Dates of growth releases and suppressions were recorded for all crossdated cores (from thirteen pink pine sites and two *Libocedrus bidwillii* sites; Chapters 2 and 5). I analysed the raw (non-standardised) ring-width series. Since the purpose of standardisation is to remove

variations due to factors other than climate (Fritts, 1976), using the raw measurements is more appropriate in disturbance studies (Veblen *et al.*, 1992; Nowacki and Abrams, 1997; Vittoz *et al.*, 2001; Wells *et al.*, 2001). For each core, I compared sequential 5-year ring-width means, and calculated the percentage growth change (*%GC*) using the formula proposed by Nowacki and Abrams (1997) (Equation 6.1):

$$\%GC = [(M_2 - M_1) / M_1] * 100 \qquad (6.1)$$

where *%GC* = percentage growth change between preceding and subsequent 5-year means, M_1 = preceding 5-year mean, and M_2 = subsequent 5-year mean. The growth change is affixed to the last year of the preceding 5-year period (M_1), thus M_1 = 1972-1976 and M_2 = 1977-1981 would be used to calculate *%GC* at the year 1976, etc.

The 5-year span, which I selected for radial-growth averaging, has been previously used in forest-disturbance studies in South America (Veblen *et al.*, 1992) and New Zealand (Vittoz *et al.*, 2001; Wells *et al.*, 2001). I did not apply the filter developed by Kitzberger *et al.* (1995) to the data, because it uses 2-year periods for the calculation, which I believe is too short to eliminate short-term growth responses related to climate. Also, in dendroecological research, only sequences of more than three marker years are considered abrupt growth changes (Schweingruber, 1990a). At the other end of the time-span spectrum would be the 10-year period used by Nowacki and Abrams (1997), but averaging over such a great length of time might obscure the detection of shorter growth responses.

I defined growth releases and suppressions as ≥ 100% changes in mean ring-width between consecutive 5-year periods. Thus, from Equation 6.1, $M_2 \geq 2M_1$ ($\%GC \geq 100$) for a release, and $M_1 \geq 2M_2$ ($\%GC \leq -50$) for a suppression. Selection of the 100% threshold was a subjective decision. In other studies, the values ranged from 25% (Nowacki and Abrams, 1997) to 250% (Veblen *et al.*, 1992; Vittoz *et al.*, 2001). The minimum threshold for disturbance recognition varied with the species investigated, site conditions, and the purpose of the research. Here, few abrupt growth changes (less than 1% of all 5-year periods) could be identified in pink pine when using the 250%, or even 150% (Wells *et al.*, 2001), thresholds. Since three major earthquakes occurred over the last 540 years (Wells *et al.*, 2001), up to 2.8% of all 5-year periods (three events in 108) could potentially show a release or a suppression. This is based on the assumption that the Alpine Fault earthquakes represented the most severe disturbances at each site. By selecting the 100% growth-change threshold, 3.1% of all 5-year periods (i.e.

one event in each core per 160 years) were identified as either a release or a suppression. This effectively covers all of the major events (and it also leaves some space for other disturbances), while not being too liberal.

In *Libocedrus bidwillii*, using the 100% threshold resulted in recognition of more abrupt changes in tree growth (9.3% of all 5-year periods; i.e. one event in each core per 53 years). A higher value, such as the 150% used for this species by Wells *et al.* (2001), might be more appropriate. However, for the purpose of comparison, I retained the same minimum threshold as for pink pine.

When a ≥100% growth change was calculated for two or more consecutive years, only the first year was identified as a release or a suppression. For example, when $\%GC \leq -50$ for 1976 (M_1 = 1972-1976; M_2 = 1977-1981) and $\%GC \leq -50$ for 1977 (M_1 = 1973-1977; M_2 = 1978-1982), I assigned the suppression to 1976 only. For each site, I combined the dates of abrupt changes for all trees, and grouped them into 5-year classes. The grouping is justified by the fact that while some trees respond to a disturbance immediately, other individuals may show a delay of several years (Veblen *et al.*, 1992; Kitzberger *et al.*, 1995; Wells *et al.*, 1999). The results were then summarised as the percentage of all cores from a site, and presented only for the periods in which the number of cores was five or greater.

6.3 Results

Figures 6.2-6.4 present the proportion of samples from each site (arranged from north to south) that show an abrupt increase or decrease in growth. At GLS (Figure 6.2), TOS and OMO (Figure 6.4), releases occurred about as often as suppressions. At the remaining ten pink pine sites, releases were nearly twice as frequent as suppressions (Figures 6.2-6.4). *Libocedrus bidwillii* shows, on the other hand, more suppressions than releases (Figure 6.3). The variability in radial growth of *Libocedrus bidwillii* is very high – compared with pink pine, about thrice as many releases and suppressions were detected in the *Libocedrus bidwillii* cores.

In pink pine, the proportion of samples with a release or suppression for any given 5-year period rarely exceeds 20%. The seemingly frequent growth changes occurring in the early part of the record (Figures 6.2-6.4) were influenced by low sample size. More recently, over 20% cores show a growth release in the 1560s (CCP, MGR, BON and ELD), in 1596-1600 (MTF), 1726-1730 (SPD), at around 1950 (MEL, CCP and BON), and in the early 1970s

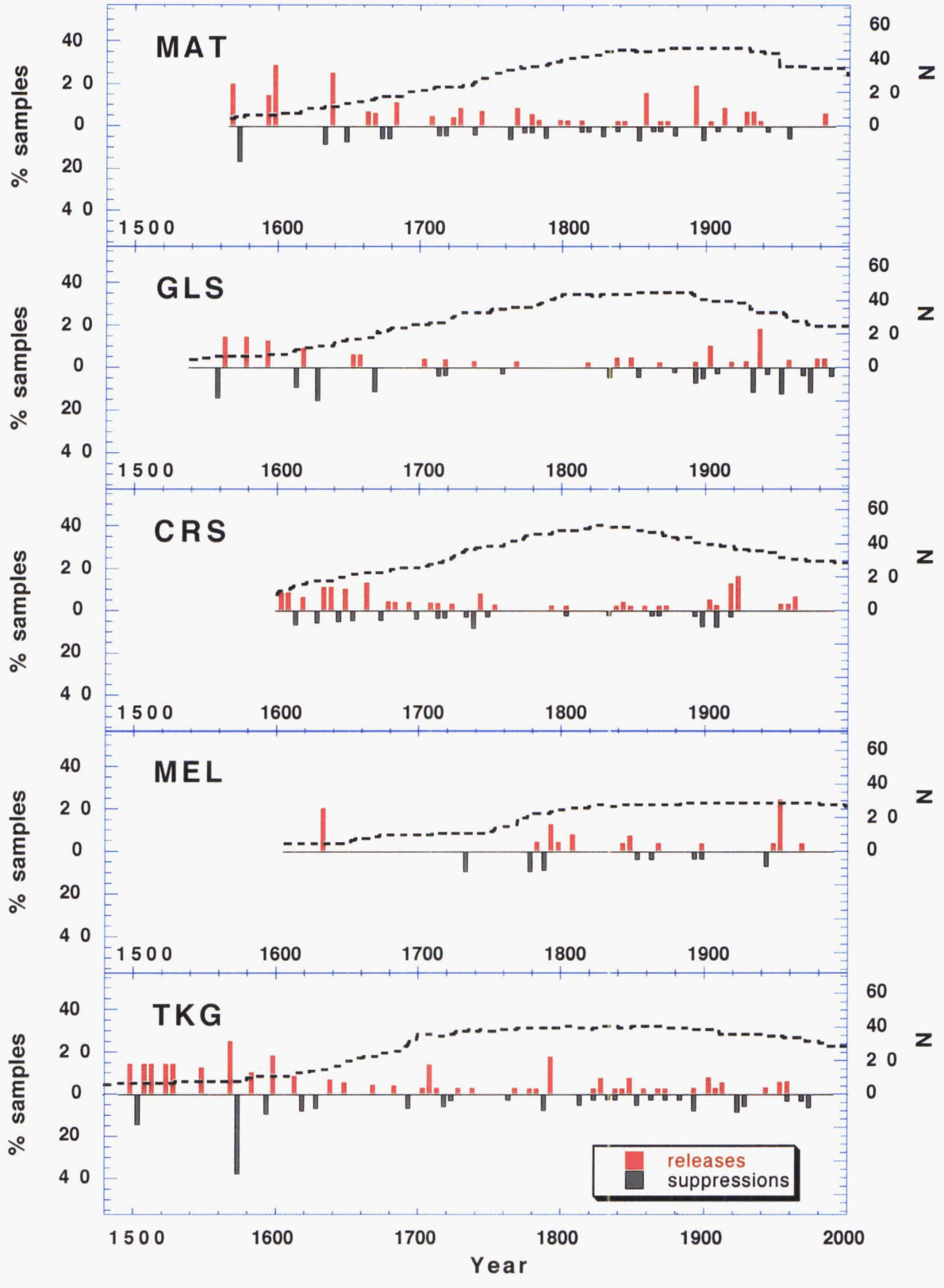

Figure 6.2 Proportion of cores showing a growth release (red) or suppression (black) for five northern sites. Dashed lines indicate the number of samples available (*N*).

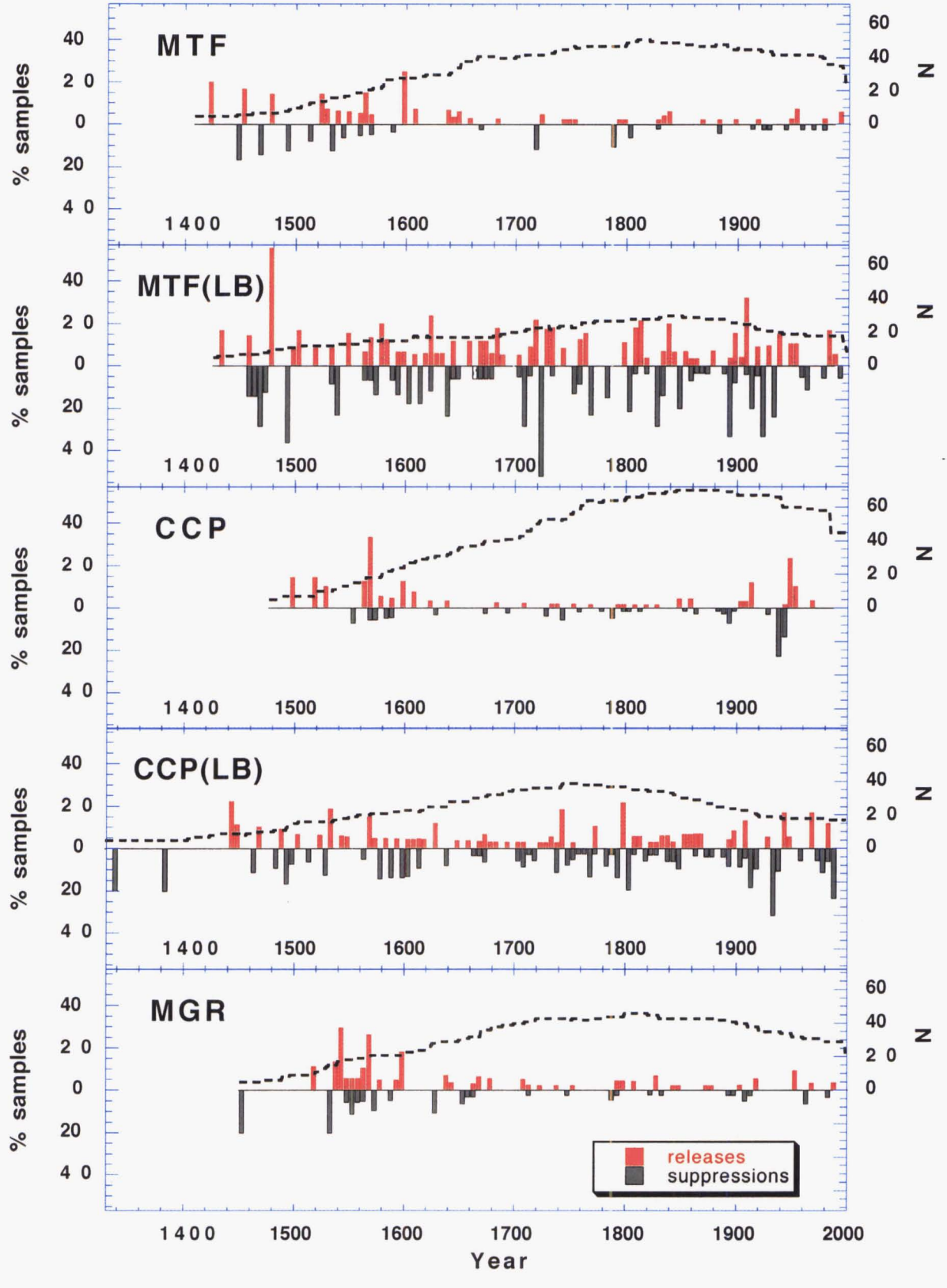

Figure 6.3 Proportion of cores showing a growth release (red) or suppression (black) for three central sites (two species). Dashed lines indicate the number of samples available (*N*).

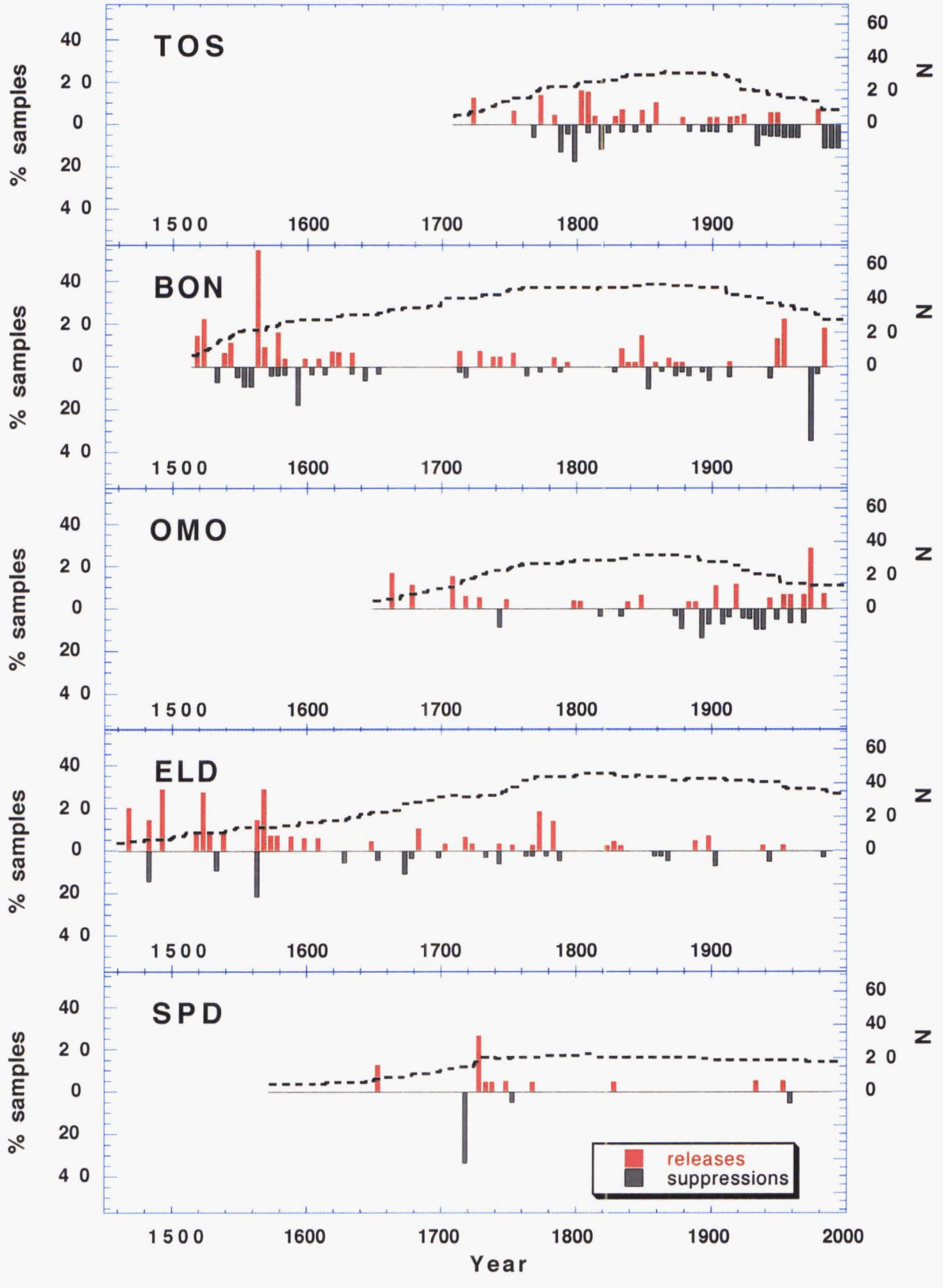

Figure 6.4 Proportion of cores showing a growth release (red) or suppression (black) for five southern sites. Dashed lines indicate the number of samples available (*N*).

(OMO). Remarkable growth suppressions occurred in 1561-1565 (ELD), 1716-1720 (SPD), 1936-1940 (CCP) and 1971-1975 (BON). The only decade, in which both releases and suppressions were frequent, is the 1560s at ELD (Figure 6.4).

Among the two *Libocedrus bidwillii* chronology sites, abrupt growth changes were more common in MTF(LB) (Figure 6.3). Frequent releases and suppressions in MTF(LB) occurred throughout the 18th century, with 52% samples showing a suppression in 1721-1725. This coincides with the 1717 Alpine Fault earthquake (Wells *et al.*, 1999). Major growth changes in MTF(LB) are also apparent in the first half of the 19th century, and in 1890-1940. In CCP(LB), more than 20% cores show a release in 1796-1800, while the growth was suppressed in the early 1930s and in the late 1980s (Figure 6.3). As for pink pine, the frequencies at both sites are high in the early period, due to small sample size.

6.4 Discussion

The results indicate that earthquakes had no major impact on the growth of pink pine. With the exception of ELD during the 1560s (Figure 6.4), I did not detect any frequent, simultaneous growth releases and suppressions, as could be expected in earthquake-affected trees (Jacoby, 1997; Wells *et al.*, 2001). Because of the low sample size, interpretation of the impacts of the oldest Alpine Fault rupture (around 1460; Wells *et al.*, 1999) is not possible. At no site are the EPS values (a measure of chronology's reliability; Chapter 2) above 0.85 for that period. The next major earthquake (around 1630; Wells *et al.*, 1999) did not result in any remarkable growth changes (Figures 6.2-6.4). The biggest growth anomaly concurrent with the latest Alpine Fault event (in 1717; Wells *et al.*, 1999) are the suppressions at SPD (Figure 6.4). However, the existence of a direct link is rather dubious, since the SPD site is located in Catlins (southeastern South Island; Figure 2.1) – of all the sites investigated, SPD lies the farthest from the fault.

According to the model published by Yetton *et al.* (1998), the 1717 earthquake resulted in MM VI intensities in Southland. Several events recorded over the last 160 years produced similar or higher intensities in parts of the study area, but none of them affected the SPD site (Table 6.2). Thus the impact of known earthquakes on SPD cannot be documented and compared with the 1717 response. It is plausible that the post-1717 growth suppressions detected in four SPD trees (five cores) were not related to the Alpine Fault rupture. It does not seem likely that trees growing on a stable, flat surface (Table 2.1) would show more damage than trees from steep slopes that were exposed to higher earthquake intensities.

Table 6.2 New Zealand earthquakes of magnitude 7 or more since 1848. Listed are only those earthquakes for which intensity reached MM VI or more in the study area. MM ≥ VI: chronology sites located between the epicentre and the MM VI isoseismal line. Based on data from Downes (1995).

Event name	Date	Magnitude	Epicentre	Depth	MM ≥ VI
Marlborough	15 Oct 1848	7.1	41.5°S, 173.8°E	Shallow	MAT, GLS
Wairarapa	23 Jan 1855	8.1 - 8.2	41.4°S, 175.0°E	Shallow	MAT, GLS
Cape Farewell	18 Oct 1868	7.0 – 7.5	40.3°S, 172.9°E	Shallow	MAT, GLS
North Canterbury	31 Aug 1888	7.0 – 7.3	42.6°S, 172.4°E	Shallow	CRS, MEL, TKG, MTF, CCP
Arthur's Pass	9 Mar 1929	7.1	42.8°S, 171.9°E	< 15 km	MAT, GLS, CRS, MEL, TKG, MTF, CCP
Murchison (Buller)	16 Jun 1929	7.8	41.7°S, 172.2°E	20 km	MAT, GLS, CRS, MEL, TKG, MTF, CCP, MGR, TOS
Charles Sound	16 Dec 1938	7.0	45.0°S, 167.0°E	60 km	ELD
Inangahua	23 May 1968	7.0 – 7.4	41.8°S, 172.0°E	15 km	MAT, GLS, CRS, MEL, TKG, MTF, CCP, MGR, TOS

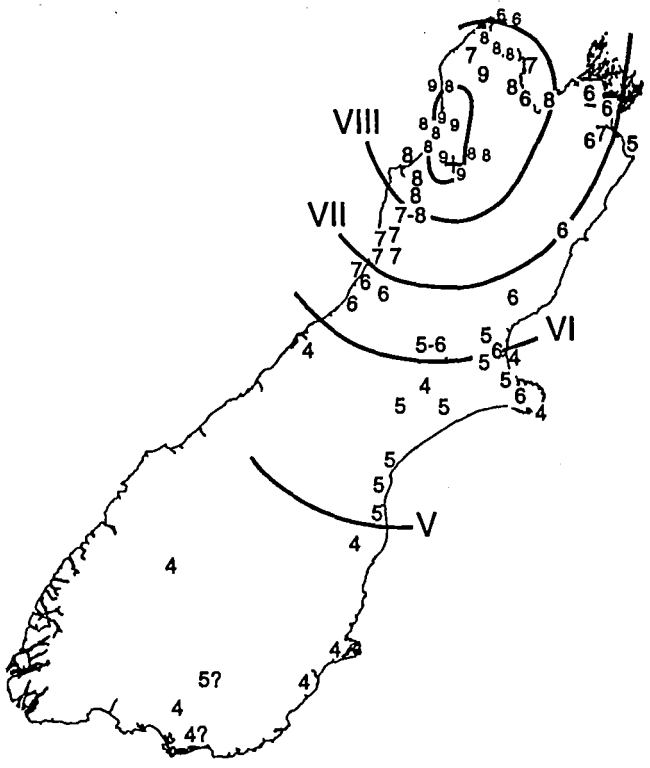

Figure 6.5 Isoseismal map of the South Island, showing the felt intensities of the 1929 Murchison earthquake. Units: the Modified Mercalli (MM) scale. (From Downes, 1995 based on Dowrick, 1994.)

Among the historical earthquakes (Table 6.2), Murchison and Inangahua had the greatest potential to induce abrupt growth changes in pink pine. The 1929 Murchison earthquake (Figure 6.5) and the 1968 Inangahua earthquake (Figure 6.6) resulted in high intensities (MM≥VII) recorded in the northern part of the study area. However, no clear signs of either event were visible in the ring-width patterns of trees from the four northernmost sites (Figure 6.2; Table 6.3).

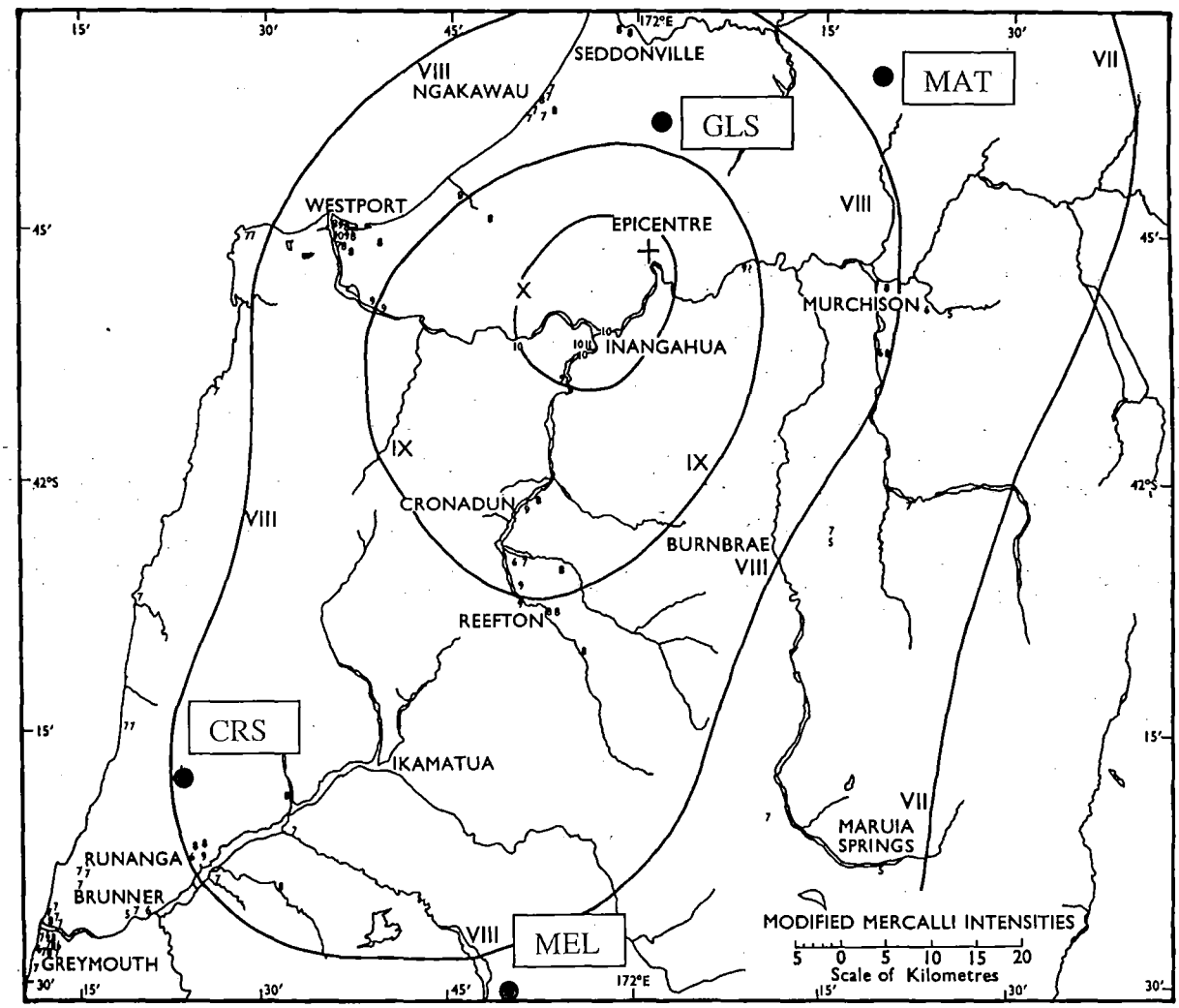

Figure 6.6 Isoseismal map showing the felt intensities of the 1968 Inangahua earthquake. Units: the Modified Mercalli (MM) scale. Indicated are the locations of four pink pine chronology sites. (Adapted from Downes, 1995.)

In Figure 6.2, abrupt growth changes were grouped into 5-year classes. Table 6.3 presents the results in more detail – it shows the annual number of releases and suppressions for the four sites nearest to the epicentres of the two historical earthquakes. At MAT, periods of increased growth were detected in only three cores out of 47 (6.4%) immediately after the 1929

Murchison earthquake, and further three cores showed a release 4-6 years later (Table 6.3). At GLS, several cores showed a suppression 3-5 years after both earthquakes (Table 6.3), but since the proportion was still very low, and no releases were detected over the same period, this cannot be considered an "earthquake signature."

Table 6.3 Number of growth releases (rel.) and suppressions (sup.) in four 5-year periods for four northern sites. Also indicated is the total number of samples available (ranging from 26 to 47). Highlighted are the years in which the Murchison (1929) and Inangahua (1968) earthquakes occurred.

Year	MAT	GLS	CRS	MEL
1926				
1927				
1928				
1929		1 / 39 (rel.)		
1930	3 / 47 (rel.)			
1931				
1932				
1933	1 / 45 (rel.)	1 / 35 (sup.)		
1934	1 / 45 (rel.)	3 / 35 (sup.)		
1935	1 / 45 (rel.)			
1966				
1967		1 / 28 (sup.)		
1968				
1969				
1970				1 / 29 (rel.)
1971		3 / 26 (sup.)		
1972				
1973				
1974				
1975				

The lack of clear, widespread earthquake signals may be surprising, considering how close the pink pine sites were to the Alpine Fault. Eight sites located between 42°30'S and 43°25'S (i.e. between and including MEL and OMO) were within 15 km of the fault. Allen *et al.* (1999) found that a *Nothofagus solandri* var. *cliffortioides* stand located 10 km of a 6.7-magnitude earthquake epicentre suffered 24% tree mortality and 23% tree injury, mainly as a result of the earthquake-induced landslides. One reason for the lack of response in pink pine could be that seven of the eight sites mentioned above (all except for CCP) were situated on the Australian Plate. With its granite bedrock, landforms on the Australian Plate are generally much more stable than the steep slopes and alluvial deposits that are characteristic of the

Pacific Plate (Figure 1.3). The *Nothofagus* stand described by Allen *et al.* (1999) was a typical example of such Pacific Plate site.

The same argument helps to explain why Wells *et al.* (1999) found supporting evidence for the 1717 earthquake in *Libocedrus bidwillii* and *Nothofagus* ssp. chronologies. All eight chronologies that showed a decrease in ring widths after 1717 were from the Pacific Plate (note: some caution is, nevertheless, required, as these results were based on 1-12 radii only). Two chronologies (14 and 25 radii) lacking this suppression were from the Australian Plate (Wells *et al.*, 1999). In a latter study, Wells *et al.* (2001) detected earthquake-related growth releases and suppressions in tree rings from the Welcome Flat area. Again, the Welcome Flat site is located on the Pacific Plate, and is surrounded by steep peaks composed of weak schist rock masses. Another, and perhaps more important, factor that contributed to the detection of abrupt growth changes by Wells *et al.* (2001) was that the authors used *Libocedrus bidwillii* in their research. Thus both the study sites (Australian Plate predominantly) and the species investigated (pink pine) might be responsible for the paucity of earthquake signals here.

Because of their asynchronicity, it appears that most releases and suppressions in pink pine were related to climate. For example, the increase in growth around 1950 (MEL, CCP, BON; Figures 6.2-6.4) is concurrent with an increase in temperature at the same time (Section 3.2.1). Similar results were obtained also for Westland *Nothofagus* (Cullen, 2001; Cullen *et al.*, 2001a). The climate link is encouraging in view of the temperature reconstruction (Chapter 4), since it indicates that disturbances did not confound the proxy record in any serious manner. Perhaps one part of the palaeotemperature series that needs to be treated with caution would be the 1560s. In Chapter 4, 1557-1566 was identified as the coldest 10-year period over the last 520 years. At about the same time, both releases and suppressions were detected at some of the central and southern sites (TKG, MTF, CCP, MGR, BON and ELD; Figures 6.2-6.4), which would suggest that a disturbance (e.g. windstorm) had occurred there.

Interesting results were obtained for the two *Libocedrus bidwillii* sites (Figure 6.3). Although the mean sensitivity values – about 0.13 for pink pine (Chapter 2) and about 0.16 for *Libocedrus bidwillii* (Chapter 5) – indicated that ring widths were slightly more variable in *Libocedrus bidwillii*, the proportion of abrupt growth changes was greater than anticipated. Another unexpected outcome was the higher occurrence of abrupt growth changes in MTF(LB), as Mt. French (MTF) is a granitic outcrop located on the Australian Plate. Fewer releases and suppressions were detected in CCP(LB), in spite of the fact that the underlying

substrate at Camp Creek (CCP) is soft schist (Pacific Plate). However, the particular area from which both pink pine and *Libocedrus bidwillii* were sampled – the upper valley at CCP – has been found to be relatively stable (Stewart and Harrison, 1987).

Age-class distribution studies have shown that both major and minor disturbances are important for the establishment of *Libocedrus bidwillii* (Norton, 1983d; Stewart and Rose, 1989; Wardle, 1991). The high proportion of suppressions and releases (Figure 6.3) implies that disturbances affect not only the establishment, but also the growth rates of *Libocedrus bidwillii*. The release that is evident in 22% cores at MTF(LB) in 1716-1720, and which is followed by a suppression in 1721-1725 (52% cores; Figure 6.3), is probably a result of the 1717 earthquake (Wells *et al.*, 1999). (Note: pink pine from the same site, MTF, shows only 12% suppressions and 5% releases over those two periods.)

Other abrupt growth changes, which were identified in *Libocedrus bidwillii*, could be attributed to frequent, smaller-scale disturbances, such as windthrow. Releases and suppressions, especially at MTF(LB), were common around the turn of the 20th century (Figure 6.3). At least two severe storms affected Westland at that time – in 1898 (Foster, 1931) and in 1905 (Benn, 1990). Abrupt growth changes in the 1890s and in the early 20th century have also been recorded in several *Nothofagus* stands in north Westland (Cullen *et al.*, 2001a; Vittoz *et al.*, 2001).

It seems that tree-growth patterns in *Libocedrus bidwillii* reflect numerous disturbances, both large and small. Without the knowledge of earthquake history, it would be very difficult to separate earthquake-induced growth changes from those caused by windstorms, erosion, or landslides of nonseismic origin. Pink pine's response to disturbances, on the other hand, appears to be very weak. Thus, in neither species could I distinguish clear earthquake signals. However, it must be acknowledged that the sampling was not suited to palaeoseismic research – the primary focus of this study was palaeoclimate. Ideally in dendroseismology, trees within a few tens of metres of the surface rupture should be sampled, and both changing growth rates and age-class distribution should be investigated (Jacoby, 1997).

6.5 Summary and conclusions

Thirteen pink pine and two *Libocedrus bidwillii* chronology sites were used to investigate the earthquake history in Westland. I screened individual samples for abrupt growth changes, assuming that earthquake disturbances would emerge in tree-growth patterns as simultaneous

releases and suppressions. These were common in *Libocedrus bidwillii*; however, the growth changes were not confined only to the years in which earthquakes occurred. This implies that *Libocedrus bidwillii* is sensitive to both large-scale and small-scale disturbances. It might be one reason why the temperature reconstruction (Chapter 5) was unsuccessful – both temperature and disturbance signals were present in the *Libocedrus bidwillii* tree-ring data.

Few abrupt growth changes were detected in pink pine. Neither historical nor prehistorical earthquakes seem to have influenced pink pine's growth rates. Since in most cases, releases and suppressions did not occur simultaneously, they could be attributed to climate. Based on the results presented in this chapter, I was unable to identify the temporal and spatial pattern of major earthquakes that affected Westland in the past centuries. However, the results reinforced the reliability of the Westland palaeotemperature series (Chapter 4). With the exception of the 1560s, when a disturbance may have affected the growth of pink pine, the temperature reconstruction is unlikely to contain any major disturbance signals.

Chapter 7

Conclusions

7.1 Summary and final discussion

Pink pine tree-ring data have been used to reconstruct temperatures back to 1480 for the Westland region of New Zealand. Especially in the high frequencies, the reconstruction captures the variations in summer (January-March) temperatures with a remarkable degree of fidelity. The calibration model explains 43% of the variance in the instrumental climate data, and all verification tests have been passed at high levels of significance. The Westland palaeotemperature record exhibits an overall positive trend, with the lowest temperatures occurring in the mid-sixteenth century, and with the maximum in the second half of the twentieth century. With a departure of 0.56 ± 0.02°C from the reconstruction mean, 1966-1990 is the warmest 25-year period over the last 520 years.

This anomalous warming is consistent with both New Zealand (Salinger *et al.*, 1992a) and global (Jones *et al.*, 1986; Jones and Briffa, 1992) instrumental records. Interpretations of the significance of the recent warming vary. Some tree-ring and multiproxy palaeoclimate studies conclude that temperatures in the 20th century have been the highest over the last millennium (Briffa *et al.*, 1995; Mann *et al.*, 1999; Jones *et al.*, 2001). Other results (Cook *et al.*, 1992; Luckman *et al.*, 1997; Cook *et al.*, 2002a; Esper *et al.*, 2002) indicate that the warming is comparable with the Medieval Warm Period (MWP). The MWP was an epoch of very high temperatures in about A.D. 1000-1300 (Lamb, 1965).

Some proxy temperature records contain distinct regional signals and do not provide any evidence of a warming trend whatsoever (Briffa *et al.*, 1992; Lara and Villalba, 1993). The Westland reconstruction (Chapter 4), on the other hand, is representative of the hemispheric climate changes – at least over the length of instrumental data (Jones *et al.*, 2001). The record high temperatures of the late 20th century could, judged by this study alone, seem beyond the natural variability of climate over New Zealand. However, with a time span of 520 years, the Westland palaeotemperature record is relatively short – it does not even approach the MWP (Lamb, 1965). The recent warming could still be a part of some low-frequency (>500 years),

natural climate cycles. Multi-millennial records are clearly essential for proper evaluation of the current trends in climate.

It may be best used in conjunction with other, longer proxy records; nevertheless, the Westland reconstruction contributes greatly to the existing set of palaeotemperature records derived from New Zealand tree rings (Norton *et al.*, 1989; Palmer, 1989; Salinger *et al.*, 1994; Xiong and Palmer, 2000b; Cook *et al.*, 2002b). The model developed in this thesis is currently the most accurate estimate of a temperature-growth relationship in the country (based on the calibration and verification statistics). The Westland palaeotemperature record is among the longest, second after the Oroko Swamp reconstruction (Cook *et al.*, 2002b). These two series are also the only ones that have been developed specifically for Westland, with the WRC covering a more extensive geographical area (Chapter 4).

Existing reconstructions of New Zealand temperatures (Norton *et al.*, 1989; Palmer, 1989; Salinger *et al.*, 1994; Xiong and Palmer, 2000b) show a varying degree of agreement, both with the Westland record and among themselves. One reason is that different authors reconstructed different variables (non-identical months or seasons; regional versus national temperatures). This mainly affected the data in higher frequencies. In lower frequencies, standardisation methods had the greatest influence. However, even when the same techniques were applied to the same data, strikingly dissimilar results were often obtained, depending merely on the choice of calibration period (Norton *et al.*, 1989; Salinger *et al.*, 1994; Xiong and Palmer, 2000b).

Xiong and Palmer (2000b) have demonstrated that when comparing year-to-year variability, tree-ring reconstructions of New Zealand temperatures were highly correlated ($P<0.02$). The proxy record that they derived from eleven *Libocedrus bidwillii* chronologies was also significantly correlated with the Westland temperatures produced in this thesis (Section 4.4). Most disagreements among the New Zealand-wide reconstructions were associated with longer-term trends (Xiong and Palmer, 2000b). Similar results were obtained for the Westland record – when comparing warm and cold periods spanning over several years (up to 25), it was not consistent with previous work (Table 7.1). For example, Palmer and Xiong (2003) identified the 1593-1617 period as one of the warmest over the last 500 years, whereas 1591-1615 was among the coldest periods in the Westland palaeoseries (Table 7.1). The 1840-1860 period, identified previously as cold (Salinger *et al.*, 1994; Table 7.1) coincides with a decade in Westland that was the warmest outside of the twentieth century (1847-1856; Table 4.3b).

Table 7.1 Cold and warm periods in New Zealand tree-ring reconstructions. Source: A – this thesis (Tables 4.3a and 4.3b); B – Norton *et al.* (1989); C – Salinger *et al.* (1994); D – Xiong and Palmer (2000b); E – Palmer and Xiong (2003).

Tree-ring reconstr.	A: 1480-2000	B: 1730-1853	C: 1731-1862	D: 1720-1987	E: 1459-1986
	1503-1527	mid-1730s	1760s	1747-1766	1623-1647
Cold	1542-1566	1760s	around 1790	1845-1864	1678-1702
periods	1591-1615	1780s	1820s	1866-1885	1796-1820
	1616-1640	mid-1840s	1840-1860	1896-1915	1881-1905
	1646-1670			1931-1950	1940-1964
	1739-1763	early 1730s	1810s	1720-1739	1463-1487
Warm	1830-1854	1750s	mid-1830s	1807-1826	1519-1543
periods	1859-1883	1770s		1825-1844	1593-1617
	1939-1963	mid-1790s		1910-1929	1728-1752
	1966-1990	1805-1815		1956-1975	1763-1787
		1830s			

Comparison of the Westland reconstruction with the Oroko series (Cook *et al.*, 2002b) provided an important test, as different input variables (species and sites) were used to estimate the same output (Hokitika's January-March temperatures). The results (Section 4.3.3) were encouraging – the two reconstructions were very similar, especially in the year-to-year variability. However, disagreements were found in the lower frequencies (Figure 4.12). In the first few decades of the common period, this could be explained by fading sample depth in the Westland series. Another reason the Westland record should be treated with caution during this period is that it was based on young trees only (this will be discussed further in relation to the RCS method). The Westland and Oroko reconstructions exhibit different longer-term trends also at the start of the 18th century and during the 19th century (Figure 4.10; Figure 4.12). The causes are currently not clear and require further investigation.

On a larger scale, the Westland series can be compared with a tree-ring reconstruction from *Lagarostrobos franklinii*, in which Tasmanian November-April temperatures have been estimated back to A.D. 900 (Cook *et al.*, 1992). The Tasmanian reconstruction shows little century-scale fluctuations and trends. There is certainly no evidence for the overall positive trend that is apparent in the Westland record. The coldest and warmest 25-year periods in the Tasmanian reconstruction are 1890-1914 and 1965-1989, respectively (Cook *et al.*, 1992). Temperatures were very low in Westland around 1900 (Figure 4.6), although because of the positive trend, this period is not among the five coldest (Table 4.3a; Table 7.1). The warmest period (1965-1989) is nearly identical to the 1966-1990 segment, in which temperatures

reached their maximum in Westland (Table 4.3b). Over the last 500 years, Tasmanian temperatures were extremely low also in 1604-1628 and 1664-1688 (Cook *et al.*, 1992), broadly coinciding with the below-average temperatures of the 17th century in Westland (Table 4.3a; Table 7.1). Prior to the recent warming, Tasmanian temperatures were above average in 1476-1500, 1855-1879 and 1808-1832 (Cook *et al.*, 1992). Of these, only the 1855-1879 period is concurrent with 1859-1883, which was the second warmest 25-year period in the Westland reconstruction (Table 4.3b).

Few hemispheric temperature reconstructions exist for the Southern Hemisphere (Jones *et al.*, 1998; Jones *et al.*, 2001; Mann and Jones, 2003). Except for the sharp increase in temperatures during the 20th century, the multi-proxy records show little trend over the last 500 years. Up until the late 19th century, the agreement between the Westland and hemispheric series is weak. However, it must be noted that the reconstruction produced by Jones *et al.* (1998) had only 16% variance in common with hemispheric land and marine instrumental data on the inter-annual timescale, and 49% on the decadal timescale. These results were markedly poorer than for the Northern Hemisphere (Jones *et al.*, 1998). It has been generally acknowledged that because of the lack of both instrumental and proxy data, it would be dangerous to place too much reliance on the Southern Hemisphere temperature reconstructions (Jones *et al.*, 1998; Jones *et al.*, 2001; Mann and Jones, 2003).

While comparing the Westland palaeotemperature series with other records, one common feature has transpired: similarities, apparent in the high frequencies, often disappear when evaluating the longer-term trends. The great amount of low-frequency variance that has been retained is one of the prominent characteristics of the Westland reconstruction. Spectral analysis of the reconstructed data in the >10-year bandwidth identified 11-year and 22-year cycles (probably linked to solar activity), and also regular oscillations on the order of 14, 45 and 125 years in length (Chapter 4). But is it absolutely certain that these long trends represent temperature change?

The low-frequency component of the Westland palaeorecord is essentially identical to that of the WRC. Any errors in the chronology development might therefore compromise the final result. The major issue, and a potential source of bias, is undoubtedly the application of RCS (Briffa *et al.*, 1992) to the tree-ring data. As with the individual site chronologies (Chapter 2), possible inaccuracies in pith-offset estimates would only have a minimal effect on the WRC (Esper *et al.*, 2003). Another point of uncertainty discussed in Section 2.5 was the inclusion of

fast-growing trees (OMO and TOS) into the CLOSED population. This is of no concern here, since the WRC is based on samples from six sites only (excluding OMO and TOS), and the RCS was redone for this new subset of data (Section 4.2.1).

The biggest caveat as regards applying the RCS method is that it is not appropriate for even-aged cohorts of trees, because commonly experienced climate throughout their lifetimes might bias the shape of RCS curve (Briffa *et al.*, 1992). The method assumes a wide and temporally homogenous makeup of the replicate samples in the series – ideally, all time periods should be represented by trees of all ages. However, in this case, only young trees contribute to the early part of the WRC, while the recent section comprises mostly old material. Although there is some variation in tree ages (the estimated values range from about 250 to over 700 years), the temporal composition of the WRC is not optimal. A more homogenous makeup of the series could be assured by collecting sub-fossil pink pine material, which should be the priority of any future research.

Cross-spectral analysis (Chapter 4) revealed that the reconstructed data are highly coherent with the instrumental record, especially at periods of 3-4 years. These frequencies are most likely related to the El Niño-Southern Oscillation (ENSO) phenomenon. A strong forcing of Westland temperatures by ENSO was also suggested by the results of correlation analyses (Chapter 3), in which positive relationships between tree growth and the Southern Oscillation Index (SOI) were identified. The correlation analyses in Chapter 3 also indicated that precipitation does not affect the growth of pink pine in Westland, and that the primary growth-limiting factor is temperature.

This work presents the reconstruction of summer temperatures. I selected the January-March temperatures for modelling because (a) the correlations between tree growth and temperatures were highest for these months (Figure 3.7), and (b) the relationships were time stable (Figure 3.8). The dependence on summer temperatures is the expected and most commonly found type of response in trees at high altitudes/latitudes (Fritts, 1976; Briffa *et al.*, 1995; Buckley *et al.*, 1997; Cullen *et al.*, 2001b; Cook *et al.*, 2002a).

However, ring-width indices are often significantly correlated with temperatures over an extended period, which, in some cases, may exceed one year (Jacoby *et al.*, 1996; D'Arrigo *et al.*, 2001). This is especially true for evergreen conifers with long needle retention. Through their photosynthetic surfaces and root system, they can integrate temperatures over a longer

time period than the actual growing season (Kramer and Kozlowski, 1979; Jacoby *et al.*, 1996). This seems to be the case with pink pine – the trees can retain their leaves for up to 50 years (Wardle, 1963), and most chronologies in this thesis were significantly correlated with mean monthly temperatures from about previous May to current June (Figure 3.7). Reconstruction of temperatures averaged over periods longer than January-March is thus conceivable.

In the following example (Table 7.2; Figures 7.1 and 7.2), the Westland Regional Chronology (WRC; Chapter 4) has been used to reconstruct annual (June-May) temperatures. The model calibrated on the late period (1948-1999) explains 51.1% of the variance in June-May temperatures (cf. 42.9% for the summer temperatures / early-period calibration; Table 7.2). Figure 7.1 demonstrates the high degree of similarity between the reconstructed values and the instrumental record (Pearson's product moment correlation coefficient: RP = 0.75, $P<0.001$, for the 1895-1999 period).

Table 7.2 Experimental reconstruction of annual temperatures – calibration and verification statistics for the late-calibration model. Values obtained for the annual temperatures are compared with those for the early-calibrated, summer-temperature model from Chapter 4 (in brackets). Stat. = statistic; P = probability level. RP = the Pearson's product moment correlation coefficient; RR = the robust correlation coefficient; RS = the Spearman's coefficient of rank correlation; PM = the product means test; ST = the sign test; RSQ = the variance explained; RE = the reduction of error; CE = the coefficient of efficiency.

Calibration (1948-1999)			Verification (1896-1947)		
Stat.	**Value**	**P**	**Stat.**	**Value**	**P**
RP	0.715 (0.655)	$< 10^{-5}$	RP	0.647 (0.661)	$< 10^{-5}$
RR	0.733 (0.667)	$< 10^{-5}$	RR	0.659 (0.656)	$< 10^{-5}$
RS	0.674 (0.704)	$< 10^{-5}$	RS	0.653 (0.653)	$< 10^{-5}$
PM	0.137 (0.483)	0.00001	PM	0.142 (0.391)	0.00217
ST	38+ 14- (41+ 12-)	0.00071	ST	40+ 12- (40+ 13-)	0.00009
RSQ	0.511 (0.429)	$< 10^{-5}$	RE	0.512 (0.557)	
			CE	0.360 (0.422)	

Because the results of calibrating any proxy data depend on the chosen seasonal temperature predictand, tree-ring series that can be used to reconstruct both summer and annual temperatures are extremely valuable (Briffa and Jones, 1993; Briffa and Osborn, 2002). This is especially true in the Northern Hemisphere, where the differences between seasonal and annual temperatures are greater (Jones and Briffa, 1992). The annual reconstruction (Figure 7.2) presented in this chapter is, however, virtually identical to the Westland summer palaeotemperature record (Figure 4.6). The reason is that the seasonal and annual temperature

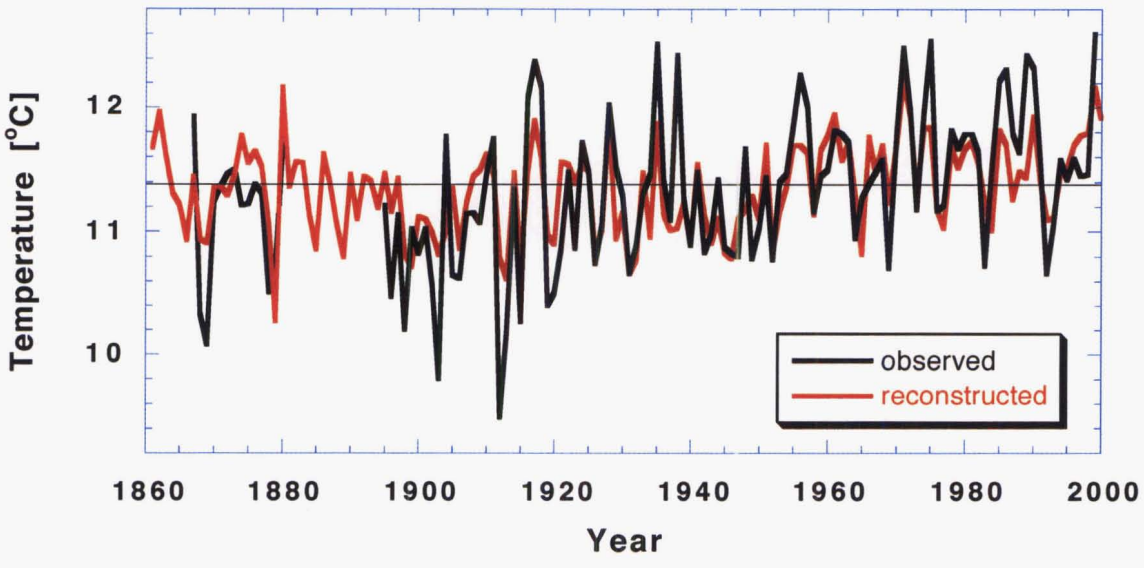

Figure 7.1 Observed (black) and reconstructed (red) Hokitika annual temperatures. Based on the 1948-1999 calibration period. The black horizontal line is the 20th century mean of Hokitika instrumental temperatures (June-May).

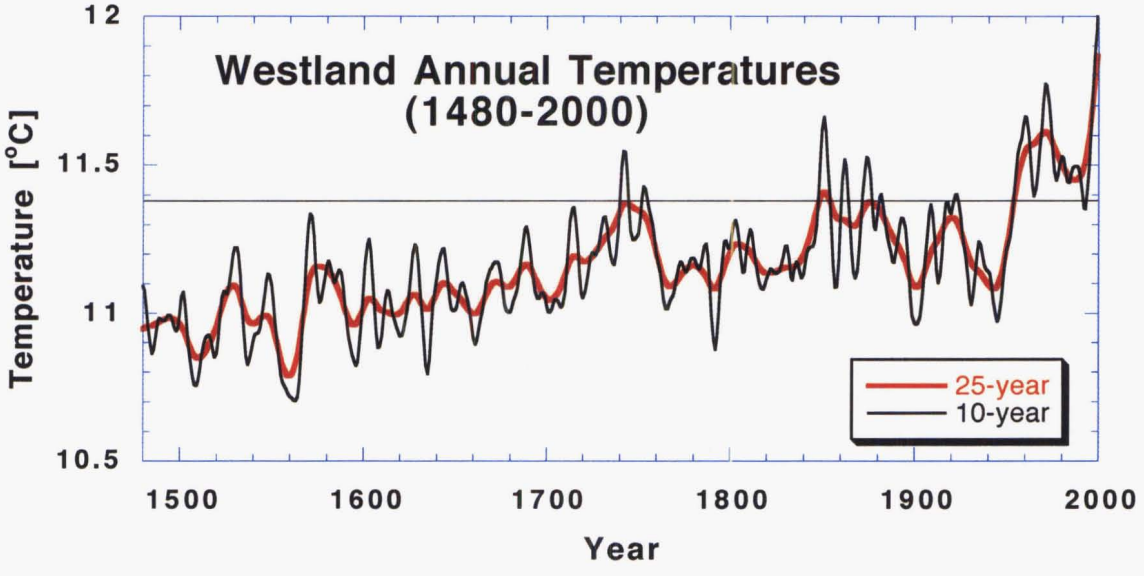

Figure 7.2 The Westland annual temperature reconstruction (1480-2000). The series has been smoothed to emphasise variance with wavelengths greater than 10 years (black) and 25 years (red). The black horizontal line is the 20th century mean of Hokitika instrumental temperatures (June-May).

anomalies are very similar in the Southern Hemisphere (Jones and Briffa, 1992), and the seasonality of proxy series is therefore of less concern here.

The response to summer (January-March) temperatures is more stable in time (as is also indicated by better verification statistics; Table 7.2), and this is a very important consideration in dendroclimatic research (Briffa *et al.*, 1998a). Thus, although the calibration statistics are higher for the annual temperatures (Table 7.2), the reconstruction is not necessarily an improvement over the one presented in Chapter 4. It merely offers another, valid alternative.

As well as reconstructing past temperatures, this thesis has compared the temperature sensitivity of pink pine with that of *Libocedrus bidwillii* (Chapter 5). While pink pine is mainly affected by summer conditions, *Libocedrus bidwillii* in Westland responds to temperatures at the start of the growing season (winter/spring). The differences in climate response are probably related to species physiology and phenology, but the exact mechanism requires further investigation. It also appears that *Libocedrus bidwillii* tree rings integrate both climate and disturbance signals (Chapter 6). Disturbances have only a small effect on the growth of pink pine (Chapter 6), which is one of the reasons why pink pine ring widths are such excellent indicators of Westland's palaeotemperatures.

Finally, this work has strengthened the New Zealand network of chronology sites by producing fifteen original ring-width chronologies. Thirteen chronologies were developed for pink pine (Chapter 2), and two for *Libocedrus bidwillii* (Chapter 5). All relevant data, including the crossdated raw measurements, will be contributed to the ITRDB in the near future.

7.2 Further research

While yielding a robust 520-year palaeotemperature record, this study has also raised several questions, and highlighted areas on which further research should focus. Extending the chronology network could be one way of increasing both the time span and the reliability of future climate reconstructions. Only six chronologies were used for the temperature reconstruction in this study. Development of new pink pine chronologies would increase the sample size (which is important for the RCS method in particular), and it would also expand the relevant area – the six chronology sites were located within only two latitudinal degrees, between 41°37'S and 43°05'S. However, the establishment of new study sites might prove difficult in the *Nothofagus*-dominated southern Westland.

Pink pine chronologies could be extended not only spatially, but also temporally. This research has shown that pink pine's longevity exceeds 650 years. Yet the reconstruction spans only 520 years. Provided that all or most stands contain trees that are older than 600 years, sampling of those specimens could improve the statistical quality in early parts of the chronologies, and thus extend the reconstruction further back in time. Besides the search for old living trees, collection of sub-fossil material should become one of the main objectives of future research. The timber of pink pine is extremely durable – possibly the most durable of New Zealand native woods (Cockayne and Turner, 1967; Salmon, 1996). Inclusion of sub-fossil material might therefore extend the chronologies by several centuries or more. It would also ensure that more than one population is represented in the sample, and that the analyses cannot be affected by the stand dynamics of a single cohort. Currently, a great volume of sub-fossil material, including pink pine, is being excavated in central Westland (Figure 7.3). Such unique opportunities, where easily accessible sub-fossil logs amount to dozens, if not hundreds, should not be missed.

Figure 7.3 Sampling of sub-fossil pink pine material at Weka Farm (January, 2003). Weka Farm is located in central Westland, about 10 km northeast of Lake Brunner.

This study has also reinforced the need for a detailed investigation into the physiology of pink pine. How exactly does climate affect the growth of this species? Correlation and response function analyses suggested a casual input-output relationship between temperature and tree growth. The increase in ring widths over the recent decades was consistent with both local and hemispheric/global instrumental records (Salinger *et al.*, 1992a; Jones and Briffa, 1992). However, can we be confident that temperature was the only forcing mechanism? Other factors than temperature may enhance tree growth. These include atmospheric CO_2 and nitrogenous pollution, both of which show positive trends over the 20th century (Cook *et al.*, 1996; Briffa and Osborn, 1999).

Cook *et al.* (1996b) reasoned that a contribution from CO_2 fertilisation in tree growth would result in overestimating the actual temperatures in the calibration process. In this thesis, the reconstructed temperatures were slightly lower than the observed data, which would indicate that CO_2 did not affect tree growth. Pollution also appears negligible in Westland. But even if we do agree that ring widths reflect only/mainly variations in temperature, further research is required to improve our understanding of the relationship. Is there any temperature threshold, above which the positive linear response of trees breaks down (Briffa *et al.*, 1998a)? Is the positive response to winter temperatures a statistical artefact (i.e. do, in fact, only summer temperatures influence the growth), or can pink pine integrate temperatures over longer periods – both within and without the growing season (Jacoby *et al.*, 1996)? And how long is the growing season for pink pine?

The issue of thresholds has been raised by Briffa *et al.* (1998a) in connection with the unstable nature of the growth response to temperature. Allen (1998) has obtained similar results. In this work, only the January-March mean monthly temperatures show a consistent, strong positive relationship with tree-ring data. The response for other months differs according to the period (early or late) over which the correlation was computed. Linear transfer functions, which are typically employed in dendroclimatic research, may be oversimplifying the relationship between tree growth and climate. The use of nonlinear methods should be considered. Woodhouse (1999) experimented with artificial neural networks, although with only moderate success – the nonlinear model performed very well in the calibration period, but poorly in the verification period. However, Woodhouse (1999) is confident that the problem of model overfit can be resolved in the future.

Being a relatively "young" science, dendroclimatology is rapidly evolving, and new techniques are being developed constantly. Thus not only transfer functions, but statistical approaches in general, offer great scope for improvement. The tree-ring data collected here may benefit from re-processing in the future, when new methods of standardisation, calibration, verification, etc., are available.

Another subject that requires attention is the instrumental climate data. Only the Hokitika temperature and precipitation records have been used in this thesis. Compiling a regional record (from a network of stations) might prove valuable. Also, the relationships between tree growth and other climate variables (e.g. minimum temperature, maximum temperature, solar radiation, the Zonal and Meridional Indices) should be explored.

Parameters other than total ring width (earlywood width, latewood width, maximum density) have provided important refinements to a number of dendroclimatic studies in the Northern Hemisphere (Briffa *et al.*, 1992; Briffa *et al.*, 1995; D'Arrigo *et al.*, 1996; Luckman *et al.*, 1997; Briffa *et al.*, 1998a; Briffa *et al.*, 1998b; Xiong *et al.*, 1998-1999; Fujiwara *et al.*, 1999; Kalela-Brundin, 1999; Meldahl *et al.*, 1999). Because pink pine occurs in cool-moist climates, maximum-density data should have the greatest potential to improve the temperature reconstruction (Schweingruber, 1990b). Yet in a preliminary densitometric study on fifteen pink pine trees from a North Island site, earlywood-related parameters were more sensitive to climate than latewood-related parameters (Xiong *et al.*, 1998). The densitometric properties of pink pine are certainly worth further investigation; however, it may be difficult to extract density data from the samples collected for this thesis (narrowness of the rings in subalpine pink pine trees; lack of facilities in New Zealand). Densitometry is probably not a priority at this stage.

Another, and I believe more promising, way of refining climate reconstructions in New Zealand is by employing multiple-species networks. With different species being sensitive to climate in different seasons, palaeoclimates could be studied with increased resolution. Utilising multiple species would also improve the coverage – although pink pine has proved to be an excellent indicator of past temperatures, its distribution is limited. Other species could fill the gaps, both in a latitudinal and a longitudinal sense (southern Westland, east coast, North Island). New insights into past climatic variation and climate-growth relationships could be also gained from sampling along altitudinal transects.

Ultimately, the data obtained in this work should be combined with long tree-ring records and other proxies from regions beyond New Zealand. New large-scale climate reconstructions would not only extend our knowledge of past climates on hemispheric or global scales, but they would also improve our understanding of the current warming trends. To what degree is the recent increase in temperatures unusual when viewed against a background of past climate variability? Has the climate change resulted purely from industrial activities, or could it be partly attributed to low-frequency cycles that are naturally present in climate? Will the global warming continue in the next years and/or decades? If so, at what rate and magnitude? By shedding more light on our past, present and future, millennia-long palaeoclimate records have the potential to answer these questions.

Acknowledgements

I wish to thank many people for their help, advice and encouragement. Firstly, to my supervisors, Glenn Stewart (for supporting me even though I did not find his beloved earthquakes) and Stuart Larsen (for being so enthusiastic about this project, and for continuing to advise me even after his departure from Lincoln University). Jonathan Palmer for getting me hooked on dendrochronology, coffee and Harihari, and for supervising me throughout the years. Jonathan's expertise, guidance and help, both at the university and in the field, are greatly appreciated. Ed Cook... How can I express my gratitude in a few words? Ed has given me advice, support, inspiration, and a bottle of Basil Hayden. Upon his invitation to LDEO, I arrived in New York with a suitcase full of cores, and left equipped with both software and hardware, and a pretty good idea what to do next in terms of data analysis. Ed has also rescued me from the fast and loose lifestyle that I was leading in Mormonland by asking me to participate in a couple of data-collecting projects for their lab. And what did he get in return? Tracy Chapman and a trip to one of my nastier pink pine sites, which he had to pay for.

Limin "the Chinese Bear" Xiong has helped on countless occasions, like when I was struggling with computers in our tree-ring lab, or with increment borers in the bush. Louise Cullen has seen both the beginning and end of my Ph.D.-student career. She took me on my first sampling trip (to assist with her project; and I ventured into her subalpine sites wearing running shoes), and she also read an early draft of this thesis. I am not sure which occasion she found more horrifying. Hannah Buckley has kindly read the final draft, and I thank both Louise and Hannah for their helpful comments.

I am grateful to the Department of Conservation for allowing me to sample trees at all requested locations. I appreciate the financial assistance provided by the Lincoln University Doctoral Scholarship. The SPES Division covered majority of my research costs, and I would also like to acknowledge the contribution made by the R. C. Bruce Trust. The Commonwealth Science Council's travel grant enabled me to present the preliminary results of this research at the 6th International Conference on Dendrochronology in Quebec. Many thanks to Roland Jaspers for all his help and support in accounting matters.

A number of people have made my stay at Lincoln University enjoyable and sometimes bearable. Christine Stark has been a great friend over the years. Lora Peacock and Chris Berry have patiently listened to my whining and assisted with printing, and I hope we can graduate together, guys! Sandy Hammond helped me in the tree-ring lab and in the workshop. Jon Sullivan fixed my computer, which was an immense relief. Thanks to Kim, Cynthia, Hazel, Richard, Pascal and all the others seventh-floorers, whose company I have enjoyed very much.

To Paul and Anna Krusic: thank you for your friendship, all those wonderful trips, the Chicago tune and Dracula night, and for showing me that a 10-month old baby, nursing mother and a blind dog make the best cliffside-dendrochronology team. To all people from LDEO, with a special mention to Ken and Brendan, thank you. My field assistants have endured cold, rain, snow and New Zealand bush, while helping me to collect hundreds of samples all over the South Island. These are my heroes: Kathy Allen, Kim Bestic, Ed Cook, Simon Fenwick, Vladimír Kolář, Anna and Paul Krusic, Lukáš Lánský, Xiong Limin, Míša Mauleová, Alice Miller, Jonathan Palmer, Lynne Sheldon-Sayer, Martin Vaňous, Pascal Vittoz and Sarah Wedde. It is a source of continuing amazement to me that some of them came twice.

Finally, I would like to thank my family, who are probably still wondering what it is that I have been studying, but have been encouraging me nevertheless. Thank you, Simon, for your love, support and patience. I would not have started, let alone have finished, this without you.

References

Ahmed, M. (1984) *Ecological and dendrochronological studies on* Agathis australis *Salisb. (kauri) in New Zealan*d. Unpublished Ph.D. thesis. University of Auckland, Auckland, New Zealand.

Ahmed, M. and Ogden, J. (1985). Modern New Zealand tree-ring chronologies III: Agathis australis (Salisb.) – kauri. *Tree-Ring Bulletin*, 45, 11-24.

Aitken, J.J. (1996). Plate tectonics for curious Kiwis. *Institute of Geological and Nuclear Sciences information series 42*. Lower Hutt: Institute of Geological and Nuclear Sciences Limited.

Aitken, J.J. (1999). *Rocked and ruptured: geological faults in New Zealand.* Auckland: Reed Books.

Aitken, J.J. and Lowry, M.A. (1995). More earthquakes explained. *Institute of Geological and Nuclear Sciences information series 35*. Lower Hutt: Institute of Geological and Nuclear Sciences Limited.

Akaike, H. (1974). A new look at the statistical model identification. *IEEE Transactions on Automatic Control*, AC-19, 716-723.

Allan, R.J. (2000). ENSO and climatic variability in the past 150 years. In H.F. Diaz and V. Markgraf (Eds.), *El Niño and the Southern Oscillation: multiscale variability and global and regional impacts* (pp. 3-55). New York: Cambridge University Press.

Allan, R., Lindesay, I. and Parker, D. (1996). *El Niño, Southern Oscillation and climatic variability*. Collingwood: CSIRO Publishing.

Allen, K.J. (1998). *A dendroclimatological investigation of* Phyllocladus aspleniifolius *(Labill.) Hook. f.* Unpublished Ph.D. thesis. University of Tasmania, Hobart, Australia.

Allen, R.B., Bellingham, P.J. and Wiser, S.K. (1999). Immediate damage by an earthquake to a temperate montane forest. *Ecology*, 80, 708-714.

Anderson, H., Beanland, S., Blick, G., Darby, D., Downes, G., Haines, J., Jackson, J., Robinson, R. and Webb, T. (1994). The 1968 May 23 Inangahua, New Zealand, earthquake: an integrated geological, geodetic, and seismological source model. *New Zealand Journal of Geology and Geophysics*, 37, 59-86.

Australian Bureau of Meteorology (Ed.). (2002, April 3*). S.O.I. Archives – 1876 to present* [Homepage of Commonwealth of Australia 2002, Bureau of Meteorology]. Retrieved November 5, 2002 from http://www.bom.gov.au/climate/current/soihtm1.shtml

Barry, R.G. (1978). Climatic fluctuations during periods of historical and instrumental record. In A.B. Pittock, L.A. Frakes, D. Jenssen, J.A. Peterson and J.W. Zillman (Eds.), *Climatic change and variability: a Southern Hemisphere perspective* (pp. 150-166). London: Cambridge University Press.

Bell, V. and Bell, R.E. (1958). Dendrochronological studies in New Zealand. *Tree-Ring Bulletin*, 22, 7-11.

Benn, J.L. (1990). *A chronology of flooding on the West Coast, South Island, New Zealand: 1846-1990.* Unpublished report to the West Coast Regional Council, Greymouth, New Zealand.

Benn, J.L. (1992). *A review of earthquake hazards on the West Coast.* Unpublished report to the West Coast Regional Council, Greymouth, New Zealand.

Berryman, K.R. (1980). Late Quaternary movement on White Creek Fault, South Island, New Zealand. *New Zealand Journal of Geology and Geophysics*, 23, 93-101.

Blasing, T.J., Solomon, A.M. and Duvick, D.N. (1984). Response functions revisited. *Tree-Ring Bulletin*, 44, 1-15.

Box, G.E.P. and Jenkins, G.M. (1970). T*ime series analysis: forecasting and control.* San Francisco: Holden-Day.

Bradley, R.S. and Jones, P.D. (1993). 'Little Ice Age' summer temperature variations: their nature and relevance to recent global warming trends. *The Holocene*, 3, 367-376.

Bridge, M.C. and Ogden, J. (1986). A sub-fossil kauri (*Agathis australis*) tree-ring chronology. *Journal of the Royal Society of New Zealand*, 16, 17-23.

Briffa, K. and Jones, P.D. (1990). Basic chronology statistics and assessment. In E.R. Cook and L.A. Kairiukstis (Eds.), *Methods of dendrochronology: applications in the environmental sciences* (pp. 137-152). Dordrecht: Kluwer Academic Publishers.

Briffa, K. and Jones, P.D. (1993). Global surface air temperature variations during the twentieth century: Part 2, implications for large-scale high-frequency palaeoclimatic studies. *The Holocene*, 3, 77-88.

Briffa, K.R. and Osborn, T.J. (1999). Seeing the wood from the trees. *Science*, 284, 926-927.

Briffa, K.R. and Osborn, T.J. (2002). Blowing hot and cold. *Science*, 295, 2227-2228.

Briffa, K.R., Jones, P.D., Bartholin, T.S., Eckstein, D., Schweingruber, F.H., Karlen, W., Zetterberg, P. and Eronen, M. (1992). Fennoscandian summers from AD 500: temperature changes on short and long timescales. *Climate Dynamics*, 7, 111-119.

Briffa, K.R., Jones, P.D., Schweingruber, F.H., Shiyatov, S.G. and Cook, E.R. (1995). Unusual twentieth-century summer warmth in a 1,000-year temperature record from Siberia. *Nature*, 376, 156-159.

Briffa, K.R., Schweingruber, F.H., Jones, P.D., Osborn, T.J., Shiyatov, S.G. and Vaganov, E.A. (1998a). Reduced sensitivity of recent tree-growth to temperature at high northern latitudes. *Nature*, 391, 678-682.

Briffa, K.R., Jones, P.D., Schweingruber, F.H. and Osborn, T.J. (1998b). Influence of volcanic eruptions on Northern Hemisphere summer temperature over the past 600 years. *Nature*, 393, 450-455.

Brown, D. and Rothery, P. (1993). *Models in biology: mathematics, statistics and computing*. Chichester: John Wiley & Sons Ltd.

Buckley, B.M. (1997). *Climate variability in Tasmania based on dendrocliamtic studies of* Lagarostrobos franklinii. Unpublished Ph.D. thesis. University of Tasmania, Hobart, Australia.

Buckley, B.M., Cook, E.R., Peterson, M.J. and Barbetti, M. (1997). A changing temperature response with elevation for *Lagarostrobos franklinii* in Tasmania, Australia. *Climatic Change*, 36, 477-498.

Buckley, B., Ogden, J., Palmer, J., Fowler, A. and Salinger, J. (2000). Dendroclimatic interpretation of tree-rings in *Agathis australis* (kauri): 1. Climate correlation functions and master chronology. *Journal of The Royal Society of New Zealand*, 30, 263-276.

Burrows, C. (1982). On New Zealand climate within the last 1000 years. *New Zealand Journal of Archaeology*, 4, 157-167.

Burrows, C.J. and Greenland, D.E. (1979). An analysis of the evidence for climatic change in New Zealand in the last thousand years: evidence from diverse natural phenomena and from instrumental records. *Journal of the Royal Society of New Zealand*, 9, 321-373.

Campbell, D.A. (1982). Preliminary estimates of summer streamflow for Tasmania. In M.K. Hughes, P.M. Kelly, J.R. Pilcher and V.C. LaMarche Jr. (Eds.), *Climate from tree rings* (pp. 170-177). Cambridge: Cambridge University Press.

Caviedes, C.N. (2001). *El Niño: storming through the ages*. Gainesville: University Press of Florida.

Changnon, S.A. (2000). *El Niño 1997-1998: the climate event of the century*. New York: Oxford University Press.

Cleaveland, M.K., Cook, E.R. and Stahle, D.W. (1992). Secular variability of the Southern Oscillation detected in tree-ring data from Mexico and the southern United States. In H.F. Diaz and V. Markgraf (Eds.), *El Niño: historical and paleoclimatic aspects of the Southern Oscillation* (pp. 271-291). Cambridge: Cambridge University Press.

Climate Prediction Center (Ed.). (2002, November 21). *El Nino / La Nina Home* [Homepage of the Climate Prediction Center, NOAA]. Retrieved November 22, 2002 from http://www.cpc.ncep.noaa.gov/products/analysis_monitoring/lanina/

Cockayne, L. and Turner, E.P. (1967). *The trees of New Zealand*. (6th ed.). Wellington: Government Printer.

Cole, J.E. and Cook, E.R. (1998). The changing relationship between ENSO variability and moisture balance in the continental United States. *Geophysical Research Letters*, 25, 4529-4532.

Cook, E.R. (1985). A time series analysis approach to tree-ring standardisation. Unpublished Ph.D. thesis. University of Arizona, Tucson, USA.

Cook, E.R. (1992). Using tree rings to study past El Niño / Southern Oscillation influences on climate. In H.F. Diaz and V. Markgraf (Eds.), *El Niño: historical and paleoclimatic aspects of the Southern Oscillation* (pp. 203-214). Cambridge: Cambridge University Press.

Cook, E.R. (1995). Temperature histories from tree rings and corals. *Climate Dynamics*, 11, 211-222.

Cook, E. and Briffa, K. (1990). A comparison of some tree-ring standardization methods. In E.R. Cook and L.A. Kairiukstis (Eds.), *Methods of dendrochronology: applications in the environmental sciences* (pp. 153-162). Dordrecht: Kluwer Academic Publishers.

Cook, E.R. and Kairiukstis, L.A. (1990). *Methods of dendrochronology: applications in the environmental sciences*. Dordrecht: Kluwer Academic Publishers.

Cook, E.R. and Peters, K. (1981). The smoothing spline: a new approach to standardizing forest interior tree-ring width series for dendroclimatic studies. *Tree-Ring Bulletin*, 41, 45-53.

Cook, E., Briffa, K., Shiyatov, S. and Mazepa, V. (1990a). Tree-ring standardization and growth-trend estimation. In E.R. Cook and L.A. Kairiukstis (Eds.), *Methods of dendrochronology: applications in the environmental sciences* (pp. 104-123). Dordrecht: Kluwer Academic Publishers.

Cook, E., Shiyatov, S. and Mazepa, V. (1990b). Estimation of the mean chronology. In E.R. Cook and L.A. Kairiukstis (Eds.), *Methods of dendrochronology: applications in the environmental sciences* (pp. 123-132). Dordrecht: Kluwer Academic Publishers.

Cook, E., Bird, T., Peterson, M., Barbetti, M., Buckley, B., D'Arrigo, R., Francey, R. and Tans, P. (1991). Climatic change in Tasmania inferred from a 1089-year tree-ring chronology of Huon pine. *Science*, 253, 1266-1268.

Cook, E., Bird, T., Peterson, M., Barbetti, M., Buckley, B., D'Arrigo, R. and Francey, R. (1992). Climatic change over the last millennium in Tasmania reconstructed from tree-rings. *The Holocene*, 2, 205-217.

Cook, E.R., Briffa, K.R., Meko, D.M., Graybill, D.A. and Funkhouser, G. (1995). The 'segment length curse' in long tree-ring chronology development for palaeoclimatic studies. *The Holocene*, 5, 229-237.

Cook, E.R., Buckley, B.M. and D'Arrigo, R.D. (1996a). Inter-decadal climate oscillations in the Tasmanian sector of the Southern Hemisphere: evidence from tree rings over the past three millennia. In P.D. Jones, R.S. Bradley and J. Jouzel (Eds.), *Climatic variations and forcing mechanisms of the last 2000 years* (pp. 141-160). Berlin Heidelberg: Springer-Verlag.

Cook, E.R., Francey, R.J., Buckley, B.M. and D'Arrigo, R.D. (1996b). Recent increases in Tasmanian Huon pine ring widths from a subalpine stand: natural climate variability, CO_2 fertilisation, or greenhouse warming? *Papers and Proceedings of the Royal Society of Tasmania*, 130, 65-72.

Cook, E.R., Buckley, B.M., D'Arrigo, R.D. and Peterson, M.J. (2000a). Warm-season temperatures since 1600 BC reconstructed from Tasmanian tree rings and their relationship to large-scale sea surface temperature anomalies. *Climate Dynamics*, 16, 79-91.

Cook, E.R., D'Arrigo, R.D., Cole, J.E., Stahle, D.W. and Villalba, R. (2000b). Tree-ring records of past ENSO variability and forcing. In H.F. Diaz and V. Markgraf (Eds.), *El Niño and the Southern Oscillation: multiscale variability and global and regional impacts* (pp. 297-323). New York: Cambridge University Press.

Cook, E.R., Palmer, J.G., Cook, B.I., Hogg, A. and D'Arrigo, R.D. (2002a). A multi-millennial palaeoclimatic resource from *Lagarostrobos colensoi* tree-rings at Oroko Swamp, New Zealand. *Global Planetary Change*, 33, 209-220.

Cook, E.R., Palmer, J.G. and D'Arrigo, R.D. (2002b). Evidence for a 'Medieval Warm Period' in a 1,100 year tree-ring reconstruction of past Austral summer temperatures in New Zealand. *Geophysical Research Letters*, 29, 10.1029/2001BLO14580.

Cooley, W.W. and Lohnes, P.R. (1971). *Multivariate data analysis*. New York: John Wiley & Sons, Inc.

Cullen, L.E. (2001). *Climate warming and disturbance influences on* Nothofagus *treelines in north Westland, New Zealand.* Unpublished Ph.D. thesis. Lincoln University, Lincoln, New Zealand.

Cullen, L.E., Stewart, G.H., Duncan, R.P. and Palmer, J.G. (2001a). Disturbance and climate warming influences on New Zealand *Nothofagus* tree-line population dynamics. *Journal of Ecology*, 89, 1061-1071.

Cullen, L.E., Palmer, J.G., Duncan, R.P. and Stewart, G.H. (2001b). Climate change and tree-ring relationships of *Nothofagus menziesii* tree-line forests. *Canadian Journal of Forest Research*, 31, 1981-1991.

D'Arrigo, R.D. and Jacoby, G.C. (1992). A tree-ring reconstruction of New Mexico winter precipitation and its relation to El Niño / Southern Oscillation events. In H.F. Diaz and V. Markgraf (Eds.), *El Niño: historical and paleoclimatic aspects of the Southern Oscillation* (pp. 243-257). Cambridge: Cambridge University Press.

D'Arrigo, R.D., Buckley, B.M., Cook, E.R. and Wagner, W.S. (1995). Temperature-sensitive tree-ring width chronologies of pink pine (*Halocarpus biformis*) from Stewart Island, New Zealand. *Palaeogeography, Palaeoclimatology, Palaeoecology*, 119, 293-300.

D'Arrigo, R.D., Cook, E.R. and Jacoby, G.C. (1996). Annual to decadal-scale variations in northwest Atlantic sector temperatures inferred from Labrador tree rings. *Canadian Journal of Forest Research*, 26, 143-148.

D'Arrigo, R.D., Cook, E.R., Salinger, M.J., Palmer, J., Krusic, P.J., Buckley, B.M. and Villalba, R. (1998). Tree-ring records from New Zealand: long-term context for recent warming trend. *Climate Dynamics*, 14, 191-199.

D'Arrigo, R., Jacoby, G., Frank, D., Pederson, N., Cook, E., Buckley, B., Nachin, B., Mijiddorj, R. and Dugarjav, C. (2001), 1738 years of Mongolian temperature variability inferred from a tree-ring width chronology of Siberian pine. *Geophysical Research Letters*, 28, 543-546.

Diaz, H.F. and Markgraf, V. (1992). *El Niño: historical and paleoclimatic aspects of the Southern Oscillation.* Cambridge: Cambridge University Press.

Diaz, H.F. and Markgraf, V. (2000). *El Niño and the Southern Oscillation: multiscale variability and global and regional impacts*. New York: Cambridge University Press.

Downes, G.L. (1995). Atlas of isoseismal maps of New Zealand earthquakes. *Institute of Geological and Nuclear Sciences monograph 11*. Lower Hutt: Institute of Geological and Nuclear Sciences Limited.

Dowrick, D.J. (1994). Damage and intensities in the magnitude 7.8 1929 Murchison, New Zealand, earthquake. *Bulletin of the New Zealand National Society for Earthquake Engineering*, 27, 190-204.

Duncan, R.P. (1989). An evaluation of errors in tree age estimates based on increment cores in kahikatea (*Dacrycarpus dacrydioides*). *New Zealand Natural Sciences*, 16, 31-37.

Dunwiddie, P.W. (1979). Dendrochronological studies of indigenous New Zealand trees. *New Zealand Journal of Botany*, 17, 251-266.

Efron, B. (1987). Better bootstrap confidence intervals. *Journal of the American Statistical Association*, 82, 171-185.

Eiby, G.A. (1966). The Modified Mercalli scale of earthquake intensity and its use in New Zealand. *New Zealand Journal of Geology and Geophysics*, 9, 122-129.

Esper, J., Cook, E.R. and Schweingruber, F.H. (2002). Low-frequency signals in long tree-ring chronologies for reconstructing past temperature variability. *Science*, 295, 2250-2253.

Esper, J., Cook, E.R., Peters, K. and Schweingruber, F.H. (2003). Tests of the RCS method for preserving low-frequency variability in long tree-ring chronologies. *Tree-Ring Research* (in press).

Folland, C.K. and Salinger, M.J. (1995). Surface temperature trends and variations in New Zealand and the surrounding ocean, 1871-1993. *International Journal of Climatology*, 15, 1195-1218.

Foster, F.W. (1931). A stand of beech regeneration of known age. *Te Kura Ngahere*, 3, 39-40.

Fouhy, E., Coutts, L., McGann, R., Collen, B. and Salinger, J. (1992). *South Pacific historical climate network: climate station histories. Part 2: New Zealand and offshore islands*. Wellington: New Zealand Meteorological Service.

Fowler, A. (1988). Climate reconstruction from tree rings. *Weather and Climate*, 8, 33-45.

Fowler, A., Palmer, J., Salinger, J. and Ogden, J. (2000). Dendroclimatic interpretation of tree-rings in *Agathis australis* (kauri): 2. Evidence of a significant relationship with ENSO. *Journal of The Royal Society of New Zealand*, 30, 277-292.

Fritts, H.C. (1976). *Tree rings and climate*. London: Academic Press.

Fritts, H.C., Guiot, J. and Gordon, G.A. (1990). Verification. In E.R. Cook and L.A. Kairiukstis (Eds.), *Methods of dendrochronology: applications in the environmental sciences* (pp. 178-185). Dordrecht: Kluwer Academic Publishers.

Fujiwara, T., Okada. N. and Yamashita, K. (1999). Comparison of growth response of *Abies* and *Picea* species to climate in Mt. Norikura, central Japan. *Journal of Wood Science*, 45, 92-97.

Glantz, M.H. (1996). *Currents of change: El Niño's impact on climate and society.* Cambridge: Cambridge University Press.

Goff, J.R. and McFadgen, B.G. (2001, August). Nationwide tsunami during prehistoric Maori occupation, New Zealand. *ITS 2001 Proceedings, Session 3, Number 3-1.* [Pages of the International Tsunami Symposium, Seattle, 7-10 August 2001]. Retrieved January 8, 2003 from http://www.pmel.noaa.gov/its2001/Separate_Papers/3-01_Goff.pdf

Gordon, N.D. (1985). The Southern Oscillation: a New Zealand perspective. *Journal of the Royal Society of New Zealand*, 15, 137-155.

Graybill, D.A. (1982). Chronology development and analysis. In M.K. Hughes, P.M. Kelly, J.R. Pilcher and V.C. LaMarche Jr. (Eds.), *Climate from tree rings* (pp. 21-31). Cambridge: Cambridge University Press.

Graybill, D.A. and Shiyatov, S.G. (1989). A 1009 year tree-ring reconstruction of mean June-July temperature deviations in the Polar Urals. In *Symposium on Air Pollution Effects on Vegetation* (pp. 37-42). USDA Forest Service, Northwestern Forest Experiment Station.

Griffiths, G.A. and McSaveney, M.J. (1983). Distribution of mean annual precipitation across some steepland regions of New Zealand. *New Zealand Journal of Science*, 26, 197-209.

Grissino-Mayer, H.D. and Fritts, H.C. (1997). The International Tree-Ring Data Bank: an enhanced global database serving the global scientific community. *The Holocene*, 7, 235-238.

Guiot, J. (1986). ARMA techniques for modelling tree-ring response to climate and for reconstructing variations of paleoclimates. *Ecological Modelling*, 33, 149-171.

Guiot, J. (1990). Methods of calibration. In E.R. Cook and L.A. Kairiukstis (Eds.), *Methods of dendrochronology: applications in the environmental sciences* (pp. 165-178). Dordrecht: Kluwer Academic Publishers.

Henderson, J. (1937). The west Nelson earthquakes of 1929. *New Zealand Journal of Science and Technology*, 19, 65-144.

Hirschboeck, K.K. (1979-1980). A new worldwide chronology of volcanic eruptions. *Palaeogeography, Palaeoclimatology, Palaeoecology*, 29, 223-241.

Holmes, R.L. (1983). Computer-assisted quality control in tree-ring dating and measurement. *Tree-Ring Bulletin*, 43, 69-78.

Howell, P. (2001). *ARAND time series and spectral analysis package for the Macintosh, Brown University.* IGBP PAGES / World Data Center for Paleoclimatology Data Contribution Series #2001-031. NOAA / NGDC Paleoclimatology Program, Boulder, Colorado, USA.

Innes, J.L., Schneiter, G., Waldner, P. and Bräker, O.U. (2000). Latitudinal variations in tree growth in southern Chile. In F.A. Roig (Ed.), *Dendrocronología en América Latina / Dendrochronology in Latin America* (pp. 177-192). Mendoza: EDIUNC.

Institute of Geological and Nuclear Sciences (1996). New Zealand adrift. *Institute of Geological and Nuclear Sciences information series 39*. Lower Hutt: Institute of Geological and Nuclear Sciences Limited.

Intergovernmental Panel on Climate Change (1996). *IPCC second assessment: Climate change 1995: a report of the Intergovernmental Panel on Climate Change.* Geneva: World Meteorological Organization.

International Tree-Ring Data Bank (Ed.). (2002, December 11*). Tree-ring data search.* IGBP PAGES / World Data Center for Paleoclimatology, NOAA / NGDC Paleoclimatology Program, Boulder, Colorado, USA. Retrieved February 5, 2003 from http://www.ngdc.noaa.gov/paleo/ftp-treering.html

Jacoby, G.C. (1997). Application of tree ring analysis to paleoseismology. *Reviews of Geophysics*, 35, 109-124.

Jacoby, G.C., D'Arrigo, R.D. and Davaajamts, T. (1996). Mongolian tree rings and 20th-century warming. *Science*, 273, 771-773.

Jones, P.D. and Briffa, K.R. (1992). Global surface air temperature variations during the twentieth century: Part 1, spatial, temporal and seasonal details. *The Holocene*, 2, 165-179.

Jones, P.D., Wigley, T.M.L. and Wright, P.B. (1986). Global temperature variations between 1861 and 1984. *Nature*, 322, 430-434.

Jones, P.D., Briffa, K.R., Barnett, T.P. and Tett, S.F.B. (1998). High-resolution palaeoclimatic records for the last millennium: interpretation, integration and comparison with General Circulation Model control-run temperatures. *The Holocene*, 8, 455-471.

Jones, P.D., Osborn, T.J. and Briffa, K.R. (2001). The evolution of climate over the last millennium. *Science*, 292, 662-667.

Kalela-Brundin, M. (1999). Climatic information from tree-rings of *Pinus sylvestris* L. and a reconstruction of summer temperatures back to AD 1500 in Femundsmarka, eastern Norway, using partial least squares regression (PLS) analysis. *The Holocene*, 9, 59-77.

Kendall, M. and Ord, J.K. (1990). *Time series.* (3rd ed.). Sevenoaks, Kent: Edward Arnold.

Kitzberger, T., Veblen, T.T. and Villalba, R. (1995). Tectonic influences on tree growth in northern Patagonia, Argentina: the roles of substrate stability and climatic variation. *Canadian Journal of Forest Research*, 25, 1684-1696.

Koopmans, L.H. (1974). *The spectral analysis of time series*. New York: Academic Press.

Kramer, P.J. and Kozlowski, T.T. (1979). *Physiology of woody plants*. New York: Academic Press.

LaMarche, V.C., Jr. and Pittock, B. (1982). Preliminary temperature reconstruction for Tasmania. In M.K. Hughes, P.M. Kelly, J.R. Pilcher and V.C. LaMarche Jr. (Eds.), *Climate from tree rings* (pp. 177-185). Cambridge: Cambridge University Press.

LaMarche, V.C., Jr., Holmes, R.L., Dunwiddie, P.W. and Drew, L.G. (1979a). *Tree-ring chronologies of the Southern Hemisphere 4: Australia.* Laboratory of Tree-Ring Research, University of Arizona, Tucson.

LaMarche, V.C., Jr., Holmes, R.L., Dunwiddie, P.W. and Drew, L.G. (1979b). *Tree-ring chronologies of the Southern Hemisphere 3: New Zealand.* Laboratory of Tree-Ring Research, University of Arizona, Tucson.

Lamb, H.H. (1965). The early medieval warm period and its sequel. *Palaeogeography, Palaeoclimatology, Palaeoecology*, 1, 13-37.

Lara, A. and Villalba, R. (1993). A 3620-year temperature record from *Fitzroya cupressoides* tree rings in southern South America. *Science*, 260, 1104-1106.

Le Quesne, C., Aravena, J.C., Alvarez García, M.A. and Fernández Prieto, J.A. (2000). Dendrocronología de *Austrocedrus chilensis* (Cupressaceae) en Chile Central. In F.A. Roig (Ed.), *Dendrocronología en América Latina / Dendrochronology in Latin America* (pp. 159-175). Mendoza: EDIUNC.

Lough, J.M. (1992). An index of the Southern Oscillation reconstructed from western North American tree-ring chronologies. In H.F. Diaz and V. Markgraf (Eds.), *El Niño: historical and paleoclimatic aspects of the Southern Oscillation* (pp. 215-226). Cambridge: Cambridge University Press.

Luckman, B.H., Briffa, K.R., Jones, P.D. and Schweingruber, F.H. (1997). Tree-ring based reconstruction of summer temperatures at the Columbia Icefield, Alberta, Canada, AD 1073-1983. *The Holocene*, 7, 375-389.

Lydolph, P.E. (1985). *The climate of the Earth.* New Jersey: Rowman & Allanheld.

Mann, M.E. and Jones, P.D. (2003). Global surface temperatures over the past two millennia. *Geophysical Research Letters*, 30, 10.1029/2003GL017814.

Mann, M.E., Bradley, R.S. and Hughes, M.K. (1999). Northern Hemisphere temperatures during the past millennium: inferences, uncertainties, and limitations. *Geophysical Research Letters*, 26, 759-762.

McBride, J.L. and Nicholls, N. (1983). Seasonal relationships between Australian rainfall and the Southern Oscillation. *Monthly Weather Review*, 111, 1998-2004.

McGlone, M.S., Salinger, M.J. and Moar, N.T. (1993). Paleovegetation studies of New Zealand's climate since the last glacial maximum. In H.E. Wright, J.E. Kutzbach, T. Webb III, W.F. Ruddiman, F.A Street-Perrot and P.J. Bartlein (Eds.), *Global climates since the last glacial maximum* (pp. 294-317). Minneapolis: University of Minnesota Press.

Meko, D.M. (1992). Spectral properties of tree-ring data in the United States Southwest as related to El Niño / Southern Oscillation. In H.F. Diaz and V. Markgraf (Eds.), *El Niño: historical and paleoclimatic aspects of the Southern Oscillation* (pp. 227-241). Cambridge: Cambridge University Press.

Meldahl, R.S., Pederson, N., Kush, J.S. and Varner III, J.M. (1999). Dendrochronological investigations of climate and competitive effects on longleaf pine growth. In R. Wimmer and R.E. Vetter (Eds.), *Tree-ring analysis: biological, methodological and environmental aspects* (pp. 265-285). Oxon: CABI Publishing.

Mendenhall, W. and Sincich, T. (1988). *Statistics for the engineering and computer sciences.* (2nd ed.). San Francisco: Dellen Publishing Company.

Mullan, A.B. (1995). On the linearity and stability of Southern Oscillation-climate relationships for New Zealand. *International Journal of Climatology*, 15, 1365-1386.

Murphy, J.O. (1993). Dendrochronological investigation of *Halocarpus biformis* (pink pine) from a site at the West Arm of Lake Manapouri in New Zealand. *Australian Systematic Botany*, 6, 481-489.

New Zealand Geological Survey (1972). *South Island. (1st ed.). Geological map of New Zealand 1:1,000,000.* Wellington: Department of Scientific and Industrial Research.

New Zealand Meteorological Service (1984). Rainfall normals for New Zealand 1951 to 1980. *New Zealand Meteorological Service miscellaneous publication 185.*

New Zealand Soil Bureau (1968). *Soil map of the South Island, New Zealand: Sheet 3.* Wellington: Department of Scientific and Industrial Research.

Norton, D.A. (1983a). *A dendroclimatic analysis of three indigenous tree species, South Island, New Zealand.* Unpublished Ph.D. thesis. University of Canterbury, Christchurch, New Zealand.

Norton, D.A. (1983b). Modern New Zealand tree-ring chronologies: I. *Nothofagus solandri. Tree-Ring Bulletin*, 43, 1-17.

Norton, D.A. (1983c). Modern New Zealand tree-ring chronologies: I. *Nothofagus menziesii. Tree-Ring Bulletin*, 43, 39-49.

Norton, D.A. (1983d). Population dynamics of subalpine *Libocedrus bidwillii* forests in the Cropp River Valley, Westland, New Zealand. *New Zealand Journal of Botany*, 21, 127-134.

Norton, D.A. (1984). Tree-growth-climate relationships in subalpine *Nothofagus* forests, South Island, New Zealand. *New Zealand Journal of Botany*, 22, 471-481.

Norton, D.A. (1987). Reconstruction of past river flow and precipitation in Canterbury, New Zealand from analysis of tree-rings. *Journal of Hydrology (N.Z.)*, 26, 161-174.

Norton, D.A. (1990). Dendrochronology in the Southern Hemisphere. In E.R. Cook and L.A. Kairiukstis (Eds.), *Methods of dendrochronology: applications in the environmental sciences* (pp. 17-21). Dordrecht: Kluwer Academic Publishers.

Norton, D.A. and Palmer, J.G. (1992). Dendroclimatic evidence from Australasia. In R.S. Bradley and P.D. Jones (Eds.), *Climate since AD 1500* (pp. 463-482). London: Routledge.

Norton, D.A., Palmer, J.G. and Ogden, J. (1987). Dendroecological studies in New Zealand. 1. An evaluation of tree age estimates based on increment cores. *New Zealand Journal of Botany*, 25, 373-383.

Norton, D.A., Briffa, K.R. and Salinger, M.J. (1989). Reconstruction of New Zealand summer temperatures to 1730 AD using dendroclimatic techniques. *International Journal of Climatology*, 9, 633-644.

Nowacki, G.J. and Abrams, M.D. (1997). Radial-growth averaging criteria for reconstructing disturbance histories from presettlement-origin oaks. *Ecological Monographs*, 67, 225-249.

Ogden, J. (1978). On the dendrochronological potential of Australian trees. *Australian Journal of Ecology*, 3, 339-356.

Ogden, J. (1982). Australasia. In M.K. Hughes, P.M. Kelly, J.R. Pilcher and V.C. LaMarche Jr. (Eds.), *Climate from tree rings* (pp. 90-103). Cambridge: Cambridge University Press.

Ogden, J. and Ahmed, M. (1989). Climate response function analyses of kauri (*Agathis australis*) tree-ring chronologies in northern New Zealand. *Journal of The Royal Society of New Zealand*, 19, 205-221.

Ortlieb, L. (2000). The documented historical record of El Niño events in Peru: an update of the Quinn record (sixteenth through nineteenth centuries). In H.F. Diaz and V. Markgraf (Eds.), *El Niño and the Southern Oscillation: multiscale variability and global and regional impacts* (pp. 207-295). New York: Cambridge University Press.

Palmer, J.G. (1982). *A dendrochronological study of kauri* (Agathis australis). Unpublished M.Sc. thesis. University of Auckland, Auckland, New Zealand.

Palmer, J.G. (1989). *A dendroclimatic study of* Phyllocladus trichomanoides *D. Don (tanekaha).* Unpublished Ph.D. thesis. University of Auckland, Auckland, New Zealand.

Palmer, J.G. and Xiong, L. (2003). New Zealand climate over the last 500 years reconstructed from *Libocedrus bidwillii* Hook. f. tree-ring chronologies. *The Holocene* (in press).

Patel, R.N. (1967). Wood anatomy of Podocarpaceae indigenous to New Zealand. *New Zealand Journal of Botany*, 5, 171-184.

Peters, K., Jacoby, G.C. and Cook, E.R. (1981). Principal component analysis of tree-ring sites. *Tree-Ring Bulletin*, 41, 1-19.

Pilcher, J.R.. (1990). Sample preparation, cross-dating, and measurement. In E.R. Cook and L.A. Kairiukstis (Eds.), *Methods of dendrochronology: applications in the environmental sciences* (pp. 40-51). Dordrecht: Kluwer Academic Publishers.

Preisendorfer, R.W., Zwiers, F.W. and Barnett, T.P. (1981). *Foundations of principal components selection rules.* SIO Reference Series, 81-4, Scripps Institution of Oceanography, La Jolla, USA.

Quinn, C.J. (1982). Taxonomy of *Dacrydium* Sol. ex Lamb. emend. de Laub (Podocarpaceae). *Australian Journal of Botany*, 30, 311-320.

Richman, M.B. (1986). Rotation of principal components. *Journal of Climatology*, 6, 293-335.

Robinson, W.J. (1990). Dendrochronology in western North America: the early years. In E.R. Cook and L.A. Kairiukstis (Eds.), *Methods of dendrochronology: applications in the environmental sciences* (pp. 1-8). Dordrecht: Kluwer Academic Publishers.

Ropelewski, C.F. and Jones, P.D. (1987). An extension of the Tahiti-Darwin Southern Oscillation index. *Monthly Weather Review*, 115, 2161-2165.

Sakai, A. and Wardle, P. (1978). Freezing resistance of New Zealand trees and shrubs. *New Zealand Journal of Ecology*, 1, 51-61.

Salinger, M.J. (1980a). New Zealand climate: 1. Precipitation patterns. *Monthly Weather Review*, 108, 174-186.

Salinger, M.J. (1980b). New Zealand climate: 2. Temperature patterns. *Monthly Weather Review*, 108, 187-194.

Salinger, M.J. (1981). *New Zealand climate: the instrumental record.* Unpublished Ph.D. thesis. Victoria University, Wellington, New Zealand.

Salinger, M.J. (1988). New Zealand climate: past and present. In *Climate change: the New Zealand response* (pp. 17-24). Proceedings of a workshop held in Wellington, 29-30 March 1988. Wellington: Ministry for Environment.

Salinger, J., McGann, R., Coutts, L., Collen, B. and Fouhy, E. (1992a). *South Pacific historical climate network: temperature trends in New Zealand and outlying islands, 1920-1990.* Wellington: New Zealand Meteorological Service.

Salinger, J., McGann, R., Coutts, L., Collen, B. and Fouhy, E. (1992b). *South Pacific historical climate network: rainfall trends in New Zealand and outlying islands, 1920-1990.* Wellington: New Zealand Meteorological Service.

Salinger, M.J., Palmer, J.G., Jones, P.D. and Briffa, K.R. (1994). Reconstruction of New Zealand climate indices back to AD 1731 using dendroclimatic techniques: some preliminary results. *International Journal of Climatology*, 14, 1135-1149.

Salmon, J.T. (1996). *The native trees of New Zealand.* (Rev. ed.). Auckland: Reed Books.

Sandercock, H.R. (1987). *Ajax ecological area, Catlins State Forest Park: a vegetation survey.* Unpublished report to the New Zealand Forest Service, Invercargill, New Zealand.

Schmelter, A. (2000). Climatic response and growth-trends of *Nothofagus pumilio* along altitudinal gradients from arid to humid sites in northern Patagonia – a progress report. In F.A. Roig (Ed.), *Dendrocronología en América Latina / Dendrochronology in Latin America* (pp. 193-215). Mendoza: EDIUNC.

Schulman, E. (1956). *Dendroclimatic changes in semiarid America.* Tucson: University of Arizona Press.

Schweingruber, F.H. (1990a). Dendroecological information in pointer years and abrupt growth changes. In E.R. Cook and L.A. Kairiukstis (Eds.), *Methods of dendrochronology: applications in the environmental sciences* (pp. 277-283). Dordrecht: Kluwer Academic Publishers.

Schweingruber, F.H. (1990b). Radiodensitometry. In E.R. Cook and L.A. Kairiukstis (Eds.), *Methods of dendrochronology: applications in the environmental sciences* (pp. 55-63). Dordrecht: Kluwer Academic Publishers.

Schweingruber, F.H., Kairiukstis, L. and Shiyatov, S. (1990). Sample selection. In E.R. Cook and L.A. Kairiukstis (Eds.), *Methods of dendrochronology: applications in the environmental sciences* (pp. 23-35). Dordrecht: Kluwer Academic Publishers.

Self, S., Rampino, M.R. and Barbera, J.J. (1981). The possible effects of large 19th and 20th century volcanic eruptions on zonal and hemispheric surface temperatures. *Journal of Volcanology and Geothermal Research*, 11, 41-60.

Sheppard, P.R., Holmes, R.L. and Graumlich, L.J. (1997). The "many fragment curse:" a special case of the segment length curse. *Tree-Ring Bulletin*, 54, 1-9.

Stahle, D.W. and Cleaveland, M.K. (1993). Southern Oscillation extremes reconstructed from tree rings of the Sierra Madre Occidental and Southern Great Plains. *Journal of Climate*, 6, 129-140.

Stahle, D.W., D'Arrigo, R.D., Krusic, P.J., Cleaveland, M.K., Cook, E.R., Allan, R.J., Cole, J.E., Dunbar, R.B., Therrell, M.D., Gay, D.A., Moore, M.D., Stokes, M.A., Burns, B.T., Villanueva-Diaz, J. and Thompson, L.G. (1998). Experimental dendroclimatic reconstruction of the Southern Oscillation. *Bulletin of the American Meteorological Society*, 79, 2137-2152.

Stewart, G.H. and Harrison, J.B.J. (1987). Plant communities, landforms, and soils of a geomorphically active drainage basin, Southern Alps, New Zealand. *New Zealand Journal of Botany*, 25, 385-399.

Stewart, G.H. and Rose, A.B. (1989). Conifer regeneration failure in New Zealand: dynamics of montane *Libocedrus bidwillii* stands. *Vegetatio*, 79, 41-49.

Stewart, K. (1984). *Collins handguide to the native trees of New Zealand.* Auckland: William Collins Publishers Ltd.

Stokes, M.A. and Smiley, T.L. (1968). *Tree-ring dating.* Chicago: The University of Chicago Press.

Sturman, A. and Tapper, N. (1996). *The weather and climate of Australia and New Zealand.* Melbourne: Oxford University Press.

Szeicz, J.M., Lara, A., Díaz, S. and Aravena, J.C. (2000). Dendrochronological studies of *Pilgerodendron uviferum* in southwestern South America. In F.A. Roig (Ed.), *Dendrocronología en América Latina / Dendrochronology in Latin America* (pp. 245-270). Mendoza: EDIUNC.

The Royal Society of New Zealand. (1988). *Climate change in New Zealand.* An abridged version of a report prepared by the New Zealand Climate Committee of the Royal Society of New Zealand as a contribution towards the Climate Change Programme of the New Zealand Government. Wellington: The Royal Society of New Zealand.

Thompson, L.G., Davis, M.E., Mosley-Thompson, E., Sowers, T.A., Henderson, K.A., Zagorodnov, V.S., Lin, P.-N., Mikhalenko, V.N., Campen, R.K., Bolzan, J.F., Cole-Dai, J. and Francou, B. (1998). A 25,000-year tropical climate history from Bolivian ice cores. *Science*, 282, 1858-1864.

Tomlinson, A.I. (1976). Climate. In I. Wards (Ed.), *New Zealand atlas*. Wellington: Government Printer.

Veblen, T.T., Kitzberger, T. and Lara, A. (1992). Disturbance and forest dynamics along a transect from Andean rain forest to Patagonian shrubland. *Journal of Vegetation Science*, 3, 507-520.

Villalba, R. (1990). Climatic fluctuations in northern Patagonia in the last 1000 years as inferred from tree-ring records. *Quaternary Research*, 34, 346-360.

Villalba, R. (1994). Climatic fluctuations in mid-latitudes of South America during the last 1000 years: their relationships to the Southern Oscillation. *Revista Chilena de Historia Natural*, 67, 453-461.

Villalba, R. (1995). *Climatic influences on forest dynamics along the forest-steppe ecotone in northern Patagonia.* Unpublished Ph.D. thesis. University of Colorado, Boulder, Colorado, USA.

Villalba, R., Leiva, J.C., Rubulis, S., Suarez, J. and Lenzano, L. (1990). Climate, tree-ring, and glacial fluctuations in the Rio Frias Valley, Rio Negro, Argentina. *Arctic and Alpine Research*, 22, 215-232.

Villalba, R., Boninsegna, J.A., Veblen, T.T., Schmelter, A. and Rubulis, S. (1997a). Recent trends in tree-ring records from high elevation sites in the Andes of northern Patagonia. *Climatic Change*, 36, 425-454.

Villalba, R., Cook, E.R., D'Arrigo, R.D., Jacoby, G.C., Jones, P.D., Salinger, M.J. and Palmer, J. (1997b). Sea-level pressure variability around Antarctica since AD 1750 inferred from subantarctic tree-ring records. *Climate Dynamics*, 13, 375-390.

Villalba, R., Cook, E.R., Jacoby, G.C., D'Arrigo, R.D., Veblen, T.T. and Jones, P.D. (1998). Tree-ring based reconstructions of northern Patagonia precipitation since AD 1600. *The Holocene*, 8, 659-674.

Vittoz, P., Stewart, G.H. and Duncan, R.P. (2001). Earthquake impacts in old-growth *Nothofagus* forests in New Zealand. *Journal of Vegetation Science*, 12, 417-426.

Wardle, J. (1974). Influence of introduced mammals on the forest and shrublands of the Grey River headwaters. *New Zealand Journal of Forestry Science*, 4, 459-486.

Wardle, P. (1960). The subalpine scrub of the Hokitika catchment, Westland. *Transactions of the Royal Society of New Zealand*, 88, 47-61.

Wardle, P. (1963). Growth habits of New Zealand subalpine shrubs and trees. New *Zealand Journal of Botany*, 1, 18-47.

Wardle, P. (1991). *Vegetation of New Zealand.* Cambridge: Cambridge University Press.

Wells, A. (1998). *Landscape disturbance history in Westland, New Zealand: the importance of infrequent earthquakes along the Alpine Fault.* Unpublished Ph.D. thesis. Lincoln University, Lincoln, New Zealand.

Wells, A., Yetton, M.D., Duncan, R.P. and Stewart, G.H. (1999). Prehistoric dates of the most recent Alpine fault earthquakes, New Zealand. *Geology*, 27, 995-998.

Wells, A., Duncan, R.P. and Stewart, G.H. (2001). Forest dynamics in Westland, New Zealand: the importance of large, infrequent earthquake-induced disturbance. *Journal of Ecology*, 89, 1006-1018.

Whitehouse, M.J. (1999). Sediments reveal their age. *Science*, 285, 58-59.

Wigley, T.M.L., Briffa, K.R. and Jones, P.D. (1984). On the average value of correlated time series, with application in dendroclimatology and hydrometeorology. *Journal of Climate and Applied Meteorology*, 23, 201-213.

Wilson, A.T., Hendy, C.H. and Reynolds, C.P. (1979). Short-term climate change and New Zealand temperatures during the last millennium. *Nature*, 279, 315-317.

Wilson, H.D. (1987a). Plant communities of Stewart Island (New Zealand). In H.D. Wilson, *Vegetation of Stewart Island, New Zealand: a supplement to the New Zealand Journal of Botany*. Wellington: DSIR Science Information Publishing Centre.

Wilson, H.D. (1987b). Vascular plants of Stewart Island (New Zealand). In H.D. Wilson, *Vegetation of Stewart Island, New Zealand: a supplement to the New Zealand Journal of Botany*. Wellington: DSIR Science Information Publishing Centre.

Winkler, S. (2000). The 'Little Ice Age' maximum in the Southern Alps, New Zealand: preliminary results at Mueller Glacier. *The Holocene*, 10, 643-647.

Woodhouse, C.A. (1999). Artificial neural networks and dendroclimatic reconstructions: an example from the Front Range, Colorado, USA. *The Holocene*, 9, 521-529.

Xiong, L. (1995). *A dendroclimatic study of* Libocedrus bidwillii *Hook.F. (kaikawaka).* Unpublished Ph.D. thesis. Lincoln University, Lincoln, New Zealand.

Xiong, L. and Palmer, J.G. (2000a). *Libocedrus bidwillii* tree-ring chronologies in New Zealand. *Tree-Ring Bulletin*, 56, 1-16.

Xiong, L. and Palmer, J.G. (2000b). Reconstruction of New Zealand temperatures back to AD 1720 using *Libocedrus bidwillii* tree-rings. *Climatic Change*, 45, 339-359.

Xiong, L., Okada, N., Fujiwara, T., Ohta, S. and Palmer, J.G. (1998). Chronology development and climate response analysis of different New Zealand pink pine (*Halocarpus biformis*) tree-ring parameters. *Canadian Journal of Forest Research*, 28, 566-573.

Xiong, L., Okada, N., Zhong, Z. and Fujiwara, T. (1998-1999). The relationship between *Schefflera delavayi* growth and climate in the Three Gorges Reservoir region of the Yangtze River, China. *Dendrochronologia*, 16-17, 99-118.

Yetton, M.D. (1998). Progress in understanding the paleoseismicity of the central and northern Alpine Fault, Westland, New Zealand. *New Zealand Journal of Geology and Geophysics*, 41, 475-483.

Yetton, M.D., Wells, A. and Traylen, N.J. (1998). *The probability and consequences of the next Alpine Fault earthquake*. Unpublished report to the Earthquake Commission, Wellington, New Zealand. EQC Research Report Number 95/193.

Appendix 1

Estimation of the pith offset

For every pink pine core, I was able to use one or several of the following methods to estimate the biological age of the first crossdated ring: (a) true pith, (b) arc, (c) 1-radius, and (d) 2-radii.

(a) true pith

I could apply the "true pith" method to the cores where pith was present, and the pith offset (*PO*) was therefore the mere count of the rings between the pith and the first crossdated ring. In several instances the innermost rings were so suppressed that the precise count was impossible, and I had to estimate their number. From the 23 cores that contained piths, I could derive the *PO* data for 20 trees / 40 cores.

(b) arc

The "arc" method was described by Duncan (1989). It is applicable to the cores that had failed to reach the pith, but in which the innermost crossdated ring forms an arc. It uses a geometric model (Equation A1.1) to estimate the missing radius *r*, assuming concentric growth from the pith to the first crossdated ring.

$$r = L^2 / 8h + h/2 \qquad \text{(A1.1)}$$

L is the length and *h* is the height of the arc. The pith offset *PO* (i.e. the number of rings in the missing radius) is then calculated by dividing the estimated length of the missing radius *r* by the mean ring width obtained from the 20 innermost rings (m_{20}) (Equation A1.2).

$$PO = r / m_{20} \qquad \text{(A1.2)}$$

(c) 1-radius

The "1-radius" method (Norton *et al.*, 1987) can be used for any samples without a pith or arching inner rings. It also assumes concentric growth, and it requires the DBH value for the

calculation. The length of the missing radius r can then be calculated as the difference between the geometric radius and the length of the core (Equation A1.3). The length of the core can be calculated by multiplying the number of crossdated rings N by their mean ring width M.

$$r = DBH / 2 - N*M \quad \text{(A1.3)}$$

I estimated the pith offset PO by dividing the length of the missing radius r by the mean ring width M (Equation A1.4). In the "arc" method, I considered m_{20} to be representative of the innermost growth, because the arcs in general appeared to be close to the pith. However, the cores without arcs often seemed to have missed the pith by several decades to several centuries. As alternating periods of slow and fast growth were typically present in the cores, the mean growth calculated from only the first 20 or 50 measured rings could potentially lead to a large over- or underestimation of the pith offset. Hence I decided to use the mean ring width M (for the entire radius) in the calculation.

$$PO = r / M \quad \text{(A1.4)}$$

(d) 2-radii

The "2-radii" method does not work with individual cores, but rather with trees. It requires the DBH value and at least two cores per tree for the calculation. The chief advantage of this method is that it does not make any assumption about the position of the pith. First, the mean ring width M_{avg} for the entire tree is calculated as a weighted average from both radii (Equation A1.5).

$$M_{avg} = (N_1*M_1 + N_2*M_2) / (N_1 + N_2) \quad \text{(A1.5)}$$

N_1 and N_2 are the number of crossdated rings from cores 1 and 2; M_1 and M_2 are their respective mean measurements. By dividing the DBH value by M_{avg}, I obtained the total number of rings that were expected to occur within the diameter of the tree. By subtracting one half of this value (i.e. the number of rings that were expected to occur within a complete radius) from the calendar year of the outermost ring (1999 for most of my sites), I thus estimated the calendar year of the pith P (Equation A1.6).

$$P = 1999 - 0.5*(DBH / M_{avg}) \quad \text{(A1.6)}$$

The pith offset of core 1 (PO_1) is then calculated by subtracting the calendar year of the pith P from the calendar year of its first (innermost) crossdated ring F_1 (Equation A1.7). Similarly is calculated the pith offset for core 2.

$$PO_1 = F_1 - P \qquad \text{(A1.7)}$$

In the "2-radii" method, I assumed that the rings in the missing radius were growing at the mean rate of M_{avg} (rather than m_{20} as in the "arc" method) for the same reasons as given before.

In many cases, I was able to use more than one method to calculate the pith offset of a particular core. As each method yielded different results, I had to decide which estimate was the most accurate. I ranked the methods in the following order: (1) true pith, (2) 2-radii, (3) arc, and (4) 1-radius. I considered the "1-radius" method to be the least precise, as it assumes that the pith lies in the geometric centre of the tree. However, the growth of many New Zealand trees is eccentric (Norton *et al.*, 1987), and this is also true for pink pine, especially when growing on steep slopes. I decided to favour the "2-radii" estimates over the "arc" estimates, after I compared them against several known dates. There were 12 cores with arcs for which I knew the precise calendar year of the pith (from the trees' second cores), and 18 trees where one of every pair of cores contained a pith. I calculated the differences between the true piths and their estimates, and I found that both methods underestimated the tree age (Table A1.1). On average, the "2-radii" method was more accurate than the "arc" method, even though the errors were more widely spread around the mean.

Table A1.1 Accuracy of the pith-offset estimates. The errors were calculated by subtracting the estimated calendar year of the pith from the true calendar year. All values in the table are in years.

Method	Mean Error	Median	St.dev.	Min.	Max.
Arc (n = 12)	-37.7	-25	50.7	-165	18
2-radii (n = 18)	-2.4	-12	111.5	-176	261

In 21 cores (out of 598), the estimated pith-offset value was negative (i.e. the pith was said to be younger than the first crossdated year; by 19.2 ± 18.3 years). To correct this obvious mistake, I changed those PO values to zero. I did the same for six other trees where I was unable to estimate the PO value due to unrecorded DBH.

Appendix 2

Tree-ring data

The data are stored on a computer disk (enclosed). Appendix 2 contains four folders:

1. "*pink pine-raw*" – crossdated raw measurements from individual sites (Chapter 2); 13 files
2. "*pink pine-chronologies*" – RCS chronologies from individual sites (Chapter 2); 13 files
3. "*WRC*" - crossdated raw measurements and the RCS chronology from Westland pink pine (Chapter 4); 2 files
4. "*Libocedrus*" – crossdated raw measurements and RCS chronologies from two *Libocedrus bidwillii* chronology sites (Chapter 5); 4 files

Appendix 3

Temperature data

The data are stored on a computer disk (enclosed). Appendix 3 contains three files:

1. "*Hokitika-monthly*" – observed mean monthly temperatures (1866-1880 and 1894-1999) from Hokitika (Chapter 3)
2. "*Hokitika-summer*" – observed January-March temperatures (1894-1999) from Hokitika (Chapter 4)
3. "*reconstruction*" – reconstructed mean of January-March temperatures (1480-2000): the Westland palaeotemperature record (Chapter 4)